

**STUDIES OF GENES SHOWING DIFFERENTIAL
EXPRESSION DURING PLASMODIUM
DEVELOPMENT IN *PHYSARUM POLYCEPHALUM***

Thesis submitted for the degree of
Doctor of Philosophy
at the University of Leicester



by

Lynnette June Cook

Department of Genetics
University of Leicester
United Kingdom

March 2000

UMI Number: U125607

All rights reserved

INFORMATION TO ALL USERS

The quality of this reproduction is dependent upon the quality of the copy submitted.

In the unlikely event that the author did not send a complete manuscript and there are missing pages, these will be noted. Also, if material had to be removed, a note will indicate the deletion.



UMI U125607

Published by ProQuest LLC 2013. Copyright in the Dissertation held by the Author.
Microform Edition © ProQuest LLC.

All rights reserved. This work is protected against
unauthorized copying under Title 17, United States Code.



ProQuest LLC
789 East Eisenhower Parkway
P.O. Box 1346
Ann Arbor, MI 48106-1346

Studies of Genes Showing Differential Expression During Plasmodium Development in *Physarum polycephalum*

by Lynnette Cook

Abstract

Uninucleate amoebae of the protist *Physarum polycephalum* develop into multinucleate, syncytial plasmodia following a developmental transition that is initiated by the multiallelic mating-type locus, *matA*. As a step towards understanding the processes involved in plasmodium development, genes that are expressed primarily during the amoebal-plasmodial developmental transition were previously identified from a subtracted cDNA library. The initial aim of the research described in this thesis was to perform sequence analysis of four such cDNA clones. This analysis revealed that the coding sequences of the four genes were incomplete. The N-terminus of the deduced P4/10P transcript contains homology to *Rhizobium* nodulation N proteins, *redB* encodes a calcium-binding protein with homology to sarcoplasmic proteins from invertebrates while both *redA* and D6/18P are novel genes. Northern blotting analysis was then performed to examine the unique expression pattern of *redA* and *redB* in more detail and confirmed that these genes are expressed primarily during the developmental transition. Southern blotting analysis indicated that *redA* and *redB* do not belong to gene families. The complete coding sequence for *redA* was deduced from a genomic clone obtained by inverse PCR and two introns were identified in the 5' region of the gene; it is possible that the 3' region of *redA* contains a third intron. To investigate the role of *redA*, gene disruption studies were initiated; however, in *P. polycephalum* such studies are limited due to considerably low transformation efficiency. A further limitation to transformation studies using *P. polycephalum* is the availability of only one selectable marker. To increase the potential use of this technique, further selectable markers were sought and preliminary trials were conducted concomitant with the *redA* gene disruption studies.

Past genetic analysis has identified many amoeba- and plasmodium-specific genes; such analysis led to the identification of the fragmin gene family. In parallel with the studies of *redA* and *redB*, northern blotting analysis was performed to examine the expression pattern for each member of the fragmin gene family during plasmodium development. These data, together with Southern blotting data, indicated that the fragmin gene family consists of three plasmodium-specific genes and one amoeba-specific gene.

ACKNOWLEDGEMENTS

I would like to thank Jenny Dee, Juliet Bailey, Jenny Foxon, Rick Kilmer-Barber, Emma Swanston, Fidelma Hernon and Angela Thomas, for their support, friendship and for providing stimulating conversation, both scientific and otherwise. I am particularly grateful to Juliet Bailey for sharing her enthusiasm and expertise in *Physarum* genetics and for her advice, patience and encouragement with the preparation of this thesis. Thanks also to Jenny Foxon for her excellent technical assistance during my early days in the *Physarum* Group and to Jenny Dee for balancing the molecular genetics with 'classical' genetics and helping me to appreciate the value of the organism as a whole.

I am grateful to The Wellcome Trust for providing financial support for my employment as a Research Assistant to Dr. Juliet Bailey (Grant No: 042524). I am also grateful to the University of Leicester for permitting my registration for a PhD whilst I was employed as a Research Assistant. I appreciate the support of the technical staff within the Department of Genetics for their contribution to the smooth running of the department and endless supply of media and consumables.

Last but not least, I am totally indebted to my mother and my fiancé, Graham, for providing unconditional love and support. Without their encouragement, financial support and faith in my abilities, I would not have reached this juncture in my life.

CONTENTS

CHAPTER 1: INTRODUCTION

1.1	CLASSIFICATION OF <i>PHYSARUM</i>	1-1
1.2	THE LIFE CYCLE OF <i>PHYSARUM POLYCEPHALUM</i>	1-2
1.2.1	Amoebae.....	1-2
1.2.2	Plasmodia.....	1-4
1.2.3	Heterothallic plasmodium development.....	1-6
1.2.4	Apogamic plasmodium development.....	1-7
1.2.5	The timing of events during plasmodium development.....	1-8
1.3	THE REGULATION AND ORGANISATION OF CELL STRUCTURAL PROTEINS.....	1-11
1.3.1	The tubulin isotypes and microtubule organisation.....	1-11
1.3.2	The actin cytoskeleton and actin-binding proteins.....	1-13
1.4	THE AMOEBAL-PLASMODIAL TRANSITION.....	1-17
1.4.1	Differentially expressed genes and proteins.....	1-17
1.4.2	Developmental mutants characterised by phenotype.....	1-20
1.4.2.1	The early acting <i>npf</i> mutants.....	1-20
1.4.2.2	The late acting <i>npf</i> mutants.....	1-21
1.4.3	Regulation of the amoebal-plasmodial transition.....	1-23
1.5	GENOME ORGANISATION.....	1-24
1.5.1	Chromosomal DNA.....	1-24
1.5.2	Repetitive elements cause instability of cloned genomic fragments.....	1-26
1.5.3	Ribosomal and mitochondrial DNA.....	1-27
1.6	DNA TRANSFORMATION IN <i>PHYSARUM POLYCEPHALUM</i>	1-28
1.6.1	Development of strains for transformation.....	1-28
1.6.2	Early transformation studies in <i>P. polycephalum</i>	1-29
1.6.3	Promoters and reporter genes.....	1-30
1.6.4	Optimisation of electroporation parameters.....	1-31
1.6.5	Selectable markers.....	1-33
1.6.6	Homologous gene replacement.....	1-35
1.6.7	Stability of introduced DNA and elements used to improve stability of transcripts.....	1-36
1.6.8	Natural suppressers of hygromycin resistance.....	1-37
1.7	AIMS.....	1-37

CHAPTER 2: MATERIALS AND METHODS

2.1	AMOEBAL CELL CULTURE AND TRANSFORMATION.....	2-1
2.1.1	Gene loci.....	2-1
2.1.2	Strains.....	2-1
2.1.2.1	<i>Escherichia coli</i> (bacterial) strains.....	2-1
2.1.2.2	<i>Physarum polycephalum</i> strains.....	2-1
2.1.3	Media.....	2-1
2.1.4	Culture and maintenance of amoebae.....	2-2

2.1.5	Encystment of amoebae for frozen stocks	2-3
2.1.6	Transfer of amoebae into axenic medium	2-3
2.1.7	Transformation of axenically grown LU352 amoebae	2-5
2.1.7.1	Optimisation of electrical parameters for electroporation using the luciferase assay	2-5
2.1.7.2	Transformation of amoebae by electroporation	2-6
2.1.8	Induction of apogamic plasmodium development	2-7
2.2	ISOLATION OF DNA	2-8
2.2.1	Isolation of genomic DNA from axenically grown amoebae	2-8
2.2.2	Quantification of nucleic acids by spectrophotometry	2-9
2.2.3	Isolation of genomic DNA for cloning, PCR and restriction mapping	2-9
2.2.4	Isolation of plasmid DNA	2-10
2.2.5	Rapid isolation of plasmid DNA	2-10
2.3	VECTOR CONSTRUCTION AND DNA CLONING	2-11
2.3.1	Restriction enzyme digestion	2-11
2.3.2	Isolation of DNA fragments	2-11
2.3.3	DNA ligation	2-12
2.3.4	Size-fractionated genomic libraries	2-14
2.3.5	Transformation of bacteria with plasmid DNA	2-15
2.4	ANALYSIS OF NUCLEIC ACIDS	2-16
2.4.1	Southern blotting	2-16
2.4.2	Northern blotting	2-17
2.4.3	Colony blots	2-19
2.4.4	Radioactive-labelling of probes	2-21
2.4.5	DNA sequence analysis and primer design	2-22
2.4.6	Polymerase Chain Reaction (PCR)	2-23

CHAPTER 3: IDENTIFICATION AND SEQUENCE ANALYSIS OF *RED* GENE cDNAs.

3.1	INTRODUCTION	3-1
3.1.1	cDNA library design and construction	3-1
3.1.2	Aims	3-6
3.2	RESULTS	3-6
3.2.1	Screening cDNA libraries for longer transcripts	3-6
3.2.2	Sequence analysis of D6/18P and P4/10P	3-7
3.2.3	Sequence analysis of D13/3D and P8/8A	3-13
3.2.4	Northern blotting analysis of D13/3D and P8/8A	3-16
3.2.5	Southern blotting analysis of <i>redA</i> and <i>redB</i>	3-20
3.3	DISCUSSION	3-23
3.3.1	Screening cDNA libraries for longer <i>red</i> gene cDNAs	3-23
3.3.2	Efficiency of subtraction of ML8A	3-25
3.3.3	Strategies for cloning differentially expressed genes	3-26
3.3.4	<i>red</i> gene expression	3-28
3.4	SUMMARY	3-30

CHAPTER 4: GENOME ORGANISATION AND SEQUENCE ANALYSIS OF *REDA*

4.1	INTRODUCTION.....	4-1
4.2	FURTHER SOUTHERN BLOTTING ANALYSIS OF <i>REDA</i>	4-1
4.3	CONSTRUCTION OF GENOMIC LIBRARIES CONTAINING <i>REDA</i>	4-2
4.3.1	Construction of <i>Hind</i> III – <i>Pst</i> I genomic libraries.....	4-6
4.3.2	Problems associated with construction of genomic libraries.....	4-8
4.3.3	Screening the <i>Hind</i> III – <i>Pst</i> I library, LL6, for <i>redA</i>	4-9
4.3.4	Construction of a <i>Hind</i> III – <i>Xho</i> I genomic library.....	4-11
4.4	USE OF PCR TO AMPLIFY GENOMIC COPIES OF <i>REDA</i>	4-12
4.4.1	Optimisation of PCR.....	4-12
4.4.2	Inverse PCR.....	4-13
4.4.2.1	Inverse PCR using <i>Taq</i> I digested genomic DNA.....	4-13
4.4.2.2	Further Inverse PCR experiments.....	4-16
4.4.2.3	Results from inverse PCR.....	4-18
4.4.3	Conventional PCR.....	4-19
4.5	DETAILED GENE MAPPING OF <i>REDA</i>	4-20
4.6	SEQUENCE ANALYSIS OF <i>REDA</i>	4-21
4.7	SUMMARY.....	4-27

CHAPTER 5: FUNCTIONAL ANALYSIS OF *REDA*

5.1	INTRODUCTION.....	5-1
5.1.1	Homologous gene replacement.....	5-1
5.1.2	Antisense RNA mutagenesis.....	5-2
5.1.3	Aims.....	5-3
5.2	CONSTRUCTION OF cDNA-BASED VECTORS FOR HOMOLOGOUS GENE REPLACEMENT OR ANTISENSE MUTAGENESIS.....	5-4
5.2.1	Construction of <i>redA</i> frameshift vectors.....	5-4
5.2.1.1	Frameshift by PCR.....	5-5
5.2.1.2	Frameshift by restriction digest.....	5-5
5.2.2	Construction of vectors where <i>PardC-hph</i> is positioned within the <i>redA</i> coding region.....	5-9
5.3	CONSTRUCTION OF A <i>REDA</i> ANTISENSE RNA MUTAGENESIS VECTOR.....	5-10
5.4	TRANSFORMATION OF AMOEBAE WITH THE GENE DISRUPTION VECTORS AND ANALYSIS OF TRANSFORMANTS.....	5-11
5.4.1	Apogamic plasmodium development of transformants.....	5-14
5.4.2	Southern blotting analysis of transformants.....	5-17
5.4.2.1	Southern blotting analysis of transformants derived from LC4 and LC5.....	5-19
5.4.2.2	Southern blotting analysis of transformants derived from LC8, LC9, LC10 and LC11.....	5-23

5.5	DISCUSSION	5-24
5.5.1	Summary of results.....	5-24
5.5.2	Optimisation of gene disruption vector design	5-25
5.5.3	Factors affecting the transformation efficiency	5-26
5.5.4	Antisense RNA-mediated gene inactivation.....	5-29
5.5.5	Future studies on <i>redA</i>	5-31
5.5.6	Other future transformation studies.....	5-32

CHAPTER 6: EXPRESSION OF THE FRAGMIN GENE FAMILY DURING PLASMODIUM DEVELOPMENT

6.1	INTRODUCTION.....	6-1
6.1.1	The role of fragmin and cell-type specific isotypes	6-1
6.1.2	Comparison of gene expression during apogamic and heterothallic development.....	6-2
6.1.3	Aims.....	6-3
6.2	RESULTS.....	6-4
6.2.1	Expression of the two control genes; <i>redA</i> and actin.....	6-4
6.2.2	Analysis of the fragmin clone by northern and Southern blotting	6-7
6.2.3	Characterisation of an amoeba-specific fragmin gene	6-10
6.2.4	Characterisation of a second plasmodium-specific fragmin gene.....	6-11
6.2.4	Characterisation of AFK by northern and Southern blotting analysis	6-12
6.3	DISCUSSION	6-14
6.3.1	Comparison of gene expression during heterothallic and apogamic development.....	6-14
6.3.2	The fragmin gene family.....	6-15
6.3.3	The role of the fragmin isotypes in amoebae and plasmodia.....	6-16
6.3.4	Regulation of the plasmodial actin microfilament system by AFK.....	6-18
6.4	SUMMARY.....	6-19

CHAPTER 7: DEVELOPMENT OF NEW SELECTABLE MARKERS FOR USE IN TRANSFORMATION STUDIES

7.1	INTRODUCTION.....	7-1
7.1.1	Aims	7-2
7.2	IDENTIFICATION OF CANDIDATE RESISTANCE GENES	7-2
7.2.1	BASTA	7-3
7.2.2	Blasticidin-S.....	7-4
7.2.3	Emetine	7-5
7.2.4	Geneticin or Neomycin.....	7-6
7.2.5	Puromycin.....	7-7
7.2.6	Zeocin.....	7-8
7.3	PRELIMINARY TRIALS OF THE G418- <i>APHI</i> TRANSFORMATION SYSTEM.....	7-9

7.4	DISCUSSION	7-13
7.4.1	Prospects for development of the zeocin selection system for use in <i>Physarum</i>	7-13
7.4.2	The G418- <i>APHI</i> transformation system	7-13
7.4.3	Summary	7-16

CHAPTER 8: GENERAL DISCUSSION

8.1	<i>PHYSARUM POLYCEPHALUM</i> AS USEFUL EXPERIMENTAL SYSTEM ...	8-1
8.2	DIFFERENTIALLY EXPRESSED GENES	8-2
8.3	THE ROLE OF <i>MATA</i> IN PLASMODIUM DEVELOPMENT	8-5
8.4	CONCLUSION	8-7

LITERATURE CITED

LIST OF FIGURES

1.1	The heterothallic life cycle of <i>Physarum polycephalum</i>	1-3
1.2	Timing of events during the amoebal-plasmodial transition in apogamic strain CL	1-10
3.1	The screening strategy for the ML8S cDNA library and stock code designation	3-4
3.2	The cDNA and deduced partial amino acid sequences for cDNA clone D6/18P isolated from subtracted cDNA library, ML8S	3-9
3.3	The cDNA and deduced partial amino acid sequences for cDNA clone P4/10P isolated from subtracted cDNA library, ML8S	3-11
3.4	Amino acid sequence for P4/10P compared with homologous sequences from BLAST database search	3-12
3.5	The cDNA and deduced partial amino acid sequences for cDNA clone D13/3D isolated from subtracted cDNA library, ML8S	3-14
3.6	The cDNA and deduced partial amino acid sequences for cDNA clone P8/8A isolated from subtracted cDNA library, ML8S	3-15
3.7	Northern blotting analysis of differentially-expressed genes during apogamic development of <i>Physarum polycephalum</i> strain CL	3-17
3.8	Southern blotting analyses of <i>redA</i> and <i>redB</i>	3-22
4.1	The location of <i>redA</i> primers and some restriction sites as deduced from cDNA sequence analysis and Southern blotting	4-3
4.2	Southern blotting analyses of <i>redA</i>	4-5
4.3	Schematic representation of inverse PCR	4-14
4.4	Detailed genomic restriction map of <i>redA</i>	4-17
4.5	Composite DNA and deduced amino acid sequences for <i>redA</i>	4-22
4.6	Schematic showing the relative positions of the <i>redA</i> cDNA and <i>TaqI</i> inverse PCR clones within the gene	4-24
5.1	Vectors for homologous gene replacement and antisense studies of <i>redA</i>	5-7
5.2	Mechanism of disruption of <i>redA</i> by LC8 and LC9 as a result of insertion of <i>PardC-hph</i>	5-8
5.3	Plasmodial morphologies	5-16
5.4	Schematic representation of possible mechanisms of disruption of <i>redA</i> by integration of LC4	5-18
6.1	Northern analysis of gene expression during heterothallic development	6-5
6.2	Northern analysis of gene expression during apogamic development	6-6

LIST OF TABLES

2.1	Distribution of cell types in CL cultures used for RNA isolation.....	2-18
2.2	Distribution of cell types in cultures of heterothallic strains used for RNA isolation	2-20
3.1	Primers used for sequencing of the four cDNA clones.....	3-8
4.1	Data from Southern blotting analyses of <i>redA</i>	4-4
4.2	Details of size-fractionated <i>HindIII</i> - <i>PstI</i> genomic libraries	4-7
5.1	Details of transformation experiments conducted using the <i>redA</i> constructs	5-13
5.2	Summary of data from the LC construct-derived stable transformants	5-15
5.3	Data from Southern blotting analyses of transformants derived from the <i>redA</i> constructs.....	5-21
6.1	Data from Southern blotting analyses of AFK and the fragmin family of genes.....	6-9
7.1	Details of preliminary transformation experiments to test the G418/ <i>APHI</i> selection system	7-12

LIST OF ABBREVIATIONS, GENE NAMES AND SYMBOLS

×g	multiple of 'gravitational force'
≥	less than or equal to
+PSA	containing sodium benzyl penicillin, streptomycin sulphate and ampicillin
A	adenine
<i>AC1-A</i>	Putative ARS consensus sequence 1-A from <i>Physarum polycephalum</i> (Accession no. X74751)
AFK	actin fragmin kinase
APH	aminoglycoside phosphotransferase
APT	amoebal-plasmodial transition
<i>ard</i>	actin encoding locus
<i>ardDA1</i>	genomic clone of <i>ardD</i> with a deletion across intron 5 and part of exon 6 of <i>ardD</i>
ARS	autonomously replicating sequence
A/T-rich	sequences that contain more than 50% A and T residues
ATP	adenosine triphosphate
axe or AXE	axenic
B145	<i>Escherichia coli</i> bacterial strain
<i>betC</i>	locus encoding the plasmodium-specific β2-tubulin isotype
bp	base pairs
BSS	basal salt solution
C	cytosine
<i>cat</i>	chloramphenicol acetyltransferase gene
cDNA	complimentary DNA
CL	Colonia Leicester strain of <i>Physarum polycephalum</i>
CLd	derivative of CL
C-terminus	carboxy-terminal region of a polypeptide
cM	centimorgan
DAPI	4'-6-diamidino-2-phenylindole
dCTP	deoxycytidine triphosphate
DNA	deoxyribonucleic acid
dNTP's	deoxyribonucleotide triphosphates
DSDM	dilute SDM
DSPB	dilute SDM with phosphate buffer

ds-RNA	double stranded RNA
EDTA	ethylene-diamine-tetra-acetic acid
EGTA	ethylene-glycol-bis[β -aminoethyl ether]- <i>N, N, N', N'</i> -tetraacetic acid
<i>endA1</i>	endonuclease mutation that improves the quality plasmid DNA isolated from bacterial hosts
F-actin	filamentous actin
FB	flagellation buffer
FKB	formalin-killed bacteria
<i>frg</i>	fragmin encoding gene
<i>fus</i>	plasmodial fusion locus
G	guanine
G-actin	monomeric, globular actin
<i>gad</i>	greater asexual differentiation locus
G/C-rich	sequences that contain more than 50% G and C residues
GFM	1.1M glyoxal, 78% formamide, 0.06 \times MOPS
HEPES	<i>N</i> -[2-hydroxyethyl]piperazine- <i>N'</i> -[2-ethanesulfonic acid]
<i>hph</i>	hygromycin phosphotransferase, hygromycin resistance gene
<i>hsdR</i>	(Host spcificity determinant) mutation that protects plasmid inserts from cleavage by the bacterial <i>EcoK</i> endonuclease system
Hyg ^r	hygromycin resistance
Hyg ^s	hygromycin sensitive
IPTG	isopropyl- β -thiogalactopyranoside
Kan ^R	aminoglycoside resistance gene
kb	kilobase pairs
<i>lacZ</i>	bacterial β -galactosidase gene
LB-agar	LB broth containing 1.5% w/v agar
LB-amp	LB-agar containing ampicillin.
LB broth	Luria Bertani broth
LB-tet	LB-agar containing tetracycline.
LU352	Leicester University <i>Physarum polycephalum</i> strain number 352
<i>luc</i>	firefly luciferase gene
Ma	macroplasmidia
<i>mat</i>	mating-type locus
MCS	multiple cloning site
Mi	microplasmidia

ML8	Madison library 8, cDNA library
ML8A	ML8 amplified
ML8S	ML8 subtracted
MOPS	3-[N-morpholino]propanesulphonic acid
MOPS buffer	20mM MOPS, 5mM sodium acetate, 100μM EDTA, pH
MTOC	microtubule organising centre
Mif	mitochondrial fusion plasmid
mRNA	messenger RNA
mtDNA	mitochondrial DNA
N-terminus	amino-terminal region of a polypeptide
NHS	nuclear homogenisation solution
NMG	<i>N</i> -methyl- <i>N</i> -nitro- <i>N</i> -nitrosoguanidine
<i>npf</i>	no plasmodium formation locus
OD	optical density
oligo-dT	oligodeoxythymilate polymer
<i>Pard</i>	<i>ard</i> gene promoter
P:C:I	phenol:chloroform:isoamyl alcohol (50:49:1 v/v)
PCR	polymerase chain reaction
PIP ₂	phosphatidylinositol-4,5-bisphosphate
poly(A) ⁺	polyadenylate residues
<i>pro</i>	profilin encoding locus
PPT	phosphinothricin
RACE-PCR	rapid amplification of cDNA ends-PCR technique
rDNA	region encoding rRNA genes
<i>recA</i>	mutation that stabilises plasmid inserts
<i>recBC</i>	mutation that abolishes exonuclease V activity in the bacterial host
RFLP	restriction fragment length polymorphism
RNaseA	endoribonuclease the cleaves 3' at pyrimidines
RNA	ribonucleic acid
RNAi	RNA interference technique
rRNA	ribosomal RNA
RT-PCR	reverse transcriptase-PCR technique
<i>sbcB</i>	exonuclease I encoding bacterial locus
SBS	live standard bacterial suspension

SDM	semi-defined medium
SDS	sodium dodecyl sulphate
SOC broth	2% w/v bacto-tryptone, 0.5% w/v bacto-yeast, 8.5mM NaCl, 2.5mM KCl, 10mM MgCl ₂ , 10mM MgSO ₄ , 20mM glucose
ss	single-stranded
10 × SSC	1.5M sodium chloride, 150mM sodium citrate
STET	8% w/v Sucrose, 5% v/v Triton X-100, 50mM EDTA, 50mM Tris, pH8
T	thymine
<i>TardC</i>	transcriptional terminator region of <i>ardC</i>
TBE	90mM Tris-Cl, 90mM boric acid, 2mM EDTA pH 8
TE	Tris-HCl, 1mM EDTA, pH 8
T _m	nucleic acid dissociation/melting temperatures
Tp	<i>Physarum</i> transposon
Tris	N-tris(hydroxymethyl)aminomethane
VC	viable count
v/v	ratio of volume to volume
<i>whiA</i>	recessive, white plasmodial colour gene
w/v	ratio of weight to volume
w/w	ratio of weight to weight
X-gal	5-bromo-4-chloro-3-indolyl-β-D-galacto-pyranoside
XL1-Blue	<i>Escherichia coli</i> bacterial strain

CHAPTER ONE

INTRODUCTION

CHAPTER 1: INTRODUCTION

1.1 CLASSIFICATION OF *PHYSARUM*

Physarum polycephalum is an acellular slime mould that belongs to the Myxomycete division of Protists (Johansen *et al.*, 1992). The Myxomycetes are separated into four phyla: Myxomycota (syncytial or plasmodial slime moulds, such as *P. polycephalum*), Acrasiomycota (cellular or pseudoplasmodial slime moulds, such as *Dictyostelium discoideum*), Labyrinthulomycota (“cell-net” slime moulds) or Plasmodiophoromycota (plasmodiophores; Johansen *et al.*, 1992). The genus *Physarum* (meaning ‘bubble’, derived from the morphology of the sporangium) was first discovered by Persoon in 1795 and the subject of this thesis, *P. polycephalum* (*poly* - ‘many’ and *cephalum* - ‘head’, also derived from the morphology of the sporangium), was first documented by Schweinitz in 1822 (Lister, 1925).

The classification of acellular slime moulds reported in the literature is somewhat confusing. The fungal-like morphology of the plasmodia and plant-like fruiting bodies have resulted in their classification as either fungi, plants or ‘fungus-animals’ (Lister, 1925; Esser & Lemke, 1994). For example, in addition to the Protist classification above, they have also been classified to the Myxomycota division of fungi, which includes the acellular (Myxomycete or Myxogastrid), cellular (Dictyostelid; e.g. *Dictyostelium discoideum*) and protostelid slime moulds (Esser & Lemke, 1994). It has been argued that the acellular slime moulds should be classified as protists, an ancient class of organisms that emerged before plants, fungi & animals, and this classification is generally accepted (Johansen *et al.*, 1992; Woese 1996). However, Nowak and Steffan (1997) recently reported the re-classification of Myxomycetes by Hausmann and Hülsmann (1996) to the new taxon of ‘Myxogastra’, belonging to the unicellular eukaryotes. Using representatives from each division of the Mycetozoa, molecular phylogenies were constructed for elongation factor-1 α -encoding genes (Baldauf & Doolittle, 1997). This data, together with phylogenies derived from actin and β -tubulin data led Baldauf and Doolittle (1997) to propose that the acellular slime moulds are ‘late-emerging’ eukaryotes and should be classified as monophyletic Mycetozoa that are more closely related to fungi and animals than to plants. The classification argument continues; future studies of *P. polycephalum* and other organisms may help scientists reach an undisputed consensus for Myxomycete classification.

1.2 THE LIFE CYCLE OF *PHYSARUM POLYCEPHALUM*

Physarum polycephalum is found in temperate vegetative areas; for example, North America where the Wisconsin strains used widely for research were first isolated. The life cycle of this eukaryote includes two distinct vegetative growth phases: uninucleate, haploid amoebae and multinucleate syncytial plasmodia. These two cell types differ vastly and are linked by an irreversible developmental transition.

1.2.1 Amoebae

In nature, *P. polycephalum* exists predominantly as haploid amoebae, 10–20 µm in diameter, that move by pseudopodia and feed by phagocytosis on microbes and spores found within their natural soil environment. In favourable conditions, when warmth, humidity and food resources are available, amoebae grow and divide by mitosis to form colonies of identical, haploid cells (Figure 1.1). During amoebal mitosis, the nuclear membrane dissociates resulting in a characteristic ‘open mitosis’ in which asters can be seen at the spindle poles (Figure 1.1; Havercroft & Gull, 1983). If conditions remain favourable, the amoebal density reaches a critical level (Section 1.2.5) at which time compatible, non-identical amoebae fuse and develop into diploid plasmodia (Section 1.2.2; Figure 1.1).

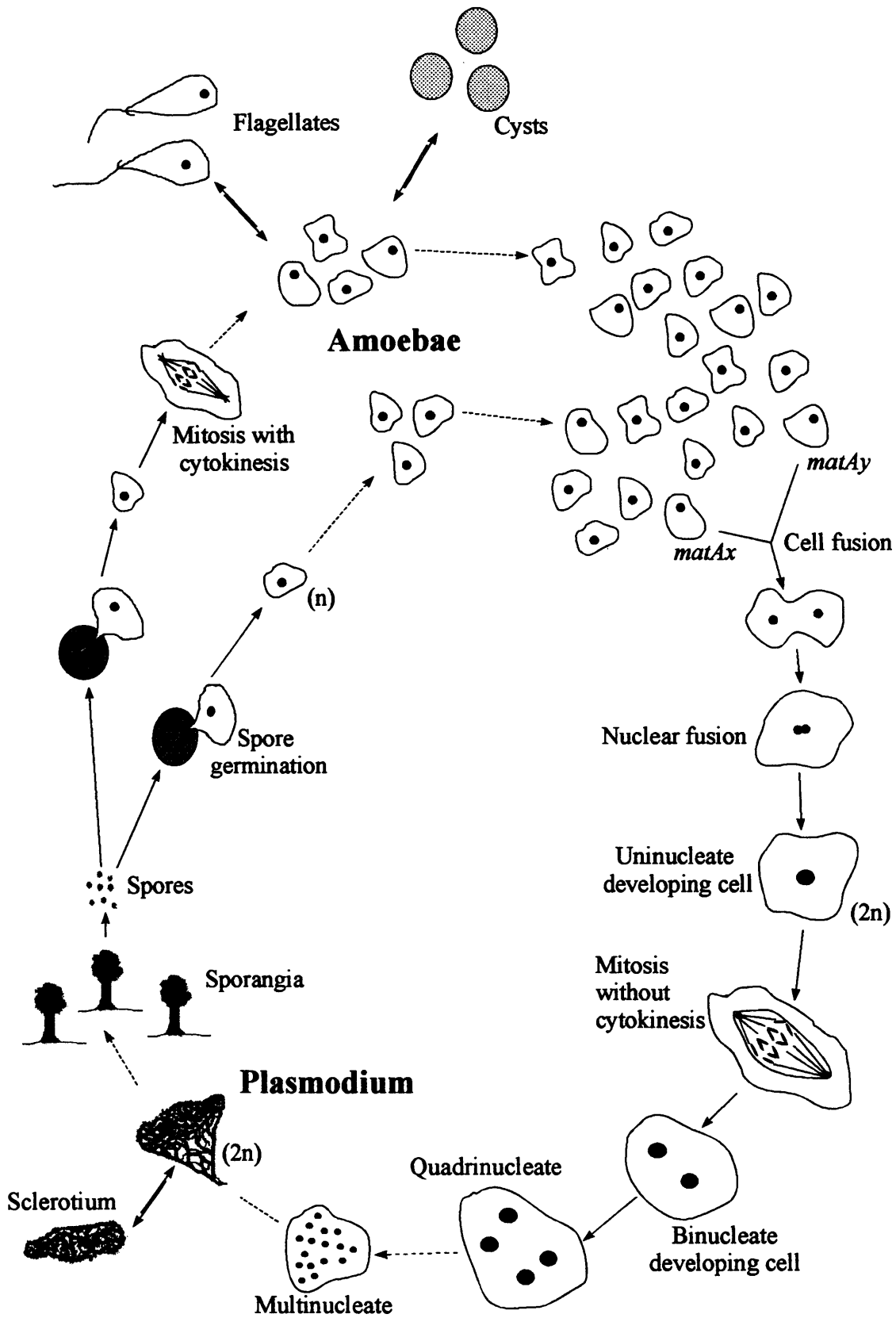
In unfavourable environmental conditions, *P. polycephalum* amoebae are capable of two reversible transitions. When immersed in water, amoebae rapidly undergo a reversible transition into swarm cells or flagellates (Figure 1.1). Amoebae can exist as flagellates for approximately 12 hours but in this form are unable to ingest food by phagocytosis, undergo cell division or fuse with genetically compatible amoebae to initiate development (Wakasugi & Ohta, 1973; Gorman & Wilkins 1980). Since flagellates are unable to feed, if they remain in water for prolonged periods they will eventually die. A flagellate possesses one long and one short flagellum that enable the cell to move rapidly with the flagella foremost, thus enabling it to seek dryer conditions where it reverts to the amoebal form (Wright, 1982). If amoebae starve or are unable to maintain vegetative growth in dryer conditions or prolonged exposure to cool temperatures (<16°C; J. Dee, personal communication), they develop a thickened cell wall to form dormant cysts, from which they are able to germinate as amoebae or flagellates when favourable conditions return

Figure 1.1: The heterothallic life cycle of *Physarum polycephalum*

Uninucleate, haploid (n) amoebae grow and divide by mitosis with cytokinesis to form dense colonies of identical cells. Under the influence of a chemical inducer secreted by the cells (Section 1.2.5) compatible amoebae of different mating-types (*matAx* and *matAy*) become competent to develop into plasmodia; cell fusion of the compatible amoebae is followed by nuclear fusion to generate a developing uninucleate diploid ($2n$) cell (Section 1.2.3). Subsequent rounds of mitosis without cytokinesis result in the formation of a multinucleate, vegetative, diploid syncytium known as a plasmodium (Section 1.2.2). Under the influence of a combination of exposure to light and starvation, the plasmodium develops sporangia. Within the sporangia, individual nuclei undergo meiosis; three of the four meiotic progeny degenerate while the fourth becomes encased as a spore (Section 1.2.2). Each spore germinates to release a single haploid amoeba, which then resumes vegetative growth, as described above.

Under the influence of certain environmental conditions, vegetative amoebae and plasmodia are able to undergo reversible cell transitions. If exposed to excess moisture, amoebae are able to transform into highly motile flagellates (Section 1.2.1). If starved or exposed to non-ambient temperatures, amoebae and plasmodia both develop thickened cell walls to form resilient dormant cells known as cysts (Section 1.2.1) or sclerotia (spherules; Section 1.2.2), respectively.

Figure 1.1



(Figure 1.1; Gorman *et al.*, 1977). Cysts are resilient and can remain dormant for several years, thus providing the cell with a survival strategy to overcome the extremes of winter.

1.2.2 Plasmodia

Wild-type *P. polycephalum* plasmodia are macroscopic, diploid, multinucleate syncytia, although haploid strains have been isolated within the laboratory (Section 1.2.4). They feed by both pinocytosis and phagocytosis on decaying vegetation, such as rotting wood and leaf litter, and the microbes that it harbours, including cannibalisation of any amoebae present. Plasmodia are naturally yellow in colour, although poorly pigmented, near-white mutants have been isolated (Anderson, 1977; Nowak & Stefan, 1997). A plasmodium contains an intricate network of veins through which protoplasmic streaming occurs, both mixing the cellular contents and providing a mechanism for locomotion (reviewed by Hatano, 1994). They are capable of vegetative growth by mitosis without cytokinesis or growth by fusion of individual plasmodia and can cover an area of several square-metres. The nuclei of a plasmodium undergo synchronous mitosis with no subsequent cytokinesis (Havercroft & Gull, 1983). This natural synchrony provides a useful model for studies of events occurring during the mitotic cycle (reviewed by Burland *et al.*, 1993b). Since no cytokinesis occurs, with every cell cycle the number of nuclei and cell volume doubles; a single plasmodium can contain several million nuclei. Unlike amoebal mitosis, the nuclear envelope remains intact and only dissociates at telophase, resulting in a characteristic 'closed', or intranuclear, mitosis in which asters are not visible at the spindle poles (Figure 1.1; Havercroft & Gull, 1983). If the nuclear membrane dissociated prior to this, errors could occur in division involving the spindle apparatus from adjacent nuclei (Havercroft & Gull, 1983).

In *P. polycephalum*, plasmodial fusion is regulated by the fusion genes (*fus*). There are three main *fus* loci: *fusA*, *fusB* and *fusC* (reviewed by Haugli *et al.*, 1980), each possessing two known alleles, although more are likely to exist in natural populations. Additional *fus* loci have recently been identified: *fusD* and *fusE* (Barber, 1998). The two known alleles of *fusA*, *fusA1* and *fusA2*, are co-dominant; plasmodia must carry identical *fusA* loci for plasmodial fusion to occur. In contrast to this, *fusB2* is dominant to *fusB1* and *fusC2* is dominant to *fusC1*; fusion can occur between any plasmodia carrying at least one dominant allele each (e.g. *fusB2/fusB1* with *fusB2/fusB2*) but not between a plasmodium carrying two recessive alleles and one carrying at least one dominant allele (e.g.

fusB1/fusB1 with *fusB2/fusBx*). Laboratory strains are generally isogenic for *fusB*, *fusD* and *fusE* loci. If two or more plasmodia that are compatible at the *fus* loci fuse, a heterokaryon is formed. Sometimes the heterokaryon is unstable and a lethal post-fusion reaction occurs. The primary targets of the lethal interaction are the nuclei. Dominant *let* or *kil* loci cause the destruction of nuclei carrying their recessive counterparts (reviewed by Haugli *et al.*, 1980). Where a heterokaryon is formed in the laboratory between diploid and haploid plasmodia (Section 1.2.4), the diploid nuclei are lost; this suggests that heterokaryon instability might be related to ploidy (Dee & Anderson, 1984). Since haploid plasmodia may not develop in nature, this kind of haploid/diploid heterokaryon instability may only occur in the laboratory.

When a plasmodium encounters unfavourable environmental conditions, it secretes a rigid cell wall to form a dormant, highly dehydrated sclerotium that can remain dormant for several years. Within a sclerotium, clusters of distinct compartments (spherules) are formed, each containing up to 14 nuclei (Gorman & Wilkins, 1980). Like the amoebal cysts, the spherules revert to vegetative growth when favourable conditions return. When a plasmodium is exposed to light and begins to starve, multi-faceted sporangia develop (Figure 1.1). These sporangia appear approximately 10 hours after light induction and mature melanised spore heads form after a further 8 hours (Schreckenbach & Werenskiold, 1986). Within these stalked structures, genetic recombination and meiosis occur; one of the four meiotic products becomes a spore and the remaining three haploid products degenerate (Laane & Haugli, 1976). Spores germinate to release single amoebae, thus completing the life cycle (Figure 1.1).

Physarum plasmodia require humidity, warmth and sufficient nutrients and are, therefore, most prevalent in nature during the early autumn months. In the laboratory, plasmodia can be maintained for only a few months. Prolonged culturing leads to a reduced growth rate and ultimately results in plasmodial senescence or cell death; different strains exhibit varied life expectancies (Poulter, 1969). McCullough *et al.* (1973) correlated an increase in DNA content and nuclear size with plasmodial senescence, while Nakagawa *et al.* (1998) recently implicated mitochondria in plasmodial senescence and suggested that a 7.9kb region of the mitochondrial DNA is necessary for plasmodial longevity. Since there are thousands of nuclei within a plasmodium, certain mutations can accumulate in a small proportion of the nuclei without detrimental effects to the cell. Presumably, once such

mutations are abundant, the cell undergoes senescence. In nature however, the plasmodium would sporulate well before such mutations could accumulate to harmful levels.

1.2.3 Heterothallic plasmodium development

Natural populations of *P. polycephalum* undergo heterothallic, or sexual, development (Figure 1.1). The fusion of two amoebae, which ultimately results in the development of a diploid plasmodium, is under strict genetic control involving three unlinked loci, the most important of which is *matA* (Youngman *et al.*, 1981). Amoebal fusion is influenced by *matB* and *matC*. Amoebae carrying different alleles of *matB* show a 100 to 1000-fold increase in frequency of cell fusions compared with homoallelic populations (Youngman *et al.*, 1981). Allelic difference at *matC* increases the range of pH over which cell fusions occur. When the *matC* alleles carried by amoebae are identical, optimal fusion occurs within the range pH 3.6–5.2. However, when the *matC* alleles are different the upper limit increases from 5.2 to 5.6–6.0 (Kawano *et al.*, 1987b). Since the *matB* and *matC* loci both affect cell fusion, rather than the events occurring after fusion, it is conceivable that they may encode cell surface receptors or pheromones. Sharpe & Goodman (1986) isolated a diffusible factor that is less than 10 kDa in size, from strain MA185 (*matA3 matB3*). This surface modifying factor (SMF; Sharpe & Goodman, 1986) is capable of inducing cell surface changes in strain RSD4 (*matA1 matB1*), which itself does not produce the SMF. Since the SMF molecule is heat stable, Sharpe and Goodman (1986) deduced it is not likely to be a degradation product of the 120 kDa developmental inducer (discussed in Section 1.2.5). Sharpe and Goodman (1986) speculated that SMF may induce cell surface changes that consequently increase the ability of the two cells to fuse. However, it is equally possible that the cell surface changes have no effect on cell fusion.

For nuclear fusion to occur and plasmodium development to be initiated, the two fusing amoebae must differ at *matA* (Figure 1.1; Dee, 1982). If the two alleles of *matA* are identical, the binucleate fusion cell usually splits apart to form two uninucleate, haploid amoebae (Bailey *et al.*, 1990). Occasionally, nuclear fusion occurs during prophase in the *matA* homoallelic binucleate fusion cell and the completion of mitosis generates two uninucleate daughter cells that are presumably diploid and are unable to develop into plasmodia (Bailey *et al.*, 1990). In a few cases, the *matA* homoallelic binucleate fusion cell undergoes mitosis without nuclear fusion giving two binucleate daughter cells, which

have similar fates to the original *matA* homoallelic fusion cells (Bailey *et al.*, 1990). The regulation of plasmodium development by *matA* is discussed further below.

Analysis of different isolates has identified 18 *matA* alleles, 15 *matB* alleles and 3 *matC* alleles (reviewed by Barber, 1998). However, more alleles of *matA*, *matB* and *matC* are considered likely to exist since new *matA* and *matB* alleles are discovered almost every time a natural isolate is brought into the laboratory.

1.2.4 Apogamic plasmodium development

Spontaneous mutations in laboratory strains generated strains of amoebae that could develop into apparently normal, haploid plasmodia. Anderson *et al.* (1976) and Bailey *et al.* (1987) used time-lapse cinematography to analyse development of one such mutant (strain CL) and confirmed the original hypothesis of Von Stosch *et al.* (1964) that the plasmodia developed apogamically (i.e. a single amoeba develops directly into a haploid plasmodium) and not as a result of homothallic development, as proposed by Wheals (1970). The haploid plasmodia formed as a result of apogamic development are able to undergo sporulation and produce viable spores. However, the spore viability is very low when compared to spores formed by diploid plasmodia. The viable spores produced by a haploid plasmodium are presumed to derive from small populations of diploid nuclei found within the plasmodium (Laffler & Dove, 1977).

The locus responsible for apogamic development, *gadA* (greater asexual differentiation) is genetically inseparable from *matA*, but has no effect on mating-type specificity (Shinnick & Holt, 1977; Adler and Holt, 1977). Since the *gadA* mutations are genetically inseparable from *matA*, the relationships of the different mutations cannot be determined by classical genetics and each new *gadA* mutation is therefore assigned a unique *gadA* designation. There are currently 29 known *gad* mutations (Anderson *et al.*, 1989); the mutation *gad-12* shows no linkage to *matA*, however, the remaining *gad* mutations are all tightly linked to *matA* (Adler & Holt, 1977; Anderson & Hutchins, 1986). Many of the *gadA* mutations are temperature sensitive and can be inhibited at 30°C; some are more sensitive to temperature than others and in such strains apogamic plasmodium development can be inhibited at 28°C (e.g. *gadA111*). The strains used for the research described in this thesis are all *matA2 gadAh* and exhibit a substantially lower incidence of

apogamic development when incubated at 30°C than that observed at 26°C (Adler & Holt, 1977).

Apogamic development is suppressed by the *npfB* and *npfC* mutations, which are closely linked to *matA* and *gadA* (Anderson *et al.*, 1989); however, these *npf* mutations have no effect on heterothallic development. Many of the strains used for the research described in this thesis carry the *npfC5* mutation, which is a leaky mutation that is able to 'revert' to a wild-type phenotype at a frequency of approximately 1×10^{-5} (R. Anderson, personal communication; Dee *et al.*, 1989), although the process by which this occurs has not been ascertained. The linkage of *gadA*, *npfB* and *npfC* to *matA* indicates that the *matA* genetic region is complex and has several roles (Anderson *et al.*, 1989; Bailey 1995). It could be a complex of several regulatory genes or a single multi-functional locus; since *matA* has not yet been cloned, this has not been established.

Apogamic strains remain haploid throughout the life cycle and, thus, the phenotypes of recessive genes are observed at all stages of the life-cycle. Apogamic strains can therefore be used to study changes in gene expression throughout the life cycle, without the added complication of changes to the genome resulting from mating. In addition, recessive mutations affecting plasmodium development or growth can be identified. Since *gadA* does not affect mating-type specificity, amoebae from apogamic strains are able to undergo normal heterothallic development; therefore, linkage studies can be performed on any mutations identified. Thus, apogamic strains are useful tools for the analysis of gene function through mutation of random loci or knockout of previously characterised genes; such analyses could help determine the events occurring during plasmodium development.

1.2.5 The timing of events during plasmodium development

During both heterothallic and apogamic development, amoebae undergo a period of vegetative growth and proliferation prior to the formation of plasmodia. By placing a filter between high and low-density populations of amoebae, Youngman *et al.* (1977) demonstrated that dense colonies of amoebae make low-density populations competent to mate or undergo apogamic development. Since the amoebal pseudopodia are unable to pass through the filters used, they concluded that the amoebae produce a diffusible chemical inducer that affects mating competence (Youngman *et al.*, 1977 & 1979).

Further studies suggest that the inducer is a 120 kDa glycoprotein (Shipley & Holt, 1982; Nader *et al.*, 1984); no further characterisation of this molecule has been performed.

Time-lapse cinematography and immunofluorescence microscopy have been used to examine the amoebal-plasmodial transition (APT; Blindt *et al.*, 1986) and the relative timing of events during apogamic and heterothallic development (Bailey *et al.*, 1987 & 1990). During heterothallic development, two genetically compatible amoebae fuse together. Approximately 2 hours later, nuclear fusion occurs to generate a uninucleate, diploid zygote that enters an extended period of growth before mitosis (Bailey *et al.*, 1990). In contrast, there is no amoebal fusion during apogamic development. Instead, the haploid amoeba enters an extended cell cycle that resembles that seen in heterothallic development following cell and nuclear fusion (Bailey *et al.*, 1987). This extended cell cycle is approximately 2.3 times the length of the mean amoebal mitotic cycle and results in a cell that becomes binucleate by mitosis without cytokinesis (Figure 1.2). During the extended cell cycle, growth continues at a constant rate; consequently the resulting binucleate cell is larger than an amoeba following mitosis and has an increased ratio of cytoplasm:DNA (Bailey *et al.*, 1987 & 1990). The extended cell cycle is followed immediately by a short cell cycle, of only 0.7 times the length of the mean amoebal mitotic cycle, which culminates in the formation of a quadrinucleate cell (Figure 1.2; Bailey *et al.*, 1987 & 1990). As a result of the short cell cycle, the ratio of cytoplasm:DNA and the periodicity of mitotic cycles return to levels similar to that found in vegetative amoebae and plasmodia (Bailey *et al.*, 1987 & 1990). Thus, the short cell cycle compensates for the alteration to the ratio of cytoplasm:DNA that occurs during the extended cell cycle (Bailey *et al.*, 1987 & 1990). The binucleate cells that are formed at the end of the extended cell cycle exhibit some plasmodial characteristics, such as the ability to undergo plasmodial fusion and phagocytose amoebae (Bailey *et al.*, 1987 & 1990; Bailey 1995). The extended cell cycle is a critical step in plasmodium development and is the time at which many of the changes to gene expression and cell organisation are initiated; this is discussed further in Sections 1.3 & 1.4.

During the extended cell cycle, the developing cell becomes committed to development (Figure 1.2). Prior to commitment, removal of developing cells from the inducer (see above) allows them to revert to amoebal growth. However, once committed to development, the cells can be removed from the influence of the inducer and will continue

Figure 1.2: Timing of events during the amoebal-plasmodial transition in apogamic strain CL (Adapted from Bailey *et al.*, 1987)

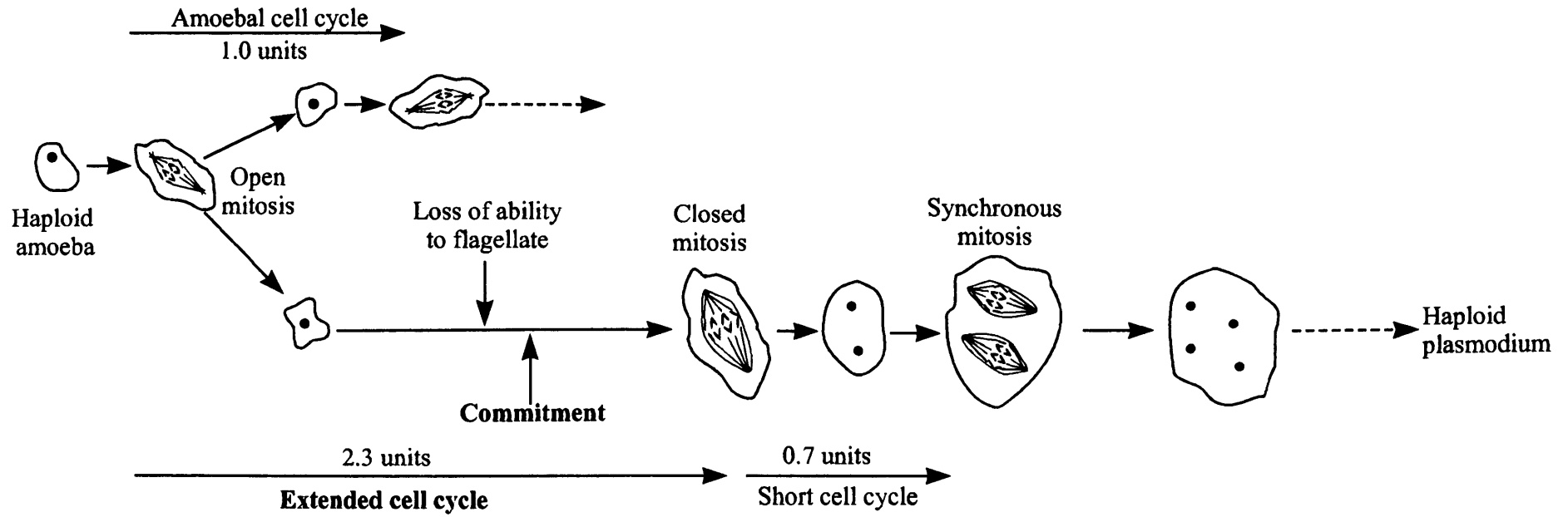
The sequence of events during the amoebal-plasmodial transition was deduced from time-lapse cinematography studies using the apogamic strain CL (Bailey *et al.*, 1987). The mean amoebal cell cycle (11.8 ± 2.2 hours; Bailey *et al.*, 1987) is shown with an arbitrary unit of 1.0; the length of the other cell cycles indicated are shown relative to this arbitrary unit. A mean plasmodial cell cycle is similar in duration to an amoebal cell cycle (Section 1.2.5). The extended (2.3 units) and short cell cycles (0.7 units) are unique to the early stages in plasmodium development (Section 1.2.4); many of the changes to gene expression and cell organisation are initiated during the extended cell cycle (Section 1.4).

The timing of commitment was deduced from replating experiments (Section 1.2.5; Bailey *et al.*, 1987). The loss of ability to flagellate was estimated by comparing the proportions of flagellates and committed cells in developing cultures (Bailey *et al.*, 1987).

‘Open mitosis’ = amoebal mitosis in which asters can be seen clearly at the spindle poles due to dissociation of the nuclear membrane (Section 1.2.1; Havercroft & Gull, 1983); this type of mitosis is accompanied by cytokinesis in *Physarum polycephalum*.

‘Closed mitosis’ = intranuclear plasmodial mitosis in which the nuclear membrane remains intact until telophase and thus asters are not observed (Section 1.2.2; Havercroft & Gull, 1983); this type of mitosis is not accompanied by cytokinesis in *P. polycephalum* and thus leads to the formation of a multinucleate cell.

Figure 1.2



to develop into plasmodia. In both apogamic and heterothallic development, loss of ability to transform into a flagellate occurs around the time of commitment (Blindt *et al.*, 1986; Bailey *et al.*, 1987, 1990 & 1992b) and is believed to be linked to a change in centriole function (Blindt 1987, Bailey *et al.*, 1987 & 1990); centrioles are necessary for flagellate formation and are not found in plasmodia (Wright, 1982; Gull *et al.*, 1985). Once a cell becomes committed to develop, the type of mitosis changes and the centrioles are no longer required.

Commitment in apogamic development was defined using replating assays (Youngman *et al.*, 1977; Burland *et al.*, 1981; Bailey *et al.*, 1987). Briefly, replica plates of plasmodium-free amoebal cultures are incubated at 26°C. At appropriate times, the cells on individual plates are harvested, replated at serial dilutions onto assay plates and then incubated at 26°C or 30°C. The number of amoebal and plasmodial plaques that develop on the assay plates are then noted at regular intervals. These data are plotted against time to determine the relative proportion of plasmodia at different times during the culture period (Youngman *et al.*, 1977). By transferring the developing cell culture to fresh assay plates, the chemical inducer is washed away and only cells that are committed to plasmodium development will generate plasmodial plaques. A committed apogamic cell can thus be defined as a cell that survives replating and continues to develop into a plasmodium. In heterothallic development, commitment is thought to occur between cell and nuclear fusion, up to 20 hours prior to the first plasmodial mitosis that generates a binucleate cell (Bailey *et al.*, 1990). During apogamic development, no cell or nuclear fusion occurs and commitment occurs much closer to the first plasmodial mitosis, up to 13.5 hours earlier (Bailey *et al.*, 1987). Since commitment is an operational definition, it has yet to be ascertained whether an apogamic committed cell is at the same developmental stage as a heterothallic one.

1.3 CELLULAR ORGANISATION AND STRUCTURAL PROTEINS

1.3.1 The tubulin isotypes and microtubule organisation

The differences in mitosis and centriole function described briefly above are just two examples of the vast differences in gene expression, behaviour and organisation that exist between amoebae and plasmodia. Microtubule organisation and tubulin expression have been an area of particular interest in *P. polycephalum* (e.g. Solnica-Krezel *et al.*, 1991; Paul *et al.*, 1992; Havercroft & Gull, 1983; Cunningham & Dove, 1993; Cunningham

et al., 1993; Salles-Passador *et al.*, 1991 & 1992). Microtubules are structural filaments found in most eukaryotic cells that form a major component of the mitotic spindle and function in the cytoplasmic skeleton. Microtubules consist primarily of heterodimers of α - and β -tubulins. In *P. polycephalum* there are three β -tubulin genes and as many as five α -tubulin genes (Schedl *et al.*, 1984a & 1984b). The tubulin isotypes were the first family of developmentally-regulated proteins extensively studied in *Physarum*.

In interphase amoebae, α 1A, α 3, β 1A and β 1B tubulin isotypes can be found within a complex of microtubules radiating from a single cytoplasmic MTOC (reviewed by Burland *et al.*, 1993a). Two centrioles form part of the MTOC of an amoeba, which is located adjacent to the nucleus (Havercroft & Gull, 1983). During mitosis, the MTOC duplicates and divides to give rise to the spindle poles (Salles-Passador *et al.*, 1992). Asters are clearly visible at each pole as a consequence of the disappearance of the nuclear envelope at mitosis (Havercroft & Gull, 1983). The centrioles are retained at the spindle poles but do not act as nucleating centres for the spindle microtubules (Havercroft & Gull, 1983). When amoebae transform into flagellates, the centrioles form the basal bodies of the two flagella and the cytoplasmic microtubules reorganise into 5 microtubular arrays (reviewed by Burland *et al.*, 1993b). Since the nucleus is attached to the MTOC, it comes to lie at the base of the flagella in flagellates. This alternate use of the MTOC may account for the lack of mitosis in flagellates.

Plasmodial microtubules also contain the α 1A and β 1B-tubulins but the amoeba-specific α 3 and β 1A-tubulins are replaced with the plasmodium-specific α 1B, α 2B, and β 2-tubulin isotypes (reviewed by Burland *et al.*, 1993b). Since plasmodia do not transform into flagellates, they do not possess centrioles (Havercroft & Gull, 1983). Although a sparse cytoplasmic microtubule network has been observed within plasmodia during interphase, it is distinct from the nuclei, which show no specific positioning within the cell (Havercroft & Gull, 1983) and is not nucleated by obvious MTOC's (Salles-Passador *et al.*, 1991). The function of such cytoplasmic microtubules in the cytoskeleton and their role in cytoplasmic streaming is unclear (Salles-Passador *et al.*, 1991).

The MTOC necessary for mitosis in plasmodia appears prior to mitosis within the nucleus and is not detectable during interphase. Although Salles-Passador *et al.* (1992) demonstrated that the amoebal and plasmodial MTOC's may share some common constituents, the plasmodial MTOC is generally believed not to be derived from the amoebal MTOC (Gull *et al.*, 1985; Solnica-Krezel *et al.*, 1991). Solnica-Krezel *et al.* (1991) stained cultures of amoebae undergoing the APT with antibodies specific to amoeba-specific $\alpha 3$ -tubulin and plasmodium-specific $\beta 2$ -tubulin. Some cells that contained a MTOC associated with a mitotic spindle typical of plasmodia ($\beta 2$ -tubulin positive and within the nuclear envelope) also contained an $\alpha 3$ -tubulin positive MTOC within the cytoplasm, indicating that the plasmodial MTOC is not derived from the amoebal MTOC (Solnica-Krezel *et al.*, 1991). Gull *et al.* (1985) and Solnica-Krezel *et al.* (1988 & 1991) also demonstrated that most uninucleate developing cells were $\beta 2$ -tubulin positive while most binucleate developing cells were $\alpha 3$ -tubulin negative. Immunolocalisation of $\beta 2$ -tubulin revealed that it begins to accumulate in the APT shortly before mitosis at the end of the extended cell cycle (Solnica-Krezel *et al.*, 1988) and is incorporated into all types of microtubule structures generated during the extended cell cycle, including chimeric (amoebal and plasmodial) and star (MTOC's and chromosomes generally located in the centre of the cell, from where the microtubules radiated) mitotic structures (Solnica-Krezel *et al.*, 1991). Therefore, although the transition from amoebal to plasmodial mitosis is complete by the end of the extended cell cycle, the acquisition of $\beta 2$ -tubulin and loss of $\alpha 3$ -tubulin takes a number of cell cycles and the lack of $\alpha 3$ -tubulin and acquisition of $\beta 2$ -tubulin is not in itself sufficient to bring about the changes to the organisation of microtubules, in particular the mitotic spindles, during the developmental transition.

1.3.2 The actin cytoskeleton and actin-binding proteins

Physarum polycephalum has four unlinked actin loci; *ardA* to *ardD* (Schedl & Dove, 1982; Hamelin *et al.*, 1988). Mendelian analysis of the four loci led Schedl and Dove (1982) to conclude that *ardB*, *ardC* and *ardD* each contain a single actin gene, while the *ardA* locus is more complex and contains at least two actin genes. Southern blotting analysis revealed that the *ardA* locus contains two actin genes, *ardA2-17* and *ardA2-7* (Hamelin *et al.*, 1988), which were subsequently re-named *ardA* and *ardE* respectively (Pallotta *et al.*, 1989). Comparison of the *ardA*, *ardB* and *ardC* sequences revealed that

ardB and *ardC* are approximately 99% homologous, whereas *ardA* shares approximately 93% homology with *ardB* and *ardC* (Hamelin *et al.*, 1988). However, despite these subtle differences, these three genes encode an identical protein (Adam *et al.*, 1991). Analysis of amoeba-specific and plasmodium-specific cDNA libraries suggested that the *ardB* and *ardC* genes encoded the majority of actin transcripts (Hamelin *et al.*, 1988). Northern blotting analysis confirmed that the majority of transcripts were from *ardB* and *ardC*, and revealed that *ardC* transcripts were the most abundant (Hamelin *et al.*, 1988). The relative abundance of the two major actin transcripts was then estimated at 3:1 *ardC*:*ardB* by dot blot analysis and S₁ mapping (Hamelin *et al.*, 1988). The *ardB* and *ardC* transcripts can be detected at all stages of the life cycle (Hamelin *et al.*, 1988); thus, actin provides an ideal internal control for northern blotting analysis. No evidence of *ardA* expression was found from northern blotting (Hamelin *et al.*, 1988). However, using nuclear RNA run-on transcription assays, Arellano *et al.* (1992) found evidence of *ardA* transcription during the late G₂ phase of the cell cycle. Analysis of the deduced *ardD* amino acid sequence revealed 84% identity to the protein encoded by *ardA*, *ardB* and *ardC* (Adam *et al.*, 1991). In contrast to *ardA*, *ardB* and *ardC*, expression of *ardD* is plasmodium-specific and is most abundant in spherules (Section 1.2.2; Adam *et al.*, 1991). The *ardE* locus is highly divergent (Pallotta, personal communication) and northern blotting analysis suggests that it may not be functional (Hamelin *et al.*, 1988).

The actin cytoskeleton is involved in several cellular functions including motility, chemotaxis, cytokinesis, phagocytosis, signal transduction and RNA localisation (Sutherland & Witke, 1999). In *Physarum* plasmodia, actin filaments are organised into two kinds of arrays:

- i. Cytoplasmic fibrils consisting of bundles of actin filaments and myosin (actomyosin), extending throughout the cytoplasmic matrix and vein network (Stockem & Brix; 1994).
- ii. A cortical actin layer consisting of a continuous irregular network of actin filaments found just under the cell surface (Kukulies *et al.*, 1987; Stockem & Brix, 1994).

The cytoplasmic fibrils form a complex network that is involved mainly in the maintenance of cell shape and mediation of cell surface adhesion sites (Stockem & Brix, 1994). The cortical actin layer is more complex and is thickest at the growing edge of plasmodia. The organisation of this layer varies depending on the distance from the

growing edge (reviewed by Stockem & Brix, 1994). In contrast, amoebae do not contain thick bundles of cytoplasmic actin filaments, instead actin filaments are localised beneath the cell membrane to form an irregular layer, located predominantly where pseudopodia form and resembling the cortical actin layer found in plasmodia (Stockem & Brix, 1994). Genetic studies of processes such as cytokinesis in *Physarum* and other systems have contributed to a better understanding of the multi-functional actin cytoskeleton (reviews: Hatano, 1994; Sutherland & Witke, 1999). Although the localisation of actin in plasmodia and amoebae has been characterised (Kukulies *et al.*, 1987; Stockem & Brix, 1994), very little is known about changes to the actin cytoskeleton that occur during plasmodium development in *P. polycephalum*.

Actin exists in two forms: globular-actin (G-actin), the monomeric form of actin, and filamentous actin (F-actin). The two forms of actin exist in an equilibrium that is regulated by actin-binding proteins (Hatano, 1994). Actin-binding proteins were initially thought to play a passive role in preventing polymerisation of actin monomers. Recent studies have shown that actin-binding proteins not only promote actin polymerisation but also regulate the formation of various actin-dependent cell structures, e.g. the contractile ring required for cytokinesis (Sun *et al.*, 1995). The first actin-binding protein to be characterised, profilin, was discovered more than 20 years ago and has been the subject of much research (reviews: Sohn & Goldschmidt-Clermont, 1994; Sun *et al.*, 1995).

Profilin is a small (12–15 kDa) ubiquitous actin monomer binding protein that regulates the polymerisation of G-actin into F-actin and is involved in at least two signal transduction pathways (Sohn & Goldschmidt-Clermont, 1994; Theriot & Mitchison, 1993). Since the concentration of profilin is higher than other actin-binding proteins (with the exception of thymosin- β 4, which is not found in *P. polycephalum*), it is believed to be one of the main regulators of actin polymerisation in non-muscle cells (reviewed by Hatano, 1994). Two profilin genes, *proA* and *proP*, have been identified in *P. polycephalum*, each being specific to only one of the two main cell types; *proA* in amoebae and *proP* in plasmodia (Binette *et al.*, 1990). These two profilins share 66% homology and, like profilins from other eukaryotes, are not as highly conserved as actin (Binette *et al.*, 1990).

Functional studies of profilin in systems such as yeast, *Dictyostelium discoideum*, *Drosophila* and the mouse have confirmed that profilin plays an important role in cell regulation and development (reviews: Sutherland & Witke, 1999; Sohn & Goldschmidt-Clermont, 1994). Using gene-targeting techniques to alter the wild-type profilin gene and introduce a null-mutation in embryonic stem cells, Sutherland and Witke (1999) generated profilin-null mouse embryos. Without functional profilin, these mouse embryos died before they reached the blastocyst stage of development (Sutherland & Witke, 1999). There are two constitutive isoforms of profilin in *D. discoideum*, profilin I and profilin II (Haugwitz *et al.*, 1994). A functional study of profilin in *D. discoideum* found that removal of just one isoform of profilin led to phenotypes virtually indistinguishable from wild-type, whereas removal of both profilin isoforms altered the growth of the cells, led to an increase in F-actin and rendered the cells unable to form fruiting bodies (Haugwitz *et al.*, 1994).

Since the two *P. polycephalum* profilin isoforms are expressed in a cell-type specific manner, it seems unlikely that they could substitute for one another in functional studies such as those performed in *D. discoideum* (Haugwitz *et al.*, 1994). Functional analysis of *proP* in *Physarum* by gene knockout through homologous recombination is in progress, however, no homologous transformant has been identified to date (D. Pallotta, personal communication). Recently, over-expression studies of the two *P. polycephalum* profilin isoforms in profilin-deficient *Saccharomyces cerevisiae* cells has suggested that they are not functionally equivalent (Marcoux *et al.*, 1999). These profilin-deficient yeast cells exhibited reduced mating efficiency, abnormalities in cortical actin localisation, no visible actin cables and no growth at 37°C or in the presence of caffeine (Marcoux *et al.*, 1999). Expression of either *P. polycephalum* profilin isotype restored the cortical actin patches and mating efficiency in the profilin-deficient yeast cells (Marcoux *et al.*, 1999). However, ProA was more effective than ProP at restoring the actin cables and ability to grow at 37°C or in the presence of caffeine (Marcoux *et al.*, 1999). Therefore, since the two *P. polycephalum* profilins do not correct the mutant phenotypes to the same extent, they are not functionally equivalent in yeast (Marcoux *et al.*, 1999); this suggests they do not have identical roles in *P. polycephalum*.

The first actin-severing protein described was gelsolin, isolated from rabbit macrophages (reviews: Hatano, 1994; Matsudaira & Janmey, 1988). Like profilin, the severing proteins

are also able to bind actin monomers. Gelsolin can sever, cap and nucleate (form new filaments from actin monomers) actin filaments in response to different conditions. The action of the molecule is regulated by calcium and polyphosphoinositides such as phosphatidylinositol-4,5-bisphosphate (PIP₂; Meerschaert *et al.*, 1998). When calcium concentrations are high, the gelsolin molecule binds to F-actin and induces cleavage of the filament. The molecule then remains bound to the end of the actin filament, preventing actin polymerisation. This capping activity is reduced in the presence of PIP₂, which binds the gelsolin molecule and dissociates it from the actin filament end (reviewed by Matsudaira & Janmey, 1988). Gelsolin-related molecules have been identified in other systems, including capG or villin in vertebrates and severin or fragmin (discussed in Chapter 6) found in the lower eukaryotes *D. discoideum* and *P. polycephalum*, respectively (reviewed by Matsudaira & Janmey, 1988).

1.4 THE AMOEBAL-PLASMODIAL TRANSITION

Initiation of plasmodium development in *Physarum polycephalum* is regulated by *matA*. The only absolute requirement for heterothallic development in *Physarum* is that the two fusing amoebae possess different alleles of *matA* (Section 1.2.3; Youngman *et al.*, 1981; reviewed by Bailey, 1995 & 1997). In addition, apogamic development can occur if an amoeba carries a *gadA* mutation at *matA* (Section 1.2.4; Shinnick & Holt, 1977; Adler and Holt, 1977). Therefore, *matA* is clearly the most important locus for initiation of plasmodium development. The *matA* region of *P. polycephalum* is multi-functional. Heterothallic development depends on genetic diversity at *matA* and yet apogamic (*gadA*) mutants are able to by-pass this dependence without changing mating-type. The frequency at which apogamic development occurs can be influenced by the *npsB* and *npsC* mutations (Section 1.2.4; Anderson *et al.*, 1989). In addition, *matA* influences uniparental inheritance of mitochondrial DNA (discussed further in Section 1.5). Therefore, *matA* is a multi-functional complex locus that has at least four roles. Studies of the APT may help to ascertain why the *matA* region can influence all these developmental events.

1.4.1 Differentially expressed genes and proteins

Comparisons of 2-D gels of abundant proteins from amoebae and plasmodia indicated that the majority of proteins (74%) were common to both stages of the life cycle but some proteins were cell-type specific (26%), i.e. differentially expressed (Turnock *et al.*, 1981). It was estimated that a quarter of the cell-type specific proteins detected on the 2-D gels

were the result of post-translational modification and were not, therefore, differentially expressed (Turnock *et al.*, 1981). Thus, approximately 20% of the abundant proteins detected were differentially expressed throughout the life cycle.

A logical progression was to investigate differences between amoebae and plasmodia at the level of gene expression (Pallotta *et al.*, 1986; Sweeney *et al.*, 1987). Pallotta *et al.* (1986) generated cDNA libraries from amoebae and plasmodia to compare the mRNA populations of the two cell types. They screened randomly selected clones from the two libraries using dot blots and identified many cell-type specific mRNAs. The majority of these randomly selected clones could not be classified due to weak hybridisation to the probes. In the plasmodial library, 10% of the clones gave a strong plasmodium-specific signal and were classified as representing abundant plasmodium-specific mRNAs. A large class of clones in the plasmodial library (30%) hybridised to both plasmodial-specific and amoebal-specific probes. A further 5.6% of the clones produced a weaker plasmodium-specific signal and probably represented moderately abundant and rare plasmodium-specific transcripts (Pallotta *et al.*, 1986). In the amoebal library, only 2.2% of the clones hybridised specifically to the amoebal probe; the remainder either hybridised to both plasmodial and amoebal probes or could not be classified (Pallotta *et al.*, 1986).

The relative abundance of the most prevalent cell-type specific clones from each library were then categorised based on the frequency of their occurrence in the libraries (Pallotta *et al.*, 1986). The most abundant plasmodium-specific clones corresponded to six sequences, representing 4.8%, 2.4%, 1.4%, 1.0%, 0.4% and 0.2% of the clones in the library (Pallotta *et al.*, 1986). The abundant amoeba-specific clones corresponded to seven different sequences, with one being most prevalent and representing 1.2% of the clones in the library (Pallotta *et al.*, 1986). It is clear from the studies of Turnock *et al.* (1981) and Pallotta *et al.* (1986) that amoebae and plasmodia possess cell-type specific proteins and it was hypothesised that the cDNA clones encoding such proteins, or the proteins themselves, may serve as markers for further analysis of the APT.

Blindt *et al.* (1986) devised a method to enrich for cells committed to plasmodium development by removing cells able to flagellate, since the ability to flagellate is lost prior to commitment in the apogamic strain they used. This involved inducing the

amoeba–flagellate transformation in the cell population and then passing the cells through a glass bead column; the flagellates passed through while the amoebae and developing cells adhered to the beads (Blindt *et al.*, 1986). Sweeney *et al.* (1987) screened cDNA libraries, constructed from populations of axenically grown cells containing different proportions of uninucleate, binucleate and multinucleate cells, which were enriched using the method of Blindt *et al.* (1986), and identified cDNA clones from developmentally–regulated genes. These clones were then used to probe northern blots containing RNA from developing populations of cells enriched for different cell–types, as before, in order to analyse changes in gene expression during the transition (Sweeney *et al.*, 1987). Some plasmodium–specific mRNA transcripts were first detected in populations containing a high proportion of uninucleate committed cells, while others were evident in populations that contained a high proportion of quadrinucleate cells (Sweeney *et al.*, 1987). These results indicated that the changes in gene expression associated with the developmental transition occur over several nuclear divisions (Sweeney *et al.*, 1987). Some amoeba–specific transcripts appeared to remain present for some time after the transition. However, since the enriched cell samples also contained vegetative amoebae, it was unclear at which stage in development the amoeba–specific transcripts were no longer evident (Sweeney *et al.*, 1987).

The transition from production of amoebal to plasmodial proteins and the associated changes in cellular organisation begin during the extended cell cycle of the APT (Figure 1.2; Section 1.2.5). During this developmental transition, α 3–tubulin gradually disappears from β 2–tubulin positive cells (Solnica–Krezel *et al.*, 1991). The timing of α 3–tubulin loss and β 2–tubulin accumulation varies for different developing cells (Solnica–Krezel *et al.*, 1991). In addition, the different types of β 2–tubulin positive spindle apparatus present in developing uninucleate cells demonstrate that the changes to tubulin expression are not sufficient to induce the formation of specific mitotic apparatus and that mitosis occurs irrespective of the changes to the mitotic spindle and cytokinesis (Solnica–Krezel *et al.*, 1991). Solnica–Krezel *et al.* (1991) suggested that the differences in the type of mitosis exhibited at the end of the extended cell cycle could reflect differences in the timing of initiation of development. The complex cytoskeletal and cellular rearrangements that occur when an amoeba develops into a plasmodium are initiated by the mating–type gene, *matA* (Section 1.2).

1.4.2 Developmental mutants characterised by phenotype

Mutagenesis of apogamic strains by exposure to UV light, caffeine, or NMG (*N*-methyl-*N*-nitro-*N*-nitrosoguanidine) has led to the identification of a class of mutants that are unable to undergo normal plasmodium development (Wheals, 1973; Anderson & Dee, 1977; Solnica-Krezel *et al.*, 1995). These were originally termed *apt* (amoebal-plasmodial transition) mutants by Wheals (1973) but the terminology that is more recently favoured is *npf* (no plasmodium formation; Anderson & Dee, 1977) mutants. Analysis of such mutants could determine their functional relationship and may reveal some of the mechanisms involved in the developmental transition (Wheals, 1973). Since the majority of the research described in this thesis is concerned with the characterisation of genes expressed primarily during the APT (Chapters 3 to 5), the *npf* mutants are described in detail below.

The *npf* mutants can be categorised as follows:

- i. Those mapping to *matA* that block the induction of development (*npfB*, *npfC*; Section 1.2.4). The majority of *npf* mutants isolated fall into this category.
- ii. Those that block development during the extended cell cycle.
- iii. Those that block development after the extended cell cycle.

Six recessive *npf* mutants were analysed extensively by Bailey *et al.* (1992a) and Solnica-Krezel *et al.* (1995). These cellular and genetics studies considered each mutation in turn and examined their phenotypes during the developmental transition. Most *npf* mutations affect development of plasmodia and have no effect on amoebal growth, with the exception of *npfM1*, which significantly slows amoebal growth (Solnica-Krezel *et al.*, 1995).

1.4.2.1 The early acting *npf* mutants

The *npfA* and *npfG* mutants are unlinked to the other studied *npf* loci or to *matA* (Solnica-Krezel *et al.*, 1995) and they both block apogamic development early in the extended cell cycle. However, crosses between two *npfA* strains or two *npfG* strains, compatible at *matA* loci, revealed that these alleles are not essential to heterothallic development, since numerous apparently normal plasmodia developed (Solnica-Krezel *et al.*, 1995). Plasmodia form at a frequency of approximately 1 in 10⁵ cells that carry the recessive *npfA1* mutation (Anderson & Dee, 1977). Spores from one such plasmodium were allowed to germinate to determine whether the mutation had reverted to wild-type.

However, since the ability to form plasmodia remained at a low frequency in the progeny, a reversion had not occurred and instead the mutation was described as 'leaky' (Solnica-Krezel *et al.*, 1995). Since only a small proportion of *npfA1* cells were β 2-tubulin positive (higher than could be attributed to the mutation being leaky) and the majority of cells showed no further signs of development and presumably died, Solnica-Krezel *et al.* (1995) concluded that the *npfA*⁺ gene product is required close to the initiation of apogamic plasmodium development.

Cells with the recessive *npfG1* and *npfG2* mutations revert to apparently normal plasmodium development at a frequency of 1 in 10⁶. Although there was evidence from tubulin studies, DAPI (4'-6-diamidino-2-phenylindole) staining and cellular studies that some *npfG* mutants initiated development, the majority of cells showed no evidence of development and presumably died, indicating that, like *npfA*⁺, the *npfG*⁺ gene product is required close to the initiation of apogamic plasmodium development (Solnica-Krezel *et al.*, 1995).

1.4.2.2 The late acting *npf* mutants

The first *npf* mutant, *npfF1*, originally termed *apt-1*, was isolated through mutagenesis of an apogamic strain derived from *Colonia* (Wheals, 1973). This allele was shown to be unlinked to all loci tested, except the plasmodial fusion gene *fusC* (Section 1.2.2; Anderson & Dee, 1977; Bailey *et al.* 1992a; Solnica-Krezel *et al.*, 1995). The recessive *npfF1* mutation affects both apogamic and heterothallic development under all conditions tested. Hardly any binucleate cells develop, although many large, uninucleate cells are observed. Time-lapse cinematography revealed that the developing uninucleate cell enters an extended period of growth, similar to the extended cell cycle, but instead of culminating in the formation of a binucleate cell, the cell usually divided and the daughter cells resumed proliferative growth (Solnica-Krezel *et al.*, 1995). The rare binucleate cells that formed at the end of the extended cell cycle possessed condensed nuclei that suggested they died in an apoptosis-like manner (see below; Solnica-Krezel *et al.*, 1995). Many of the *npfF* cells contained β 2-tubulin and had no detectable α 3-tubulin indicating that some cellular changes had been initiated although development was blocked (Solnica-Krezel *et al.*, 1995). The *npfF*⁺ gene product is therefore believed to play an important role in development towards the end of the extended cell cycle (Solnica-Krezel *et al.*, 1995).

Another recessive mutation that blocks development late in the APT is *npfK* (Solnica-Krezel *et al.*, 1995). The *npfK* gene is linked to the plasmodial fusion gene, *fusA* (Section 1.2.2). Plasmodium development in *npfK* mutants generates multinucleate cells that are unable to fuse with one another. These large cells contain a few hundred nuclei, display rapidly moving pseudopodia but barely any motility and do not develop veins or display the rhythmic pulsations characteristic of plasmodia of a similar size (Solnica-Krezel *et al.*, 1995). Since the abnormalities appear after the extended cell cycle, it was concluded that this is when the *npfK*⁺ gene product is required (Solnica-Krezel *et al.*, 1995). In addition, since the multinucleate *npfK* cells rarely fuse with one another or engulf amoebae and display abnormal pseudopodia along with little or no locomotion, it was suggested that the *npfK*⁺ gene may play an essential role in plasmodial membrane structure (Solnica-Krezel *et al.*, 1995).

In *npfM* mutants, abnormalities are first detected after the extended cell cycle and small multinucleate cells develop; *npfM* is recessive and unlinked to all loci tested (Solnica-Krezel *et al.*, 1995). These multinucleate cells exhibit plasmodia-like morphology but lack the ability to fuse with other plasmodia. They are incapable of phagocytosis and unable to develop into macroscopic plasmodia (Solnica-Krezel *et al.*, 1995). Therefore, as with *npfK*, the *npfM*⁺ gene may affect the plasmodial membrane.

The recessive *npfL* mutation has been the subject of extensive research (Bailey *et al.*, 1992a). Time-lapse cinematography of developing *npfL1* cells (Bailey *et al.*, 1992a) revealed that the abnormalities in cell behaviour and structure caused by *npfL1* appear at the end of the extended cell cycle (Bailey *et al.*, 1992a). Abnormalities in mitotic characteristics suggest that the transition from amoebal to plasmodial nuclear structure is incomplete by the end of the extended cell cycle (Bailey *et al.*, 1992a). However, the *npfL* cells display some apparently normal plasmodial characteristics, such as the ability to ingest passing amoebae and fuse with other developing cells that are still capable of locomotion (Bailey *et al.*, 1992a). The nuclei condense and the cells become rounded and highly vacuolated, exhibiting rapid cytoplasmic activity that resembles the characteristic 'boiling' phenotype observed during apoptosis (Bailey *et al.*, 1992a). The *npfL* mutants possess condensed nuclei similar to those observed in *npfG*, *npfM* and some *npfF* mutants (Solnica-Krezel *et al.*, 1995) and undergo an apoptosis-like cell death (Bailey *et al.*,

1992a). This apparent apoptosis is probably a response to the block in development and not a direct result of the *npf* mutation.

The fact that some aspects of the APT appear normal, while others are abnormal in many of these *npf* mutants suggests that a number of developmental pathways are involved in plasmodium development. Analysis of double mutants could provide evidence to support the existence of such developmental pathways. In *npfK-npfL* double mutants, both mutant phenotypes are observed and therefore neither is dependent on the other suggesting that they probably lie on different developmental pathways. In *npfG-npfF* double mutants, however, only the *npfG* phenotype is observed (Solnica-Krezel *et al.*, 1995). Solnica-Krezel *et al.* (1995) suggested that *npfG* and *npfF* act in the same developmental pathway. However, since it is unclear exactly when cell death occurs in *npfG* mutants, the earlier action of *npfG* may have resulted in cell death prior to the point at which *npfF* expression normally occurs and therefore they may be expressed in different pathways, as with the *npfK-npfL* double mutant.

1.4.3 Regulation of the amoebal-plasmodial transition

Initiation of the APT depends upon the multi-functional *mata* region (see above). It is interesting that many of the *npf* mutations block development during the extended cell cycle, the time at which many of the structural changes are beginning and regulatory genes controlling the transition are believed to function (Bailey, 1995 & 1997). The analysis of *npf* mutants provides further evidence of the importance of the extended cell cycle during the APT. Some of the *npf* mutations may have occurred at loci that are important for the regulation of the developmental transition. There may be several regulatory pathways involved in the APT, as suggested by the study of double mutants containing *npfK1* and *npfL1* (Solnica-Krezel *et al.*, 1995) and the *npfL1* study (Bailey *et al.*, 1992a). It is possible that some genes will function transiently whilst others will be required throughout plasmodium growth.

Dee (1975) speculated that “plasmodial properties are acquired simultaneously by multiple gene activation or inactivation under the influence of regulatory genes”. Similarly, Gorman and Wilkins (1980) hypothesised that “there should exist a set of control genes specific to the transition”. However, it was only during the 1980’s that biochemical and genetic evidence of differential gene expression in amoebae and plasmodia was obtained

(Section 1.4.1; Turnock *et al.*, 1981; Pallotta *et al.*, 1986; Sweeney *et al.*, 1987). Time-lapse cinematography and immunolocalisation studies of plasmodium development in wild-type and the *npf* mutants demonstrated that the extended cell cycle is a critical stage in the APT and is when many of the changes in gene expression and cell organisation are initiated (Sections 1.2.5, 1.3.1 & 1.4.2; Bailey *et al.*, 1987 & 1990; Solnica-Krezel *et al.*, 1991; Bailey *et al.*, 1992a; Solnica-Krezel *et al.*, 1995). These studies led back to the idea that a set of APT-specific regulatory genes exist (Bailey *et al.*, 1992b). Studies to isolate and characterise APT-specific genes form a major part of the research described in this thesis and are discussed in detail in Chapters 3, 4 and 5. Such studies may help to determine the regulatory events occurring during the transition as well as identifying a hierarchy of gene transcription during developmental cascades, such as those proposed as a result of the *npf* studies. Identification and characterisation of these genes could clarify how *matA* initiates plasmodium development and may ultimately lead to a greater understanding of complex developmental processes in other eukaryotic cells (reviewed by Bailey, 1995 & 1997).

1.5 GENOME ORGANISATION

Some procedures involving genomic DNA, e.g. the construction and screening of genomic libraries, are facilitated by an understanding of the organisation of the genome being utilised. Since genomic DNA was used in this thesis, some properties of the *Physarum polycephalum* genome and technical considerations are discussed below.

1.5.1 Chromosomal DNA

Studies on ploidy throughout the life cycle of *P. polycephalum* have generally revealed approximately 40 chromosomes within haploid *P. polycephalum* nuclei although this varies dramatically from one isolate to the next, ranging from 25–75 (reviewed by Mohberg & Babcock, 1982). The variety of chromosome numbers in different strains probably reflects differences in ploidy that have arisen through laboratory culture (Mohberg *et al.*, 1973). The Colonia isolate, from which all strains utilised in this thesis were derived, contains 35–40 chromosomes per haploid nucleus (Mohberg *et al.*, 1973; Mohberg, 1977). Since *P. polycephalum* nuclei possess so many chromosomes, it is no surprise that many gene loci examined to date are unlinked. The DNA content in the haploid unreplicated nucleus is estimated at 0.3pg, which corresponds to approximately 2.7×10^8 bp per haploid genome (reviewed by Burland *et al.*, 1993b).

Studies on the *HpaII*-resistant, methylated fraction of *Physarum* genomic DNA, which represents 4–20% of the genome, identified a large repetitive element whose length was estimated to exceed 5.8kb (Peoples & Hardman, 1983). Further analysis of this element revealed that it forms part of a larger repetitive structure (approximately 8.6kb in size), found in scrambled clusters of up to 50kb, which shares several features with transposable elements (Pearston *et al.*, 1985). This *HpaII*-repeat element was renamed Tp1 (Transposon *Physarum* 1; McCurrach *et al.*, 1990) and contains homologies to the protease, endonuclease, reverse transcriptase and nucleic acid-binding domains of *copia* and other retrotransposons (Rothnie *et al.*, 1991). Although northern blotting analysis suggests that Tp1 is transcribed, no full-length transcript was detected (Rothnie *et al.*, 1991). McCurrach *et al.* (1990) identified a smaller retrotransposon-like sequence within the large scrambled clusters of Tp1, which was named Tp2. Tp2 is much smaller than Tp1, at 1.7kb, and does not contain all components required for independent mobilisation (McCurrach *et al.*, 1990). Retrotransposons contain highly conserved elements, e.g. reverse transcriptase, which can be used to determine evolutionary pathways and aid classification through phylogenetic studies (Rothnie *et al.*, 1991). The Tp elements may be useful for integrative DNA transformation studies, since DNA flanked by such sequences would be targeted for integration by retrotransposition. However, there could be associated problems with stability or multiple integration, since there are numerous target integration sites. In addition, since Tp1 sequences have only been found in association with methylated DNA (Rothnie *et al.*, 1991) there may be problems with the activity of such integrated fragments; since there is generally a negative correlation between methylation and gene activity, DNA inserted at these sites might have reduced or little activity due to *de novo* methylation (Rothnie *et al.*, 1991).

In addition to the methylated repetitive elements described above, moderately repetitive sequences that are A/T-rich are also found in the genome. Kruse *et al.* (1993) examined one such sequence and discovered that certain regions of the element were likely to form secondary structures. Furthermore, the sequence contains a region that is almost identical to a highly conserved 11bp core consensus sequence from autonomously replicating sequence (ARS) elements in yeast that suggested it could be a replicator sequence (Kruse *et al.*, 1993). However, the existence of an interspersed sequence typical of yeast replicator sequences does not prove an involvement in replication. Indeed, replication

origins in *P. polycephalum* have been identified in the promoter regions of *proP*, *ardB* and *ardC* and do not contain any ARS-like sequences (Bénard & Pierron, 1992; Pierron *et al.*, 1999).

Reassociation kinetic analysis by Hardman *et al.* (1980) revealed three sequence components in the nuclear DNA; foldback DNA dispersed approximately once every 7kb (6%), repetitive sequences including the *HpaII*-repeat element (31%) and single-copy sequences (63%). Hardman *et al.* (1980) estimated that as many as 80 families of repetitive elements exist in the *Physarum* genome, spaced on average once every 1300 nucleotides. The single copy sequences encode the majority of genes and are interspersed at regular intervals by the foldback DNA and repetitive elements (Hardman *et al.*, 1980).

Evidence from cloned *P. polycephalum* genes shows that they tend to have several short introns and exons (e.g. Nader *et al.*, 1986; Binette *et al.*, 1990; Hamelin *et al.*, 1988; Kozlowski *et al.*, 1993). Introns in *P. polycephalum* vary from approximately 50bp–300bp in size (e.g. Nader *et al.*, 1986; Binette *et al.*, 1990), but are generally 100bp–150bp. Similarly, exons generally vary from approximately 50bp–350bp (e.g. Nader *et al.*, 1986; Binette *et al.*, 1990). Because the introns and exons are small, the genes are generally small and are not spread over large areas of the genome. In addition, reassociation kinetic analysis of genomic DNA by Hardman *et al.* (1980) indicates that most genes are contained between the foldback DNA and repetitive elements throughout the genome.

1.5.2 Repetitive elements can cause instability of cloned genomic DNA

Repetitive elements in *Physarum* genomic DNA can cause instability in genomic libraries carried by plasmids or phage λ in bacterial hosts (Nader *et al.*, 1985; Nader *et al.*, 1986; Kruse *et al.*, 1993). Kruse *et al.* (1993) encountered problems with cloning an A/T-rich repetitive element. Recombination deficient strains were required and it was suggested that the instability was caused by sequence-specific secondary structures (Kruse *et al.*, 1993). Exonuclease I (*sbcB*) and V (*recBC*) activity in some bacterial hosts results in removal of DNA by recombination between repetitive sequences (Nader *et al.*, 1985). Nader *et al.* (1985) cloned a region of *Physarum* genomic DNA in the proximity of the *ardA* locus and discovered that a region of 360bp, which was subsequently found to contain poly(dT) and poly(dC) homopolymeric sequences (single nucleotide repeats;

Nader *et al.*, 1986), had been deleted. Similar losses were observed by Trzcinska-Danielewicz *et al.* (1996) across poly(dC) homopolymeric regions of the *Ppras1* gene. Using recombination deficient (*recBC⁻*, *sbcB⁻*) bacterial hosts reduced the frequency at which the 360bp *ardA* region was lost from the vector and enabled Nader *et al.* (1985 & 1986) to clone the gene. Nader *et al.* (1986) proposed that the homopolymeric regions were becoming single-stranded (ss) under torsional stresses and that these ss regions were targeted by the endonuclease activity of the *recBC* enzyme, leading to deletion or degradation of the region located between the nucleotide repeats. In addition, Nader *et al.* (1986) suggested the poly(dT) regions might be degraded by exonuclease I (*sbcB*). However, Nader *et al.*, (1986) concluded that the instability of the 360bp *ardA* region may have depended on a particular conformation of several homopolymeric regions, since similar instability was not evident in regions containing single homopolymeric sequences.

Hardman and Jack (1978) estimated that foldback repeats (inverted complimentary repeat sequences) are dispersed approximately once every 7kb throughout the *P. polycephalum* genome; the majority of foldback duplexes are up to 800bp in size. Since foldback repeat structures may resemble intermediates of DNA recombination, they may serve as targets for cleavage by exonucleases I and V and could, therefore, be unstable in *recBC sbcB* hosts (Nader *et al.*, 1986). Restricting DNA fragments for cloning to 7kb or less should reduce the occurrence of such repeats on the same fragment, although the presence of other factors (such as single nucleotide repeats) may also cause instability, in particular with *recA⁺* hosts (Nader *et al.*, 1986).

1.5.3 Ribosomal and mitochondrial DNA

Other well-characterised DNA components from *Physarum* are the ribosomal RNA (rRNA) genes and mitochondrial DNA (mtDNA). In *P. polycephalum*, the rRNA genes are present on 60kb, linear mini-chromosomes (rDNA) found within the nucleolus, at approximately 150 copies per haploid nucleus (Burland *et al.*, 1993b); rDNA constitutes approximately 1–2% of the total DNA content (Hardman & Jack, 1978). The molecule contains two sets of rRNA genes on 13.3kb regions separated by a 23kb non-transcribed spacer containing varied repetitive elements (Burland *et al.*, 1993b). Every rDNA molecule typically replicates once per cell cycle. The complete nucleotide sequences for

the 26s, 5.8s (Otsuka *et al.*, 1983) and 19s rRNA (Johansen *et al.*, 1988) genes have been determined.

Mitochondrial DNA represents 5–10% of cellular DNA from *P. polycephalum* (reviewed by Burland *et al.*, 1993b). The mtDNA is a linear molecule (Sasaki *et al.*, 1994) that has been estimated to vary between 56–86kb in size (reviewed by Burland *et al.*, 1993b). Different strains of *P. polycephalum* carry mtDNA molecules with distinct RFLP (Restriction Fragment Length Polymorphism) patterns. Using RFLP markers, Kawano *et al.* (1987a) demonstrated that mitochondria show uniparental inheritance during heterothallic development. Subsequent studies established that mtDNA inheritance is subject to a linear hierarchy, governed by the *matA* allele carried by the two parent strains (Kawano & Kuroiwa, 1989; Meland *et al.*, 1991). In heterothallic development, the loss of one parental mitochondrial genotype is virtually complete by the second plasmodial mitosis following zygote formation (Meland *et al.*, 1991). Since the mitochondria of one parental type are lost much faster than expected from passive dilution alone, an active process of elimination is thought to be involved (Meland *et al.*, 1991). Presence of the 16kb linear mitochondrial fusion plasmid (Mif; Kawano *et al.*, 1991) results in fusion of mtDNA into larger ‘knotted’ mitochondria (Kawano *et al.*, 1991). On spore germination, these large mitochondria are resolved into smaller mtDNA molecules in which recombination of mtDNA RFLP markers can be observed (Kawano *et al.*, 1991). The Mif plasmid is nearly always inherited by the progeny and, where present, the hierarchical uniparental inheritance of mtDNA is not seen (Kawano *et al.*, 1991).

1.6 DNA TRANSFORMATION IN *PHYSARUM POLYCEPHALUM*

Stable DNA transformation provides a means by which the genome of an organism can be manipulated. This provides the opportunity to examine the function of a gene of interest either by removal of a particular gene’s function, e.g. through homologous gene replacement with an altered copy of the gene (Section 1.6.6) or by mis-expression, e.g. by constitutive expression of a cell-type specific gene.

1.6.1 Development of strains for transformation

Improvements in culture methods and the isolation of strains of amoebae able to grow in liquid, semi-defined or axenic (axe) medium (Dee *et al.*, 1989) allowed easy growth of the high numbers of amoebae required for transformation. Without axenic strains, several

agar plates would be required to grow the number of amoebae required (100mls of axenic culture contains the equivalent number of amoebae as would grow on 100 plates). In addition, the cells grown on plates would need thorough washing to remove the background bacterial cells and agar debris; a procedure which would be both time consuming and problematic.

The early axe strains such as CLd-AXE (CL-derived axenic strain; McCullough *et al.*, 1978) became abnormal in ploidy and development after continuous growth in axenic conditions for several years (reviewed by Dee *et al.*, 1989). The extent to which these abnormalities occur varies from one strain to the next (Dee *et al.*, 1989). The frequency of *npfC* reversion (Section 1.2.4) decreased and the few revertant plasmodia that developed no longer produced viable spores. This led Dee *et al.* (1989) to develop new axenic strains and investigate the stability of such strains after a prolonged period of growth in axenic conditions. Dee *et al.*, (1989) took CLd-AXE amoebae and crossed them with heterothallic strains. The progeny from these crosses were tested for axenic growth properties, inheritance of abnormal characteristics and were classified for known genetic markers, such as *matA*, *fusA* and *whiA*. Several progeny were tested, but one in particular, LU352, grew well in both axenic and monoxenic culture and readily produced *npfC5* revertant plasmodia that were morphologically normal and gave rise to viable spores (Dee *et al.*, 1989). The strains were maintained in axenic conditions for up to sub-culture 28 to assess the growth of the axe strains during “prolonged culture”. The doubling time for LU352 decreased from approximately 55 hours to 25–30 hours over the first 5–10 sub-cultures and then remained at this level (Dee *et al.*, 1989). In addition, DNA content remained haploid. LU352 exhibited a decreased frequency of flagellate formation after prolonged culture and Dee *et al.* (1989) suggested that continuous axenic culture could lead to a complete loss of this transition.

1.6.2 Early transformation studies in *P. polycephalum*

DNA transformation provides a means by which genes can be added or removed from the genome or the expression of genes can be altered. Early attempts at transformation in *Physarum* included treatment with calcium chloride or polyethylene glycol (Haugli & Johansen, 1986); both methods had previously been successfully applied to other systems. Haugli and Johansen (1986) used the aminoglycoside resistance gene (Kan^R) in conjunction with G418 (geneticin) as a selectable marker for their preliminary

transformation experiments. Preliminary results suggested that transformation could be achieved in *P. polycephalum* using both methods, albeit at a low frequency (approximately 10^{-7} ; Haugli & Johansen, 1986). McCurrach *et al.* (1988) compared the efficiency of transformation using the calcium chloride treatment and electroporation techniques with the reporter gene chloramphenicol acetyltransferase (*cat*) under the control of a putative promoter from the *HpaII*-repeat (Tp1; Section 1.5.1). They reported similar levels of *cat* activity for both methods, although Burland *et al.* (1992a) were unable to reproduce their findings, perhaps due to background *cat* activity in the amoebae. Recent advances in transformation techniques in *Physarum* have focussed on electroporation (Burland *et al.*, 1992b; Burland & Bailey, 1995; Burland & Pallotta, 1995).

1.6.3 Promoters and reporter genes

Promoters play a vital role in transformation, without which the reporter gene/selectable marker cannot function. Using several vectors that exhibited *cat* expression in the fission yeast, *Schizosaccharomyces pombe*, but failed to do so in *Physarum polycephalum*, Burland *et al.* (1992a) demonstrated that *P. polycephalum* can only recognise *P. polycephalum* promoter sequences. A similar situation exists for *Dictyostelium discoideum*, this contrasts to some experimental systems, such as the yeast *Saccharomyces cerevisiae*, which are able to utilise promoters from foreign systems.

Two constitutive actin gene promoters from *P. polycephalum*, *PardB* and *PardC*, were tested with the reporter genes *cat* and *luc* (firefly luciferase; Promega Notes) in transient expression studies by Burland *et al.* (1992a) and Bailey *et al.* (1994) respectively. The *ardB* and *ardC* actin transcripts are known to account for most of the actin mRNA found within cells at all stages of the life cycle (approximately 5%; Section 1.3.2; Pallotta *et al.*, 1986) and it was estimated that *ardC* accounted for approximately two-thirds of the mRNA and *ardB* for approximately one-third (Hamelin *et al.*, 1988). Using *cat*-based vectors, Burland *et al.* (1992a) confirmed that *PardC* exhibited higher promoter activity than *PardB*; for this reason, *PardC* is generally favoured for use in *Physarum* transformation studies. Bailey *et al.* (1994) tested *PardC* and *PardB* using *luc* as a reporter and, interestingly, the relative levels of *luc* activity generated by the two promoters were more similar (5:4 respectively) than predicted from previous studies (Hamelin *et al.*, 1988). This may have been due to differences in the vector sequence

immediately downstream of the *luc* gene affecting the stability of the transcript (Section 1.6.8).

The reporter gene, *luc* (Brasier & Ron, 1992; Luehrsen *et al.*, 1997), has been used extensively in transient and stable expression studies under the control of *PardC* to determine the effect of various DNA elements on transcription (Burland *et al.*, 1992b; Bailey *et al.*, 1994). Oxidation of luciferin by luciferase, releases light which can be measured on a luminometer. The luciferin molecule is relatively short lived and therefore provides a good indication of mRNA abundance; the higher the levels of light emitted, the higher the transcriptional activity of the particular element of DNA under investigation. In *Physarum*, luciferase activity from a non-integrated plasmid peaks 2–5 hours after electroporation and drops rapidly thereafter (Bailey *et al.*, 1994). Such a rapid decline in luciferase activity does not occur in other systems, such as mammalian cells, where the luciferase appears to be more stable accumulating for 48–72 hours after transfection (Brasier & Ron, 1992). The rapid decline in *Physarum* is not thought to be associated with plasmid loss at cell division since the level declines faster than that expected for a non-replicating plasmid; it is likely that some active mechanism is responsible for the rapid decline of luciferase expression (Bailey *et al.*, 1994). Protease inhibitors are added to the cell lysate from the transformed *Physarum* cells to stabilise the luciferase sufficiently for an assay to be performed (Bailey *et al.*, 1994). The luciferase assay is simple to perform, reliable and inexpensive. Other reporter genes, such as *cat*, involve costly and time-consuming assays and are often associated with high levels of background activity. Compared to *cat*, the luciferase assay is approximately 100 times more sensitive (Bailey *et al.*, 1994). In addition, the *cat* assay is potentially more hazardous than the *luc* assay, since it involves the use of radiolabelled probes (Burland *et al.*, 1992a). Although the *cat* system was the first reporter gene tested for use in *P. polycephalum* (McCurrach *et al.*, 1988; Burland *et al.*, 1992a), it has been used very little since the *luc* system was developed (Bailey *et al.*, 1994).

1.6.4 Optimisation of electroporation parameters

Electroporation has been widely adopted by researchers for transformation/transfection experiments (reviewed by Lurquin, 1997). When a cell is exposed to an electric field, pores open within the cell membrane. Under the influence of the electrical charge, the negatively-charged DNA outside the cell passes into the cytoplasm through these pores.

Pore formation is reversible and, provided the electrical parameters are not too severe, the cell survives the treatment (Lurquin, 1997).

The optimum conditions required for electroporation vary for each cell system. Several factors are important; for example, the temperature and ionic strength of the medium can affect the electrical resistance, which in turn will affect the current. The size of the cell can affect the electrical field required for membrane poration; generally smaller cells require higher electrical fields (reviewed by Lurquin, 1997). Extensive studies were, therefore, conducted on *P. polycephalum* amoebae to optimise the buffer, temperature, electrical parameters, cell concentration and volume used for electroporation (Burland *et al.*, 1992a & 1992b; Burland & Bailey, 1995). It has not yet been possible to transform plasmodia.

Burland *et al.* (1992a) conducted the early optimisation procedures using the reporter vector *PardC-cat* and the apogamic, axenic strain, LU352 (Section 1.6.1). Several electroporation buffers at different concentrations and pH were tested. The optimum buffer from these studies contained 30mM sucrose buffered by 8–10mM HEPES (*N*-[2-hydroxyethyl]piperazine-*N'*-[2-ethanesulfonic acid]) at pH 8.2 (Burland *et al.*, 1992a).

Once the electroporation buffer had been optimised, other factors affecting the efficiency of electroporation were considered. The optimum temperature and period of incubation of the cells before and after electroporation was established, together with the best cell density and cuvette temperature for electroporation (Burland *et al.*, 1992a). The expression of *cat* was highest when the cells were pre-incubated on ice overnight and then electroporated in a cuvette pre-chilled to 0°C (Burland *et al.*, 1992a). However, the overnight pre-incubation step was impractical and thus a 2-hour period is routinely used (Burland & Bailey, 1995). Immediately following electroporation, optimum expression is obtained if the cells are allowed a recovery period of 20 minutes at 30°C before the axenic medium is added; if the outgrowth temperature is reduced to 26°C (or less) or is increased to 37°C, there is a reduction in the level of expression of *cat* (Burland *et al.*, 1992a). Although Burland *et al.* (1992a) had optimised the electrical parameters for their studies, these are routinely optimised for each new sub-line of axenic amoebae, or once every 10–20 subcultures, to account for cell culture variation.

Further optimisation of buffers was performed by Burland and Bailey (1995) using the reporter gene *luc*. They confirmed that sucrose was the best osmotic stabiliser for the electroporation buffer but found, for their luciferase vectors, that 40mM sucrose was more effective than 30mM sucrose; largely due to differences in the electrical parameters selected for electroporation (Lurquin, 1997). As a result of the optimisation procedures (Burland *et al.*, 1992a; Burland & Bailey, 1995) the efficiency of transformation was improved from 1×10^{-8} to approximately 1×10^{-7} per cell (Burland *et al.*, 1992b).

1.6.5 Selectable markers

To identify individual cells with integrated DNA resulting from transformation, selectable markers are required. Different selectable markers are available that facilitate the isolation of transformant cells. These include nutritional markers, for example leucine or tryptophan requirement in *Saccharomyces cerevisiae* (Zhang *et al.*, 1996), and drug resistance genes such as the antibiotic resistance genes commonly used in plasmid vectors, e.g. ampicillin and tetracycline. *P. polycephalum* is naturally resistant to many drugs that are suitable for use in transformation experiments. This natural resistance is discussed further in Chapter 7.

The hygromycin phosphotransferase gene, *hph* (Gritz & Davies, 1983; Zalacain *et al.*, 1986), confers resistance to hygromycin and has been used under the control of *PardC* for transformation of *P. polycephalum* (e.g. Burland *et al.*, 1992b; Burland *et al.*, 1993a). At concentrations of $50\mu\text{g ml}^{-1}$, approximately 1 in 10^5 amoebae exhibit hygromycin resistance (Burland *et al.*, 1993a). Therefore, the working concentration of hygromycin used for selection of transformants was increased to $100\mu\text{g ml}^{-1}$; at this concentration no spontaneous hygromycin resistance was detected amongst more than 10^{10} amoebae (Burland *et al.*, 1993a). The best frequency of hygromycin-resistant stable transformants was approximately 1×10^{-7} per cell and was obtained following transformation with *PardC-hph* (Burland *et al.* 1992b). With this vector, transformants arising through homologous integration at *PardC* are unlikely to be recovered, since *ardC* is an essential actin gene (Section 1.3.2). Southern blotting analysis demonstrated that each transformant had a single copy of *PardC-hph* integrated at a random site within the genome (Burland *et al.*, 1992b & 1993a). This contrasts to *Dictyostelium discoideum* where multimerisation occurs at the site of integration, leading to an increased copy number (Barth *et al.*, 1998). Genetic analysis of *PardC-hph* transformants in the absence of selection revealed that the

hygromycin resistance is stable through mitosis and can be inherited through meiosis (Burland *et al.*, 1993a).

Transformation in some systems has been shown to be more effective when linear DNA is used instead of circular, for example *Tetrahymena thermophila* (Gaertig *et al.*, 1994). In contrast, other systems exhibit their highest transformation efficiencies when circular plasmids are used, for example *D. discoideum* (Pang *et al.*, 1999; Barth *et al.*, 1998). Therefore, Burland & Pallotta (1995) tested both linear and circular constructs and revealed that, like *T. thermophila*, linear fragments integrate more efficiently in *P. polycephalum*; recovery of *Physarum* transformants from experiments using circular constructs has not been reported to date.

Based on the frequency of transformants generated per cell using the different sized DNA fragments, Burland and Pallotta (1995) concluded “smaller DNA fragments transform *Physarum* amoebae with higher efficiency”. The effect of varying plasmid size from 2.9–12.6kb in *Bacillus subtilis*, on the efficiency of transformation was investigated by Ohse *et al.* (1995). Although the transformation efficiency (transformants per μg DNA) was seen to decrease for larger molecules, the molecular efficiency (transformants per plasmid molecule) remained constant. By adjusting the transformation efficiency figures of Burland and Pallotta (1995) from number of transformants per μg DNA to number of transformants per plasmid molecule, as suggested by Ohse *et al.* (1995), the transformation efficiency for the larger fragment improved from 6.4×10^{-8} to 2.8×10^{-7} ; this is much closer to the efficiency of 1.8×10^{-7} obtained using the smaller fragment.

Recently, Pierron *et al.* (1999) demonstrated that introduced DNA is sometimes only partially integrated following electroporation. Southern blotting analysis indicated that only 2.1kb of an 8.4kb linear plasmid had been integrated and sequence analysis revealed that the *hph* gene was truncated and missing the last 18 amino acids of coding sequence. However, the hygromycin resistance was unaffected (Pierron *et al.*, 1999). Since functional hygromycin resistance must be maintained in order for the amoebae to survive the selection procedure, the *PardC-hph* component of integrated DNA must be integrated. However, additional sequences included in the transformation construct, such as targets for homologous gene replacement (see below), may be lost through such truncation events.

1.6.6 Homologous gene replacement

Homologous gene replacement in *P. polycephalum* was achieved for the plasmodium-specific *ardD* gene (Burland & Pallotta, 1995). The *ardD* gene is the least conserved actin gene in *P. polycephalum* (Section 1.3.2; Adam *et al.*, 1991); thus simplifying northern and Southern blotting analysis of transformants since there would be no cross hybridisation with the other actin genes under stringent hybridisation conditions. The *ardD* gene was also suited to these studies because it is developmentally regulated; exhibiting its highest level of expression in developing spherules, low levels of expression in plasmodia and no detectable expression at any other stage in the life cycle (Adam *et al.*, 1991). Thus, any deleterious effects resulting from the replacement of *ardD* should not affect the amoebae. Burland and Pallotta (1995) utilised a genomic clone (*ardDΔ1*), which contained a “natural” deletion of approximately 1kb across intron 5 and part of exon 6 of *ardD* (Adam *et al.*, 1991), to construct gene knockout vectors. They positioned the selectable marker, *PardC-hph*, either at the 3' end of *ardDΔ1* or within *ardDΔ1*, close to the end of exon 2. This created two vectors for transformation, one in which the homology to the target gene was positioned to one side of the selectable marker and one in which the homology flanked the selectable marker. Electroporation was performed using these two vectors either undigested (circular) or linearised by single or double digestion, which generated different-sized linear fragments for each vector.

Burland and Pallotta (1995) did not recover transformants from experiments using the construct where *PardC-hph* was flanked by *ardDΔ1* sequence. This suggested that this design of vector for transformation of *Physarum polycephalum* might not be effective. However, since this is the only homologous gene knockout study that has been performed for *P. polycephalum*, there is insufficient data to determine which design of vector is the most effective in targeting homologous gene replacement (Burland & Pallotta, 1995). Further studies are required before it is clear which designs are best for stable transformation and homologous gene replacement in *Physarum*. Analysis of 38 independent transformants revealed two independent homologous integration events at *ardD* using the vector where the selectable marker was positioned at the 3' end of *ardDΔ1* (Burland & Pallotta, 1995). Approximately 1 in 20 of the integration events were homologous. Therefore, to be certain that a transformant is generated by homologous recombination, it may be necessary to analyse as many as 60 transformants in future

experiments (95% confidence limit; Burland & Pallotta, 1995). However, since this is the only homologous gene replacement study that has been reported for *P. polycephalum*, this figure may differ significantly from one gene to the next

1.6.7 Stability of introduced DNA and elements used to improve stability of transcripts

Circular plasmids carrying *PardC* are not maintained within amoebae (Burland *et al.*, 1993a; Bailey *et al.*, 1994; Burland & Pallotta, 1995) and one of several explanations for this was a lack of replication origin on the plasmid. However, recent studies by Pierron *et al.* (1999) demonstrated that *PardC* contains an origin of replication that is able to promote early replication within plasmodia, even when integrated into a late-replicating chromosomal fragment. Therefore, since *PardC* contains an active origin of replication, the lack of maintenance of non-integrated plasmid molecules may be due to problems associated with extrachromosomal DNA molecules, such as inability of the amoebae to replicate circular plasmid molecules or active degradation of the plasmid molecule.

Types of sequence known to improve levels of expression in other systems, such as yeast, have been included in vectors for transformation in *Physarum polycephalum* (Burland *et al.*, 1992a; Bailey *et al.*, 1994). These include *TardC*, a transcriptional terminator containing a polyadenylation site located downstream from the *ardC* gene (Burland *et al.*, 1992a), and *AC1-A*, a sequence from *Physarum polycephalum* which contains homology to a budding yeast ARS (Bailey *et al.*, 1994). The *AC1-A* sequence, which confers ARS activity on budding yeast, was shown to display some characteristics expected for enhancer elements in a transient study using luciferase (Bailey *et al.*, 1994).

The transcriptional terminator, *TardC*, had no measurable effect on the activity of *cat* when first tested (Burland *et al.*, 1992a). However, recent experiments using *luc*-based plasmids have indicated that transcription terminates more effectively if *TardC* is included (Hernon, 1996; E. Swanston, unpublished data). *TardC* prevents transcription of *luc* from progressing too far beyond the end of the gene, which can adversely affect the stability of the luciferase transcript. Therefore, since the site of integration in non-transient studies is generally random, it follows that different mRNA transcripts for the *hph* gene may be produced for each unique integration event if *TardC* is not included, which may be detrimental to hygromycin resistance.

1.6.8 Natural suppressers of hygromycin resistance

Burland *et al.* (1993a) demonstrated that the *hph* gene is stable following mitosis and meiosis. Subsequent genetic analysis of the segregation of hygromycin resistance (Hyg^r) amongst progeny derived from crosses of transformant amoebae with non-transformed amoebae indicated that natural suppressers of Hyg^r may exist in *P. polycephalum* (Burland & Pallotta, 1995). Southern blotting analysis provided no evidence of genetic recombination of *PardC-hph* within the progeny that would account for the reduction in Hyg^r (Burland & Pallotta, 1995). Burland and Pallotta (1995) crossed one of the hygromycin sensitive (Hyg^s) progeny, which was shown to contain *hph* by Southern blotting analysis, with a wild-type strain. The progeny from this cross were both Hyg^r and Hyg^s, suggesting that a dominant unlinked suppresser of Hyg^r existed in some strains (Burland & Pallotta, 1995). Such natural suppressers of Hyg^r could complicate transformation studies; therefore, development of other selectable markers may prove useful for future transformation work.

1.7 AIMS

The two vegetative cell types in *Physarum polycephalum*, amoebae and plasmodia, differ in gene expression and cell organisation and are linked by a developmental transition. The complex cytoskeletal and cellular rearrangements that occur during the APT are initiated by the mating-type gene, *matA*. A combination of gene expression, time-lapse cinematography and immunofluorescent microscopy studies have demonstrated that although some aspects of the transition are usually complete by the end of the extended cell cycle (e.g. transfer from amoebal to plasmodial type of mitosis), the acquisition of some plasmodium-specific proteins and loss of amoeba-specific proteins can take a number of cell cycles (e.g. β 2 and α 3-tubulin; Solnica-Krezel *et al.*, 1991). In addition, the timing of protein accumulation and loss varies for different developing cells (Solnica-Krezel *et al.*, 1991). The mixture of abnormal and normal plasmodial characteristics in the *npf* mutants and evidence from the *npfK1* and *npfL1* double mutants suggest that a number of developmental pathways are involved in plasmodium development (Bailey *et al.*, 1992a; Solnica-Krezel *et al.*, 1995). The idea that the APT is controlled by a set of regulatory genes activated by *matA* has been suggested several times within the last 25 years (e.g. Dee, 1975; Gorman & Wilkins, 1980; Sweeney *et al.*, 1987; Bailey *et al.*, 1992b; Bailey 1995 & 1997). Studies to isolate and characterise such genes

form a major part of the research described in this thesis and are discussed in detail in Chapters 3, 4 and 5.

Actin is present at all stages of the life-cycle (Hamelin *et al.* 1988). However, amoebae and plasmodia possess notably different actin localisation and cytoskeletal structures. The various actin-binding regulatory proteins, such as profilin and fragmin, co-operate to regulate the polymerisation of actin and the formation of the various actin-dependent cell structures, e.g. the contractile ring required for cytokinesis (Sun *et al.*, 1995). During the course of the studies described in this thesis, I became involved in some collaborative work to characterise the *P. polycephalum* fragmin gene family; this is described in Chapter 6.

DNA transformation by electroporation has been developed for *Physarum*. Functional analyses by gene knockout or mis-expression studies provide an opportunity to characterise the role of a gene. However, the only selectable marker that has been developed for use in *P. polycephalum* is hygromycin resistance. Development of a second selectable marker would expand the usefulness of transformation, for example by simplifying multiple gene knockout analysis. The final aim of the research described in this thesis was to develop a second selectable marker for use in future transformation studies in *P. polycephalum*; this work is discussed in Chapter 7.

CHAPTER TWO

MATERIALS AND METHODS

CHAPTER 2: MATERIALS AND METHODS

2.1 AMOEBAL CELL CULTURE AND TRANSFORMATION

2.1.1 Gene loci

- matA* mating-type locus affecting initiation of development (Section 1.2.1).
- gadA* greater asexual differentiation mutation, genetically inseparable from *matA*, permitting apogamic development (Section 1.2.2).
- npfC5* no plasmodium formation mutation, genetically inseparable from *matA*, blocks apogamic plasmodium development (Section 1.4.1).
- matB, matC* mating-type loci affecting frequency of amoebal fusion (Section 1.2.1).
- fusA, fusC* Plasmodial fusion loci (Section 1.1.3).
- whiA* Recessive white plasmodial colour gene (*whiA1*; Anderson, 1977). Wild-type, *whiA*⁺, plasmodia are yellow.

2.1.2 Strains

2.1.2.1 *Escherichia coli* (bacterial) strains

- XL1-Blue *recA1 endA1 gyrA96 thi-1 hsdR17 supE44 relA1 lac [F' proAB lacI^q ZAM15 Tn10 (Tet^r)]*
- B145 *thre⁻ leu⁻ thi⁻ his⁻ arg⁻ lac⁻ gal⁻ xyl⁻ mal^{T-} man⁻ str⁻ T1^R T2^S T6^R λ^R colI^R F⁻ (K12)*

2.1.2.2 *Physarum polycephalum* strains

- LU352 *matA2 gadAh npfC5, matB3, matC1, fusA1, fusC1, whiA⁺.*
- CL *matA2 gadAh npfC⁺, matB1, matC1, fusA2, fusC1, whiA⁺.*

2.1.3 Media

(Unless stated otherwise sterile distilled water was used as a solvent for all media and chemicals utilised in the studies described throughout this thesis).

- SDM Semi-defined medium (Blindt *et al.*, 1986).
- SDM-agar 1.5% w/v agar containing 50% v/v SDM (Blindt *et al.*, 1986).
- DSDM Dilute SDM (Blindt *et al.*, 1986). 1.5% w/v agar containing 6.25% v/v SDM.

DSPB	Dilute SDM with phosphate buffer (Dee <i>et al.</i> , 1997). DSDM containing 10mM sodium phosphate buffer, pH 6.8 (Sambrook <i>et al.</i> , 1989).
SDM+PSA	SDM containing 150µg ml ⁻¹ sodium benzyl penicillin (GlaxoWellcome), 250µg ml ⁻¹ streptomycin sulphate (Sigma) and 100µg ml ⁻¹ ampicillin (Sigma).
LB broth	Luria Bertani broth (Sambrook <i>et al.</i> , 1989). 0.5% w/v bacto-peptone (Difco), 0.25% w/v bacto-yeast (Difco), 250mM NaCl, pH 7.0.
LB-agar	LB broth containing 1.5% w/v agar (Sambrook <i>et al.</i> , 1989).
LB-amp	LB-agar containing 100µg ml ⁻¹ ampicillin (Sigma).
LB-tet	LB-agar containing 10 - 100µg ml ⁻¹ tetracycline (Sigma).
SOC broth	2% w/v bacto-tryptone (Difco), 0.5% w/v bacto-yeast (Difco), 8.5mM NaCl, 2.5mM KCl, 10mM MgCl ₂ , 10mM MgSO ₄ , 20mM glucose (Sambrook <i>et al.</i> , 1989).
SBS	Live standard bacterial suspension (Burland <i>et al.</i> , 1981) prepared by washing a lawn of <i>Escherichia coli</i> (strain B145; Leicester University), grown on a 9cm LB-agar plate at 37°C for 16-24 hours, with 5ml of sterile distilled water.
FKB	Formalin-killed bacteria (Dee 1986; Dee <i>et al.</i> , 1997). FKB were used as a food source for culture of amoebae in transformation experiments and for analysis of transformants. Live bacteria are resistant to hygromycin at the concentrations used to aid selection of transformants and would produce false positive results due to inactivation of the drug within the plate. Using FKB for culture of stable transformants was also useful when the transformant strains were transferred back to axenic conditions. A background of live SBS within the axenic culture required treatment with antibiotics and delayed isolation of genomic DNA. Otherwise, SBS was used as a food source for all amoebal culture.

2.1.4 Culture and maintenance of amoebae

Amoebae were cultured from cysts stored frozen in 15% v/v glycerol (Dee, 1986). The frozen stocks were thawed, 20-100µl of the stock was mixed with 100µl of SBS or FKB, as a food source, and then spread to cover a 9cm DSPB plate using a sterile glass spreader. The plate was incubated at 26°C for 1-5 days to allow excystment and enable the culture

to become established. Since LU352 and LU352-based transformant amoebae carry the *npfC5* allele, these amoebae were incubated at 26°C for up to 5 days; the low ‘reversion’ rate of *npfC5* meant plasmodia would rarely form during this period of culture (Section 1.2.4). Strains that carry *npf*⁺ more readily form plasmodia; amoebae of this type only require pre-incubation at 26°C for 24 hours to allow excystment; if *npf*⁺ amoebae are left at 26°C for longer periods, plasmodia will develop.

After incubation at 26°C, the amoebae were incubated at 30°C to block apogamic development into plasmodia (Section 1.2.4). Once confluent, a sterile toothpick was used to sub-culture a small sample of the amoebae into 100µl of bacterial suspension on a fresh DSPB plate. The amoebal/bacterial cell suspension was spread evenly across the plate surface using a sterile glass spreader and the plate was then incubated as described above. Confluent plates were stored at 4°C for periods of up to four months and served as the resource for amoebae used in subsequent experiments, thus preserving the frozen stocks.

2.1.5 Encystment of amoebae for freezer stocks

Amoebal stocks remain viable for longer periods if the amoebae are stored as cysts in frozen stocks (J. Dee, personal communication). Amoebae grown to confluence on DSPB form resistant cysts when their food source is depleted. Since exposure to cold is also known to induce encystment (Dee *et al.*, 1997), confluent plates were incubated at 4°C for 24 hours, to ensure complete encystment. The cysts were harvested from each plate using 3ml of cold (4°C), sterile 15% v/v glycerol, transferred to two 1.5ml sterile, screw-cap cryo-tubes and stored at -80°C (Dee, 1986). Frozen stocks prepared in this way remain viable for several years.

2.1.6 Transfer of amoebae into axenic medium

Confluent amoebae were washed from a 9cm DSPB plate into a sterile, conical-base, screw-cap 15ml polystyrene tube (Sterilin) using 5ml of flagellation buffer (FB; 10mM phosphate buffer, pH 6; Gorman *et al.*, 1977; Sambrook *et al.*, 1989). The amoebae and cysts were pelleted by centrifugation at 400 ×g for 1.5 minutes and the supernatant was discarded to remove excess bacteria, which do not pellet under such low centrifugation. The cells were then resuspended in 3ml of FB and the cell density was determined using a haemocytometer. The tube was transferred to a reciprocating shaker, at room temperature, for up to 4 hours to induce amoebal excystment and flagellation. After 1 hour, and every

30 minutes thereafter, a haemocytometer was used to determine the proportion of flagellates. The cells were transferred to SDM+PSA after 4 hours, or sooner if the proportion of flagellates reached $\geq 50\%$. For the majority of strains used in these studies, the proportion of flagellates did not reach 50% during the 4-hour period. However, if left in FB for a period longer than this, those cells that had become flagellates generally began to die.

The cells were pelleted at $400 \times g$ and were then resuspended in SDM+PSA at cell densities of 5×10^5 for new LU352 axenic cultures or 2×10^5 for stable transformants and 'sub-culture 10' LU352 amoebae (see below), based on the final haemocytometer count; LU352 'sub-culture 10' and LU352-based transformant strains more readily adapt when returned to axenic conditions and therefore a lower starting density of 2×10^5 cells ml^{-1} was used. The cell suspensions were then split into four 1.5ml aliquots, each in a sterile 15ml screw-cap tube, and incubated at $30^\circ C$ on a reciprocating shaker (Dee *et al.*, 1989). Cells were sub-cultured to fresh SDM before the cell density reached 1×10^7 cells ml^{-1} . When actively growing, the amoebae divide once every 24–48 hours resulting in a doubling of cell density. At cell densities exceeding 1×10^7 cells ml^{-1} , amoebae become dormant and can take several weeks to return to active growth (Dee *et al.*, 1997). Once the LU352 amoebae reached sub-culture 15–20, they were cultured in 100ml SDM at $30^\circ C$ using 500ml screw-cap conical flasks, to enable growth of the large number of cells required for transformation.

New LU352 cultures took approximately 10 sub-cultures to show consistent, active growth in axenic conditions. To reduce the time required to establish the amoebae in axenic culture for use in transformation studies, frozen glycerol stocks were made from cultures that had reached sub-culture 10. Once at sub-culture 10, amoebae were plated on 9cm DSPB plates at 5×10^6 cells per plate. These plates were then incubated at $30^\circ C$ for six days to induce encystment. To guarantee viability in the frozen stock and standardise the conditions for re-initiation of axenic culture from the stock (described below), a triton test (Dee *et al.*, 1997) was performed to determine the proportion of cysts; cysts will not stain with trypan blue in the presence of Triton-X100. The cells from one plate were washed into 2ml distilled water and a triton test was performed (Dee *et al.*, 1997). If the proportion of cysts was less than 50%, the plates were maintained at $4^\circ C$ for

a further 48 hours to increase the level of encystment and the triton test was repeated. Once the proportion of cysts was $\geq 50\%$, the remaining plates were used to make frozen stocks of 'sub-culture 10' amoebae (Section 2.1.5).

To return the stock to axenic conditions, the contents of a 1.5ml frozen aliquot were thawed, transferred to a 15ml screw-cap tube and the cells pelleted by centrifugation at $400 \times g$ for 1.5 minutes. The supernatant was discarded and the cell pellet washed once in 1ml FB and then resuspended in 1ml FB. The starting cell density was determined using a haemocytometer and the cells were then transferred to a reciprocating shaker for flagellation and subsequent culture in SDM+PSA as described above.

2.1.7 Transformation of axenically grown LU352 amoebae

Transformation experiments were conducted using a Bio-Rad Gene Pulser™ with pulse controller and 4mm cuvettes (Bio-Rad). Axenically grown amoebae of strain LU352 were prepared for electroporation as described by Bailey *et al.* (1994) with the exception that ultrapure 50mM sucrose, 10mM HEPES (pH 8.2), was used for washing and resuspending the cells. Each transformation was performed using 5×10^7 cells and 1–10 μ g DNA.

Optimum electrical parameters were determined for each new LU352 axenic culture line used in transformation experiments and thereafter at intervals of approximately 6–12 weeks using the luciferase assay (see below). This was necessary in order to maximise the transformation efficiency, since the amoebae changed after prolonged culture in axenic conditions (Section 1.6.1). Therefore, when the cell survival was seen to increase to 70% or more, or a noticeable decrease in luciferase activity was evident, a new optimisation test was performed as below.

2.1.7.1 Optimisation of electrical parameters for electroporation using the luciferase assay

Immediately prior to electroporation, 1 μ g of undigested *pPardC-luc* plasmid DNA (Bailey *et al.*, 1994) was added to each aliquot of 5×10^7 cells. The first aliquot was electroporated using Gene Pulser™ settings of 0.65 kV (voltage), 400 Ω (resistance) and 2.5 μ F (capacitance). The settings were varied for each subsequent aliquot, using voltage increments of 0.05 kV (to a maximum of 0.90 kV) combined with resistance settings of 400, 600, 800 or “ ∞ ” Ω respectively. A negative control was included to determine the

background luciferase activity in the amoebae and was electroporated at 0.65kV, 800 Ω and 2.5 μ F. Each sample was assayed for luciferase activity approximately 2.5 hours after electroporation as described by Burland & Bailey (1995). The optimum electrical parameters were those which resulted in the highest photon (light) emission, as measured over a 30 second period, and allowed approximately 50% cell survival, these parameters were used for subsequent transformation experiments.

2.1.7.2 Transformation of amoebae by electroporation

Transformation experiments were performed using the optimised parameters and included one *pPardC-luc* (positive) and two 'No DNA' (negative) controls. The positive control and one negative control were harvested approximately 2.5 hours after electroporation to confirm the transformation had worked before proceeding with the outgrowth and selective plating as described by Burland & Bailey (1995). Details of the selective plates and vectors used are described in the relevant Chapters (Chapters 5 & 8). The remaining samples, including the second negative control, were transferred to sterile screw-cap conical flasks containing 50ml SDM+PSA and incubated on a reciprocating shaker at 30°C for a 2 day outgrowth period. During the outgrowth period, the surviving cells continued active growth, generally undergoing 2–3 cell divisions. After outgrowth, assuming 50% survival and three cell divisions following transformation, as many as 2×10^8 cells were present.

The cells were counted using a haemocytometer and pelleted by centrifugation at 2500 \times g for 3 minutes. The supernatant was discarded and 600–800 μ l FKB was added to each pellet (plus residual liquid) to produce a final volume of 800 μ l–1ml. Plates used to determine the viable count (VC) were prepared by diluting up to 100 μ l of the negative control sample to approximately 10^3 cells ml⁻¹ in SDM and inoculating 100 μ l (approximately 100 cells) to DSDM with 100 μ l FKB, in duplicate. These VC plates were then incubated as described below. The remaining negative control cell suspension and all other transformation cell suspensions were plated evenly across 4–5 selective plates per sample, corresponding to 150 μ l FKB and a maximum density of 7.5×10^7 amoebae per plate. Based on the reported transformation efficiency of 2×10^{-7} (Burland & Pallotta, 1995), this density of plating was expected to yield 4 colonies per plate.

The selective and VC plates from the electroporation experiments were incubated at 26°C and were inspected for colony growth every 3–4 days. The final VC was determined after 10 days and the selective plates were maintained for 3–4 weeks. The VC was used to determine the percentage of cells surviving electroporation and replating. The VC, together with the luciferase result, gave an indication of the efficiency of transformation. Any colonies appearing on the selective plates were transferred to new selective plates once the colony was approximately 3mm in diameter. This was achieved using a sterile toothpick to ‘streak’ amoebae from the colony across 100µl FKB in the centre of the new plate. In this instance, the amoebal/bacterial suspension was not spread over the entire surface of the plate because cells plated in close proximity to one another grow more efficiently. These plates were incubated at 26°C, until growth was evident and then incubated at 30°C to prevent apogamic plasmodium development. The sub-culture to a second selective plate was included in the transformation experiments to exclude false positives arising as a result of reduced activity of the selective agent in the original plates, thereby reducing the need for laborious Southern analysis to confirm integration of the selectable marker.

Once growth had been established for individual colonies on the second selective plates, the amoebae were sub-cultured onto three DSPB plates with FKB and grown to confluence (Section 2.1.4). Cells from the first plate were used to produce a frozen stock (Section 2.1.5). The second plate was used to provide cells to determine whether apogamic plasmodium development was possible (Section 2.1.8) and then stored at 4°C to provide a convenient contingency stock. The cells from the third plate were grown in axenic conditions for 2–3 weeks and then their genomic DNA was isolated (Section 2.2.1) for Southern blotting analysis.

2.1.8 Induction of apogamic plasmodium development

Transformants, grown to confluence on DSPB plates as described above, were sub-cultured using a sterile toothpick into 100µl SBS on DSDM plates and were then incubated at 26°C until small plasmodia developed; DSDM plates have a pH of 4.8 and are more suitable for growth of plasmodia than DSPB, which have a higher pH of 6.5. Once a plasmodium had grown to 25mm², the block of agar with the plasmodium was excised and transferred to a fresh 9cm SDM agar plate and incubated at 26°C for 3–5 days or until the plasmodium had almost grown to cover the surface of the plate. The

plasmodium was then sub-cultured onto fresh SDM agar by transferring a 1cm² block from the growing edge, as before. The morphologies of the plasmodia were noted throughout this period. Plasmodia can be maintained in this manner for 2–3 months; culture beyond this was avoided in order to minimise the risk of plasmodial senescence (Section 1.2.2).

2.2 ISOLATION OF DNA

2.2.1 Isolation of Genomic DNA from axenically grown amoebae

Genomic DNA was isolated from axenically grown amoebae using a method modified from one devised by D. Pallotta (personal communication). The method is quick and simple, but the DNA isolated is impure and generally contaminated with extranuclear materials. DNA isolated using this method was suitable for Southern blotting analysis. Where genomic DNA was required for cloning, PCR or genome restriction enzyme mapping, a method that yields purer DNA was used (Section 2.2.3).

Cells that had been maintained for at least 2 weeks in axenic conditions were used to prepare four tubes each containing 5×10^5 cells ml⁻¹ and the cells were grown to between 5×10^6 and 1×10^7 cells ml⁻¹, at 30°C, for DNA isolation. The cells were not allowed to grow to stationary phase because actively growing cells generally yielded better quality DNA (personal observation). The cells from the four tubes were pooled and pelleted by centrifugation at 400 ×g for 1.5 minutes. The pellet was washed once in 5ml BSS (basal salt solution; 14mM citric acid, 24mM KH₂PO₄, 4.3mM NaCl, 850µM MgSO₄, 340µM CaCl₂, pH 5.0; Bailey *et al.*, 1994), then resuspended in the residual liquid and gently lysed in 1.5ml of 4M guanidium thiocyanate (filter sterilised) using a sterile pasteur pipette. The cell debris was pelleted by centrifugation at 1400 ×g for 5 minutes and the supernatant was then transferred to a fresh sterile tube. The DNA was precipitated by addition of 3.5ml of ethanol and 150µl of 3M sodium acetate (pH 5.2). The DNA was then pelleted by centrifugation at 1400 ×g for 3 minutes. The pellet was washed with 1ml of 75% v/v ethanol and transferred to a sterile eppendorf tube and re-pelleted using a microfuge at 13800 ×g for 1 minute. The supernatant was removed and the DNA pellet was allowed to dry slightly before resuspension in 400µl of 10mM TE (Tris-HCl, 1mM EDTA, pH 8; Sambrook *et al.* 1989). The DNA was initially treated with 100µg ml⁻¹ RNaseA for 15 minutes at 65°C and then an equal volume of Phenol:Chloroform:Isoamyl

alcohol (P:C:I; 50:49:1 v/v) for 20 minutes with gentle agitation to extract impurities and proteins. The RNaseA/P:C:I-treated mixture was centrifuged at $13800 \times g$ and the aqueous phase transferred to a fresh eppendorf, where the DNA was recovered by ethanol precipitation, as described above. The supernatant was discarded and the DNA pellet was air-dried and resuspended in 50 μ l of sterile distilled water.

2.2.2 Quantification of nucleic acids by spectrophotometry

Spectrophotometric quantification of the DNA was performed using a 1:500 dilution of DNA as described by Sambrook *et al.*, (1989). Briefly, 0.5–1ml of DNA diluted in sterile distilled water was transferred to a 1ml quartz cuvette. Absorbency readings were taken using a Hitachi U-2000 spectrophotometer at wavelengths of 260nm and 280nm against a background reference sample of sterile distilled water. For DNA diluted to 40 μ g ml⁻¹ the absorbency reading at 260nm was 1.0, whilst for RNA, which is single stranded, a reading of 1.0 was obtained when the RNA concentration was 50 μ g ml⁻¹. The purity of the sample was assessed by comparing the absorbencies at 260nm and 280nm. For a pure DNA sample, the absorbency at 260nm was 1.8 times greater than at 280nm, for a pure RNA sample this ratio increased to 2.0. Ratios were often slightly lower than these, due to contamination from proteins, which also absorb light at 280nm and, therefore, reduce the ratio. If a purer sample was required, further P:C:I extractions were performed to remove the contaminating proteins (Section 2.2.1).

2.2.3 Isolation of Genomic DNA for cloning, PCR and restriction mapping

Clean genomic DNA was isolated from microplasmodia, of strains CL or LU352, grown essentially as described by Daniel and Rusch (1961). A 1cm² block of agar, cut from the growing edge of a macroplasmodium on SDM agar (Section 2.2.1), was transferred to 50ml SDM in a 500ml screw-cap conical flask. The plasmodia were incubated on a reciprocating shaker at 26°C or 30°C. The action of the shaker prevented plasmodial fusion, resulting in small or microplasmodia containing several hundreds of nuclei. The culture density was maintained such that large quantities of 'slime' and starvation-induced spherulation were avoided, generally by sub-culturing 2–10ml into 50–100ml fresh SDM every 3–4 days. Microplasmodia were used for genomic DNA isolation because they are easier to harvest than plasmodia grown on SDM agar (macroplasmodia) and grow more rapidly than axenic amoebae. However, microplasmodia were not used for crude genomic DNA isolation (Section 2.2.1) because

they produce large quantities of extracellular protein, including lipopolysaccharides, which are not removed by the single P:C:I extraction.

Genomic DNA was isolated as described by T'Jampens *et al.* (1997). Using this method, intact nuclei were released by gentle homogenisation in nuclear homogenisation solution (NHS; 250mM sucrose, 0.1% v/v Triton X-100, 15mM CaCl₂, 10mM Tris-HCl, pH 7.5). The nuclei were washed once in NHS:percoll (7:2 v/v) and twice in NHS, prior to lysis with 100mM EDTA, 0.5% v/v Triton X-100, 25mM Tris-HCl, pH 8. The percoll creates a gradient which traps the 'slime' at the top and thus separates it from the nuclei. The lysed nuclei were then treated with 100µg ml⁻¹ Proteinase K and 1mg ml⁻¹ DNase-free RNaseA to remove contaminant proteins and RNA. After a series of extractions using phenol, P:C:I and chloroform:isoamyl alcohol (49:1 v/v), the purified genomic DNA was recovered by ethanol precipitation and then washed twice with 75% v/v ethanol. The DNA was resuspended gently in sterile water at 1mg ml⁻¹ (or less) and quantitated spectrophotometrically (Section 2.2.2). To minimise possible damage to the DNA, vortexing was avoided and the DNA was stored at 4°C rather than frozen.

2.2.4 Isolation of plasmid DNA

Frozen stocks of bacterial strains were stored in 10% v/v glycerol at -80°C. A sterile nickel loop was used to inoculate a small sample of bacteria from the top of frozen stocks without thawing, onto 9cm LB-amp or LB-tet plates. By avoiding repeated freeze-thawing of the stocks, they remain viable for longer periods. The plates were incubated overnight at 37°C, individual colonies were then inoculated into 10ml or 100ml LB-broth containing relevant antibiotics and grown overnight using a shaker at 37°C. Plasmid DNA was isolated using Qiagen kits in accordance with the manufacturers instructions (Qiagen, UK).

2.2.5 Rapid isolation of plasmid DNA

Individual colonies, grown on selective media, were inoculated into 1ml LB-broth in an eppendorf tube and to fresh LB-amp plates using a sterile nickel loop. Both the plates and broth were incubated at 37°C overnight. The plates were then stored at 4°C until required. Plasmid DNA was isolated using the 'lysis by boiling method' (Sambrook *et al.* 1989). With this method, the cells in LB-broth were pelleted using a microfuge at maximum speed for 45 seconds. The pellet was resuspended in 100µl of STET buffer

(8% w/v Sucrose, 5% v/v Triton X-100, 50mM EDTA, 50mM Tris, pH8) and 10 μ l of 10mg ml⁻¹ lysozyme. After 2 minutes at ambient room temperature, the tube was transferred to a boiling water bath for 40 seconds and then centrifuged in a microfuge at maximum speed for 10 minutes to pellet the cell debris. Next, 65 μ l of supernatant was transferred to a fresh eppendorf tube containing 65 μ l of Propan-2-ol. The tube was vortexed and placed at -20°C for 10 minutes before recovery of the DNA by centrifugation. The pellet was air-dried and the plasmid insert was then checked by restriction enzyme digestion and gel electrophoresis. Once the desired plasmid was identified, the plate stored at 4°C was used to set up 100ml LB-broth cultures for plasmid isolation (Section 2.2.4).

2.3 VECTOR CONSTRUCTION AND DNA CLONING

2.3.1 Restriction enzyme digestion

Restriction enzyme digestion was performed using Gibco enzymes in accordance with manufacturers instructions, except where stated otherwise (Gibco BRL). Plasmid DNA was digested at 50ng μ l⁻¹ for 1 hour at 37°C. The level of digestion was confirmed by running 200–500ng on a 0.8% agarose gel (Section 2.3.2). If digestion was incomplete, further enzyme was added and incubation was continued overnight at 37°C. Genomic DNA was digested at 25ng μ l⁻¹ overnight at 37°C using a 5 to 10-fold excess of enzyme to ensure complete digestion. For double digestions in which the enzyme buffers were incompatible, the DNA was digested to completion using one of the enzymes, recovered by ethanol precipitation and then digested with the second enzyme. Digested DNA was recovered by precipitation with 2 volumes ethanol and ¹/₁₀ volume 3M Sodium Acetate (pH 5.2) at -20°C for a minimum of 1 hour, followed by a wash with 75% ethanol.

2.3.2 Isolation of DNA fragments

DNA was restriction digested to release the desired fragment(s) (Section 2.3.1). The digested DNA was cleaned by 'P:C:I extraction' (Section 2.2.1) followed by ethanol precipitation. The DNA was resuspended in sterile distilled water and electrophoresed in a 0.8–1.5% w/v agarose gel containing approximately 200ng ml⁻¹ ethidium bromide. All agarose gels were prepared using SeaKem[®] LE or GTG grade agarose (FMC) in 1 \times TBE, (90mM Tris-Cl, 90mM boric acid, 2mM EDTA pH 8; Sambrook *et al.*, 1989). The concentration of agarose used varied depending on the size separation required.

Generally, 0.8% w/v agarose was used, however 1.1% w/v agarose was used to separate plasmid fragments running close together in the range 1kb to 10kb and 1.5% w/v agarose for fragments smaller than 3kb. DNA samples were loaded using $\frac{1}{10}$ volume loading buffer (0.25% w/v bromophenol blue in 40% w/v sucrose; Sambrook *et al.* 1989).

The required fragment or genomic fraction was located using a hand-held UV lamp, in order to minimise risk of UV-induced damage to the DNA, relative to λ *HindIII* and ϕ X174 *HaeIII* DNA size markers (Gibco BRL). The desired fragment or fraction was isolated from the gel using Na45-DEAE cellulose membrane (Schleicher & Schuell Inc.; Sambrook *et al.*, 1989) or by filtration of the section of agarose gel containing the desired fragment(s) through mineral wool. With the latter of these procedures, a small plug of mineral wool was placed loosely into the bottom of an eppendorf tube that had been pierced with a hypodermic needle to create a small hole in the bottom. The section of agarose containing the desired fragment was excised from the gel and then placed on the wool in the eppendorf tube. The eppendorf was positioned at the top of a sterile 15ml polystyrene conical-based tube (Sterilin) and both tubes were then centrifuged at 800 \times g for 15 minutes. The DNA was recovered from the eluate that had collected in the 15ml tube by 'P:C:I extraction' and ethanol precipitation (Section 2.2.1); the DNA pellet was resuspended in water at 0.5 – 1 μ g ml⁻¹. The mineral wool filtration method produces a crude DNA extract but was suited to preparation of size-fractionated genomic DNA, especially where large fractions were prepared. For all plasmid purification and preparation of some small genomic DNA fractions, DEAE membrane was used.

Plasmid fragments were used either as templates for radio-labelled probes (Section 2.4.4) or cloned into a suitable vector (Section 2.3.3). Digested vector molecules were also separated from uncut plasmid in this manner. Genomic fractions were used to construct size-fractionated genomic libraries or for PCR.

2.3.3 DNA ligation

Most plasmids were constructed using pBluescript[®] II (Stratagene). Bluescript II is a convenient high-copy number ColEI-based vector, derived from pUC19, that was designed to simplify commonly used cloning and sequencing procedures. It has the convenience of ampicillin resistance and the *lacZ* blue-white colour selection system. In addition, the multiple cloning site (MCS) contains a series of unique restriction sites that

generate all possible overhangs. This MCS is flanked by T3 and T7 RNA polymerase promoters and sites for several primers, including the universal reverse and M13 -40 primers. In addition to the bacterial ColEI origin, Bluescript II contains the f1(+) filamentous phage origin, which allows recovery of single-stranded phagemids in the presence of helper phage.

Generally, the MCS in pBluescript II provided ample choice of restriction sites and could be digested to generate compatible ends of DNA for cloning. Occasionally, no suitable sites were available, for example when the DNA fragment was derived from PCR. In these instances, a blunt-end generating site such as *EcoRV* was used. During construction of some complex plasmids, blunt-end generating restriction sites were not always available. In such cases, the overhangs on both the vector and insert fragment were removed by DNA polymerase I large (Klenow) fragment (Gibco BRL, UK), which fills 5' overhangs with deoxynucleotide triphosphates (dNTPs) or removes 3' overhangs (Sambrook *et al.*, 1989).

To prevent self-ligation, plasmid vector molecules were treated with shrimp alkaline phosphatase (Amersham Life Sciences) to remove the 5' phosphate group. Reactions were performed for 1 hour at 37°C using 50–100 $\mu\text{g ml}^{-1}$ DNA and an excess of shrimp alkaline phosphatase (1 unit μg^{-1}) in accordance with the manufacturers guidelines. The phosphatase was inactivated by incubation at 65°C for 15 minutes and the DNA was then recovered by 'P:C:I extraction' and ethanol precipitation. The efficiency of phosphatase treatment was determined through self-ligation of 1 μg of treated DNA and compared to ligation of 1 μg vector plus insert. Following transformation to XL1-Blue (Stratagene), as described below, the number of colonies per ligation reaction were compared. Background levels for self-ligation of $\leq 10\%$ compared to vector plus insert were considered acceptable. If self-ligation was $>10\%$, the phosphatase treatment was repeated. High levels of background from the vector were avoided because they would increase the level of screening required to identify single plasmids and, within genomic libraries, would lead to a dramatic decline in insert-bearing vectors following amplification of the library.

Ligation reactions were performed using T4 DNA ligase in 10 μl volumes in accordance with the manufacturers guidelines (Gibco BRL). Three different vector:insert DNA ratios,

based on the DNA concentration ($\mu\text{g ml}^{-1}$), were used; generally 3:1, 1:1 and 1:3. Ligations were incubated at ambient room temperature or 4°C for 24–36 hours. From each 10 μl ligation reaction, 3–5 μl was used to transform *E. coli* XL1–Blue competent cells (Stratagene) as described in Section 2.3.5.

2.3.4 Size–fractionated genomic libraries

Genomic DNA, isolated from CL microplasmodia (Section 2.2.3), was digested to completion and the required fragments were size–fractionated either using DEAE membrane or by mineral wool filtration (Section 2.3.2). A small amount of the digested genomic DNA fraction was used to test three different vector:insert ligation ratios as described above. For each ratio, 18 colonies were selected at random for plasmid isolation (Section 2.2.5). The plasmids were digested to release the insert DNA and the proportion of inserts was determined. The vector:insert ratio that produced plasmids containing a single genomic fragment and gave the highest proportion of inserts was selected for the construction of the library. Where the expected background of self–ligation (approximately 10%) was not observed, this was assumed to be a result of insufficient vector:insert and in these circumstances double inserts were often also observed. Such ratios would lead to loss of genomic inserts either through self–ligation or because of insufficient vector and were, therefore, not selected for construction of the library. If the initial ratios did not yield a sufficient proportion of single inserts, three additional ratios were tested, adjusted as appropriate to alter the deficit or excess of vector DNA.

Once a suitable ratio had been identified, the remainder of the digested genomic DNA fraction was used to prepare multiple 10 μl ligation reactions (Section 2.3.3). After ligation, the reactions were pooled. If the pooled volume was >45 μl , the ligation mixture was ethanol precipitated and resuspended in 30 μl of sterile distilled water to reduce the total number of individual transformations required to 10. The pooled ligation reactions were precipitated, rather than increasing the volume used for each transformation, as there was an increased risk of electrical arcing if volumes higher than 3 μl were used, due to the electrolytes present in the ligation buffer. The entire ligation mixture was used in 3 μl aliquots for transformation to bacteria as described below.

2.3.5 Transformation of bacteria with plasmid DNA

The bacterial host strain XL1-Blue (Stratagene) was used for transformation throughout these studies. XL1-Blue is a recombination deficient strain that supports growth with some vectors and is particularly suited to Bluescript-based plasmids. The strain is recombination deficient (*recA*), which helps to stabilise the insert, especially where repetitive sequences occur, and endonuclease deficient (*endA1*), which improves the quality of plasmid DNA preparations. In addition to this, the *hsdR* mutation protects the inserts from cleavage by the *EcoK* endonuclease system, however, the transfected DNA can still be modified by exonucleases I and V (*sbcB* & *recBC*). It was anticipated that this strain would be sufficiently recombination deficient to improve the stability of *Physarum* genomic DNA fragments.

Competent *E. coli*, strain XL1-Blue, were prepared as described by Miller (1994) and stored in 10% v/v glycerol at -80°C as 200µl aliquots, sufficient for 5 transformations. Electroporation was as described by Miller (1994) with the exception that the shocking chamber and electroporation cuvettes were stored at -20°C before use and the cells were allowed a 1-hour period of outgrowth. A Bio-Rad Gene Pulser™ with pulse controller was used to apply a pulse of 12.5 kV cm⁻¹ (2.5 kV, 25 µF, 200 Ω) across 40µl of competent bacteria plus DNA using 2mm cuvettes (Bio-Rad). The cells were then transferred to 1ml SOC broth for outgrowth at 37°C for 1 hour. In addition to vector alone and vector plus insert ligations, positive (100ng pGEM7Zf+; Promega, UK) and negative (3µl sterile distilled water) controls were included in each bacterial electroporation experiment.

Selective plates (LB-amp or LB-tet) were inoculated with 100µl or 10µl from each experimental sample (two plates for each sample), 200µl from the negative control or 0.01µl from the positive control and incubated at 37°C overnight. For genomic libraries, sterile 50% v/v glycerol was added to the remaining electroporated bacteria to a final concentration of 10% v/v. This suspension was transferred to cryo-tubes in 1ml aliquots, frozen rapidly using a dry-ice/ethanol bath and then stored at -80°C until required. The remainder of other bacterial transformation suspensions were stored at 4°C for re-plating in the event of technical problems. Occasionally, 40µg ml⁻¹ X-gal (5-bromo-4-chloro-3-indolyl-β-D-galactopyranoside) and 0.1mM IPTG (isopropyl-

β -thiogalactopyranoside) were added to the selective plates to aid selection of insert-bearing plasmids. The β -galactosidase activity of the *lacZ* gene is disrupted by insertion of a DNA fragment in the MCS and the cells appear white; without an insert the cells appear blue (Sambrook *et al.*, 1989).

A 10-fold difference in plating volumes for the vector alone and vector plus insert DNA ligations was used to ensure individual colonies could be isolated and to account for individual differences in transformation and ligation efficiencies. If the plating density was too high or low, the plating density was adjusted accordingly using the bacteria stored at 4°C. Since no colonies were expected on the negative control plate, any colonies present indicated the competent cells were contaminated with plasmid DNA and the transformation was therefore repeated. The positive control was included to check the transformation efficiency. Freshly prepared competent cells generally yielded transformation efficiencies of 1×10^9 colonies ml^{-1} , but this declined after prolonged storage at -80°C. To check the efficiency of insert ligation and isolate the desired plasmid, 18 colonies were chosen at random from the selective plates for plasmid isolation (Section 2.2.5).

2.4 ANALYSIS OF NUCLEIC ACIDS

2.4.1 Southern blotting

DNA for Southern blotting was fractionated using 0.8% w/v agarose gels containing approximately 200ng ml^{-1} ethidium bromide. DNA markers (λ *Hind*III and ϕ X174 *Hae*III markers; Gibco BRL) were loaded in the first and last lanes of the gel, at least one lane of the gel was left empty between the markers and the DNA samples to allow easy removal of the markers before blotting. The digested genomic DNA was run at 26V overnight on a gel 20cm in length to ensure complete separation of the fragments. Plasmid DNA was run at 100V for approximately 4 hours. The gels were photographed against a fluorescent ruler using Kodak T_{MAX} 100 film. The fluorescent ruler provided an accurate scale to allow the size of bands to be determined after hybridisation. Lanes containing DNA markers were then cut away from the gel and the section containing the DNA samples was treated with depurinating (250mM HCl), denaturing (1M NaCl, 500mM NaOH) and neutralising (500mM Tris, 3M NaCl, pH 7.5) solutions for 15–20 minutes each as described by Sambrook *et al.* (1989). The DNA was transferred from the gel to

Hybond™-N membrane (Amersham Life Sciences) using the $10 \times$ SSC (1.5M sodium chloride, 150mM sodium citrate; Sambrook *et al.*, 1989) alkaline transfer method described by Sambrook *et al.* (1989). The DNA was fixed to the membrane prior to hybridisation by UV irradiation using an UV Crosslinker (Amersham Life Sciences, UK) with an energy setting of $700 \times 100\mu\text{J cm}^{-2}$.

2.4.2 Northern blotting

Total RNA was isolated from amoebae, plasmodia and developing cells using the method of Chomczynski & Sacchi (1987), with modifications by Puissant & Houdebine (1990). Briefly, the cells were cooled and then lysed in a solution containing 4M guanidium thiocyanate, 25mM sodium citrate, pH 7.0, 0.5% v/v sarcosyl and 100mM β -mercaptoethanol; the guanidium thiocyanate and sodium chloride are both protein denaturants and lyse the cells, β -mercaptoethanol is a potent RNase inhibitor that prevents degradation of the RNA. The RNA was then separated from the DNA by phenol extraction under acidic conditions. This was followed by several washes in 4M lithium chloride to remove contaminant polysaccharides (Puissant & Houdebine, 1990); polysaccharides are soluble in water and have an absorbency in UV light that interferes with the correct quantification of nucleic acids (Puissant & Houdebine, 1990).

Total RNA from crossed microplasmodia (LU648 \times CH508) was isolated using the commercially available RNAzol™ B method (AMS Biotechnology) which was modified to include two lithium chloride washes to remove polysaccharides (Barber, 1998). All RNA samples were quantitated spectrophotometrically (Section 2.2.2) and the integrity of each RNA sample was determined prior to northern blotting by running approximately $3\mu\text{g}$ of denatured RNA on a small $1 \times$ MOPS gel as described below.

The RNA from strain CL undergoing apogamic development was isolated and assayed by Bailey *et al.*, (1992b); the results of this assay are shown in Table 2.1. Briefly, 100 plates each containing 5×10^5 CL amoebae, on initial culture, were harvested for each RNA sample. The cells were harvested from each plate in 5ml sterile distilled water and the total cell density was determined using a haemocytometer. The cell suspension was examined by phase microscopy to determine the number of amoebae and bi- or multinucleate cells. Serial dilutions of the suspension were plated onto fresh DSDM and incubated at 26°C . After 2–3 days, committed cells were seen as small plasmodia

Table 2.1

Sample Code	Amoebae (%)	Uninucleate Developing Cells (%)	Multinucleate Developing Cells (%)	Total Developing Cells (%)
A	100	0	0	0
1%	98.9	1.1	0	1.1
4%	95.9	3.4	0.7	4.1
10%	90.4	9.3	0.3	9.6
11%	89.3	10.4	0.3	10.7
22%	77.9	21.2	0.9	22.1
23%	77.3	18.8	3.9	22.7
38%	62.3	32.5	5.2	37.7
39%	61.0	34.7	4.3	39.0
56%	44.0	46.1	9.9	56.0
Mi	0	0	100	100
Ma	0	0	100	100

Distribution of cell types in CL cultures used for RNA isolation (Bailey *et al.*, 1999)

A: amoebal RNA, 1% - 56%: total percentage of developing cells, Mi: microplasmodia, Ma: macropasmodia.

The percentage of total developing cells was determined using replating assays (Section 1.2.5). The percentage of uninucleate developing cells was determined by subtracting the percentage of multinucleate cells, determined by microscopic analysis, from the percentage of total developing cells.

(plateable plasmodia) and after a further 1–2 days the non-committed cells formed amoebal colonies (Bailey *et al.*, 1987).

The RNA samples used to study expression patterns in heterothallic development were isolated and assayed by Barber (1998) and the results of this assay are shown in Table 2.2. Briefly, flagellates from the mating strains were mixed together in equal proportions and plated as $60 \times 10\mu\text{l}$ spots onto 9cm SM-2 plates (Blindt, 1987) at a density of 3×10^4 cells per spot. For each RNA isolation, 100 plates were prepared and incubated at 26°C until required. At the time of harvest, two plates from each batch of 100 were used to determine the number of plateable plasmodia, as above. The cell suspension was also examined using phase microscopy to determine the number of amoebae, fusion cells, zygotes and multinucleate developing cells present (Barber, 1998).

Northern blots were performed using 10 μg total RNA per sample and 3 μg RNA size markers (Promega, UK). The RNA was denatured at 50°C for 20min in GFM (1.1M glyoxal, 78% v/v formamide, 0.06 \times MOPS). RNA loading buffer (4% v/v formamide, 5% v/v glycerol, 0.1 \times MOPS, 0.0825% w/v xylene cyanol, 0.0025% w/v bromophenol blue) was added to each denatured RNA sample and these were size fractionated in 1.1% w/v agarose made using 1 \times MOPS buffer (20mM MOPS, 5mM sodium acetate, 100 μM EDTA, pH 7) as described by Murray *et al.* (1994). The lane(s) containing the RNA size markers were cut away from the gel and stained for 10 minutes in 1 \times MOPS containing approximately 100ng ml⁻¹ ethidium bromide. A photograph of the markers was taken against a fluorescent ruler using Kodak T_{MAX} 100 film. The remaining RNA was transferred from the unstained gel to Hybond™-N membrane (Amersham Life Sciences, UK) using the 20 \times SSC alkaline transfer method described by Sambrook *et al.* (1989). The RNA was fixed to the membrane by UV irradiation in an UV cross-linker as before.

2.4.3 Colony blots

Bacterial stocks were plated onto 9cm LB-amp plates at a density of 1000–3000 colonies per plate, and incubated overnight at 37°C. An 82mm Hybond-N circle (Amersham Life Sciences, UK) was then placed gently onto the surface of each plate. The filter was pierced using a sterile hypodermic needle to uniquely code the filter and to aid re-orientation later. After 2 minutes, the filter was gently lifted from the surface and placed, colony side up, onto 3MM™ blotting paper to dry. The LB-amp plates were placed

Table 2.2

Sample Code	Amoebae (%)	Fusion Cells (%)	Zygotes (%)	Multinucleate Developing Cells (%)	Total Developing Cells (%)
CH508	100	0	0	0	0
LU648	100	0	0	0	0
2%	97.7	0.8	1.5	0	2.3
4%	95.7	2.1	2.2	0	4.3
17%	82.8	3.7	13.5	0	17.2
24%	76	1.2	14.4	8.4	24
38% [†]	62	4.1	25.7	8.2	38
41% [†]	59	4.9	29.1	7.0	41
Mi	0	0	0	100	100
Ma	0	0	0	100	100

Distribution of cell types in cultures of heterothallic strains used for RNA isolation (Barber, 1998)

CH508 and **LU648**: amoebal RNA, **2%** – **24%**: total percentage of developing cells in cultures derived from LU648 × CH508 (2-strain cultures), **38%**[†] & **41%**[†]: total percentage of developing cells in cultures derived from 10-strain cultures (strains below; Barber, 1998), **Mi**: microplasmodia derived from LU648 × CH508, **Ma**: macroplasmodia derived from LU648 × CH508.

The percentage of fusion cells, zygotes and multinucleate cells was determined by microscopic analysis, the total percentage of developing cells was determined from these figures. Replating assays were also performed and the figures closely resembled those shown here (Barber, 1998).

[†] Derived from 10-strain cultures using strains: CH508 (*matA2*, *matB3*, *matC2*); LU648 (*matA1*, *matB1*, *matC1*); DP14 (*matA7*, *matB7*, *matC6*); DP15 (*matA8*, *matB8*); DP74 (*matA12*, *matB5*); DP75 (*matA11*, *matB6*); DP89 (*matA15*, *matB12*, *matC5*); DP90 (*matA16*, *matB13*, *matC4*); PpII1.17-100 (*matA5*, *matB10*); PpII1.17-80 (*matA6*, *matB11*).

at 37°C for a 4–6 hour recovery period to allow re-growth of the colonies, before being stored at 4°C.

Once dry, the Hybond-N filters were transferred, colony side up, onto a double thickness of filter paper soaked with denaturing solution (0.5N NaOH, 1.5M NaCl) for 7 minutes. They were then moved to filter paper soaked in neutralising solution (1.5M NaCl, 0.5M TRIS-HCl, pH 7.4) for 3 minutes. The neutralising step was repeated before the filters were washed in $2 \times$ SSC to remove cellular debris and dried, colony side up, on dry 3MM paper. The DNA was fixed to the membrane by UV irradiation. The filters were then hybridised with the appropriate radiolabelled probe (Section 2.4.4) and, following exposure, the position of each filter and orientation marks were clearly marked on the X-ray film. The film was then laid on an illumination box and positive 'spots' on the film were aligned with colonies on the plates using the orientation marks for reference. These positive colonies were inoculated individually to LB-broth for plasmid isolation (Section 2.2.4). The integrity of the plasmid DNA was then confirmed by restriction digestion.

2.4.4 Radioactive-labelling of probes

Radio-labelled DNA probes were synthesised by the random primer method of Feinberg & Vogelstein (1983) using DNA fragments isolated as described in Section 2.3.2. A Klenow reaction in the presence of 200–500ng of DNA template (Section 2.3.2), 10mCi ml^{-1} $\alpha\text{-P}^{32}$ dCTP, 1.5–2.5mM dNTPs (excluding dCTP; Pharmacia) and 0.8–1.4 OD units of hexa-deoxyribonucleotides (Pharmacia) was used to generate P^{32} -labelled probe fragments. Unincorporated P^{32} -dCTP and small labelled fragments, which would produce background hybridisation, were removed by ethanol precipitation in the presence of 90 μg unshered salmon sperm DNA (Sigma). The resulting pellet was resuspended in 500 μl sterile distilled water and heat denatured for 5 minutes in a boiling water bath followed by rapid cooling on ice prior to hybridisation.

Hybridisation was performed in 0.5M Na_2HPO_4 (pH 7.5), 1mM EDTA, 7% w/v SDS using approximately 0.2ml cm^{-2} of membrane in a rotisserie dual hybridisation oven (Hybaid). The blot was incubated at 65°C (or 50–55°C for lower stringency probing) in the hybridisation solution for a period of 2–6 hours prior to the addition of the

radio-labelled probe. The denatured probe was then added and incubation was continued for a further 18 hours. Two 10-minute post-hybridisation washes were performed at the hybridisation temperature for each wash solution using approximately 1 ml cm⁻² of 0.2M Na₂HPO₄ (pH 7.5), 1% w/v SDS and then 0.1M Na₂HPO₄ (pH 7.5), 1% w/v SDS (based on Church & Gilbert, 1984). If background hybridisation was high following the fourth wash, an additional 10-minute wash was performed using 0.04M Na₂HPO₄ (pH 7.5), 1% w/v SDS.

The filter was then covered with saran wrap and exposed to X-ray film (Fuji RX) in the presence of a SMIT rapid intensifying screen at -80°C for up to 3 weeks. The exposure time required was assessed using a hand-held Geiger counter. Generally, the blot was exposed for an initial period of 24-72 hours if the signal was strong (<50 cps) or 1-3 weeks if the signal was low (>50 cps). Where the signal was strong and the initial exposure resulted in saturation of the film, a second shorter exposure was performed; where the film was under-exposed a second longer exposure was performed. So that blots could be re-probed after the exposures were complete, radioactive probes and background activity were removed using boiling 1% w/v SDS as described by Sambrook *et al.* (1989). The blots were treated this way and re-used in further hybridisations up to four times.

2.4.5 DNA sequence analysis and primer design

Sequencing reactions were performed manually or using an 'in-house' automated sequencing facility with an Applied Biosystems, 337 or 337XL ABI automated sequencer (Protein and Nucleic Acids Laboratory; PNAACL, Leicester University). Manual sequencing was performed using a T7 DNA polymerase Sequenase Version 2.0 kit in accordance with the manufacturers instructions (Pharmacia) together with the Sequagel™ sequencing acrylamide gel system (National Diagnostic) and BioRad sequencing apparatus. Sequencing gels were run in 1.1 × TBE at a constant temperature of 50°C for 2-6 hours and gels were dried onto 3MM blotting paper using a vacuum gel dryer (BioRad). The gel was exposed to X-ray film (Fuji RX) without an intensifying screen at ambient room temperature for up to 3 weeks.

The sequence analysis and primer design utilised the Wisconsin Package, Genetics Computer Group (GCG; Madison, USA) on the Leicester University mainframe computer.

Databases comparisons were performed using the BLAST, FASTA, and TFASTA programs.

All primers were designed with 17–22 nucleotides homology to the sequence of interest and melting temperatures (T_m) of 50–55°C, this generally correlated to approximately 50% G–C content. Keeping the T_m over a narrow range ensured primer combinations would anneal in standardised conditions and reduced potential problems resulting from primer dimerisation. Primers were synthesised using an ABI 394 DNA synthesiser (Perkin Elmer) at a concentration of 40nM by PNACL (Leicester University). The primers were recovered by precipitation with one volume propan–2–ol overnight at –20°C followed by centrifugation in a microfuge at 13800 ×g for 10 minutes; the pellet was resuspended in 100µl sterile distilled water. The primer concentration was determined after spectrophotometric analysis (Section 2.2.2) using molar extinction coefficients in the following calculation, where A_n , T_n , G_n and C_n are the number of respective bases in the sequence.

$$\text{Concentration (mM)} = \frac{\text{OD}_{260} \times \text{dilution}}{(A_n \times 15.4) + (T_n \times 8.8) + (G_n \times 11.7) + (C_n \times 7.7)}$$

2.4.6 Polymerase Chain Reaction (PCR)

DNA polymerases synthesise DNA in the 5' to 3' direction using a single–stranded template starting from a region that is double–stranded. In PCR, DNA polymerase is used to amplify a region of DNA between two primers that are complementary to opposite strands of the DNA. The template is denatured and allowed to anneal in the presence of an excess of primers. Since the primers are in excess, they anneal to the template preferentially and the action of the DNA polymerase leads to synthesis of a new strand from the 3' end of the primer. Several cycles result in an exponential synthesis of the region of DNA flanked by the two primers. Several factors can affect the efficiency of PCR, these are discussed in Chapter 4 (reviewed by McPherson *et al.* 1991 & 1995).

PCR cycles were performed using an OmnE[®] Hybaid thermal cycler (Hybaid). Generally, 50µl reactions were set up in 0.5ml eppendorf tubes using 50mM KCl, 10mM Tris–Cl (pH 8.4), 1.5mM MgCl₂, 150mM dNTPs, 200nM primers, 8µg ml⁻¹ plasmid DNA or 20µg ml⁻¹ genomic DNA template and 1 unit *Taq* DNA polymerase I (5units µl⁻¹;

Applied Biosystems). Where genomic DNA was utilised as a template, the PCR reactions were prepared using 0.5–1.0µg of DNA. This ensured that sufficient copies of the gene were present for effective PCR, since the *Physarum* genome is comparatively large at 2.7×10^8 bp (Burland *et al.*, 1993b), and also compensated for problems associated with the structural complexity of the DNA. Control reactions were included in all PCR experiments. Negative controls were used to determine whether the primers were contaminated and generally included the primer pair without a DNA template and single primer:template reactions. Positive controls were set up using the primer pair and $8\mu\text{g ml}^{-1}$ cDNA plasmid as a template to confirm the enzymatic activity of the polymerase and primer viability.

Thermal cycles included denaturing, annealing and extension steps. The denaturing step (94°C) separated the double-stranded DNA template strands, the annealing step (50–53°C) enabled the primers to bind to the single-stranded DNA template and the extension step (70°C or 72°C) was optimal for strand synthesis by *TaqI* DNA polymerase. An additional final prolonged extension step at 72°C or 77°C was sometimes included (McPherson *et al.*, 1991 & 1995). It is generally recommended that a 1-minute extension period is allowed for each 1kb of DNA to be amplified, although *TaqI* DNA polymerase actually transcribes at 2–4kb per minute (McPherson *et al.*, 1995). Therefore, for amplification of large fragments, the extension period was increased accordingly (e.g. Program 2, see below). The thermal cycle programs used in these studies were as follows:

Program 1:

94°C 40 seconds }
 53 °C 1 minute } × 25 cycles
 72 °C 1 minute }
 72 °C 15 minutes

Program 2:

94°C 40 seconds }
 53 °C 1 minute } × 25 cycles
 72 °C 4 minutes }
 72 °C 15 minutes

Program 3:

94°C 30 seconds }
 50 °C 30 seconds } × 25 cycles
 70 °C 2 minutes }

Program 4:

94°C 1 minute }
 53 °C 1.5 minutes } × 40 cycles
 72 °C 3 minutes }
 77 °C 15 minutes

CHAPTER THREE

IDENTIFICATION AND SEQUENCE

ANALYSIS OF *RED* GENE cDNAS

CHAPTER 3: IDENTIFICATION AND SEQUENCE ANALYSIS OF *RED* GENE cDNAS.

3.1 INTRODUCTION

As discussed in Chapter 1, although it is possible that the mating-type gene *matA* directly regulates all the genes involved in the amoebal-plasmodial transition (APT), it is more likely that *matA* initiates a cascade of gene transcription, which concludes with the formation of a plasmodium. The phenotypes of strains carrying mutations in the late acting *npf* genes, such as *npfK1* and *npfL1*, suggest that they probably act towards the end of any such cascade (Section 1.4.1). A cascade of gene function within the early oocyte of *Drosophila* establishes morphogenic gradients of transcription factors (e.g. the homeobox containing transcription factors) that regulate the expression of the zygotic segmentation genes. This induces a second regulatory cascade that ultimately subdivides the embryo. As these early oocyte genes are only required to establish the expression of more stable genes, such as the homeotic genes, their expression is short and transient (Tautz & Schmid, 1998). It is possible that similar genes function transiently during the developmental transition in *Physarum polycephalum*.

Bailey *et al.* (1992b) sought to clone and analyse genes expressed at highest levels during the APT by screening a cDNA library that they constructed from a culture containing a high proportion of developing cells. The culture used to construct the library contained 46% uninucleate committed cells, 10% multinucleate cells and 44% amoebae (Bailey *et al.*, 1992b & 1999). Since the library would contain cDNAs from constitutively-expressed, amoeba-specific and plasmodium-specific genes, it was subtracted against poly(A)⁺ RNA from amoebae and plasmodia to enrich for genes expressed at high levels during the developmental transition. A detailed description of the construction of the cDNA library was published (Bailey *et al.*, 1999). However, since this library and clones derived from it have been used extensively during the course of these studies, this process is summarised below.

3.1.1 cDNA library design and construction

An oligo (dT) column was used to purify poly(A)⁺ RNA from total RNA, isolated from the developing cell culture. The poly(A)⁺ RNA was then used as a template for cDNA synthesis with RNase H-free Moloney Murine Leukaemia Virus Reverse Transcriptase

and the Oligo(dT)₁₅ *NotI* primer (Promega). Second strand synthesis was performed with DNA polymerase in the presence of RNase H, to remove the original poly(A)⁺ RNA template, dNTPs, DNA ligase and P³² α-dCTP. The population of cDNA molecules were then phosphorylated (phosphate groups added) with T4 Kinase, treated with T4 DNA polymerase to generate blunt-ends and size-fractionated to remove molecules smaller than 500bp. Transcripts smaller than 500bp were removed from the cDNA library since, with the occasional exception (e.g. haemagglutinin I; Mortia, 1998), *Physarum* mRNA molecules are rarely smaller than this. It is considered that the majority of cDNAs smaller than 500bp were the product of incomplete reverse transcription of the poly(A)⁺ RNA during the library construction.

Next, *EcoRI* adapters were added to the blunt-ended cDNAs using T4 DNA ligase and these cDNAs were phosphorylated with T4 kinase. Restriction digestion was performed using *NotI*, which cut within the Oligo(dT)₁₅ primer sequence at the poly(A)⁺ end of the cDNA. A spin column was used to remove the cut primer ends and excess adapters from the cDNAs, which were then ligated to pBluescript II KS⁻ (Stratagene) prepared with *NotI*-*EcoRI* cloning ends. The resulting plasmids were transformed to XL1-Blue to generate the cDNA library ML8 (Madison Library 8). This primary cDNA library consisted of 1×10^7 phagemid-carrying cells, approximately 95% of which contained cDNA inserts. The insert size varied from 500bp – 2kb, with a mean of approximately 900bp (Bailey *et al.*, 1992b). Approximately 30% of ML8 was amplified to produce ML8A (ML8 Amplified) and following this amplification, approximately 70% of the plasmids contained inserts (Bailey *et al.*, 1992b).

For cDNA subtraction, M13 helper phage were added to 3.2×10^{10} colony forming units of ML8A for 6 hours at 37°C in the presence of Kanamycin. This resulted in the synthesis of single-stranded phagemids, since Bluescript II contains an M13-related f1 filamentous phage origin of replication. The newly synthesised single-stranded phagemids were pelleted by centrifugation in the presence of 4% v/v polyethylene glycol and 500mM NaCl and purified using a caesium chloride gradient. The phagemids were then lysed and the DNA was harvested. The single-stranded phagemids were hybridised to an excess of biotinylated amoebal and plasmodial poly(A)⁺ RNA and the hybridised abundant, constitutive, amoeba- and plasmodium-specific phagemids were then removed using streptavidin, which is a high-affinity biotin-binding protein. Contaminants were then

removed from the non-hybridised phagemids by phenol:chloroform extraction and the resulting purified phagemids were finally transformed into *Escherichia coli* strain DH5 α MCR to produce the subtracted library, ML8S (ML8 Subtracted; Bailey *et al.*, 1999). Since non-insert-containing phagemids were not removed through subtraction, approximately 15% of the subtracted library still contained inserts (Bailey *et al.*, 1999).

Approximately 5% of ML8S was screened using three replica colony blots against amoeba-specific (A), plasmodium-specific (P) or developmental-transition enriched (D) probes (Bailey *et al.*, 1999). The A and P probes were enriched for low-abundance constitutive transcripts by subtraction against the mRNA from which they were derived. By removing the more abundant transcripts from these two probes, the sensitivity of detection was improved. Such transcripts would constitute the majority of the labelled probe if they were not removed and hence, greater proportions of the labelling components would be required to ensure all low abundance transcripts were detected. The D probe was enriched by subtraction against mRNA from amoebae and plasmodia. By subtracting amoeba and plasmodium specific transcripts, the majority of abundant constitutive and cell-type specific transcripts were removed.

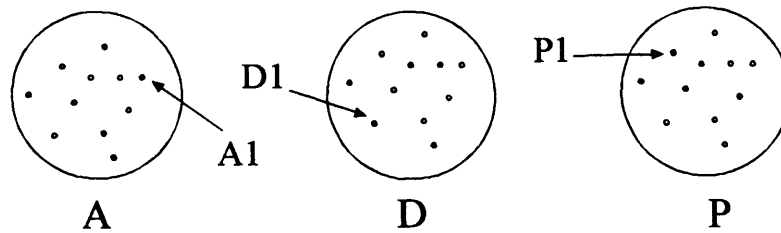
Each clone that hybridised to only one or two of the probes was assigned a unique code based on the hybridisation pattern produced. If a clone produced a signal with just the D probe, it was assigned the letter D and a unique number (e.g. D1; Figure 3.1, step 2). If a signal was observed using the A or both the A and D probes, it was assigned the letter A plus a number (e.g. A1; Figure 3.1, step 2). Similarly, a clone that produced a signal with just the P or with both the P and D probes was assigned the letter P and a number (e.g. P1; Figure 3.1, step 2). This preliminary screen identified 150 colonies that failed to hybridise to all three probes. Any colonies that hybridised to all three probes were considered to represent constitutive transcripts and were not investigated further.

Since the preliminary screening was performed on plates containing a high density of colonies, the 150 stocks often contained mixed populations of cDNAs and secondary screening was necessary to enable individual positive colonies to be identified. Of the 150 colonies assigned to the A, D and P categories, approximately 30 were selected at random for secondary screening. These were re-plated individually on LB-amp to a density of approximately 200 colonies per plate (Figure 3.1, step 3). Individual colonies were then

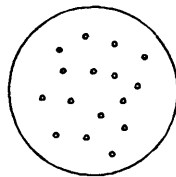
Figure 3.1

The screening strategy for the ML8S cDNA library and stock code designation

1. Plate cDNA library ML8S, make three replica filters and then probe with the A, D or P probes

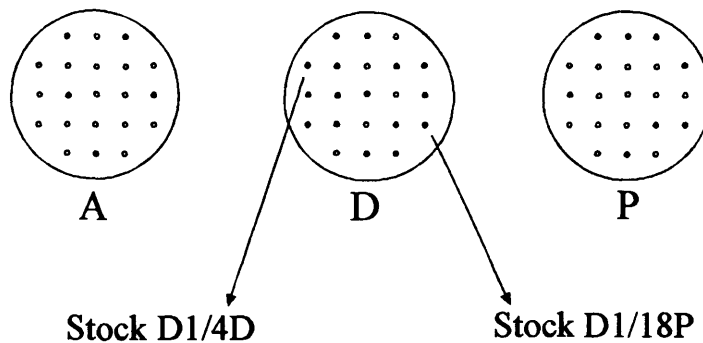


2. Categorise the colonies based on the pattern of hybridisation observed and make freezer stocks for 150 colonies.
3. Dilute stock and plate out approximately 200 colonies.



4. Transfer 21 colonies onto three replica filters and a stock plate in the pattern shown. Probe the filters with the A, D or P probes.

1	2	3
4	5	6 7 8
9	10	11 12 13
14	15	16 17 18
19	20	21



5. Assign positive colonies to new stocks based on the position of the colony in the ordered array.

transferred from the stock plate to a fresh LB-amp plate and three replica Hybond-N filters, supported on LB-amp plates, in an ordered array of 21 colonies (Figure 3.1, step 4) and grown overnight at 37°C. The plasmid DNA was fixed to the filters (Section 2.5.3) and the filters were screened against the A, D or P probes, as before (Figure 3.1, step 4). Individual clones were then assigned a two-part code. The first part of the code relates directly to the A, D or P stock from which they were derived. The second part of the code relates to the signal obtained from the probing and the position of the clone in the ordered array. For example, if screening of stock D1 identified a clone with a plasmodium-specific expression pattern in position '4' on the array, this clone would be designated D1/4D (Figure 3.1, step 5). Often more than one type of classification (A,D or P) was assigned to individual colonies from the same stock sample (e.g. D1/4D and D1/18P; Figure 3.1, step 5); this reflected differences in the nature of mixing in the original stock due to the high density of plating, as described above.

Following the secondary screen, 12 clones were analysed in detail using northern blotting against RNA prepared from amoebae, plasmodia and a culture containing a high proportion of developing cells. Comparison of the sizes of the transcripts from the northern analysis and the cDNA inserts revealed that many clones were shorter than the corresponding mRNAs, suggesting that they were missing the start of their coding sequences (J. Bailey, personal communication). Three different results were observed on these preliminary northern blots.

- i. Some of the clones failed to produce a discernible signal. This was generally considered to be associated with a very low transcription rate below the level of sensitivity of northern blots, although plasmid instability or associated problems could not be ruled out (J. Bailey, personal communication).
- ii. Some clones produced a weak pattern of expression across all the samples and therefore represented low abundance constitutive genes. These were not eliminated during the colony screening due to uneven transfer of the bacterial colonies resulting in an apparent failure of the colony to hybridise to all three probes.
- iii. Finally, some of the clones produced a unique pattern of expression unlike the others. These clones were selected for further screening.

The fact that none of the clones produced an amoeba- or plasmodium-specific expression pattern indicates that the subtraction step was a success.

Four of the 12 clones exhibited an apparently novel pattern of expression (D6/18P, D13/3D, P4/10P and P8/8A). Comparison of the sizes of these cDNA clones and their corresponding transcripts, detected by the preliminary northern analysis, indicated that they were all partial cDNAs. It was anticipated that more complete transcripts might exist within the cDNA library ML8A, since inserts of up to 2kb in size were evident in this library (Bailey *et al.*, 1992b).

3.1.2 Aims

The first aim of the work presented in this Chapter was to screen the ML8A and ML8S cDNA libraries to identify longer transcripts of D6/18P, D13/3D, P4/10P and P8/8A. The second aim was to then complete the preliminary sequence analysis of the cDNA clones, adding any additional sequence obtained from the screen for longer transcripts.

Once the sequence analysis was completed, the final aim of the work presented in this Chapter was to further characterise D13/3D and P8/8A using detailed northern and preliminary Southern blotting analysis to determine whether the genes are members of multi-gene families and to confirm their expression patterns.

3.2 RESULTS

3.2.1 Screening cDNA libraries for longer transcripts.

Initially, the amplified cDNA library, ML8A, was screened for longer transcripts of D6/18P, D13/3D, P4/10P and P8/8A by colony blotting (Section 2.4.3). The ML8A library was an appropriate resource for such screening, since the library from which the original clones were isolated, ML8S, was derived from it. In addition, a large volume of ML8A was available containing several thousands of colonies, whereas ML8S was a much more limited resource. Two rounds of screening were performed on ML8A using approximately 30,000 colonies and then 21,000 colonies, distributed over 10 and 14 plates respectively. For the second screen, the colonies were plated at a lower density to simplify the isolation of a single cDNA clone. Finally, a third screen was performed using approximately 10,500 colonies from the subtracted library, ML8S, distributed over 10 plates. For each round of screening, the filters were probed individually for D6/18P, D13/3D, P4/10P and P8/8A. In addition, the filters were stripped of radioactivity between each probing to reduce the level of background signal (Section 2.4.4). The order of

probing for each cDNA was varied for the three sets of filters, with the exception that P8/8A was consistently probed last since this probe often produced a strong signal that was difficult to reduce by high stringency ‘stripping’ and generated a high background signal. The reason for this background became apparent later (Section 3.2.3).

The screening of libraries ML8A and ML8S identified the following additional clones:

	D6/18P	D13/3D	P4/10P	P8/8A
ML8A	none	1 smaller clone	none	5 smaller clones
ML8S	1 smaller clone	none	none	2 larger clones

With the exception of P8/8A, the screening of the cDNA libraries did not identify longer cDNA molecules. The cDNA libraries were a limited resource and the fact that only a few positive clones were detected despite screening a large number of colonies suggests that full length cDNAs are unlikely to be present in these libraries. Therefore, no further screening was performed. The sequences of the longest clone for P8/8A, obtained from screening ML8S, together with the three original cDNA clones for D6/18P, D13/3D and P4/10P were then analysed in detail, as described below, in order to identify any domains, motifs or homologies to genes from other systems that may provide indicate the roles of the four genes in *Physarum polycephalum*.

3.2.2 Sequence analysis of D6/18P and P4/10P

Initial sequencing of D6/18P and P4/10P was performed using just the universal reverse and –40 primers located in the vector (Table 3.1). Since Oligo(dT)₁₅ *NotI* primers were used for the construction of the cDNA library, ML8, all cDNAs are orientated such that the –40 primer will amplify the reverse strand of the cDNA, beginning in the poly(A)⁺ region. With manual sequencing, approximately 200 nucleotides of good sequence can be generated, thus there were errors in the mid-region of the preliminary sequences, since these were furthest away from the primer sites. Therefore, internal primers (Table 3.1) spaced at intervals of between 200–300 nucleotides were designed and further sequencing was performed (Section 2.4.5).

The sequence of the 516bp D6/18P cDNA clone, including the location of the putative polyadenylation signal (AAATTTA) and the stop codon (TAA) together with the deduced amino acid sequence is shown in Figure 3.2. The coding region ends with a TAA stop

Table 3.1

Primer code	Sequence	Strand synthesis
Reverse	5'-GGAAACAGTATGACCATG-3'	Forward
M13 -40	5'-GTTTTCCCAGTCACGAC-3'	Reverse
D6/18P-1	5'-GCCATCAAGGGAGTTAAGG-3'	Forward
D6/18P-2	5'-AGCACATGGCTTTGATCC-3'	Forward
D6/18P-3	5'-GCATTTGGGCCAACATTC-3'	Reverse
D6/18P-4	5'-CTCTGGTTAAATGGATCAAAGC-3'	Reverse
D6/18P-5	5'-GCAGTGTCTGACCTTTTCCC-3'	Forward
D13/3D-1	5'-TGGTGTAGTCCCTTCCCTCC-3'	Reverse
D13/3D-2	5'-GGCTGTTACGGTGTTAATTGG-3'	Reverse
D13/3D-3	5'-TTGGGTGACGCTGTGTGGGC-3'	Reverse
D13/3D-4	5'-GCACTTGAATCAGAGAATT-3'	Reverse
D13/3D-5	5'-GCAATAAGGAGGGAAGGGAC-3'	Forward
D13/3D-6	5'-CAAATGCCACCTTCACTATG-3'	Forward
D13/3D-7	5'-TATTGACAAGAAACCAGGC-3'	Reverse
P4/10P-1	5'-CTTACTCCCATATCTGGTGGTG-3'	Forward
P4/10P-2	5'-AACCCTGGAAATTCGCC-3'	Reverse
P4/10P-3	5'-GCAGGTTTGAAGGAATACGTAG-3'	Forward
P4/10P-5	5'-AAACGACACGTCCTTACG-3'	Reverse
P4/10P-6	5'-GATTGCTCCTTATCCTTGCC-3'	Forward
P4/10P-7	5'-CGTAGCAGCACTTCATTG-3'	Reverse
P8/8A-1	5'-TCCACTCGTAGATTCCGTCG-3'	Reverse
P8/8A-2	5'-TTGGCGATTTGTAGCTTACC-3'	Reverse
P8/8A-3	5'-TTCACAGCCTTCCATCATCC-3'	Reverse
P8/8A-4	5'-GATGATGGAAGGCTATGAAC-3'	Forward
P8/8A-5	5'-TTCAAGCGCCAATGGTAAGC-3'	Forward
P8/8A-6N	5'-CAGCCGATAAGAACAAGGAC-3'	Forward
P8/8A-7N	5'-AGATTCTCGGCACAAATG-3'	Reverse
P8/8A-8	5'-CAAGTTCACCGCTGCTGGAG-3'	Forward
P8/8A-9	5'-GAGCGAACTTTTCCGTCC-3'	Reverse

Primers used for sequencing of the four cDNA clones

Primers were designed using the Wisconsin Package, Genetics Computer Group (Madison, USA) on the Leicester University mainframe computer and synthesised as described in Section 2.4.5.

Figure 3.2: The cDNA and deduced partial amino acid sequences for cDNA clone D6/18P isolated from subtracted cDNA library, ML8S.

The nucleotide and deduced amino acid sequence of the 516bp D6/18P cDNA clone, isolated from ML8S (Section 3.1.1) is shown. The D6/18P cDNA clone was considerably smaller than the transcript detected on northern blots, 516bp compared to approximately 2500 nucleotides and is therefore incomplete (Section 3.2.2). The sequence of both the forward and reverse strands were determined manually using T7 DNA polymerase and the Sequagel™ sequencing system (Section 2.4.5) with the Reverse, -40 and D6/18P primers listed in Table 3.1. The sequences obtained from each primer were aligned using the Wisconsin Package, Genetics Computer Group (Madison, USA) on the Leicester University Mainframe computer. All regions of sequence discrepancy identified in the overlapping regions were clarified by further sequencing.

The standard single-letter code for the deduced partial amino acid sequence is shown. The coding region ends with a TAA stop codon at base 414 (TAA), this is indicated by an asterix in the amino acid sequence (*). The coding region is followed by a short 3' untranslated region of 85bp. The putative polyadenylation signal is located 11bp ahead of the poly(A)⁺ residues and is shown underlined (AAATTTA). Since an Oligo(dT)₁₅ primer was used for construction of the cDNA library, ML8S (Section 3.1.1), the cDNA sequence ends with 15 'A' residues.

Figure 3.2

1 AGCTCTTGTT TAAGCCATTT TGTAATGAAG AAAATAGACG CATGTTTTTTT
L L F K P F C N E E N R R M F F

51 ATAAACTATG CACAATCCCA TTCATTTGAC CCCCTAAGCC CCAAAGCATG
I N Y A Q S H S F D P L S P K A W

101 GTATCAACAC ACTCGTGATA TGTTCCCTGAA CCACAATAAG GGAGCAGCTA
Y Q H T R D M F L N H N K G A A S

151 GTGTACTIONTAT GCACCATAAC AATAGCTACA CACAGGCAGT GTCTGACCTT
V L M H H N N S Y T Q A V S D L

201 TCCCTGAAAT TGGCATTGTG CAGGAATGTT GGCCCAAAGC ACATTGGGCA
S L K L A L C R N V G P K H I G H

251 TACCCTTCAA ATAGGATTAA GATATTTACT GGATATGCAA AAGCACATGG
T L Q I G L R Y L L D M Q K K M A

301 CTTTGATCCA TTAAACCAG AGAACTGGTA CCATCAACCA ATTGCACATA
L I H L N Q R T G T I N Q L H I

351 TATTGGCCAT CAAGGGAGTT AAGGAAGTTG TGTGGTATCA TAAAAATCGA
Y W P S R E L R K L C G I I K I E

401 ATCAGTAGGG CTTTAAATTGA TCTTTTTCCA AATACTAAAT TCATAGCCTC
S V G L *

451 CAAATTTTCAT AGAGCTTTGT AGATTATTA TGTAATTTA GCTTTTGTGT

501 CAAAAAAAAA AAAAAA

codon at base 414; *P. polycephalum* exhibits a bias towards use of this stop codon (e.g. Green & Dove, 1988; Binette *et al.*, 1990). The 3' untranslated region of D6/18P is 85bp, which is also consistent with previous observations (e.g. Binette *et al.*, 1990). The low abundance of the transcript meant that it was difficult to accurately define the D6/18P expression pattern using northern blots. Further northern analysis of D6/18P indicated a plasmodium-specific expression pattern, which was contradictory to the preliminary findings (E. Swanston, Unpublished data). The D6/18P cDNA clone was considerably smaller than the transcript detected on northern blots, 516bp compared to approximately 2500 nucleotides. Since a longer cDNA for D6/18P could not be found and no homologues were identified, the analysis of D6/18P was suspended.

The sequence analysis of P4/10P was completed under my supervision as part of a MSc project (Evans, 1997). The sequence of the 634bp P4/10P cDNA clone, including the location of putative polyadenylation signal (AAATTAA) and the stop codon (TAA) together with the deduced amino acid sequence is shown in Figure 3.3. As with D6/18P, the coding region ends with a TAA stop codon at base 590 and is followed by a short 3' untranslated region (27bp; Figure 3.3). Preliminary northern blotting analysis revealed that P4/10P encodes a mRNA of approximately 900 nucleotides. Allowing for a poly(A)+ tail of approximately 50 residues (discussed in Section 3.3.1), comparison of the size of transcript detected on northern blots and the cDNA clone suggest that the cDNA clone is missing approximately 230bp of coding and 5' untranslated sequences. Since the 5' untranslated region can be as small as 15bp (Binette *et al.*, 1990), this could account for up to 70 amino acid residues.

Further analysis of P4/10P was performed at Leicester University by Evans (1997), who failed to identify any P4/10P-related sequences in the computer databases (Section 2.4.5). I recently repeated the database comparisons and identified genes with significant identity to the C-terminal region of P4/10P (Figure 3.4). The protein most closely related to the protein encoded by P4/10P is a predicted 16.5kDa protein, encoded on chromosome A3(2) in *Streptomyces coelicolor*, that exhibits 54% identity and a further 11% similarity in amino acid residues (Figure 3.4). Two other proteins that exhibit high levels of similarity to the protein encoded by P4/10P are the nodulation N protein from *Rhizobium leguminosarum* (46% identity, 17% similarity) and the hypothetical 16.0kDa protein from *Mycobacterium tuberculosis* (46% identity, 15% similarity; Figure 3.4). In addition to

Figure 3.3: The cDNA and deduced partial amino acid sequences for cDNA clone P4/10P isolated from subtracted cDNA library, ML8S.

The nucleotide and deduced amino acid sequence of the 634bp P4/10P cDNA clone, isolated from ML8S (Section 3.1.1) is shown. The sequence analysis of P4/10P was completed under my supervision as part of a MSc project (Evans, 1997). Preliminary northern blotting analysis revealed that P4/10P encodes a mRNA of approximately 900 nucleotides, thus the P4/10P cDNA clone is incomplete (Section 3.2.2). The sequence of both the forward and reverse strands were determined manually using T7 DNA polymerase and the Sequagel™ sequencing system (Section 2.4.5) with the Reverse, -40 and P4/10P primers listed in Table 3.1. The sequences obtained from each primer were aligned using the Wisconsin Package, Genetics Computer Group (Madison, USA) on the Leicester University Mainframe computer. All regions of sequence discrepancy identified in the overlapping regions were clarified by further sequencing.

The standard single-letter code for the deduced partial amino acid sequence is shown. The coding region ends with a TAA stop codon at base 590 (TAA), this is indicated by an asterisk in the amino acid sequence (*). The coding region is followed by a short 3' untranslated region of 23bp. The putative polyadenylation signal is located 10bp ahead of the poly(A)⁺ residues and is shown underlined (AAATTAA). Since an Oligo(dT)₁₅ primer was used for construction of the cDNA library, ML8S (Section 3.1.1), the cDNA sequence ends with 15 'A' residues.

Figure 3.3

1 AGCCACCAGA AGGATTCACG CTATTCAGCA ACACCTTGCC CCTATCAGCC
A T R R I H A I Q Q H L A P I S P

51 CTGCAAATGA ATTGCAAGCA CAGCCAACCA GCAATGAAGT GCTGCTACGT
A N E L Q A Q P T S N E V L L R

101 CAGTTCATAA TGAACCCCAA GCAAGCCCCC AAACCTCCCTC CTGTCAAAGG
Q F I M N P K Q A P K L P P V K G

151 CCTTGCAGGT TTGAAGGAAT ACGTAGGAAA GGAGCTTGGA GTAACAGACT
L A G L K E Y V G K E L G V T D Y

201 ACTTCAATGT TTCTCAAGAA AGAATCAACG CCTTCGCAGA TACAACAGGC
F N V S Q E R I N A F A D T T G

251 GATTTCCAGT GGATTCACGT AGATGTGGAG CGCGCATCCA ACGAATCTCC
D F Q W I H V D V E R A S N E S P

301 GTTTGGAGGA CCAATCGCCC ACGGATTGCT CACCTTATCC TTGGCCCCTT
F G G P I A H G L L T L S L A P Y

351 ATTTTGTGTC CCAGACTCTC CCCAGGTCG AGGGCGTCAA GTACGGCGTC
F V S Q T L P Q V E G V K Y G V

401 AACTATGGAT TCAACAAGGT CAGATATGTT AGCCCAGTGA AAGCGGGACG
N Y G F N K V R Y V S P V K A G R

451 AAACGTAAGA GGACGTGTCG TTTTACAAGA ACTTACTCCC ATATCTGGTG
N V R G R V V L Q E L T P I S G G

501 GTGCGCAAGT CATTGCCAAG ATCACATTCTG AGATTGAGGG AAGTGATAAG
A Q V I A K I T F E I E G S D K

551 CCCGCAGCCG TTGCAGAATG GATCCTTCGT TACTATGAGT **AAATTGTCGC**
P A A V A E W I L R Y Y E *

601 ACAAATTAAT TCGAAACACA AAAAAAAAAA AAAA

Figure 3.4: Amino acid sequence for P4/10P compared with homologous sequences from BLAST database search

Sequence alignment generated from the BLAST database comparison of the putative protein encoded by P4/10P with the *Streptomyces coelicolor* predicted 16.5kDa protein from A3 (2) chromosome (Accession number: CAB46796), *Mycobacterium tuberculosis* predicted 16.0kDa protein (Accession number: P96807) and the *Rhizobium leguminosarum* (biovar viciae) and *Rhizobium meliloti* nodulation proteins N (Accession numbers: P08634 and P25200, respectively).

The black boxes (A) indicate regions of amino acid identity to P4/10P whilst the shaded boxes (B) indicate regions of amino acid similarity to P4/10P. Gaps in some sequences were necessary to obtain the best sequence alignment and these are indicated by a dot (.). The sequence alignment between the other sequences is not shown.

R. leguminosarum, P4/10P shares significant homology with *R. meliloti* nodulation N protein (Figure 3.4). These *Rhizobium* nodulation N proteins are known to be involved in production of host-specific root hair deformation factors although their exact role is unclear (Surin & Downie, 1988). Unfortunately, none of these homologies indicate a role for P4/10P in *Physarum polycephalum*. However, the fact that this homology only extends to the C-terminal half of the protein suggests that P4/10P may have a second functional domain at the N-terminus and does not function in a manner related to the genes described above.

Following further northern analysis, a constitutive expression pattern for P4/10P was observed (Evans, 1997), therefore, since this gene does not exhibit the novel pattern of gene expression observed during the APT, no further characterisation has been performed.

3.2.3 Sequence analysis of D13/3D and P8/8A

Sequencing of D13/3D and P8/8A was performed initially using the universal primers and then using internal primers designed as required (Table 3.1). The original clone and one of the longer clones for P8/8A were sequenced completely. All regions of discrepancy were clarified by further sequencing of both clones. The longer clone contained an additional 15bp of coding region. The sequence and deduced amino acid sequences for D13/3D (Accession number: Y18123; Bailey *et al.*, 1999) and P8/8A (Accession number: Y18124; Bailey *et al.*, 1999) are presented in Figures 3.5 & 3.6. The putative polyadenylation signals are underlined (AATAAA) and the stop codons are shown in bold type (**TAA**). As with P4/10P and D6/18P, the coding regions of both cDNAs ends with a TAA stop codon and are followed by 3' untranslated regions of up to 80 nucleotides. Both the D13/3D and P8/8A cDNAs contain the putative polyadenylation signal, AATAAA, located 16bp ahead of the poly(A)⁺ tract, consistent with previous findings (e.g. Hamelin *et al.*, 1988; Kozlowski *et al.*, 1993; Morita, 1998). The D13/3D and P8/8A cDNAs were compared with the sequence databases. No significant sequence homologies, domains or motifs were identified in D13/3D. Further analysis of D13/3D is discussed in Chapters 4, 5 & 6.

A pair of well conserved EF-hand calcium-binding domains was identified in P8/8A (Bailey *et al.*, 1999); EF-hand calcium-binding domains have a consensus sequence of 13 amino acids and generally occur in pairs (Figure 3.6). Unfortunately these domains occur

Figure 3.5: The cDNA and deduced partial amino acid sequences for cDNA clone D13/3D isolated from subtracted cDNA library, ML8S.

The nucleotide and deduced amino acid sequence of the 674bp D13/3D cDNA clone, isolated from ML8S (Section 3.1.1) is shown (Accession number: Y18123; Bailey *et al.*, 1999). Northern blotting analysis revealed that D13/3D encodes a mRNA of approximately 800 nucleotides, thus the D13/3D cDNA clone is incomplete (Section 3.3.1). The sequence of both the forward and reverse strands were determined manually using T7 DNA polymerase and the Sequagel™ sequencing system (Section 2.4.5) with the Reverse, -40 and D13/3D primers listed in Table 3.1. The sequences obtained from each primer were aligned using the Wisconsin Package, Genetics Computer Group (Madison, USA) on the Leicester University Mainframe computer. All regions of sequence discrepancy identified in the overlapping regions were clarified by further sequencing.

The standard single-letter code for the deduced partial amino acid sequence is shown. The coding region ends with a TAA stop codon at base 600 (TAA), this is indicated by an asterix in the amino acid sequence (*). The coding region is followed by a short 3' untranslated region of 57bp. The putative polyadenylation signal is located 16bp ahead of the poly(A)⁺ residues and is shown underlined (AATAAA). Since an Oligo(dT)₁₅ primer was used for construction of the cDNA library, ML8S (Section 3.1.1), the cDNA sequence ends with 15 'A' residues. The sequence shown in bold-type, beginning at base 115, denotes the *Xcm*I restriction site used during the construction of cDNA-based vectors for homologous gene replacement of the D13/3D gene (*redA*; Section 5.2)

Figure 3.5

1 GAAAGAAGCA AGTAAATATG CTGAAAGTTG TGATTTTGTG AGTTCTTCTG
K K Q V N M L K V V I L S V L S

51 ATTGGCCTGG TTTCTTGTC AATATGTGATA CACCAAGAAT TCTCTGATTC
I G L V S C Q Y V I H Q E F S D S

101 CAAGTGCTCA AATGCCACCT **TCACTATGGT** CGCCCCAACT GCTTGTGTTG
K C S N A T F T M V A P T A C V E

151 AAGCTGAAGA TGGAAAATAC CACAAATCCG TATGTGCAAG TGATTCTGTG
A E D G K Y H K S V C A S D S V

201 CAGCTGTTTG AATGCAATGA CCAGGCTTGT ACCGACTGCC CTCGTAAAGA
Q L F E C N D Q A C T D C P R K E

251 AACAAATGAAC ACAACGTGCA ACCCAACCAT GAACAAAGAA TATTCTCAGT
T M N T T C N P T M N K E Y S Q Y

301 ACTCGTGCGC AGCTACCGTC CCGACCGGCC CACACAGCGT CACCCAAGCT
S C A A T V P T G P H S V T Q A

351 ATATATCCTG AAACCGCGGG AGGATGTAAG GGAAC TTTCT CAACGGCTTT
I Y P E T A G G C K G T F S T A F

401 TGTGGACTTT GGGTTGATTG GCAGTTGCAA TAAGGAGGGA GGGACTACAC
V D F G L I G S C N K E G G T T P

451 CATGCTGTCT TGCGACTCCA ATAACAGCCG TAACAGACCA AGACCTGCAG
C C L A T P I T A V T D Q D L Q

501 CGGATGACAA GTGCTCCACG GAGCTGCCAC GAGCAAAGC TCGAGTCTTG
R M T S A P R S C H E Q K L E S C

551 CGAACATTCA GAACATGGGT TTGGATACAC AGGCTTCACC TGCACAGCAT
E H S E H G F G Y T G F T C T A *

601 **AAATGGAAGC** GATATGTTTC TATTTGCAGA TCATAGGAAT AAACTGATAA

651 CAGTAGACTA AAAAAAAAAA AAAA

Figure 3.6: The cDNA and deduced partial amino acid sequences for cDNA clone P8/8A isolated from subtracted cDNA library, ML8S.

The nucleotide and deduced amino acid sequence of the 660bp P8/8A cDNA clone, isolated from ML8S (Section 3.1.1) is shown (Accession number: Y18124; Bailey *et al.*, 1999). Northern blotting analysis revealed that P8/8A encodes a mRNA of approximately 800 nucleotides, thus the P8/8A cDNA clone is incomplete (Section 3.3.1). The sequence of both the forward and reverse strands were determined manually using T7 DNA polymerase and the SequageTM sequencing system (Section 2.4.5) with the Reverse, -40 and P8/8A primers listed in Table 3.1. The sequences obtained from each primer were aligned using the Wisconsin Package, Genetics Computer Group (Madison, USA) on the Leicester University Mainframe computer. All regions of sequence discrepancy identified in the overlapping regions were clarified by further sequencing.

The standard single-letter code for the deduced partial amino acid sequence is shown. The coding region ends with a TAA stop codon at base 563 (TAA), this is indicated by an asterix in the amino acid sequence (*). The coding region is followed by a 3' untranslated region of 80bp. The putative polyadenylation signal is located 16bp ahead of the poly(A)⁺ residues and is shown underlined (AATAAA). Since an Oligo(dT)₁₅ primer was used for construction of the cDNA library, ML8S (Section 3.1.1), the cDNA sequence ends with 15 'A' residues. The boxed regions (D K) denote the location of two putative EF-hand calcium-binding domains (Section 3.2.3). The sequence shown underlined in italics (438bp: CC GG) indicates the location of a *Msp*I restriction site that was used to prepare template DNA for generation of radio-labelled probes as discussed in Section 3.2.3.

Figure 3.6

1 CAAGAGAGAA ACATGGCAGA CTTCAGAGCA CGCTGGGAGG GATACTTCAA
K R E T W Q T S E H A G R D T S R

51 GGCACCTCGAT GGCAACTCGA ATGGCTTCCT CGAGCCTTCG GACAGCCCTC
H S M A T R M A S S S L R T A L

101 ATTTGTGCCG AGAATCTGGC CAAGGGACTC AAGTTCACCG CTGCTGGAGC
I C A E N L A K G L K F T A A G A

151 AGAGGCCTTG AAGCAAGCTC AGATTTCGCAC ATATTCCGAG TGGGTGAAAG
E A L K Q A Q I R T Y S E W V K A

201 CAGCCGATAA GAACAAGGAC GGAAAAGTTT CGCTCCCCGA GTTTCTTGAG
A **D K N K D G K V S L P E F** L E

251 TATGCTGAGA AGCATTTCGC TGGAAAGAAA TACGAGGAGA TCCCATCTTT
Y A E K H F A G K K Y E E I P S F

301 TTTCCGTGAC GACTTGGAGG GCCAGGCCCA GCACTTTGAC GCAAATGGAG
F R D D L E G Q A Q H F **D A N G D**

351 ATGGCATTAT TACTTTGGAT GAATGGAAGG CTATGAACAG CAGCTACCCT
G I I T L D E W K A M N S S Y P

401 AACCACGCTC CCGAGGCCGA GTTTGTGCT GCTTTCCACC GGTTTGCTGG
N H A P E A E F V A A F H R F A G

451 AGGAGACAAA TTGGACTTAG CCAAGCTCAA GCACGGAATC TACGAGTGGA
G D K L D L A K L K H G I Y E W T

501 CCTCGACCAA GGGCCCCGTC CCCGACCTCG AAATCCTTTT CCCGTTTTTC
S T K G P V P D L E I L F P F F

551 AAGCGCCAAT **GGTAAG**CTAC AAATCGCCAA TTTTGGCAAA ACTACCATTT
K R Q W *

601 TGTAGCTAGG CAAATTTATA TTTAATAAAA TTGTAAATTC CATTTAAAAA

651 AAAAAAAAAA

in genes with several different functions and thus do not indicate a role for P8/8A during plasmodium development. Analysis of P8/8A was continued by J. Bailey and subsequently revealed homologies to sarcoplasmic calcium-binding proteins from invertebrates. Unfortunately, the exact role of these proteins is unclear at this time and, therefore, they provide no indication of the role of P8/8A (Bailey *et al.*, 1999).

The P8/8A probe often generated a high background signal on colony blots. Sequence analysis revealed that two small regions, located at the 3' end of the P8/8A cDNA, were homologous to sequences in the Bluescript II vector molecule and were a likely cause of the unusually high background signal. The level of background hybridisation was reduced considerably in subsequent probes by truncation of the template DNA to eliminate this 3' region, using an *MspI* site located 438bp into the cDNA sequence (CCGG, Figure 3.6).

3.2.4 Northern blotting analysis of D13/3D and P8/8A

To confirm the expression pattern of D13/3D and P8/8A observed during preliminary northern analysis, more detailed northern analysis was performed using total RNA isolated from amoebae, microplasmodia, macroplasmodia and cultures of developing cells of the apogamic strain CL (Section 2.4.2). The proportions of different cell types represented in the samples used are shown in Table 2.1. The northern blots were probed for D13/3D, P8/8A, amoeba- and plasmodium-specific profilins (*proA* [pLAV3-1a] and *proP* [pLAV5-1]; Binette *et al.*, 1990) and constitutively expressed actin (p*PpA35*; Hamelin *et al.*, 1988). Hybridisation was conducted at low (55°C) and high (65°C) stringency for both D13/3D and P8/8A probes and at 65°C for all other probes (Section 2.4.4).

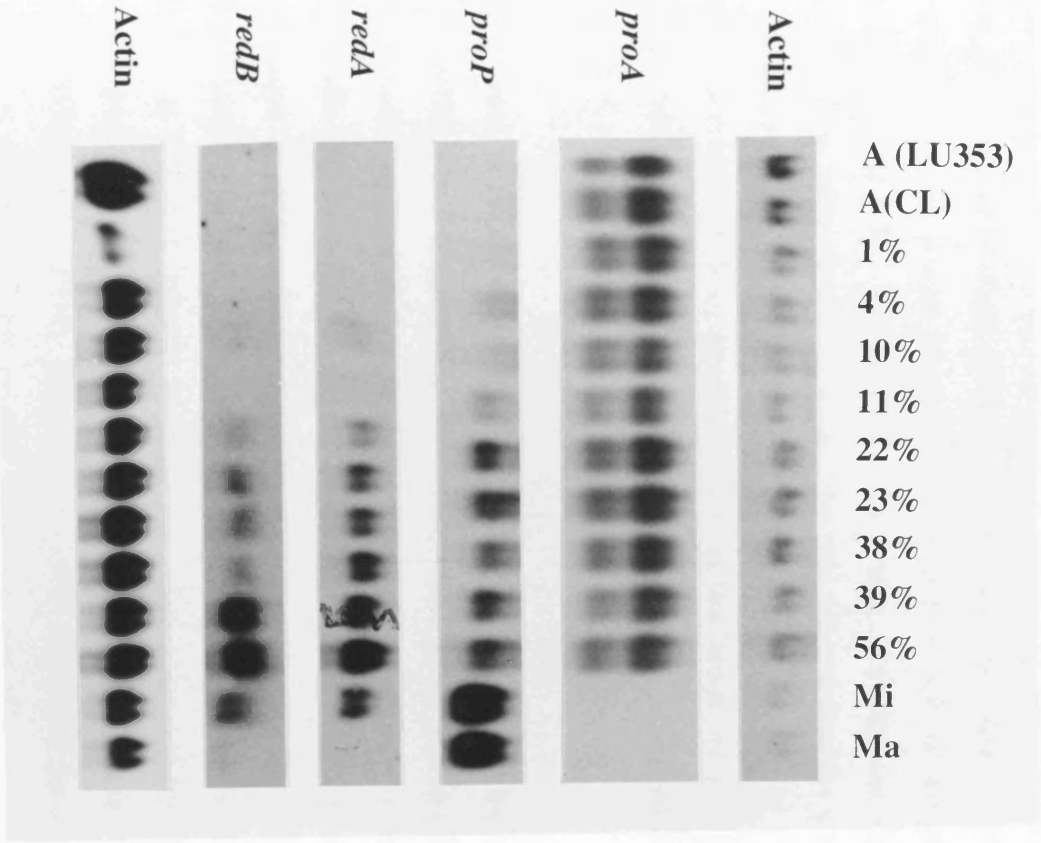
Actin is expressed at a steady state throughout all stages of the life cycle and constitutes a large proportion (approximately 4–5%; Pallotta *et al.*, 1986) of mRNA. Therefore, actin was used as a control for sample loading and transfer to the membrane and to check the integrity of the RNA. The actin probe, p*PpA35*, encodes the *P. polycephalum ardC* actin gene and hybridises to a 1400 nucleotide transcript. Since the genes for *ardB* and *ardC* differ by just 16 nucleotides, this probe cross-hybridises to both *ardB* and *ardC* transcripts (Section 1.3.2; Hamelin *et al.*, 1988). Representative results from three northern blotting experiments are shown in Figure 3.7 and the actin signals from two of these are included. The actin signal shown at the top of this Figure ('upper actin') was derived from the same blot as *proA* and *proP*, whilst the actin signal shown at the bottom

Figure 3.7: Northern blotting analysis of differentially-expressed genes during apogamic development of *Physarum polycephalum* strain CL

Total RNA was isolated from amoebae (**A**), plasmodia (**Mi**: microplasmodia, **Ma**: macropasmodia) and populations of developing cells (1-56%) of the apogamic strain CL and amoebae of the heterothallic strain LU353 as described in Section 2.4.2; for more information on the CL RNA samples see Table 2.1. 10µg denatured total RNA and 3µg denatured RNA size markers (Promega) were size-fractionated in 1.1% agarose gels as described in Section 2.4.2. The sample RNA was blotted to Hybond-N membrane using the 20 × SSC alkaline transfer method (Sambrook *et al.*, 1989) and the RNA was fixed to the membrane by exposure to UV (Section 2.4.1). The RNA size markers were stained and photographed as described in Section 2.4.2 and were used to estimate the transcript sizes detected on autoradiographs following probing (see below).

The cDNA clones for **actin** (pPpA35; Hamelin *et al.*, 1988), amoebal- and plasmodial-specific profilins (**proA** [pLAV3-1a] and **proP** [pLAV5-1] respectively; Binette *et al.*, 1990), D13/3D (**redA**) and P8/8A (**redB**) were radio-labelled using the method of Feinberg and Vogelstein (1983), as described in Section 2.4.4. These radio-labelled probes were hybridised at high stringency (65°C) to northern blots; the results shown are representative of the signals obtained from three independent blots containing the same samples.

The probes hybridised to transcripts of the following sizes, as estimated from the RNA size markers: Actin, 1400 nucleotides; **proA**, 600 and 500 nucleotides; **proP**, 520 nucleotides; **redA** (D13/3D), 800 nucleotides; **redB** (P8/8A), 800 nucleotides.



(‘lower actin’) was derived from the same blot as D13/3D (*redA*) and is representative of the actin signal obtained using the blot probed for P8/8A (*redB*).

All lanes produced clear actin bands with minor smearing, suggesting there was negligible degradation of the samples used. The hybridisation pattern for the ‘upper actin’ is somewhat uneven, probably due to slight differences in the loading and/or transfer of the samples to the membrane. The lowest intensity of hybridisation was to the plasmodial samples (Mi & Ma; Figure 3.7). However, since a strong hybridisation signal was obtained for the *proP* probe using these samples and this blot was not used for the genes in question, these differences bear little relevance to the general observations. The low intensity of hybridisation to the A (CL) amoebal sample in the ‘lower actin’ (Figure 3.7) could be attributed to under-loading, which resulted from technical problems during the quantitation of the RNA sample.

The profilin genes were included as examples of amoeba- and plasmodium-specific genes to confirm that the newly characterised genes exhibited a novel expression pattern. Although the expression patterns for *proA* and *proP* were previously examined in amoebae and plasmodia (Binette *et al.*, 1990), this study provided the first opportunity to compare the expression in cells undergoing apogamic development. The *proA* probe hybridised to 500 nucleotide and 600 nucleotide transcripts and *proP* hybridised to a 520 nucleotide transcript as expected (Binette *et al.*, 1990). The *proA* transcripts are the product of a single gene and are known to differ in the lengths of their 5’ and 3’ non-coding regions (Binette *et al.*, 1990). Binette *et al.* (1990) found that the largest *proA* mRNAs were twice as abundant as the smaller transcripts and this observation was reflected in my analysis with the strongest hybridisation occurring to the 600 nucleotide transcripts (Figure 3.7). In contrast to *proA*, the *proP* gene produces a single transcript (Binette *et al.*, 1990). The *proA* transcripts were detected in all samples containing amoebae but neither of the plasmodial samples (Mi & Ma; Figure 3.7), while *proP* transcripts were first detected in samples containing as little as 4% developing cells and gradually increased as the percentage developing cells increased to reach a peak in plasmodia (Ma; Figure 3.7). There are less than half as many amoebae in the sample containing 56% developing cells than in the amoebal sample and yet the level of expression of *proA* appears to remain constant (Figure 3.7). Therefore, *proA* transcripts must also be present in the developing cells. Since the sample containing 56% developing

cells only contained approximately 10% multinucleate cells, this indicates that *proA* mRNA may be present well into the extended cell cycle.

Studies of expression of the plasmodium-specific *betC* locus, encoding the $\beta 2$ -tubulin isotype, revealed that *betC* transcripts begin to accumulate early in the APT (Solnica-Krezel *et al.*, 1988). The pattern of *betC* expression observed by Solnica-Krezel *et al.* (1988) resembles the pattern detected for *proP* (Figure 3.7). Using antibodies to $\beta 2$ -tubulin, Solnica-Krezel *et al.* (1988) demonstrated that there is a delay in relation to *betC* expression before the $\beta 2$ -tubulin protein accumulates, which correlates to later in the extended cell cycle, shortly before mitosis. Solnica-Krezel *et al.* (1991) expanded the analysis of the transition using antibodies to the amoeba-specific $\alpha 3$ -tubulin and plasmodium-specific $\beta 2$ -tubulin isotypes as markers to study the reorganisation of the mitotic spindle in populations of cells undergoing plasmodium development. The $\beta 2$ -tubulin isotype was not detected in cultures that lacked committed cells and therefore it was deduced that $\beta 2$ -tubulin is only expressed in cells committed to development (Solnica-Krezel *et al.*, 1991). In contrast, the amoeba-specific $\alpha 3$ -tubulin could be detected in committed cells up to the bi- and quadrinucleate stage of development (Solnica-Krezel *et al.*, 1991). Solnica-Krezel *et al.*, (1991) observed that some developing cells that contained $\beta 2$ -tubulin, and were thus committed to development, were able to undergo at least one amoebal-type mitosis before binucleate cell formation. The presence of $\alpha 3$ -tubulin in bi- and quadrinucleate cells demonstrated that the changes to the mitotic spindle are not caused by a lack of $\alpha 3$ -tubulin. This is consistent with the notion that the changes associated with this transition are regulated by independent factors (Section 1.4).

An important question concerning profilin expression is whether a single cell committed to development can express both *proA* and *proP* at the same time. The expression patterns observed on the northern blots described in this Chapter provide evidence in favour of *proA* expression only declining once *proP* expression has been established. Immunofluorescence using isotype-specific antibodies on populations of cells undergoing the developmental transition would confirm the existence of both profilins in a single cell, as was observed for $\alpha 3$ - and $\beta 2$ -tubulin. Since profilin has been shown to be essential for cytokinesis and, in addition, is implicated in the regulation of actin filament dynamics

(Schlüter *et al.*, 1997), it is likely that the two profilins have different roles. Recent over-expression of the two *P. polycephalum* profilin isoforms in profilin-deficient *Saccharomyces cerevisiae* cells, provide evidence to suggest that they are not functionally equivalent (Section 1.3.2; Marcoux *et al.*, 1999).

Having established the expression patterns of constitutive (actin), amoeba-specific (*proA*) and plasmodium-specific (*proP*) genes, the expression of D13/3D (*redA*; see below) and P8/8A (*redB*; see below) was investigated. A single transcript was detected for *redA* and *redB* at both low and high stringency, suggesting that these genes do not have any closely related *Physarum* homologues. The *redA* and *redB* mRNAs are both of approximately 800 nucleotides; however, these are not the same since they do not cross-hybridise. No expression of these two genes is detected in amoebae (A; Figure 3.7). Expression of both genes is first evident when as few as 4% committed cells are present in the culture (1–4%; Figure 3.7) and reaches their peak level when the number increases to 56% (Figure 3.7). Both genes are detected at reduced levels in microplasmodia (Mi; Figure 3.7) and lower still in macroplasmodia (Ma; Figure 3.7).

Although the expression pattern for *redA*, *redB* and *proP* appear similar in populations of cells containing small proportions of developing cells, the expression is clearly different in populations of cells containing a high proportion of developing cells and in plasmodia (Figure 3.7). The *red* gene transcripts reach their highest levels in populations of cells containing a high proportion of developing cells whereas *proP* transcripts are most abundant in plasmodia (Figure 3.7). The expression patterns for *redA* and *redB* differ dramatically from the amoeba-specific *proA* and constitutive actin transcripts (Figure 3.7). Since the expression patterns for *redA* and *redB* differ from constitutive, amoeba- and plasmodium-specific genes, they therefore represent a new class of differentially expressed genes that are up-regulated during the developmental transition. These genes were therefore re-named *red* genes (regulated in development; Bailey *et al.*, 1999); this nomenclature is included in Figure 3.7 and used for the rest of the thesis. The expression of *red* genes is discussed further in Section 3.3.4.

3.2.5 Southern blotting analysis of *redA* and *redB*

Southern blotting was performed to confirm that *redA* and *redB* were single copy genes, as suggested by the northern blotting analysis. Southern blots (Section 2.5.1) were prepared

using 3µg of genomic DNA isolated from CL microplasmodia (Section 2.3.2), digested to completion using a variety of restriction enzymes (Section 2.4.1). The Southern blots were probed for *redA* and *redB* at both low and high stringency and data from the high stringency probing are shown in Figure 3.8.

At high stringency, only fragments from the gene being probed and highly conserved homologues can be detected. Digestion with *HindIII* generated a single 6.6kb band that hybridised to the *redA* probe at high stringency (Figure 3.8a). Since only a single band was observed, a homologous gene could only exist if it were either also located on the same restriction fragment or if, by coincidence, the restriction fragments were of the same size. The cDNA sequence identified a *TaqI* site within the coding region of *redA* and digestion with *TaqI* generated three fragments, 1.8kb, 1.5kb and 900bp (Figure 3.8b). Since only one internal site exists, the generation of the three fragments can be explained by three possibilities:

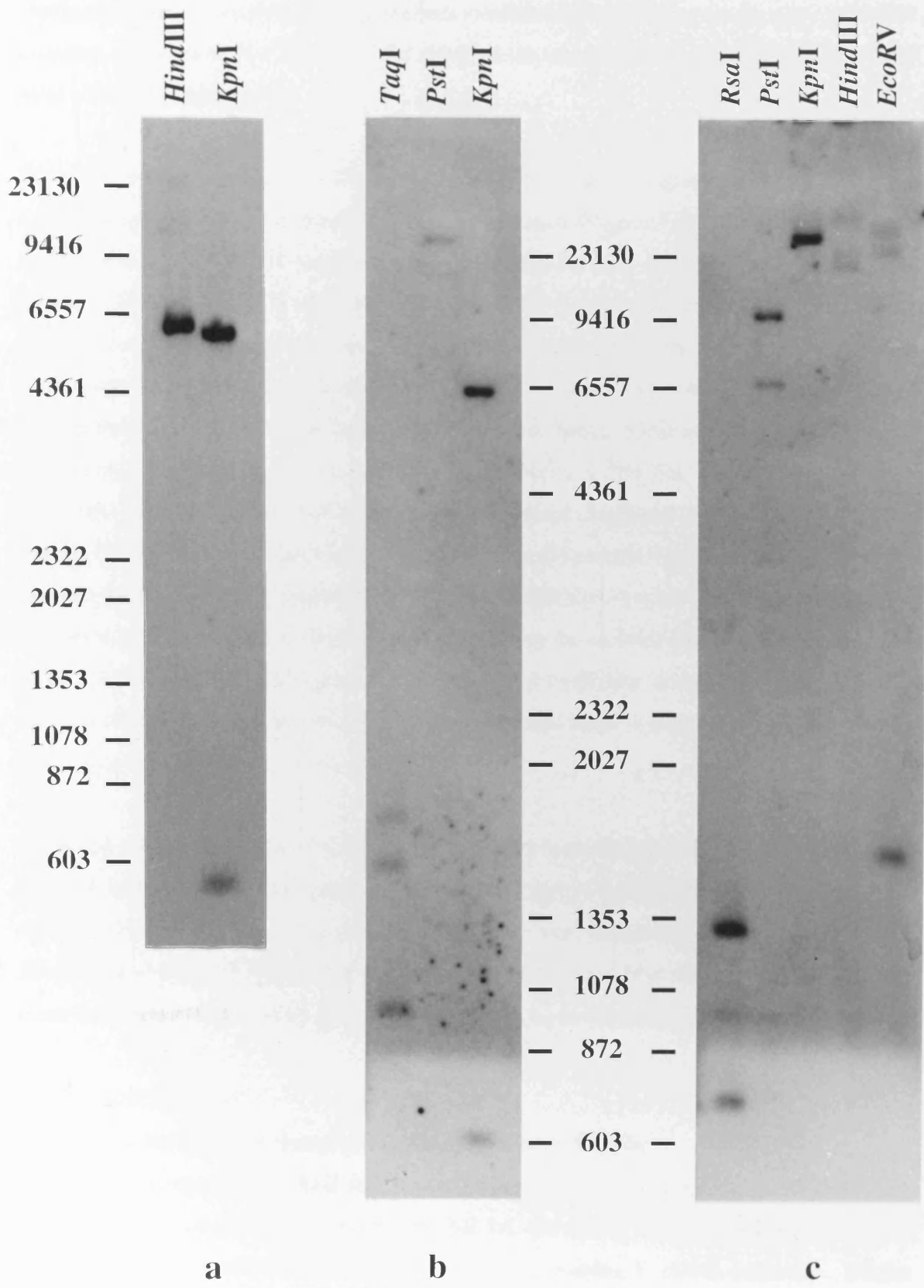
- i. The third fragment could indicate that a homologue of *redA* exists in the *P. polycephalum* genome.
- ii. If one of the fragments is the product of digestion within an intron, the gene must be a minimum of 1.1kb in size, since the smallest *TaqI* fragment is 900bp in size, the internal *TaqI* site is located some 120bp from the 3' end of the cDNA and the third fragment must also contain sufficient homology to the probe to generate a strong signal (at least 100bp). This would suggest the presence of a further intron(s) to account for the size of the internal fragment (minimum 900bp).
- iii. Alternatively, the third fragment could be the product of partial digestion, which may or may not suggest the presence of an intron, depending on which end of the restriction fragment the partial digestion occurred.

Digestion with *KpnI* generated two bands, 6.5kb and 600bp, when the Southern blot was probed for *redA* at high stringency (Figure 3.8a & 3.8b). However, the cDNA sequence data indicate that the *redA* coding region contains no *KpnI* sites. This result therefore suggests either the presence of a second gene related to *redA* or the presence of at least one intron, containing a *KpnI* site, in the gene for *redA*. Since additional Southern blots generated single *redA* restriction fragments, similar to *HindIII*, (Chapter 4) and only a single transcript was detected on northern blots when probed for *redA*, it is considered

Figure 3.8: Southern blotting analyses of *redA* and *redB*

3µg of genomic DNA, isolated from microplasmodia of the apogamic strain CL (Section 2.3.2), was digested to completion with the restriction enzymes indicated (Section 2.3.1) and size-fractionated in 0.8% agarose gels (Section 2.4.1). The size-fractionated DNA was denatured and blotted to Hybond-N membrane using the 10 × SSC alkaline transfer method (Sambrook *et al.*, 1989) as described in Section 2.4.1 and the DNA was fixed to the membrane by exposure to UV (Section 2.4.1).

Radio-labelled probes for *redA* (panels a. and b.) and *redB* (panel c.) were prepared using the method of Feinberg and Vogelstein (1983) as described in Section 2.4.4 and were hybridised at high stringency (65°C) to the Southern blots. The autoradiographs shown were exposed to the blots for a 2-3 week period. The relative migration of λ *Hind*III and φX174 *Hae*III DNA size markers (bp) is shown.



more likely that the two *KpnI* fragments were the result of digestion within an intron. Further extensive Southern blotting analysis confirmed that *redA* is a single copy gene that contains an intron with a *KpnI* site and clarified the reason for the presence of three *TaqI* bands for *redA* (Chapter 4).

Digestion by *KpnI* generated a single band for *redB* at high stringency, suggesting *redB* is a single copy gene with no closely related homologues (Figure 3.8c). No *RsaI* sites were identified from the cDNA sequence data but digestion with *RsaI* generated two intense bands, 1.3kb and 800bp in size, and one weak band, 3kb in size, suggesting the presence of two introns containing *RsaI* sites in the *redB* gene (Figure 3.8c). Similarly for *PstI*, no sites were identified from the cDNA sequence but digestion with *PstI* generated two intense bands, 10kb and 6.6kb in size, and two weak bands, 3.4kb and 3.0kb (Figure 3.8c) suggesting the presence of at least one intron containing a *PstI* site. The *HindIII* digestion for *redB* was unsuccessful and only partially digested fragments were observed (Figure 3.8c). Digestion with *EcoRV* generated two large fragments, in excess of 20kb in size, and one 1.6kb fragment (Figure 3.8c). Since no *EcoRV* sites were identified in the cDNA sequence, this restriction pattern suggests there may be at least one intron containing an *EcoRV* site within the *redB* gene. The analysis of *redB* was continued by Juliet Bailey and a *redB* genomic clone was isolated that indicated *redB* is a single copy gene with at least three introns (Bailey *et al.*, 1999).

Reducing the stringency of hybridisation generally permits cross hybridisation of probe DNA to less closely related genes. When low stringency hybridisation was applied to the *redA* and *redB* Southern blots, no additional bands were observed (data not shown). The Southern and northern analysis of *redA* and *redB* at low and high stringency indicates that these are unique single-copy genes that do not belong to gene families.

3.3 DISCUSSION

3.3.1 Screening cDNA libraries for longer *red* gene cDNAs

The cDNA clones for the four *red* genes investigated in this study were all missing a proportion of 5' sequence. Screening the ML8A and ML8S cDNA libraries identified a *redB* clone that contained an additional 15bp of the missing 5' cDNA sequence. ML8A was also used by T'Jampens *et al.* (1997) to isolate a cDNA clone for *fragminP* (*frgP*), which was also missing some of the 5' sequence. Often, the reverse transcription reaction

used to generate cDNAs does not go to completion, resulting in a variety of different length cDNAs for the same poly(A)⁺ RNA (Sagerström *et al.*, 1997). Since the reverse transcription proceeds from the poly(A)⁺ region, it is the 5' region of the transcript that is incomplete. It is not surprising, therefore, that it is difficult to identify full-length transcripts from ML8S and ML8A. Since the primary library, ML8, contained inserts from 500bp to 2kb in size, it was not unreasonable to anticipate that some of the longer transcripts would be from the four *red* genes under investigation. However, amplification of this library would enrich for phagemids bearing smaller, or no inserts; this is reflected by the enrichment of non-insert bearing phagemids from 5% to 30% upon production of ML8A. Thus, the proportion of longer transcripts would be reduced in the amplified and subtracted libraries.

Both *redA* and *redB* hybridised to mRNA transcripts that were approximately 800 nucleotides in size (Figure 3.7). The coding regions of both cDNAs ends with a TAA stop codon and were followed by 3' untranslated regions of up to 80 nucleotides that contained the putative polyadenylation signal, AATAAA, situated 16bp ahead of the poly(A)⁺ tract (Figures 3.5 & 3.6), all of which are consistent with previous findings (e.g. Hamelin *et al.*, 1988; Kozlowski *et al.*, 1993; Morita, 1998).

By comparing the size of the transcripts detected on northern blots and the cDNA clones, it was possible to estimate the number of nucleotides missing from the cDNAs; the cDNA clones for these genes are 660bp and 645bp respectively (Figures 3.2 & 3.3). The first consideration when making such an estimate concerns the proportion of the 800 nucleotide transcripts, detected by northern analysis, likely to represent the poly(A)⁺ tail. There is conflicting evidence on the length of poly(A)⁺ tails in mRNA from *P. polycephalum*. Size estimates have varied from 65 to 250 nucleotides (reviewed by Brown & Hardman, 1981). By minimising degradation of mRNA, Brown & Hardman (1981) estimated that the length of poly(A)⁺ tails ranged from 140 to 220 nucleotides and suggested that the discrepancy with previous estimates was due to variation in degradation by endonucleases. They also demonstrated that poly(A)⁺ tails become shorter as the population of mRNA molecules ages. Green & Dove (1988) found a notable reduction in the length of the poly(A)⁺ tract of α -tubulin following mitosis and correlated this directly with mRNA stability. When most stable, in G2 phase, the poly(A)⁺ tract contained 80 nucleotides. However, when the mRNA is destabilised following mitosis, it is reduced to less than 30

nucleotides (Green & Dove, 1988). Using a similar approach to Green & Dove (1988), Binette *et al.* (1990) established that the poly(A)⁺ tails of the *proA* mRNAs contained approximately 50 residues. Using an estimated 50 nucleotides for poly(A)⁺ tract from previous gene studies (e.g. Green & Dove, 1988, Binette *et al.*, 1990), approximately 100bp of coding and 5'untranslated regions are missing from the *redA* and *redB* cDNA clones. The 5' untranslated regions can be as small as 15 nucleotides (Binette *et al.*, 1990). Therefore, at most approximately 80bp of coding sequence are missing from these cDNA clones.

3.3.2 Efficiency of subtraction of ML8A

The initial screen of the subtracted library involved only a small fraction of the total library; the majority of the clones identified were unique. It is therefore likely that this library contains additional *red* gene clones. Of the 12 clones selected for northern analysis, two were unquestionably *red* genes (*redA* and *redB*) and four failed to give a positive result. A single subtraction step was used to generate ML8S, had further subtraction been performed, the level of false positives may have been reduced (Sagerström *et al.*, 1997). However, there is no doubt that the subtraction of ML8A did lead to enrichment of genes expressed primarily during the APT. By comparing the frequency at which the *red* genes were identified in ML8A and ML8S, Bailey *et al.* (1999) estimated that there was at least a 10-fold enrichment of *red* genes within the subtracted library. The degree of enrichment by subtraction has been reported to vary from 10-fold to over 5000-fold, probably as a result of differences in the procedures used and variation in the complexity of the system under investigation (Sagerström *et al.*, 1997). The screening for *redB* generated the most new clones and, the frequency at which *redB* was identified in the two libraries was 1 in 5,250 for ML8S and 1 in 10,200 for ML8A. However, since these libraries contain different proportions of cells bearing plasmids with cDNA inserts, this equates to 1 in 780 of the insert-bearing colonies from ML8S containing *redB* clones compared with 1 in 7140 for ML8A. Further experiments are required to provide a more accurate estimation of the frequency at which *redB* clones are observed in the two libraries.

The 150 potential *red* gene clones were obtained from screening 30,000 colonies from the ML8S library, 4500 of which contained cDNA inserts. Only 12 of the 150 potential *red* genes identified in the preliminary screening of ML8S were analysed during the course of

these and previous studies, which lead to the discovery of *redA* and *redB*. However, four of the 12 clones failed to produce a discernible signal on the northern blots. Therefore, approximately 1 in 4 of the clones that gave a result were *red* genes.

Recently, E. Swanston, L. King and A. Kobayashi isolated two new *red* genes (*redE* and *redF*) by continued screening of the 150 clones (Bailey *et al.*, 1999; E. Swanston, unpublished data). The most interesting of these is *redF*, which was renamed *mynD*, after sequence analysis revealed that it was homologous to myosin type II heavy chain (Bailey *et al.*, 1999). The *mynD* cDNA clone contains approximately 1kb from an estimated 6500 nucleotide transcript and represents the 3' region encoding part of the myosin II tail region (Bailey *et al.*, 1999). This is the first myosin type II heavy chain gene to be cloned from *Physarum polycephalum* and northern data indicates that it is neither the amoebal nor the plasmodial myosin II identified biochemically in previous studies (Bailey *et al.*, 1999; Stockem & Brix, 1994).

3.3.3 Strategies for cloning differentially expressed genes

The method of screening subtracted cDNA libraries is a popular technique used to isolate differentially expressed genes (Sagerström *et al.*, 1997). The libraries used in this study were constructed several years ago (Bailey *et al.*, 1992b) and since then, the variety of techniques available has expanded and several alternative approaches now exist. More recently developed techniques include expressed sequence tag (EST) sequencing (Adams *et al.*, 1991), EST-based serial analysis of gene expression (SAGE; Velculescu *et al.*, 1995) and PCR-based techniques of representational difference analysis (RDA; Lisitsyn *et al.*, 1993), differential display (Liang & Pardee, 1992), closely related RNA arbitrary primed PCR (RAP-PCR; Welsh *et al.*, 1992) and differential subtraction display (DSD; Pardinias *et al.*, 1998). The development of such techniques has simplified the analysis of differentially expressed genes.

EST's are generated from cDNA libraries; random clones are sequenced from the 3' or 5' end of the cDNA resulting in approximately 300bp of unique sequence. The method is costly and time consuming, but can yield highly informative data. Carulli *et al.*, (1998) analysed over 9000 EST's from differentiating rat osteoblast cells and 10% of the genes identified were un-related to sequences in the databases. Screening of ML8 using EST's may reveal homology to known developmental genes from other systems and would

enable a screen of the entire library. Such a screen would also allow most duplicate clones to be identified and would help identify the longest transcripts for each individual gene represented. However, using such screening, several thousand genes would be identified of different types and it is possible that some *red* genes could be overlooked, for example, those that share no homology with database sequences, such as *redA* and *redB*. Given the cost and time involved, high-throughput EST analysis seems an unlikely candidate for studies in *Physarum polycephalum* at present.

Differential display and RAP-PCR based techniques have become popular in recent years (reviewed by Liang & Pardee, 1995). These techniques rely upon comparison of 3' fragments of cDNA generated through PCR of RNA from different cell types using arbitrary primers. Although differential display techniques provide a rapid method for isolation of differentially expressed genes, technical problems often result in false positives and limit the isolation of rare transcripts. Although less than 1µg of total RNA or mRNA are required for this procedure (Carulli *et al.*, 1998), the sequence generated is generally short and often corresponds to the 3' untranslated region (Wan *et al.*, 1996; Sagerström *et al.*, 1997). The sequence is often insufficient for database comparisons, since it may represent a poorly conserved region in the sequence. To obtain full-length cDNAs for further analysis, additional cloning is required. Therefore, the rate-limiting step for the technique is verification of the results. The specificity of the sequence generated depends largely on the primers selected and, although abundant and rare transcripts can be identified (Wan *et al.*, 1996), there is often a bias towards abundant mRNAs (Bertioli *et al.*, 1995). As the differential display techniques have become popular, refinements are continually appearing in the literature to overcome such problems (reviewed by Liang & Pardee, 1995; Matz & Lukyanov, 1998; Pardinias *et al.*, 1998).

Wan *et al.*, (1996) compared electronic subtraction (e.g. EST and SAGE), differential display and subtractive hybridisation. Interestingly, none of the differentially-expressed genes identified were common to all three screening techniques (Wan *et al.*, 1996). In order to identify all differentially expressed genes in *P. polycephalum*, such as the *red* genes, it is likely that a combination of techniques such as screening subtracted cDNA libraries and differential display is required. At this time, the ML8S cDNA library represents the most logical resource for identifying further *red* genes. The construction of the ML8 cDNA library was time consuming but has generated a valued resource for

identification of the genes for which it was originally designed (Bailey *et al.*, 1999). ML8A has also been used successfully to isolate cDNA clones for amoeba-specific, plasmodium-specific and constitutive genes, such as *frgP*, *frgA* and actin-fragmin kinase (T'Jampens *et al.*, 1997 & 1999; Eichinger *et al.*, 1996). Therefore, ML8A represents a valuable resource that could be used in conjunction with other screening techniques to obtain longer length cDNAs for a gene of interest.

3.3.4 *red* gene expression

The expression pattern of *redA* and *redB* was highest in cultures containing a high proportion of developing cells (56%; Figure 3.7), suggesting the genes were most active during the APT. This expression pattern is clearly different to that produced by amoeba- and plasmodium-specific genes (*proA* and *proP*; Figure 3.7). A relatively strong signal was detected for *redA* and *redB* in samples prepared from microplasmodia (Mi; Figure 3.7). The microplasmodia used for northern blotting analysis in these studies were prepared by transferring macroplasmodia into axenic shaken culture, and therefore are not derived from the intermediate stage in plasmodium development between the extended cell cycle and the formation of macroplasmodia. The increase in expression of these genes in microplasmodia compared to microplasmodia may be a response to the fission of the plasmodia in shaken culture and not a consequence of exposure to liquid axenic media. This idea is supported by the lack of expression of the *red* genes in amoebae growing in the same media and culturing conditions (Bailey *et al.*, 1999).

Macroplasmodia differ from microplasmodia in possessing an extensive network of veins, which provides a basis for locomotion by protoplasmic streaming. Therefore, it is likely that microplasmodia, which are constantly being broken in axenic shaken culture, are continuously trying to remodel their microfilaments to establish this network of veins. The largest microplasmodia contain several hundred nuclei and are vein-like or dumbbell-shaped. These exhibit some protoplasmic streaming, although this does not provide a basis for locomotion and does not occur through well defined veins (Kukulies *et al.*, 1987; Stockem & Brix, 1994). Microfilaments are organised into two kinds of actin cytoskeleton in plasmodia; a random cortical actin system located at the plasma membrane or organised fibrillar actin microfilaments (Section 1.3.2; Kukulies *et al.*, 1987). The extent to which these are observed in microplasmodia varies from one culture to the next, although the latter is only observed in dumbbell-shaped and vein-like microplasmodia.

Kukulies *et al.* (1987) also correlated differences in the turnover of actin with the type of microplasmodia observed, with the highest turnover occurring in the small amoeboid-like microplasmodia. Similar dynamic rearrangements are necessary during the transition from amoeba to macroplasmodia (Section 1.3) and some genes that are up-regulated during both the transition and in microplasmodia will undoubtedly be involved with regulating such rearrangements.

Bailey *et al.* (1999) reported that it was possible to obtain populations of cells undergoing the APT in which more than 60% were committed to development. The majority of these committed cells were multinucleate and were therefore not suitable for construction of the cDNA libraries. However, it would be interesting to compare the expression levels of the *red* genes and the constitutive, amoeba-specific and plasmodium-specific in such samples. The multinucleate cells in such cultures would be much smaller than a typical microplasmodium. Nevertheless, the expression level for *redA* and *redB* genes in such cultures may resemble that seen in microplasmodia. However, in contrast to microplasmodia, a *proA* signal should also be detected since some amoebae will still be present in the cell population. It would also follow, therefore, that expression of some as yet undiscovered *red* genes may not occur in microplasmodia.

The *red* genes may ultimately fall into different sub-categories. Genes such as *mynd*, may provide a purely structural role and be involved in the dynamic cytoskeletal rearrangements that occur during the developmental transition. Other *red* genes may have short transient regulatory roles, similar to the regulatory genes that exist in *Drosophila* (Tautz & Schmid, 1998). The category to which *redA* and *redB* belong remains to be determined. It is also likely that some *red* genes may be involved earlier in the amoeba-plasmodium transition than *redA* and *redB* and could exhibit an earlier peak in expression. Future analysis, including immuno-localisation of the RedA, RedB and MynD proteins to determine when in development the proteins are present and whether they co-localise to particular cell structures, is planned (J. Bailey, personal communication). Such analysis is more sensitive than northern analysis, since the expression can be pinpointed to a specific cell rather than a mixed population of cell-types. This information, together with data from a functional analysis by gene knockout or antisense studies (discussed in Chapter 5), may lead to a better understanding of the processes by which plasmodia develop from amoebae.

3.4 SUMMARY

Prior to the studies reported in this Chapter, Bailey *et al.* (1992b) sought to clone and analyse genes expressed at highest levels during the amoeba-plasmodial transition by screening a cDNA library that they constructed from a culture containing a high proportion of developing cells. Preliminary northern analysis of four genes (D6/18P, D13/3D, P4/10P and P8/8A), which were identified by screening the library, revealed that they exhibited an apparently novel pattern of gene expression during plasmodium development.

I continued screening of the ML8A and ML8S cDNA libraries to identify longer transcripts of D6/18P, D13/3D, P4/10P and P8/8A. This screening identified just a few positive clones and only one clone that was longer than the original (P8/8A). Since so few positives clones were identified from the screening of a large numbers of colonies, full length cDNAs are probably not present in these libraries. Therefore no further library screening was performed.

The longest clone for P8/8A, obtained from screening ML8S, and the three original cDNA clones for D6/18P, D13/3D and P4/10P were sequenced and database comparisons were made in order to identify any domains, motifs or homologies to genes from other systems that may suggest roles for the four genes in *Physarum polycephalum*.

No homologies, domains or motifs were identified for the clone D6/18P. The D6/18P cDNA clone was considerably smaller than the transcript detected on northern blots, 516bp compared to approximately 2500 nucleotides. Further northern analysis of D6/18P revealed a plasmodium-specific expression pattern and this gene was therefore no longer in the category of genes with a novel expression pattern (E. Swanston, Unpublished data). Since a longer cDNA for D6/18P could not be found and no homologues were identified, the analysis of D6/18P was suspended.

The C-terminal half of the protein for P4/10P contained homology to *Rhizobium* nodulation N proteins, which are involved in production of host-specific root hair deformation factors, although their exact role is unclear (Surin & Downie, 1988). However, these homologies do not indicate a role for P4/10P in *Physarum polycephalum*.

In addition, the fact that the homology only extends to the C-terminal half of the protein suggests that P4/10P may have a second functional domain at the N-terminus and may not function in a manner related to the nodulation genes. Further northern analysis revealed that P4/10P exhibited a constitutive expression pattern (Evans, 1997). Since this gene does not exhibit the novel pattern of gene expression observed on the preliminary northern blots, no further characterisation was performed.

The expression pattern of D13/3D and P8/8A, observed during preliminary northern analysis, was studied in more detail by further northern analysis using total RNA isolated from amoebae, microplasmodia, macroplasmodia and cultures of developing cells of the apogamic strain CL. The expression of these genes was highest in cultures containing a high proportion of developing cells (56%; Figure 3.7), suggesting the genes were most active during the APT. Since this expression pattern is clearly different to that produced by constitutive or amoeba- and plasmodium-specific genes, they represent a new class of differentially expressed genes that are up-regulated during the developmental transition; the *red* genes (regulated in development; Bailey *et al.*, 1999). The genes were therefore named *redA* (D13/3D) and *redB* (P8/8A) since they were the first two genes cloned and identified in this manner. Southern blotting confirmed that *redA* and *redB* are single copy genes with no closely related homologues in *Physarum polycephalum*.

The database search for domains and motifs in *redB* identified a pair of well conserved EF-hand calcium-binding domains (Bailey *et al.*, 1999). However, these domains occur in genes with several different functions and thus do not suggest a role for *redB* during plasmodium development. Further analysis of *redB* by J. Bailey revealed sequence homologies to sarcoplasmic calcium-binding proteins from invertebrates that, unfortunately, provide no indication of the role of *redB* (Bailey *et al.*, 1999).

No sequence homologies were identified in *redA*. The analysis of *redA* function and genome organisation was continued and is described in Chapters 4 & 5.

CHAPTER FOUR

**GENOME ORGANISATION AND
SEQUENCE ANALYSIS OF *REDA***

CHAPTER 4: GENOME ORGANISATION AND SEQUENCE ANALYSIS OF *REDA*

4.1 INTRODUCTION

Southern and northern blotting analysis indicate that *redA* is a single-copy gene and not a member of a multi-gene family (Chapter 3). No full-length transcript of *redA* was obtained by screening the ML8A and ML8S cDNA libraries and therefore, to complete the sequence of the coding region, *redA* genomic DNA clones were sought. Before genomic clones could be identified, further extensive Southern blotting analysis was performed to generate a restriction map of the *redA* genomic region and to identify suitable restriction fragments for the construction of genomic libraries and for PCR.

As discussed previously, cloned *P. polycephalum* genomic fragments are sometimes unstable in bacterial hosts (Section 1.5.2); therefore, PCR-based strategies were sought as an additional approach to clone *redA*. One benefit of PCR-based strategies is that fragments generated by PCR can be sequenced without cloning to bacterial hosts, if necessary. This could be particularly useful in light of the potential problems associated with cloning *Physarum* genomic sequences. Conventional PCR using genomic DNA and gene-specific primers would enable the number and location of any introns to be determined, but would be limited to the region covered by the cDNA clone and therefore, would not help identify the missing 5' coding region (McPherson *et al.*, 1991). Inverse PCR is a technique that allows amplification of regions of DNA flanking previously identified sequences by using the simple approach of circularising genomic DNA fragments. Thus, primers that would ordinarily be incompatible for PCR, due to facing in opposing directions in the sequence of interest, can be used to amplify the 5' and 3' sequences (Ochman *et al.*, 1988; Section 4.4.2). It was anticipated that Inverse PCR would enable the missing 5' coding sequence and intron sequences of *redA* to be determined.

4.2 FURTHER SOUTHERN BLOTTING ANALYSIS OF *REDA*

The preliminary data from Southern blotting analysis of *redA* indicated that there was at least one intron in this gene (Chapter 3). To map the *redA* genomic region in detail and identify suitable restriction fragments for genomic library construction and inverse PCR, Southern-blotting analysis was performed using single and double restriction digests

(Section 2.3.1). Digests generating fragments less than 7kb were potentially suitable for construction of genomic libraries or PCR. As discussed previously (Section 1.5.1), fragments larger than this are regarded unsuitable for cloning purposes due to problems with stability thought to be caused by the various repetitive DNA elements found within the genome.

Initially, Southern-blotting analysis of *redA* was performed with single restriction digestion using enzymes that had 4–6bp recognition sequences, several of which were known to cut at a single internal site from the cDNA sequence (Figure 4.1 & Chapter 3). However, the smallest *redA* genomic fragment generated from these digestions was 8kb (*Bam*HI; Table 4.1) and was larger than desired for cloning.

Further Southern blotting analysis was performed using single and double restriction digestion (Table 4.1). For some double restriction digestion, *Ava*I was selected as an ‘anchor’ for gene mapping purposes and this mapping is discussed in detail in Section 4.5. Digestion with *Ava*I generated a 20kb *redA* fragment (Figure 4.2 & Table 4.1). It was anticipated that combining *Ava*I digestion with restriction enzymes that do not cut at internal sites may reduce the 20kb *Ava*I fragment to a more suitable size for cloning and PCR purposes and would simplify the mapping. The sequence data from the cDNA clone indicate that a single *Ava*I site is located close to the 3’ end of the coding region (Figure 4.1). The 3’ sequence beyond the *Ava*I site contains only 120bp of the cDNA from which the probe is generated. Therefore, the signal intensity for fragments carrying this 3’ portion would be low when compared to fragments bearing the larger 5’ region. In addition to the major 20kb *Ava*I fragment, a faint 1.2kb *Ava*I fragment was sometimes observed on the Southern blots and this was presumed to be the 3’ fragment (Table 4.1; Southern blot not shown). Provided no further *Ava*I sites exist within introns in the *redA* gene, fragments greater than 600bp generated by double digestion would contain the missing 5’ coding sequence and any introns located ahead of the *Ava*I site. Further discussion of the Southern blotting analysis is included in Sections 4.3 to 4.5.

4.3 CONSTRUCTION OF GENOMIC LIBRARIES CONTAINING *REDA*

Genomic libraries provide a convenient means of cloning fragments of the genome and are a valued resource for isolation of individual genes or gene families. Libraries can be constructed from complete genomes, although there is often a bias for the smaller

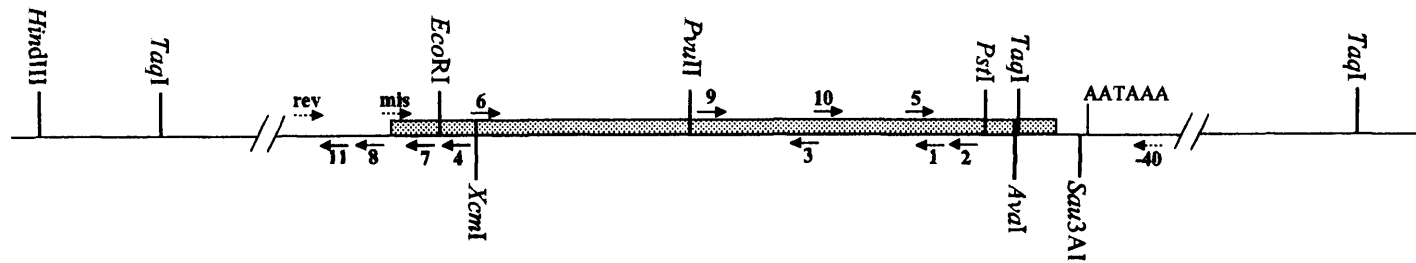
Figure 4.1: The location of *redA* primers and some restriction sites as deduced from cDNA sequence analysis and Southern blotting

The preliminary sequence of *redA* was determined manually using T7 DNA polymerase and the Sequagel™ sequencing system (Section 2.4.5) with the universal reverse and M13-40 primers located in the vector sequence. Gene-specific primers were then designed against this sequence for further sequence analysis and PCR of *redA* using the Wisconsin Package, Genetics Computer Group (Madison, USA) on the Leicester University mainframe computer and synthesised as described in Section 2.4.5.

The locations and directions of the primers used in these studies are indicated using arrows (—▶). The universal reverse and -40 primers located in the vector sequence flanking the cDNA are denoted by a broken arrow (- - -▶). The sequence of each primer and the studies for which it was used are shown in the table. Where cloning sites were added at the 5' end of the primer, the restriction enzymes are named. The gene-specific primers were all designed from the original cDNA clone (D13/3D) and are therefore named accordingly.

The area indicated by a shaded box (▒) represents the region of *redA* covered by the cDNA clone. All other regions are indicated by a single line (—). The relative position of a few important restriction sites and the putative polyadenylation signal (AATAAA), identified from sequence analysis of the cDNA clone, are included on this map. The sites located in the regions flanking *redA* are not shown to scale. Although an intron containing a *Kpn* I site was identified by Southern blotting analysis (Chapter 3), its location could not be determined from the Southern blot data available at the time and, therefore, it has been excluded from this map.

Figure 4.1



Number	Primer Stock Code	Primer Sequence	Used for
1	D13/3D-1tag	5'- <i>XhoI/HincII/SaII</i> :TGGTG TAGTCCCTTCCCTCC-3'	PCR
2	D13/3D-2	5'-GGCTGTTACGGTGTTAATTGG-3'	Sequencing, PCR
3	D13/3D-3	5'-TTGGGTGACGCTGTGTGGGC-3'	Sequencing, PCR, Inverse PCR
4	D13/3D-4	5'-GCACTTGGAATCAGAGAATT-3'	Sequencing, PCR
5	D13/3D-5	5'-GCAATAAGGAGGGAAGGAC-3'	Sequencing, PCR, Inverse PCR
6	D13/3D-6tag	5'- <i>XbaI/NotI</i> :CAAATGCCACCTTCACTATG-3'	Sequencing, PCR, Inverse PCR
7	D13/3D-7tag	5'- <i>XbaI/NotI</i> :TATTGACAAGAAACCAGGC-3'	Sequencing, PCR, Inverse PCR
8	D13/3D-8	5'-CCGAGATATTATCATTCTCC-3'	Sequencing, PCR
9	D13/3D-9	5'-TTGAATGCAATGACCAG-3'	Sequencing, PCR
10	D13/3D-10	5'-GTCACCCAAGCTATATATCC-3'	Sequencing, PCR
11	D13/3D-11	5'-ATGGTAGAAATTGCATGGC-3'	Sequencing, PCR
-40	M13 -40 primer	5'-GTTTTCCCAGTCACGAC-3'	Sequencing, PCR
rev	reverse primer	5'-GGAAACAGTATGACCATG-3'	Sequencing, PCR
mis	D13/3D-mis	5'- <i>EcoRV/EcoRI</i> :GAAAGGAAGC-3'	Creation of frameshift by PCR

Table 4.1: Data from Southern blotting analyses of *redA*

These data were compiled from several Southern blots and some digestions were repeated up to six times. When a particular digestion was repeated (e.g. *KpnI*; Figure 3.8 & Figure 4.2), there were sometimes small discrepancies with the calculated size of the fragment(s) produced as an artefact of the blotting procedure. In these cases the range of estimated sizes is given. The sizes of the bands were determined relative to λ *HindIII* and ϕ X174 *HaeIII* DNA size markers.

Restriction digests marked with a 'cross' (†) are included in Figure 4.2 and those marked with a 'double cross' (‡) are included in Figure 3.8. Fragments shown in **bold** were used in conjunction with sequence data to generate a map of the genomic region containing *redA* (Figure 4.4). Fragments thought to be generated by star activity involving *HindIII* (Section 4.5) are marked by an asterisk (*). Fragments shown in (brackets) produced a low intensity signal on the Southern blot and are thought to be either the product of asymmetric digestion within the *redA* gene (e.g. the 1.2kb *AvaI* fragment; Section 4.5) or partial digestion (e.g. the 1.8kb *TaqI* fragment; Section 4.6). The deduced fragment ends from double digests and the location of sites identified from the sequence data are shown where possible.

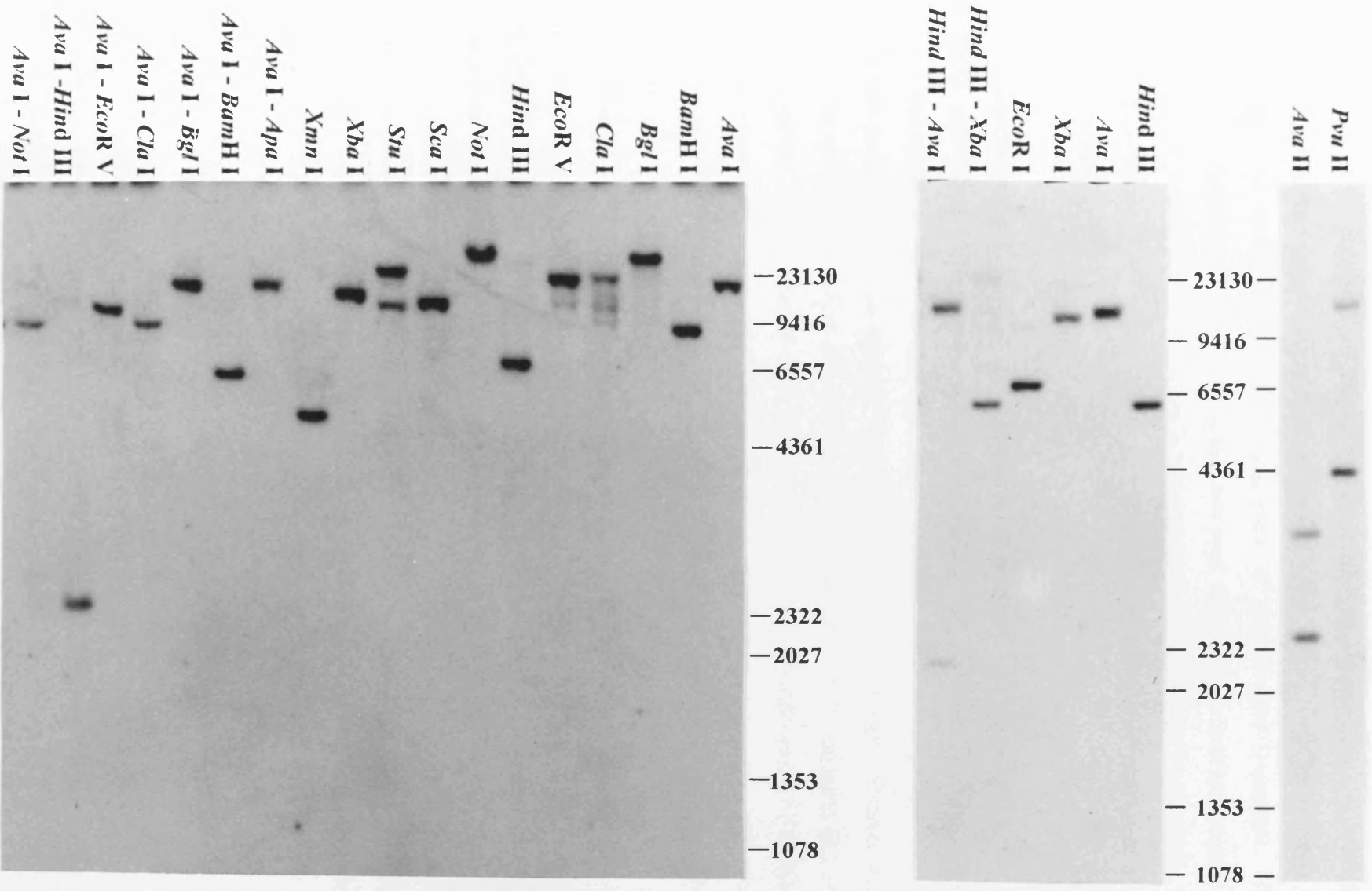
Table 4.1

Restriction digest		Fragment size(s)	Additional information
† <i>Ava</i> I	-	20kb, (1.2kb)	<i>Ava</i> I site 539bp into cDNA clone
† <i>Ava</i> II	-	3kb, 2.5kb	<i>Ava</i> II site in intron 2
† <i>Bam</i> HI	-	8kb	No internal site
† <i>Eco</i> RI	-	7kb, (2.2kb) (9.4kb)	<i>Eco</i> RI site 87bp into cDNA
† <i>Eco</i> RV	-	19-20kb	No internal site
† <i>Hind</i> III	-	6.2-6.8kb (Av. 6.6kb)	No internal site
<i>Hpa</i> I	-	21kb	No internal site
‡ <i>Kpn</i> I	-	6.0-6.6kb, 580-700bp	<i>Kpn</i> I sites 2bp into coding region and at start of intron 2
† <i>Not</i> I	-	≥23kb	No internal site
‡ <i>Pst</i> I	-	≥23kb or (15kb) & (9kb)	<i>Pst</i> I site 494bp into cDNA
† <i>Pvu</i> II	-	(20kb) or 4.4-4.8kb, (3kb), (3.5kb)	<i>Pvu</i> II site 201bp into cDNA clone
‡ <i>Taq</i> I		(1.8kb), 1.5kb, 900bp	<i>Taq</i> I sites in intron 2 and 540bp into cDNA clone
† <i>Xba</i> I	-	15-16kb	No internal site
<i>Xcm</i> I		6.6-6.7kb	<i>Xcm</i> I site 115bp into cDNA clone
† <i>Xmn</i> I		5kb	No internal site
† <i>Ava</i> I	<i>Apa</i> I	20kb	<i>Ava</i> I only
<i>Ava</i> I	<i>Ava</i> II	3kb, 2.5kb, (2kb), (1.8kb)	-
† <i>Ava</i> I	<i>Bam</i> HI	6kb	<i>Bam</i> HI- <i>Ava</i> I
† <i>Ava</i> I	<i>Bgl</i> I	20kb	<i>Ava</i> I only
† <i>Ava</i> I	<i>Cla</i> I	9.5kb	<i>Cla</i> I- <i>Ava</i> I
† <i>Ava</i> I	<i>Eco</i> RV	14kb	<i>Eco</i> RV- <i>Ava</i> I
† <i>Ava</i> I	<i>Hind</i> III	2.4kb*, (20kb), (1.2kb)	(<i>Ava</i> I only)
† <i>Ava</i> I	<i>Not</i> I	10kb	<i>Not</i> I- <i>Ava</i> I
<i>Ava</i> I	<i>Pst</i> I	20kb	<i>Ava</i> I- <i>Pst</i> I
<i>Ava</i> I	<i>Sca</i> I	9.5-10kb	<i>Sca</i> I- <i>Ava</i> I
<i>Ava</i> I	<i>Xba</i> I	4kb, (20kb)	<i>Xba</i> I- <i>Ava</i> I, (<i>Ava</i> I only)
<i>Ava</i> II	<i>Eco</i> RI	3kb, 2.5kb	<i>Ava</i> II only
<i>Ava</i> II	<i>Pst</i> I	3kb, 2.5kb	<i>Ava</i> II only
<i>Ava</i> II	<i>Pvu</i> II	3kb, 2.3kb	<i>Ava</i> II- <i>Ava</i> II, <i>Pvu</i> II - <i>Ava</i> II
<i>Eco</i> RV	<i>Hind</i> III	6.4kb	<i>Hind</i> III only
<i>Eco</i> RV	<i>Xba</i> I	8kb	-
<i>Hind</i> III	<i>Kpn</i> I	6kb, 600bp	<i>Kpn</i> I only
<i>Hind</i> III	<i>Pst</i> I	6.2-6.6kb	<i>Hind</i> III- <i>Pst</i> I
† <i>Hind</i> III	<i>Xba</i> I	2.4kb* or 6.2-6.8kb	(<i>Hind</i> III only)
<i>Kpn</i> I	<i>Sma</i> I	6.6kb, 600bp	<i>Kpn</i> I only
<i>Pst</i> I	<i>Xba</i> I	16kb	<i>Xba</i> I only

Figure 4.2: Southern blotting analyses of *redA*

3µg of genomic DNA, isolated from microplasmodia of the apogamic strain CL (Section 2.3.2), was digested to completion with the restriction enzymes indicated (Section 2.3.1) and size-fractionated in 0.8% agarose gels (Section 2.4.1). The size-fractionated DNA was denatured and blotted to Hybond-N membrane using the 10 × SSC alkaline transfer method (Sambrook *et al.*, 1989) as described in Section 2.4.1 and the DNA was fixed to the membrane by exposure to UV (Section 2.4.1).

Radio-labelled probes for *redA* were prepared using the method of Feinberg and Vogelstein (1983) as described in Section 2.4.4 and were hybridised at high stringency (65°C) to the Southern blots. The autoradiographs shown were exposed to the blots for a 9-day period. The relative migration of λ *Hind*III and φX174 *Hae*III DNA size markers (bp) is shown.



fragments within the library. This bias can occur during the outgrowth period immediately following transformation or during any subsequent bacterial culture since the bacteria with small plasmids are able to replicate, and thus divide, more rapidly than bacteria harbouring larger plasmids. However, this effect can be limited by size-fractionation of the digested DNA into pools of similar-sized fragments. This concentrates fragments of the desired size into one pool, which can be used to construct an enriched library with reduced variation in plasmid sizes. Similar size-fractionation has been used successfully by other research groups to clone *Physarum polycephalum* genes (e.g. Binette *et al.*, 1990).

4.3.1 Construction of *HindIII* – *PstI* genomic libraries

Initially, size-fractionated genomic libraries of *HindIII*–*PstI* digested CL genomic DNA were constructed. This digestion generated fragments 6.4kb in size for *redA* and 4.4–4.6kb for *redB* (data not shown). Therefore, *HindIII*–*PstI* genomic libraries would not only be useful for isolation of a *redA* genomic clone, but also for isolation of a *redB* genomic clone. Eight fractions were produced relative to λ *HindIII* and ϕ X174 *HaeIII* DNA size markers: 500bp–1kb, 1–2kb, 2–2.5kb, 2.5–4.4kb, 4.4–6.6kb, 6.6–9.4kb, 9.4–15kb and 15kb+ (Section 2.3.4). The first five fractions were ligated individually to pBluescript® II (Stratagene) with *HindIII*–*PstI* phosphatased cloning ends and transformed into XL1–Blue to generate libraries LL2–LL6 (Leicester Library; Table 4.2; Section 2.3.4). For each library, the total number of colony forming units (cfu) was determined by plating 10 to 10⁹-fold serial dilutions and counting the number of colonies. The percentage of vectors bearing inserts was estimated by determining the number of plasmids with inserts in a random sample of 10–20 colonies (Table 4.2). A fraction of each library was amplified by inoculating 10 × 9cm LB–amp plates with 600–1800 colonies per plate. After overnight incubation at 37°C, the colonies were suspended in 2ml LB–broth per plate, pooled and sterile glycerol was added to a final concentration of 10%. A small amount of the pooled suspension was used in serial dilutions to assess the final cell density and percentage inserts for the amplified libraries as described before.

The construction of *HindIII*–*PstI* size-fractionated genomic libraries was not taken further than fraction 4.4kb–6.6kb. For fractions larger than this, test ligations indicated that the number of colony forming units containing genomic fragments would have dropped to close to zero in the primary library (data not shown; Table 4.2). In addition,

Table 4.2: Details of the size-fractionated *HindIII-PstI* genomic libraries

Ten duplicate *HindIII-PstI* digestions (Section 2.3.1) of 3-5 μ g of genomic DNA isolated from microplasmidia of the apogamic strain CL (Section 2.3.2) were size-fractionated across ten lanes of a 0.8% agarose gel. Using λ *HindIII* and ϕ X174 *HaeIII* DNA size markers for reference, the DNA fractions indicated were isolated from the appropriate section of the gel by mineral wool filtration (Section 2.3.2). Five *HindIII-PstI* digested genomic DNA fractions were ligated to pBluescript II prepared with *HindIII-PstI* cloning ends that had been treated with phosphatase to prevent self-ligation (Section 2.3.3); these were then transformed into XL1-Blue competent cells to generate the five basic libraries (LL2-LL6; Section 2.3.5). For each library, the total number of colony forming units (cfu) was determined by counting the number of colonies that grew after 16 hours at 37°C using 10 to 10⁹-fold serial dilutions (Section 4.3.1). Each library was amplified by overnight incubation (37°C) of ten replica plates, each containing an inocula of 600-1800 cfu; the colonies from each plate were then suspended in 2ml-LB broth, pooled and sterile glycerol added to a final concentration of 10% for storage as 1ml aliquots at -80°C. The percentage of plasmids bearing inserts was estimated from random sampling of 10-20 colonies from each library (Section 2.2.5).

Library LL6 was not amplified since it was predicted that amplification would have led to a loss of inserts (Section 4.3.1). The apparent decline in the percentage of inserts observed for the larger genomic fragments (LL5-LL6) was deduced to be associated with repetitive elements within the *Physarum* genome and/or plasmid stability in the bacterial host (Section 4.3.2).

Table 4.2

Library code	DNA Fraction (kb)	Basic Library			Amplified Library		
		cfu ml ⁻¹	Total colonies	% inserts	cfu ml ⁻¹	Total colonies	% inserts
LL2	0.5 - 1.0	9.1 x 10 ³	1.4 x 10 ⁶	95	6.8 x 10 ⁵	1.4 x 10 ⁷	79
LL3	1.0 - 2.0	9.0 x 10 ²	2.2 x 10 ⁴	90	2.2 x 10 ⁵	4.2 x 10 ⁶	83
LL4	2.0 - 2.5	2.8 x 10 ³	6.4 x 10 ⁴	60	8.7 x 10 ⁵	1.8 x 10 ⁷	20
LL5	2.5 - 4.4	2.6 x 10 ⁴	2.9 x 10 ⁵	40	1 x 10 ⁶	2.2 x 10 ⁷	0
LL6	4.4 - 6.6	4.9 x 10 ³	6.9 x 10 ³	30	-	-	-

such fragment were reaching the upper size-limit for plasmid stability (Section 1.5.2). Overall in these libraries, as the size of fragments increased, the number of plasmids with inserts decreased (Table 4.2). Several factors may have caused the steady decline in cfu's bearing inserts, some of which are discussed below.

4.3.2 Problems associated with construction of genomic libraries

Screening LL6 for *redA* suggests that recombination may have occurred in the plasmid, since some inserts were only 2kb or less in size (data not shown). As discussed in Chapter 1, the repetitive elements in the *P. polycephalum* genome have been known to cause problems with stability of genomic fragments cloned into bacterial hosts. Recombination of repetitive elements in the genomic fragment (Nader, 1986) would result in some vectors containing a truncated insert.

The major repetitive element, Tp1, contains two *HindIII* sites (Pearston *et al.*, 1985) and is located in scrambled clusters throughout the genome (Section 1.5.1). However, since the Tp1 element does not contain any *PstI* sites, it was anticipated that the majority of these repetitive elements would be contained on *HindIII* fragments and would be excluded from the *HindIII*-*PstI* libraries through design (*HindIII*-*PstI* cloning ends). The Tp1 elements were therefore, less likely to cause instability in these libraries. However there is a possibility that recombination may have occurred across 'foldback' repeats or single nucleotide tracts (discussed in Section 1.5.2) to generate the smaller fragments in the 4.4-6.6kb library, LL6.

When the libraries were amplified, the number of plasmid-free cells increased (data not shown). For example, when LL3 was amplified, 100% of the colonies investigated contained plasmids, however, when LL5 was amplified, approximately 30% of the colonies investigated were plasmid-free. In addition to problems associated with stability of cloned genomic fragments due to recombination within the cloned genomic fragment, plasmid stability in the bacterial host can be problematic. At cell division, *E. coli* cells distribute plasmids randomly and provided the copy number remains high, plasmid-free cells are rarely formed. However, some vectors are notoriously bad when it comes to maintaining plasmid stability, e.g. the pUC series of vectors (Summers, 1998); pBluescript® II is a pUC-based vector. Such plasmids are normally maintained at over 100 copies per cell but are often lost at high frequency when the cells are grown in

non-selective conditions. The copy number can be regulated by the cell: if the copy number is too low each plasmid replicates more than once for each generation; if too high, the opposite occurs (Summers, 1998). Multimers formed by recombination out-replicate monomers by virtue of the fact they carry multiple replication origins (Summers, 1998). Eventually the population could reach a point at which most cells contain only multimers (the dimer catastrophe model; Summers *et al.*, 1983). Although the copy number of multimer containing cells may be correct, the plasmid distribution at division is uneven and permits a high frequency of plasmid-free cells forming (Summers, 1998). In reality, this kind of multimerisation is avoided because multimer containing cells grow slower than those containing monomers (Summers, 1998). Natural plasmids, such as ColE1, are able to resolve plasmid multimers back to monomers by site-specific recombination (Summers, 1998). However, many man-made plasmids, including Bluescript II, often lack the components required for multimer resolution and therefore suffer from instability. Although selective conditions were used when growing the *HindIII-PstI* genomic libraries, there is a possibility that the antibiotic had suffered a loss in activity sufficient to enable plasmid loss to contribute to the decline in inserts within the libraries.

One reason it is so difficult to clone fragments larger than 6kb, and another possible cause for the reduction in insert bearing vectors, is that once the vector was the smallest fragment within the ligation, the larger molecules of genomic DNA may be more likely to ligate to one another at random than to the vector. Fragments of genomic DNA ligating to each other to form circular molecules would be lost, since they would not be resistant to antibiotics and would not carry any of the components required for bacterial transfer or maintenance. This would result in a smaller library with a high proportion of self-ligated vector. In addition, subsequent amplification of such libraries would lead to an increase in the proportion of self-ligated vector, since bacteria containing these plasmids would be able to outgrow those with the larger plasmids, consisting of vector plus genomic fragment. This general trend is apparent in these libraries (Table 4.2).

4.3.3 Screening the *HindIII – PstI* library, LL6, for *redA*

Approximately 6,000 colonies (1,200 colonies × 5 plates) from the library containing 4.4–6.6kb *HindIII-PstI* fragments (LL6; Table 4.2) were screened for *redA* using colony blot hybridisation (Section 2.4.3). This screening generated a high level of background activity and was therefore repeated using a second batch of newly prepared colony filters.

Most of the putative positive clones selected for further analysis contained inserts that were notably smaller than expected suggesting there may be a problem; only 2 of the 12 clones from the second screen contained inserts larger than 4kb while the remaining clones contained inserts less than 2kb in size. Following Southern blotting analysis of these putative positive clones, it became apparent that none contained a *redA* genomic fragment. However, some of the small inserts were of a similar size, suggesting there was a bias for one particular clone. Subsequent sequence analysis of this clone revealed that the *redB* cDNA had contaminated at least two of the libraries: LL5 and LL6.

One factor common to construction of both LL5 and LL6 was the source of cloning vector and this is the most likely route of *redB* cDNA contamination. A fresh batch of phosphatased *HindIII*–*PstI* digested Bluescript II was prepared for construction of LL5 and LL6. The initial tests to determine the cloning suitability of the digested vector generated a relatively high level of apparent background self ligation. The vector fragment was re-purified using DEAE membrane to eliminate fragments smaller than 3kb and re-phosphatased to reduce this background ligation. A small fragment was observed at low frequency in most of the digests performed during and after the construction of these libraries, but at the time was thought to be the product of internal digestion of the ligated genomic fragment. There are several possible routes by which the *redB* cDNA could have contaminated the vector; these are discussed below.

Had the *redB* cDNA contaminated the vector prior to digestion with *HindIII*–*PstI*, a linear 3.6kb band would have been observed on the agarose gel following electrophoresis, since the *redB* cDNA contains no *PstI* sites. If this was of low abundance, it may not have been visible or may have been mistaken for uncut plasmid. In addition, subsequent phosphatasing of this 3.6kb *HindIII* fragment should have then excluded it from self-ligation, thus no cDNA plasmid molecules would have been detected in the library.

It is more plausible that a small amount of pure undigested *redB* plasmid contaminated the vector supply shortly after it was digested with *HindIII*–*PstI*. This would then be included in the transformation and would constitute a substantial proportion of the library. Unfortunately, this means that these libraries are unsuitable for the *redA* or *redB* screening that they were designed for, since the *redB* cDNA containing clones would outgrow the genomic clones.

4.3.4 Construction and screening of a *HindIII*–*XhoI* genomic library

Since there were problems constructing *HindIII*–*PstI* libraries with genomic fragments larger than 6.6kb, smaller fragments for cloning were sought. Libraries containing fragments approximately 2kb in size have been used successfully to obtain genomic clones for *redB* and *redE* (Bailey *et al.*, 1999; E. Swanston; personal communication). Southern blotting analysis indicated that *HindIII*–*AvaI* digestion generated a 2.4kb *redA* fragment (Figure 4.2 & Table 4.1). Therefore, this digestion was selected for construction of a size-fractionated genomic library. The 1.4–4.4kb fraction of *HindIII*–*AvaI* digested CL genomic DNA (10µg) was isolated using a QIAquick gel extraction kit (Qiagen), pooled, precipitated and resuspended in 20µl of sterile distilled water.

The *AvaI* site located in *redA* has an identical recognition sequence to *XhoI* and generates the same overhang (C▼TCGAG). The vector, pBluescript II, was prepared with *HindIII*–*XhoI* cloning ends since *AvaI* is not a unique site in Bluescript II and was therefore unsuitable for cloning. The 1.4–4.4kb fraction of *HindIII*–*AvaI* digested CL genomic DNA was ligated to *HindIII*–*XhoI* digested Bluescript II and transformed to XL1–Blue to generate a *HindIII*–*XhoI* genomic library (4.8×10^5 colonies, 50% inserts). Five 9cm LB–amp plates were prepared (350 colonies per plate) for colony hybridisation against *redA* (Section 2.4.3). Following hybridisation, plasmid DNA was isolated from the putative positive clones and digested with *PvuII* to determine whether they were genuine *redA* genomic clones. An internal *PvuII* site, situated near the middle of the *redA* cDNA (Figure 4.1) and two *PvuII* sites that flank the MCS in Bluescript II provide a diagnostic digest that was used for much of the cloning. If the vector contained no insert, 2.95kb and 430bp fragments were observed. If the vector contained the *redA* cDNA, 2.95kb (vector), 630bp and 450bp fragments were observed. Banding patterns that differed from these were investigated further to determine whether they contained the desired clone.

Unfortunately, none of the colonies contained a genomic clone for *redA*. It subsequently became apparent that the 2.4kb *HindIII*–*AvaI* fragment detected by Southern blotting may be an artefact of star activity involving *HindIII* in some double digests (discussed in Section 4.5). Therefore, it was considered unlikely that this library would contain a *redA* genomic fragment. Since there were problems with identifying suitable fragments for

further construction of genomic libraries and due to time constraints, different approaches to cloning the *redA* gene were sought.

4.4 USE OF PCR TO AMPLIFY GENOMIC COPIES OF *RED A*

4.4.1 Optimisation of PCR conditions

The polymerase chain reaction is sensitive to several factors, including reaction conditions and nucleic acid sequence composition. Therefore, optimisation of conditions such as buffers, primers and the choice of thermal cycle is often necessary.

During the analysis of *redA*, nine primers were designed spanning the forward and reverse strands of the cDNA clone (Figure 4.1). Since all of these primers were designed using the cDNA sequence, there was a possibility that one or more of them may lie on an intron/exon splice site and would not, therefore, function with genomic DNA. To rule out potential problems with the primer design, PCR program 2 (Section 2.4.6) was used to test all possible combinations of the primers (see Figure 4.1) against genomic DNA using the cDNA as a positive control. PCR performed using the cDNA generated clean bands of the anticipated sizes. However, despite several attempts, PCR using genomic DNA did not generate any bands.

The PCR buffer used routinely by the Leicester *Physarum* group contains 50mM KCl, 10mM Tris-Cl and 1.5mM MgCl₂. The concentration of Mg²⁺ can affect PCR in two ways. If the Mg²⁺ concentration is too high, primer specificity may be affected resulting in spurious annealing to generate non-specific PCR fragments (McPherson *et al.* 1995). Alternatively, if the Mg²⁺ concentration is too low (less than 0.5μM), *TaqI* DNA polymerase will not work (McPherson *et al.* 1995). The presence of Mg²⁺ chelators, such as EDTA, can artificially lower the Mg²⁺ concentration. Therefore, in order to optimise the concentration of Mg²⁺, the concentration of MgCl₂ in the PCR buffer was varied from 0.75mM to 3.75mM, in increments of 0.75mM, and PCR was performed against the cDNA clone using PCR program 1 (Section 2.4.6). The highest concentration of MgCl₂ generated the greatest proportion of transcript. However, no positive results were obtained using this higher concentration MgCl₂ buffer with genomic DNA as a template.

Genomic DNA is a more complex template for PCR than plasmid DNA and therefore, it is often necessary to optimise the reaction conditions to enable the primers to anneal to the

template (McPherson *et al.*, 1995). Primers are only able to function in PCR provided they can anneal to the DNA template. Each round of PCR begins at 94°C, which is sufficient to denature the DNA. The temperature of the reaction is then lowered to allow the primers to anneal to the template. KCl is a standard component of many PCR buffers, however, in some instances it is replaced with NaCl, which has superior denaturing properties for sequences that are G/C-rich (McPherson *et al.* 1995). Replacing the KCl with 40mM NaCl had no effect on the PCR when genomic DNA was used as a template. Since none of the different buffers had a discernible effect on the PCR when using genomic DNA as a template, the standard PCR buffer was used for these studies. Further optimisation could be achieved by varying the pH of the PCR buffer, annealing temperature or the relative concentrations of the template and primers. However, due to time constraints, no further optimisation experiments were performed.

4.4.2 Inverse PCR

As an alternative to direct cloning of genomic DNA, PCR-based strategies were sought. Inverse PCR was selected as a means of identifying the missing 5' coding and promoter sequences (Figure 4.3). Using Southern blotting analysis a suitable-sized restriction fragment is identified containing the gene of interest; it is generally advised that fragments smaller than 3kb are selected, since fragments larger than 3kb are often difficult to amplify (McPherson *et al.*, 1991). Genomic DNA is digested with the chosen restriction enzyme and then self-ligated to form circular molecules (Figure 4.3). These molecules are then subjected to PCR with gene-specific primers designed against a previously characterised region of the gene. The primer pair face in opposite directions such that when the fragment is circularised, the flanking regions of the restriction fragment are amplified (Figure 4.3). The PCR fragment consists of the two flanking regions joined at the restriction site (R; Figure 4.3). The cDNA sequence and Southern blot data were used to identify potential restriction fragments for inverse PCR (Chapter 3, Figure 4.2 & Table 4.1).

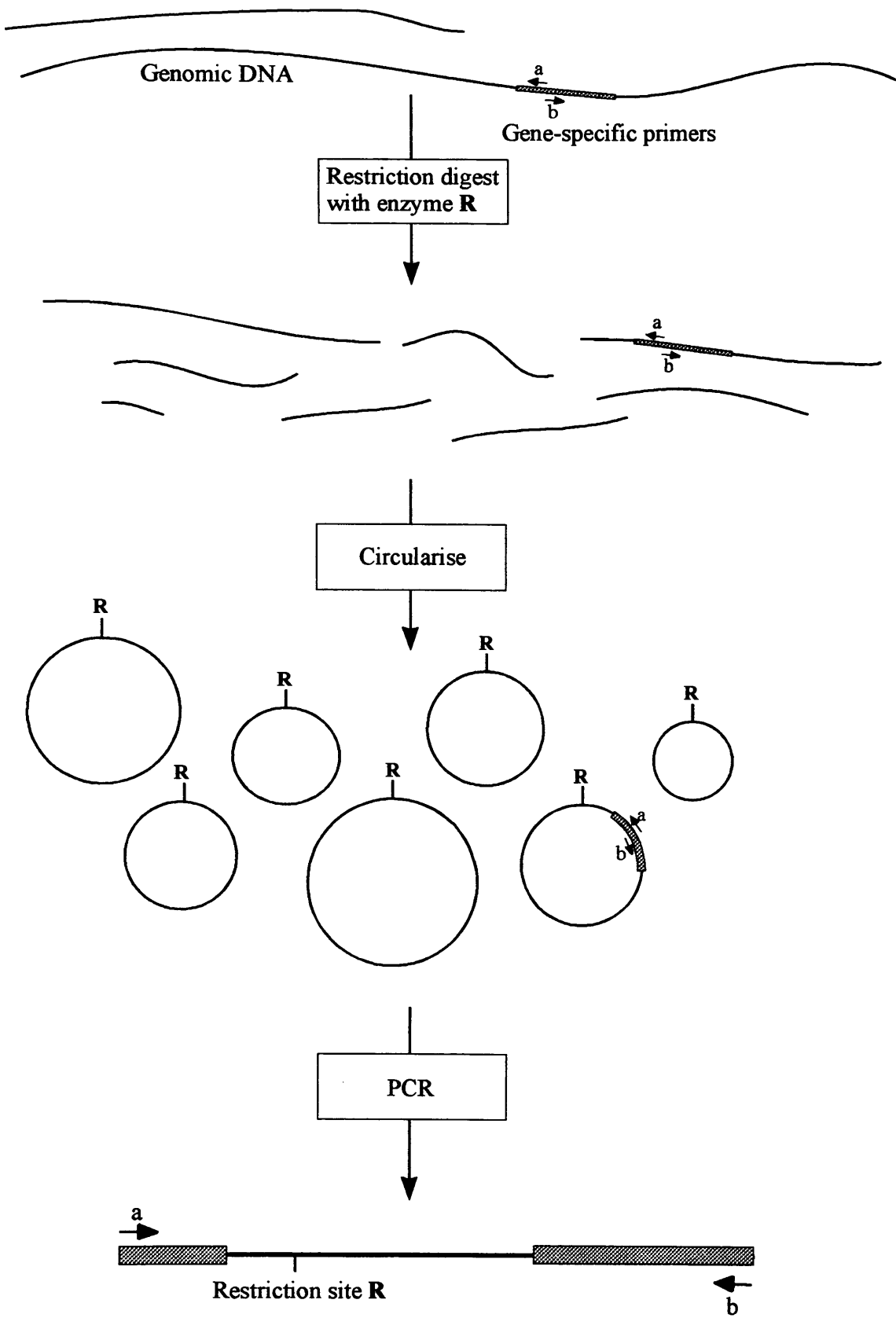
4.4.2.1 Inverse PCR using *TaqI* digested genomic DNA

Sequence data from the cDNA clone highlighted the presence of a single *TaqI* restriction site close to the 3' end of the gene (Figure 4.1). Digestion of genomic DNA with *TaqI* generated three *redA* fragments: 1.8kb, 1.5kb and 900bp (Figure 3.8) which were all of a suitable size for inverse PCR (see above). The intensity of the signal obtained for the

Figure 4.3: Schematic representation of inverse PCR

Using Southern blotting analysis (Section 2.4.1), a suitable-sized restriction fragment is identified containing the gene of interest (——). Genomic DNA is digested with the chosen restriction enzyme, **R** (Section 2.3.1), and self-ligated to circularise the fragment (Section 2.3.3). These molecules are then subjected to rounds of PCR (Section 2.4.6) with gene-specific primers (\leftarrow^a & \rightarrow^b) designed against a previously characterised region of the gene (Section 2.4.5). The primer pair face in opposite directions such that when the fragment is circularised, PCR leads to amplification of the flanking regions. The PCR fragment generated consists of the two regions that flank the gene joined at the restriction site, **R**.

Figure 4.3



1.8kb fragment was notably lower than the other two when *TaqI* was included on a second Southern blot (data not shown); suggesting that this band may be the product of partial digestion. This was subsequently confirmed (see below).

The missing 5' region of *redA* was estimated to be no more than 80bp in size (Section 3.3.1). The internal *TaqI* site is located 541bp into the *redA* cDNA clone. Since *P. polycephalum* exons vary from approximately 50bp–350bp in size (e.g. Nader *et al.*, 1986; Binette *et al.*, 1990), it is likely that the genomic region leading to the internal *TaqI* site contains at least one intron. Introns vary from approximately 50bp–280bp in size (e.g. Nader *et al.*, 1986; Binette *et al.*, 1990), but are generally 100bp–150bp in size. Therefore, allowing for introns, it was anticipated that even the smallest of the *TaqI* genomic fragments (900bp) would contain sufficient sequence to enable the missing 5' coding sequence to be determined.

Genomic DNA was digested to completion with *TaqI* and self-ligated using T4 DNA ligase at $2\mu\text{g ml}^{-1}$, for four hours at 4°C followed by 16 hours at ambient room temperature. The highly dilute conditions of the ligation reaction reduce the chance of inter-molecule ligations and thereby increase the efficiency of circularisation of the genomic DNA through self-ligation (McPherson *et al.*, 1991). The ligation mixture was P:C:I extracted, ethanol precipitated and the DNA was then pelleted and resuspended at $100\text{ng }\mu\text{l}^{-1}$ in sterile distilled water. PCR was performed using 500ng of the circularised DNA with primers D13/3D-6tag and D13/3D-7tag (Figure 4.1) and PCR program 3 (Section 2.4.6). The primers used were both designed with restriction sites at their 5' ends for ease of cloning (Figure 4.1). A second round of amplification was performed using 10% of the original PCR reaction in the same conditions. The PCR fragment was approximately 900bp in size and, therefore, corresponded with the smallest fragment observed on Southern blots (Figure 3.8). This fragment was isolated using DEAE membrane, digested at the *NotI* cloning sites located in the primers and then ligated to pBluescript II prepared with *NotI* phosphatased, cloning ends. Following transformation into XL1-Blue, plasmid DNA was isolated from several clones and two were selected that contained the inverse PCR fragment in different orientations. The two PCR fragments were then sequenced and analysed using the GCG software program (Section 2.4.5). The findings of this analysis are discussed in detail below (Section 4.6). Briefly, analysis of

the *TaqI* inverse PCR fragment revealed that *redA* contains at least two introns and enabled the full coding region to be identified (discussed in Section 4.6).

A *TaqI* site was identified in intron 2; therefore, the full sequence of this intron was not amplified by the inverse PCR (Section 4.6). The presence of a *TaqI* site within the second intron explains the presence of three *TaqI* fragments on the Southern blots (Figure 3.8). The sequence data from the *TaqI* inverse PCR fragments and the cDNA clone indicate that the two internal *TaqI* sites are separated by a minimum of 286bp (Figure 4.4). Since the 1.5kb and 1.8kb fragments differ in size by approximately 300bp, it was concluded that the 1.8kb fragment was the product of partial digestion at the second *TaqI* site (discussed in detail in Section 4.6). This also accounts for the lower intensity of hybridisation to the 1.8kb fragment on the second Southern blot (data not shown).

It was possible that the circularised DNA prepared for the *TaqI* inverse PCR also contained the second, smaller internal *TaqI* genomic fragment. The data from the 900bp *TaqI* inverse PCR fragment indicated that the two *TaqI* sites in the *redA* gene are separated by approximately 300bp (discussed in Section 4.6) and that this small region contained binding sites for primers D13/3D-5 and D13/3D-3 (Figure 4.1), which are suitable for inverse PCR. Therefore, a second *TaqI* inverse PCR reaction was performed using the remainder of the circularised *TaqI* genomic DNA and these primers. Following two rounds of PCR, no fragment was observed. This may have been associated with the small size of the fragment causing problems with the circularisation step (McPherson *et al.*, 1991).

4.4.2.2 Further Inverse PCR experiments

In an attempt to obtain genomic sequence data for the entire *redA* gene, further inverse PCR experiments were performed using different restriction fragments. Digestion with *XmnI* generated a single fragment approximately 5kb in size (Figure 4.2). No *XmnI* site was identified in *redA* from the sequence data for either the cDNA or *TaqI* inverse PCR clones. Therefore, it was anticipated that the entire *redA* gene is located on the 5kb *XmnI* fragment. Genomic DNA was digested with *XmnI* and prepared for inverse PCR with primers D13/3D-6tag and D13/3D-7tag (Figure 4.1), as described for the *TaqI* inverse PCR. The PCR was performed using PCR program 2, which included a longer extension step (72°C; as discussed in Section 2.4.6) and an optimal annealing temperature that was

Figure 4.4: Detailed genomic restriction map of *redA*

This detailed genomic restriction map for *redA* was compiled using Southern blot and sequence data from the cDNA and *TaqI* inverse PCR clones (Section 4.5; Figure 3.5; Figure 4.2; Table 4.1; Figure 4.5). The 1.5kb region covering the *redA* gene has been enlarged as indicated. The areas indicated by shaded boxes () represent the coding region for *redA*. All other regions are indicated by a solid line (). The location of the putative polyadenylation signal is indicated by AATAAA. Restriction sites are shown in their approximate location. The region of intron 2 marked with an 'X' was not cloned and is, therefore, of undetermined size; it is possible that the region beyond this intron may contain a third intron (Section 4.6).

slightly higher than in the program used for *TaqI* inverse PCR. Although a 5kb band was expected, a band approximately 1.4kb in size was obtained. This was isolated and cloned into pBluescript II using the *NotI* cloning sites, as before. The 1.4kb fragment was sequenced and, although the two primer sequences flanked the fragment as expected, the fragment contained no sequence homology to *redA*. Therefore, this 1.4kb band appears to be the product of non-specific primer annealing.

Digestion with *PvuII* generated two fragments that hybridised to *redA*: 4.6kb and approximately 20kb (Table 4.1, Figures 4.1 & 4.2); the 4.6kb fragment was selected for inverse PCR. A *PvuII* site is located 220bp into the cDNA clone (Figure 4.1). However, the Southern blot data was insufficient to ascertain whether the 4.6kb fragment was located 5' or 3' of the *PvuII* site. Either would be informative, since the fragment located 5' of the *PvuII* site would contain further 5' untranslated promoter sequences, while the fragment located 3' of the *PvuII* site would contain the remainder of intron 2, any additional introns and the 3' untranslated region of the gene. The 2.2–6.6kb fraction of *PvuII* digested CL genomic DNA was isolated using DEAE membrane (Section 2.3.2). Size-fractionation was performed to not only enrich the DNA for the fragment of interest but to also eliminate the 20kb fragment identified by Southern blotting analysis. The DNA was circularised and two separate PCR reactions were set up as for the *XmnI* inverse PCR (see above) using primers D13/3D-6tag & D13/3D-7tag or D13/3D-3 & D13/3D-5 (Figure 4.1). Unfortunately, no genomic fragments were amplified.

4.4.2.3 Results from inverse PCR

With the exception of *TaqI*, none of the inverse PCR experiments were successful. There are several possible explanations for these failures:

- i. *PvuII* and *XmnI* both generate blunt cloning ends, whereas *TaqI* generates a 3' overhang. Blunt ended fragments are hard to ligate and therefore few circular molecules may have been generated for the primers to act upon.
- ii. The DNA template for PCR can adversely affect the reaction if it contains traces of EDTA, salts or other contaminants such as phenol, which lead to inhibition of the polymerase (McPherson *et al.*, 1995). Although the template was prepared by ethanol precipitation, there may still have been traces of contaminants that contributed to the PCR failure.

- iii. The ends of the fragments may have been damaged during the short period of exposure to UV light used to visualise the DNA to be purified in the size-fractionation of the *PvuII* fragments. This would have meant that the ends were no longer compatible and prevented them from circularising.
- iv. In addition, the possibility that the second set of primers (D13/3D-3 & D13/3D-5; Figure 4.1) were to blame for the failure of the *PvuII* inverse PCR cannot be ruled out. Although these primers worked well against the cDNA, they never worked against genomic DNA (Section 4.4.1). If a third intron exists in *redA*, the binding site for either D13/3D-5 or D13/3D-3 may be interrupted by it and these primers will, therefore, not work against genomic DNA.
- v. Finally, despite adjusting the PCR program to compensate for the larger sizes of the target sequences (4.6kb for *PvuII* and 5kb for *XmnI*), there was still a chance that the fragments were too large to allow amplification by inverse PCR (McPherson *et al.*, 1991).

4.4.3 Conventional PCR

It was anticipated that the sequence for the missing portion of intron 2 and any unidentified introns could be obtained using conventional PCR. Once the sequence for the coding region was completed (see below), primers were designed to span the entire cDNA clone (Figure 4.1). Since numerous PCR experiments were performed, the exact details of each experiment are not provided. Briefly, intact or excess digested genomic DNA, which had been prepared for the inverse PCR experiments (*XmnI* and *PvuII*), was used as a template for PCR with programs 1, 2 or 4 (Section 2.4.6) using most of the compatible combinations of primers. The bands generated by PCR with genomic DNA would be larger than those obtained using the cDNA, due to the presence of introns. Therefore, the cDNA was included as a positive control in all experiments. It was anticipated that digested DNA might be less complex than undigested and could improve the efficiency of the PCR (McPherson *et al.*, 1995).

PCR with the cDNA generated clean bands of the sizes expected, however, despite several attempts no bands were obtained using genomic DNA. In my hands, PCR using genomic DNA as a template generally proved problematic. Although all possible combinations of primers were used and despite attempts to optimise the PCR (Section 4.4.1), no *redA*

genomic fragment was amplified, with the exception of the *TaqI* inverse PCR fragment. Due to time constraints no further PCR experiments were performed.

4.5 DETAILED GENE MAPPING OF *REDA*

A more extensive map of the region of genomic DNA containing the *redA* gene was produced (Figure 4.4), using the Southern blot data (Figure 4.2 & Table 4.1) together with sequence data from the cDNA (Figure 3.5) and *TaqI* inverse PCR clones (Section 4.6). A systematic and logical approach was used to determine the relative position of restriction sites that could not be positioned from the sequence data.

Some sites were positioned with relation to a site previously identified from the DNA sequences (discussed in Section 4.4). For example, *AvaI* is located 120bp before the end of the cDNA (Figure 4.1). Therefore, the majority of the *redA* probe would hybridise to sequence located 5' of this site. As the most intense *AvaI* band containing *redA* is approximately 20kb in size, it can be deduced that an *AvaI* site lies some 20kb 5' of this internal site (Figure 4.4). A second, less intense, 1.2kb band was seen when this digest was repeated (Table 4.1; Southern blot not shown). A third *AvaI* site is therefore, located 1.2kb 3' of the internal *AvaI* site (Figure 4.4).

Some sites could only be positioned on the map with reference to a second site. For example, digestion with *BamHI* generated a single, 8kb band containing *redA* (Figure 4.2 and Table 4.1). No internal *BamHI* sites were identified from the sequence data and so, without the use of a second restriction digest, it would be impossible to determine where on this 8kb fragment the *redA* gene is located. However, *BamHI*-*AvaI* double digestion reduces the 8kb fragment to 6kb (Figure 4.2 and Table 4.1). Therefore, since we already know the location of *AvaI* (Figure 4.4), we can conclude that a *BamHI* site exists 6kb 5' of the internal *AvaI* site and that a second *BamHI* site must be situated approximately 2kb from the internal *AvaI* site in the 3' direction (Figure 4.4). Several other sites were also positioned relative to *AvaI* using similar rationale, these include *EcoRV*, *NotI*, *PstI* and *XbaI* (Figure 4.4).

Some data were insufficient to determine the location of a restriction site (e.g. *XmnI*; Table 4.1) since no 'anchor' was used; these have been excluded from the map. In addition, some Southern blot data were inconsistent and provided conflicting evidence on the

possible location of restriction sites. Digestion with *Hind*III generated a band approximately 6.6kb in size (Figure 4.2), when *Hind*III–*Pst*I was used, the band was reduced in size by approximately 200bp (Table 4.1; Southern not shown). An internal *Pst*I site is located towards the 3' end of *redA* (Figure 4.1). Therefore, using this data, it can be deduced that a *Hind*III site exists just outside the 3' end of the gene and approximately 6kb 5' of the gene (Figure 4.4). However, when *Hind*III was used in conjunction with *Xba*I or *Ava*I, a 2.4kb band was often observed (Figure 4.2). This is inconsistent with the idea that a *Hind*III site is located approximately 6kb upstream of *redA*. *Hind* III, *Ava*I and *Xba*I all require the same buffer conditions for optimal digestion. Therefore, to save time both enzymes were used for a single step digestion. According to the manufacturers data sheet, *Hind*III is prone to star activity in the presence of Mn^{2+} . Although none of the buffers used contained Mn^{2+} , star activity is the most likely reason that the 2.4kb fragment was observed. Therefore, the detailed genomic map was produced excluding the 2.4kb *Hind*III – *Ava*I and *Hind*III – *Xba*I fragments (Figure 4.4).

Time constraints prevented me from fully utilising the data from this map for further cloning of the *redA* gene. However, this map should simplify future cloning of genomic fragments containing *redA*, since some pairs of restriction digests that would reduce the *redA* fragment to less than 3kb can be identified. For example, the 1.5kb *Ava*II–*Eco*RI and the 1kb *Eco*RI–*Hind*III fragments (Figure 4.4) could be cloned. Then the two fragments could be ligated at the *Eco*RI site to generate a genomic clone for *redA* that would contain promoter sequences and all the introns. Such a clone may be suitable for gene knockout studies to determine the function of *redA* (discussed in Chapter 5).

4.6 SEQUENCE ANALYSIS OF REDA

The 900bp *Taq*I inverse PCR fragment was successfully cloned into pBluescript II KS+. Two clones were isolated, which contained the inverse PCR fragment in different orientations. The complete sequence of one clone was obtained and used together with the cDNA sequence to construct a composite sequence for *redA* (Figure 4.5). The isolation and sequence analysis of this *redA* genomic clone was recently published, together with the northern and Southern blotting analysis described in Chapter 3 and further analysis of *redB* and *mynD* (Bailey *et al.*, 1999).

Figure 4.5: Composite DNA and deduced amino acid sequences for *redA*.

The sequence of both the forward and reverse strands were determined either manually using T7 DNA polymerase and the Sequagel™ sequencing system or using the PNACL in-house automated facility (Section 2.4.5) with the Reverse, M13 -40 and D13/3D primers listed in Figure 4.1. The sequences obtained from each primer were aligned using the Wisconsin Package, Genetics Computer Group (Madison, USA) on the Leicester University Mainframe computer. All regions of sequence discrepancy identified in the overlapping regions were clarified by further sequencing.

The sequence shown was compiled from the *TaqI* inverse PCR and cDNA clones (Section 4.6; Section 3.2.3). The genomic sequence, derived from inverse PCR (Section 4.4.2), spans the first 889bp and is flanked by *TaqI* restriction sites (tcga). Intron 2 is incomplete because of the *TaqI* site and the sequence has been broken to denote this (-----). Beyond this point, the cDNA sequence is shown and this may contain a further intron (see Section 4.6). The introns and non-coding regions are shown in lowercase. The start of the coding region is at base 238 and is shown italicised in bold type (***atg***); this is discussed further in Section 4.6. The complete coding region (669bp) is shown in uppercase and the standard single letter code for the deduced amino acid sequence (223aa) is shown below it. The stop codon is shown as bold (**TAA**) in the nucleic acid sequence or an asterix (*) in the amino acid sequence. The putative polyadenylation signal is underlined (aataaaa) and the location of the poly(A)⁺ tail is indicated by the final *aaaaaaaa*. The overlap with the cDNA clone (D13/3D) begins at base 308. Two small discrepancies in the coding region between the cDNA and *TaqI* inverse PCR clones have been italicised and underlined (*ctg*); these are discussed in Section 4.6. A third discrepancy was identified in the second intron at base 789 (a), this was an artefact of PCR (Section 4.6).

Figure 4.5

1 tcgaatatctaaaaaagagtattactatctctaaccgactgaaatcaaaataaagtcatt
61 tttattactatcgttggtgataaaaacacaaaaaatgtgggattaatggagatgaataa
121 cgtccgtgcttcgccatgatgccatgcaatttctaccattctaaaaatgtcatatgcagg
181 gagaatgataatatctcggcagcctaacttccattaagactaaaaaatttgtaga**ATG**
M
241 GTACCAGGCCTACGCGCGTCAAGTATTTCTTTTTTGCTTTTGTGGTTTGTAGTTTATTTCAA
V P G L R A S S I S F L L L F C S L F Q
301 GGAGAAAGAAAGAAGCAAGTAAATAT_TCTGAAAGTTGTGATTTTGTGAGTTCTTCTGATT
G E R K K Q V N I L K V V I L S V L S I
361 GGCCTGGTTTCTTGTCAATATGTGATACACCAAGAATTCTCTGATTCCAAGTGCTCAAAT
G L V S C Q Y V I H Q E F S D S K C S N
421 GCCACCTTCACTATGGTCGCCCAACTGCTTGTGTTGAAGCTgtatgaattttaatatat
A T F T M V A P T A C V E A
481 gataatcatgatttcttattatTTTTTTTatttcgaccagccgagattgtaaaatatttt
541 cttgtttgacgtagaaaataatgtcaccaagaacaaaaatataattattagaggatac
601 gtttaattcatttcctacagGAAGATGGAAAATACCACAAATCCGTATGTGCAAGTGATT
E D G K Y H K S V C A S D S
661 CTGTGCAGCTGTTTGAATGCAATGACCAGGCTTGTACCGACTGCCCTCGTAAAGAAACGg
V Q L F E C N D Q A C T D C P R K E T
721 taccgtattattaactatTTTatcaataagataaggggtattttctcccctgtgacttatc
781 cccctca_gttgagaaatatacattttggggtagctacttggtcctcccctacttttag
841 taaaggtctaaatagctatatatgggggggggggggctaatttcga-----ATGAACA
M N T
895 CAACGTGCAACCCAACCATGAACAAAGAATATTCTCAGTACTCGTGCGCAGCTACCGTCC
T C N P T M N K E Y S Q Y S C A A T V P
955 CGACCGGCCACACAGCGTCACCCAAGCTATATATCCTGAAACCGGGGAGGATGTAAGG
T G P H S V T Q A I Y P E T A G G C K G
1015 GAACTTTCTCAACGGCTTTTGTGGACTTTGGGTTGATTGGCAGTTGCAATAAGGAGGGAG
T F S T A F V D F G L I G S C N K E G G
1075 GGACTACACCATGCTGTCTTGGCGACTCCAATAACAGCCGTAACAGACCAAGACCTGCAGC
T T P C C L A T P I T A V T D Q D L Q R
1135 GGATGACAAGTGCTCCACGGAGCTGCCACGAGCAAAAGCTCGAGTCTTGGCAACATTGAG
M T S A P R S C H E Q K L E S C E H S E
1195 AACATGGGTTTGGATACACAGGCTTACCTGCACAGCATAAatggaagcgatatgtttct
H G F G Y T G F T C T A *
1255 atttgcagatcataggaataaactgataacagtagactaaaaaaaa

First it was necessary to reconstruct the *redA* sequence from the inverse PCR clone, since it was 'inverted' (Figures 4.3 & 4.6). The first step in the reconstruction process was identifying the *TaqI* restriction site. Then, using the GCG software package to examine the sequence situated either side of the *TaqI* site, the regions where the cDNA sequence overlapped with the inverse PCR clone were identified (Figure 4.6). The inverse PCR clone contained 852bp of sequence that began with primer D13/3D-7tag (Inverse PCR fragment 1; Figure 4.6c) and continued in the 3'-5' direction of the gene for 380bp until reaching a *TaqI* site (Figure 4.6c). At this point the sequence jumped to a previously unsequenced region located towards the middle the gene, which was subsequently identified as an intron, and continued in the 3'-5' direction of the gene for a further 472bp until reaching the D13/3D-6tag primer site (Inverse PCR fragment 2; Figure 4.6c).

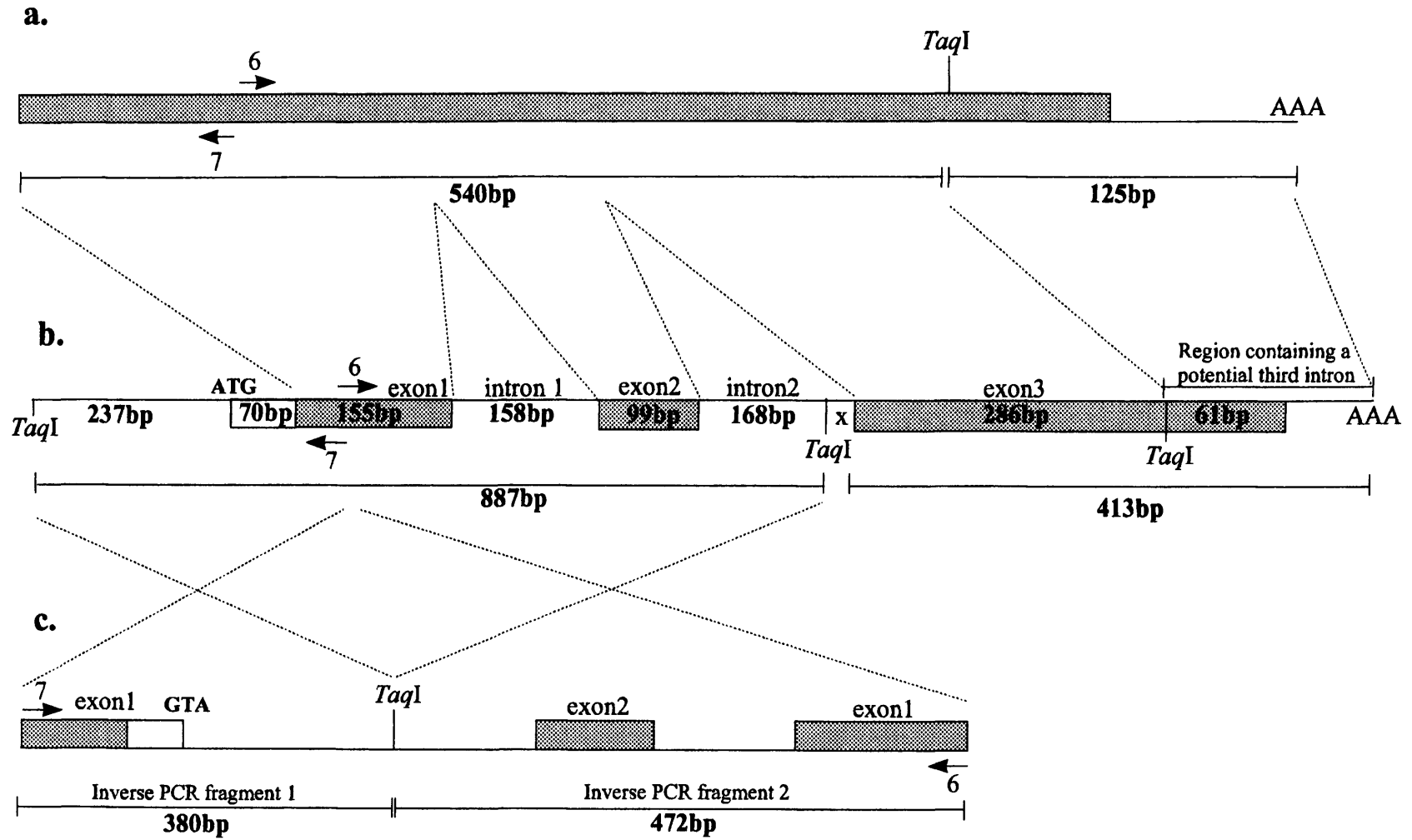
Homology to the cDNA clone began 307bp beyond the *TaqI* site of Inverse PCR fragment 1 (Figure 4.6). There was a gap of 35bp compared to the cDNA sequence before the next region of sequence overlap, which corresponded to the region of the gene not covered by the two primers (Figure 4.5). Although an intron could be located in this 35bp gap, it was considered unlikely since the fragment size (852bp plus the 35bp in the gap: 887bp) was close to that estimated from Southern blotting analysis of genomic DNA (900bp; Figure 3.8). Inverse PCR fragment 1 overlapped with the cDNA for 47bp beginning with the D13/3D-6tag primer (Figure 4.6). At this point, the inverse PCR sequence contained a region, 158bp long, which was not homologous to the cDNA sequence (Figure 4.6). Beyond this 158bp region, the homology continued at the next base in the cDNA, suggesting that it was an intron (Figure 4.6). The 158bp region was flanked by an intron splice consensus sequence, confirming it was the first *redA* intron (Figure 4.5). The homology between the two sequences extended beyond this intron for 99bp (Figure 4.6). The remaining 168bp of the inverse PCR sequence were not homologous to the *redA* cDNA (Figure 4.6) and since this region began with the intron consensus sequence, GTA, it was considered likely to be the second *redA* intron (Figure 4.5). This intron ended at an internal *TaqI* site and did not return to the cDNA sequence; therefore, the sequence for this intron is incomplete (x; Figure 4.6; Figure 4.5). Finally, the sequence from the two portions of the inverse PCR fragment were rearranged (Accession number Y18122; Bailey *et al.*, 1999) and used to construct a composite sequence for *redA* (Figure 4.5).

Figure 4.6: Schematic showing the relative positions of the *redA* cDNA and *TaqI* inverse PCR clones within the gene

The areas indicated by shaded boxes () represent the coding region for *redA* deduced from the cDNA clone (Section 3.2.3). The area indicated by an unshaded box (), represents the 70bp coding region that was obtained by inverse PCR (Section 4.4.2). Introns and other non-coding regions are represented by a solid line (). The location of introns was deduced from comparison of the cDNA and *TaqI* inverse PCR clones (Section 3.2.3; Section 4.6; Figure 4.5). Arrows () indicate the location of the two primers used to generate the *TaqI* inverse PCR clone (Section 4.4.2); the location of *TaqI* restriction sites is included for reference.

Broken lines indicate the relative location and orientation of regions of sequence identity between the *redA* cDNA clone (panel a.), the deduced *redA* gene (panel b.) and the *TaqI* inverse PCR fragment (panel c.). The sizes of the different sequence components are shown. The region of the *redA* gene (panel b.) marked 'X' was not cloned and is, therefore, of unknown size.

Figure 4.6



Comparison of the *TaqI* inverse PCR clone and the cDNA clone resulted in some discrepancy over certain coding regions. Bases 355 to 357 of the inverse PCR clone are unquestionably AAA, however, the corresponding region of the cDNA clone consists of CTG. Although this does not affect the reading frame, using the inverse PCR sequence a leucine is substituted by a lysine, 39 residues into the protein (Figure 4.5). Similarly at base 327: in the inverse PCR clone this is a 'G' residue whilst in the cDNA clone it is a 'T' residue, thus using the inverse PCR sequence an isoleucine is substituted by a methionine (Figure 4.5). PCR is a technique that is prone to base substitutions; a variety of factors effect the degree to which such errors occur, such as a disproportionate concentration of a particular nucleotide (reviewed in McPherson *et al.*, 1995). The extent to which these errors occur depends on the DNA polymerase selected for the procedure. Some polymerases possess 3'-5' endonuclease activity which remove mis-incorporated nucleotides to regenerate a correct sequence (e.g. *pfu* DNA polymerase). During the course of these studies, no such 'proof-reading' polymerase was used. Therefore, it is considered likely that the sequence errors are derived from the inverse PCR. Additional sequence analysis of other *redA* cDNA or genomic clones would clarify these anomalies.

The extent to which errors occur within the non-coding regions of the inverse PCR clone is unclear at this time. Sequencing the second inverse PCR clone identified a discrepancy between the two PCR fragments at base 789 (Figure 4.5). In one clone, the residue at 789 was an 'A' and, in the other, it was a 'G'. This discrepancy lies within the second intron and has no effect on the deduced amino acid sequence. Since this base substitution lies in an intron, the sequence could not be clarified using the cDNA data. A genomic DNA clone containing *redA* would clarify the sequence of this residue and the sequence discrepancies between the inverse PCR and cDNA clones identified at the start of the gene.

When genomic DNA was digested with *TaqI*, three bands were observed, one of which was thought to be the product of partial digestion (Section 4.4.2.1). The composite sequence data shows the two *TaqI* sites to be separated by a minimum of 286bp of cDNA (Figure 4.5). The smallest fragments retained on the agarose gels used for Southern blotting were often smaller than this, but there was no sign of any fragment smaller than 900bp in *TaqI* digested DNA (data not shown). However the intensity of signal generated by such fragments would be low and therefore may not have been apparent. Since the

difference between the 1.8kb and 1.5kb *TaqI* fragments is 300bp, the 1.8kb *TaqI* fragment is probably the result of partial digestion and, since this figure is close to the 286bp measured from the cDNA sequence, it also suggests there are no additional introns in the region ahead of the second *TaqI* site (Figures 4.5 & 4.6). The second *TaqI* site is situated 61bp ahead of the TAA stop codon; if a third intron exists in the gene, it may be located in this 61bp region or in the 3' untranslated region beyond it.

Physarum genes tend to have short introns and exons (e.g. Nader *et al.*, 1986; Binette *et al.*, 1990; Hamelin *et al.*, 1988; Kozlowski *et al.*, 1993). Introns in *P. polycephalum* vary from approximately 50bp–280bp in size (e.g. Nader *et al.*, 1986; Binette *et al.*, 1990), but are generally approximately 100bp–150bp. Similarly, exons generally vary from approximately 50bp–350 bp (e.g. Nader *et al.*, 1986; Binette *et al.*, 1990). The sequence for the second *redA* intron stopped at a *TaqI* site. It would be unusual for a *P. polycephalum* gene if this intron were much larger than the 158bp already identified. The transcribed region that follows this second intron is 413bp and thus is large enough to accommodate a third intron. However, an unusually large exon of approximately 900bp was recently identified in a *Physarum* gene (E. Swanston; Unpublished data). Therefore, although the *TaqI* data suggests that no further introns are situated in this 3' region, the possibility that a third intron exists cannot be excluded without further Southern analysis or a genomic clone covering this region.

The new 5' sequence was added to the start of the cDNA, in order to identify the start of the coding region (ATG). Several ATG triplets were located in this region, however, only one produced an open reading frame of the size estimated from northern blotting analysis (Chapter 3). Stop codons are located in all three reading frames within the 35bp region immediately upstream of this start codon, confirming that this was the correct ATG (Figure 4.5). Thus, an additional 70bp of 5' *redA* coding sequence were identified that were missing from the cDNA clone (Figures 4.5 & 4.6). This closely matched the previous estimate of up to 80 nucleotides (Section 3.3.1).

The sequence databases were screened using BLAST, FASTA and TFASTA search programs against the complete coding region of *redA*. Homology was found with the Owl Monkey involucrin gene, *atinvla* (Accession number M25313) over the first 250bp of *redA* coding sequence (tfasta; E(): 0.0036); proteins with an E() value of ≤ 0.01 are

generally considered homologous. However, this homology is probably artefactual since it was not confirmed by the more stringent BLAST search and was not in the open reading frame of the involucrin gene. In addition, the involucrin sequence consists of numerous repeat units of about 30bp each; a level of repetition that is not evident in *redA*. The complete coding region for *redA* (669bp) encodes a 223 amino acid protein (Figure 4.5) with an overall charge of -4 and a predicted weight of 24.1 kDa. The sequence was also screened for domains and motifs, using the GCG software. Such analysis had previously identified the EF-hand calcium-binding motifs in *redB* (Section 3.2.3; Bailey *et al.*, 1999). The *redA* sequence was found to contain only commonly identified motifs, such as putative N-glycosylation or N-myristoylation sites that suggest the protein may be modified. However, biochemical analysis would be required to confirm the activity of such sites.

4.7 SUMMARY

Inverse PCR amplification generated an 852bp fragment, corresponding to the smallest *TaqI-redA* fragment identified on the Southern blot (Figure 3.8). Sequencing revealed two introns and 307bp of new 5' sequence containing the transcriptional start codon (ATG) located 70bp ahead of the beginning of the cDNA clone, which completed the coding region for the gene (Figure 4.5). The 5' non-coding region ahead of the start codon in the *TaqI* inverse PCR clone contains 237bp of the promoter sequence (Figure 4.5). The clone stopped within the second intron at a *TaqI* site and this intron is, therefore, incomplete (Figure 4.6). The *TaqI* inverse PCR fragment spans the first 254bp of the cDNA clone. This leaves 413bp of cDNA sequence for which there is no corresponding genomic information (Figures 4.5 & 4.6). The 223 amino acid RedA sequence encodes a protein with a predicted molecular weight of 24.1kDa that shares no significant homology with other proteins in the databases and contains only commonly identified motifs.

CHAPTER FIVE

FUNCTIONAL ANALYSIS OF *REDA*

CHAPTER 5: FUNCTIONAL ANALYSIS OF *REDA*

5.1 INTRODUCTION

As discussed in Chapter 4, sequence analysis of *redA* revealed no significant homologies to previously characterised genes, nor any domains or motifs that may have indicated the roles of *redA*. Since no putative function could be determined by database comparisons, a functional study using homologous gene replacement and antisense RNA mutagenesis was undertaken.

5.1.1 Homologous gene replacement

The analysis of gene function by homologous gene replacement is commonly used in many systems (e.g. *Dictyostelium*, reviewed by Kuspa *et al.*, 1995; *Chlamydomonas reinhardtii*, Nelson & Lefebvre, 1995). Using a genomic clone for *ardD* that contained a deletion of approximately 1kb (*ardDΔ1*; Adam *et al.*, 1991), Burland & Pallotta (1995) designed constructs for transformation that successfully targeted the genomic *ardD* gene in *Physarum polycephalum* for homologous gene replacement (Section 1.6.6). Two *ardD* construct designs were selected:

- A. The selectable marker, *PardC-hph*, was positioned at the 3' end of *ardDΔ1* such that homology to *ardD* was at the 5' end of the construct.
- B. The *PardC-hph* was positioned approximately 750bp into the *ardDΔ1* sequence, such that homology to *ardD* flanked the construct.

Analysis of the homologous transformants generated from these constructs provided no evidence that the *ardDΔ1* deletion has any effect on growth or development in *Physarum* (Burland & Pallotta, 1995). Approximately 1 in 20 of the transformants generated using Design A were homologous and this design generated 38 transformants in total; however, no transformants were generated using Design B (Burland & Pallotta, 1995). This may indicate that the latter design is less efficient than the first. In other systems, designs similar to this are often necessary to target homologous integration (e.g. *Dictyostelium*, reviewed by Kuspa *et al.*, 1995); therefore, there is no reason to assume that this design will not work in *P. polycephalum*. Since the study of Burland & Pallotta (1995) is the only homologous gene knockout experiment that has been performed in *P. polycephalum*, further studies are required to determine the most effective construct design.

It is possible that the regions of homology that flanked *PardC-hph* in Design B from Burland & Pallotta's study (1995) may have been insufficient to target homologous gene

replacement. The 5' region of this construct contained approximately 750bp of homology to the *ardD* gene before going into the *PardC* sequence, while the 3' region comprised approximately 1.4kb of *ardD* sequence before the deletion and a further 450bp of the 3' region of the *ardD* gene after the deletion. Thus, the largest region of homology lies after *PardC-hph* and corresponds to the middle 1.4kb of the *ardD* gene. In *D. discoideum*, 100bp to 1kb of homologous DNA flanking the selectable marker is generally sufficient to target homologous gene replacement (reviewed by Kuspa & Loomis, 1994). This strongly suggests that the regions of homology flanking the selectable marker in Design B from Burland & Pallotta's study (1995) should have been sufficient to target the *ardD* sequence.

Homologous replacement of *redA* with an altered copy of the gene could provide some indication of the role of *redA* during the APT and may help clarify the most effective design for transformation vectors.

5.1.2 Antisense RNA mutagenesis

Antisense RNA mutagenesis has been used successfully to investigate gene function in several systems, including *D. discoideum* and mammalian cells (reviewed by Kuspa *et al.*, 1995). Antisense RNA gene inactivation is achieved by introduction of stable constructs where the cDNA for the gene of interest is placed such that an antisense RNA is produced; i.e. the gene is transcribed in reverse to produce a molecule that is complimentary to the native RNA transcript. How the antisense RNA affects the function of a gene is unclear. It is generally thought that the antisense RNA forms duplexes with the mRNA produced by the wild-type copy of the gene and prevents or reduces translation into a functional protein (reviewed by Vanhée-Brossollet & Vaquero, 1998). However, such duplexes may instead serve as targets for degradation by double-stranded RNA specific enzymes or may activate RNAses that degrade single-stranded RNA (reviewed by Vanhée-Brossollet & Vaquero, 1998). Other theories on how antisense RNA affects gene function revolve around the translation of the antisense RNA into an antisense peptide. It is predicted that antisense peptides are able to interact with the sense peptides or proteins, thus influencing the normal function of the gene (reviewed by Root-Bernstein & Holsworth, 1998).

A major benefit of antisense transformation studies is that they do not depend on homologous integration at the target gene. Provided the antisense cDNA is linked to a

functional promoter, integration can occur anywhere in the *Physarum* genome to generate antisense transcripts. However, if insufficient antisense transcripts are produced, there may be little or no effect on the phenotype. The timing and level of expression of antisense RNA can be controlled through the choice of promoter. For example, use of abundant, constitutive promoters such as *PardB* and *PardC* should lead to high levels of antisense RNA at all times during the life-cycle while cell-type specific promoters, such as the *proP* promoter (Binette *et al.*, 1990), would generate plasmodium-specific expression.

5.1.3 Aims

The aim of the work described in this Chapter was to investigate the possible role of *redA* during plasmodium development using a combination of antisense RNA mutagenesis and homologous gene replacement. In previous transformation experiments using *Physarum*, both homologous and non-homologous integration occurred with different vector designs but no one design seems more effective for transformation in *P. polycephalum* than another (Burland *et al.*, 1993a; Burland & Pallotta, 1995). Therefore, several different vector designs were selected for these studies. Since the only genomic clone available for *redA* was derived from inverse PCR (Chapter 4) and could not easily be rearranged to correlate with the gene sequence, the vectors were constructed using the *redA* cDNA clone.

Amoebae carrying an altered copy of *redA* can be maintained in culture as normal, since *redA* is not expressed in amoebae. The *redA* gene is first transcribed during the APT, suggesting that plasmodium development may be affected by mutation of *redA*. Removal of *redA* function may block the apogamic development of plasmodia, as seen with many of the *npf* mutations (Section 1.4.2), leading to phenotypically abnormal plasmodia or may have no discernible effect on plasmodium development. Therefore, all stable transformants were tested for the ability to undergo normal apogamic plasmodium development.

Following electroporation, amoebae typically undergo two or three cell divisions during the outgrowth period before selective plating (Section 2.1.7). Transformants from the same experiment may therefore be unique or sibling clones. Southern blotting analysis was performed to check the site of integration of the transformation construct and to

determine the relationship between transformants derived from the same transformation experiment.

5.2 CONSTRUCTION OF cDNA-BASED VECTORS FOR HOMOLOGOUS GENE REPLACEMENT

The optimum vector design for homologous gene replacement is unclear from the previous studies, therefore, two basic designs were chosen for these studies (similar to those used by Burland & Pallotta 1995; Section 5.1.1):

- i. Frameshift within the coding region of *redA* (Section 5.2.1).
- ii. Insertion of the selectable marker within the coding region of *redA* (Section 5.2.2).

Both of these strategies would generate a hybrid mRNA encoding part of RedA and part nonsense (see below).

5.2.1 Construction of *redA* frameshift vectors

The introduction or removal of nucleotides within the coding region of *redA* would alter the peptide encoded by the sequence and thus alter the function of the gene. From the sequence data (Figure 4.5), it is clear that stop codons occur earlier in the two non-coding reading-frames of *redA*. Therefore, any proteins produced from a frameshift would be smaller and would also be chimeric; containing the start of RedA followed by new amino acids. Frameshifts were engineered in two locations using PCR or restriction-based strategies (see below).

The selectable marker, *PardC-hph*, was excised from pTB37 (Burland *et al.*, 1993a) using *HindIII* and *KpnI*. Since there were limited restriction sites available in the cDNA vector that were suitable for cloning, the *EcoRV* or *NotI* sites situated either side of the cDNA insert were selected as insertion sites for the selectable marker. The selectable marker and digested frameshifted cDNA plasmid (see below) were both treated with DNA Polymerase I large (Klenow) fragment prior to ligation; this created blunt cloning ends on both fragments that could be easily joined (Section 2.3.3). Consequently, *PardC-hph* ligation could occur in either orientation at these sites and thus, four different plasmids could be created for each unique frameshift.

5.2.1.1 Frameshift by PCR

The first *redA* frameshift was generated at the start of the cDNA clone by PCR, using a primer that included some of the restriction sites from the vector and the first 9bp of 5' cDNA sequence (D13/3D-mis; Figure 4.2). The frameshift was created by including an additional guanine (G) residue in the primer sequence between nucleotides 4 and 5 of the cDNA clone (Figure 3.5). A similar strategy was successfully used to generate frameshift vectors for *redB* (J. Bailey, personal communication).

One round of PCR was performed (PCR program 1; Section 2.4.6) against the cDNA clone using D13/3D-mis and the universal -40 primer (Figure 4.2). The PCR fragment was isolated using DEAE membrane and digested with *EcoRV* and *NotI* to generate cloning ends (Sections 2.3.2 & 2.3.1). The fragment was ligated to pBluescript[®] II KS+ (Stratagene) prepared with the same cloning ends and transformed into XL1-Blue (Section 2.3.5). The correct plasmid was identified, purified and the sequence analysed, confirming that the additional G residue was present (Sections 2.2.4 & 2.4.5). However, during cloning the *EcoRV* and *NotI* sites had been lost through mis-ligation; *EcoRV* had ligated to *NotI*, and *vice versa*, despite the fact the two fragment cloning ends should have been incompatible. This meant that the *EcoRV* and *NotI* sites intended for the integration of *PardC-hph* were no longer available and no alternative sites could be identified. Consequently, and in view of time constraints, this approach was not used further for the analysis of *redA*.

5.2.1.2 Frameshift by restriction digest

When a fragment is integrated into the *Physarum* genome the ends of the DNA are occasionally lost (Pierron *et al.*, 1999; D. Pallotta, personal communication). Hence, there was a possibility that the PCR frameshift, only five nucleotides into the cDNA clone, may have been lost on integration to the genome. A second frameshift was therefore designed utilising an *XcmI* site located 120bp into the cDNA clone (Figure. 3.5). Since this is situated further into the sequence, it was anticipated that it may be less likely to be lost on integration to the genome. However, a larger proportion of the *redA* transcript will be normal and therefore there is a possibility that it may be less effective in disrupting *redA* function.

The *redA* cDNA plasmid was digested with *XcmI* (New England BioLabs) and treated with DNA Polymerase I large (Klenow) fragment to remove the single-nucleotide 3' overhang (Section 2.3.3). Some of this plasmid was then re-circularised, transformed into XL1-Blue and purified (Sections 2.3.5 & 2.2.4). Sequencing confirmed that one cytosine (C) residue at base 121 of the cDNA clone had been removed, generating a 1bp frameshift at the *XcmI* site (Section 2.4.5). Klenow-treated *PardC-hph* was then ligated to this vector at the *EcoRV* site to generate LC8 and LC9 (Figure 5.1) or at the *NotI* site to generate LC10 and LC11 (Figure 5.1). In all cases, the orientation of the selectable marker was confirmed using the diagnostic digest *EcoRI* (Figure 5.1).

If integrated homologously, the protein produced from such a frameshift would contain the first 63 amino acids of *redA* fused to a new reading frame encoding a further 45 amino acids before reaching a stop codon at base 279 of the cDNA clone. This frameshift is illustrated below; the novel transcript generated by the frameshift is shown in bold-type. The wild-type RedA sequence is included for comparison; the region corresponding with the start of the cDNA clone begins at the 25th residue (K).

Wild-type *redA* transcript (223 amino acids)

```

1  MVPGLRASSI SLLLLFCSLF QGERKKQVNM LKVVILSVLS IGLVSCQYVI HQEFSDSKCS
61  NATFTMVAPT ACVEAEDGKY HKSVCASDSV QLFECNDQAC TDCPRKETMN TTCNPTMKE
121 YSQYSCAATV PTGPHSVTQA IYPETAGGCK GTFSTAFVDF GLIGSCNKEG GTTPCCLATP
181 ITAVTDQDLQ RMTSAPRSCH EQKLESCEHS EHGFGYTGFT CTA*

```

XcmI frameshift (107 amino acids)

```

1  MVPGLRASSI SLLLLFCSLF QGERKKQVNM LKVVILSVLS IGLVSCQYVI HQEFSDSKCS
61  NATLLWSPQL LVLKLMENNTT NPYVQVILCS CLNAMTRLVP TALVKKQ*

```

If the LC8 and LC9 constructs were integrated by homologous recombination at *redA*, as shown in Figure 5.2, transcription would proceed first through the 70bp of *redA* not covered by the cDNA clone and then through *PardC-hph*, thus producing a chimeric transcript. In the case of LC9, the chimeric transcript would contain antisense *hph* RNA (Figure 5.2). However, this should not affect the hygromycin selection process since the *redA* promoter is not activated until the APT is initiated and hygromycin selection is only applied to amoebae. Therefore, although both of these vectors contained the frameshift, it would be the introduction of *PardC-hph* into *redA* that causes the disruption to the *redA*

Figure 5.1: Vectors for homologous gene replacement and antisense studies of *redA*.

Schematic representation of the structure of the *redA*-based disruption (LC4-LC5: Section 5.2.2; LC8-LC11: Section 5.2.1.2) and antisense (LC17: Section 5.3) constructs. The 1.1kb *PardC* region (▨) promotes constitutive expression of the 1.3kb *hph* gene (▩), which serves as a selectable marker for all of these constructs, conferring resistance to hygromycin on stably transformed cells. *PardC-hph* was excised from pTB37 as a 2.4kb *HindIII-KpnI* restriction fragment (Burland *et al.*, 1993a). In all cases, the transcription start site within the promoter and direction of transcription is indicated by a small bent arrow (↵). The *redA* cDNA sequences are shown as lightly shaded boxes (▨). The 5' end of the *redA* cDNA is indicated (5') to aid orientation.

During construction of LC4 and LC5, the selectable marker was inserted at a *XcmI* site in *redA* (Figure 3.5); the smallest portion of the *redA* cDNA is indicated by the letter 'A' for these two constructs. Full details of the construction of vectors LC4 and LC5 are outlined in Section 5.2.2. The *redA* cDNA insert was modified to contain a 1bp frameshift (▼) in vectors LC8 to LC11; full details of the construction of these vectors are outlined in Section 5.2.1.2.

In addition to *PardC-hph*, LC17 contains the putative transcriptional terminator, *TardC* (▩), and the 1.9kb *PardB* promoter region (▩) positioned such that it would express antisense *redA* transcripts (Section 5.3). The 635bp fragment of the *redA* cDNA clone used to construct the antisense RNA vector, LC17, is shown as 'rev-*redA*' to denote the fact that it is reversed. Full details of the construction of vector LC17 are outlined in Section 5.3.

The location of the *EcoRI* sites, used to confirm the orientation of the components in each vector, are shown. *HindIII-SstI* (LC4-LC11) or *KpnI-SstI* (LC17) digestion was used to linearise the constructs prior to transformation (Section 5.4).

Figure 5.1

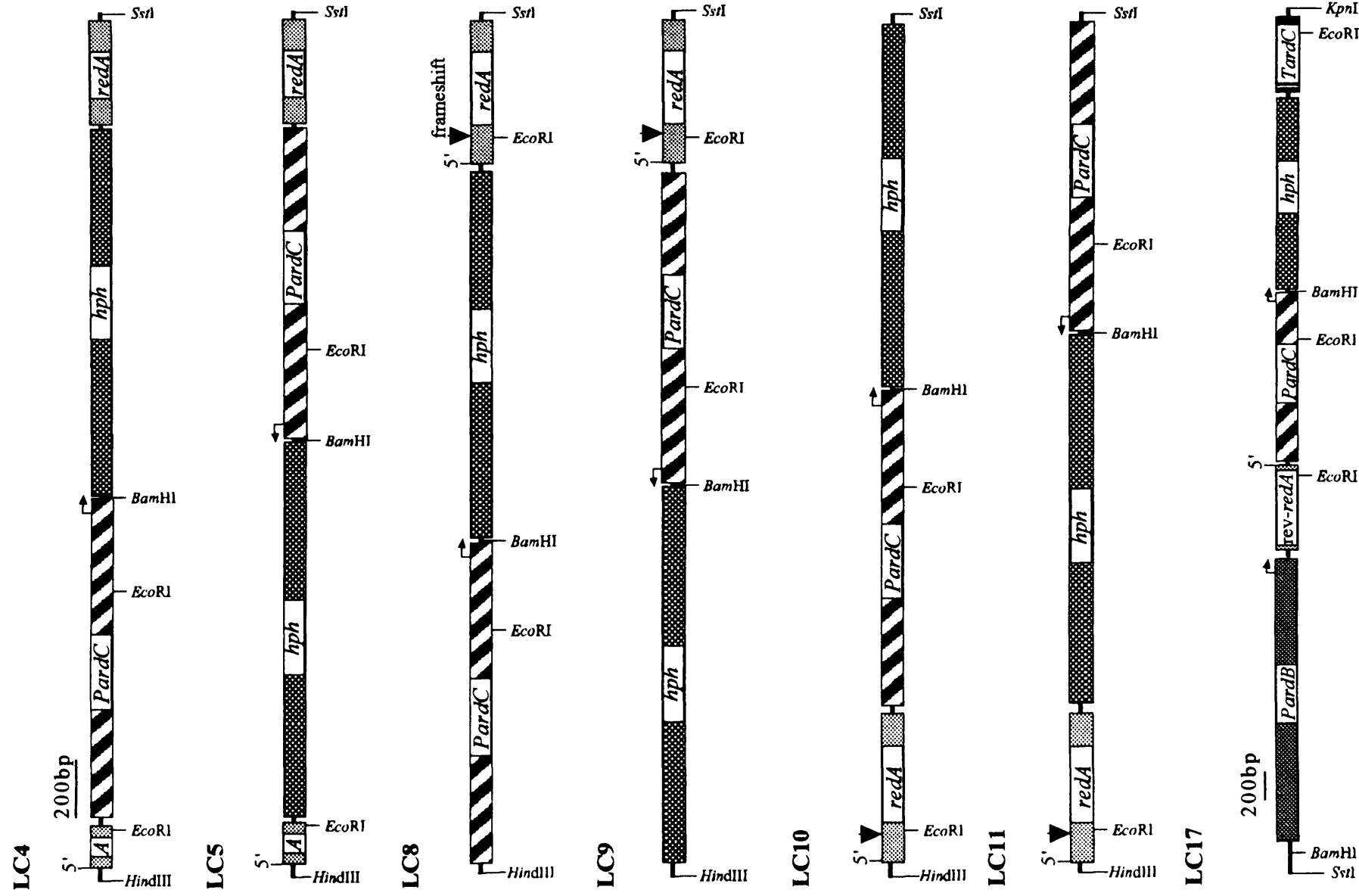
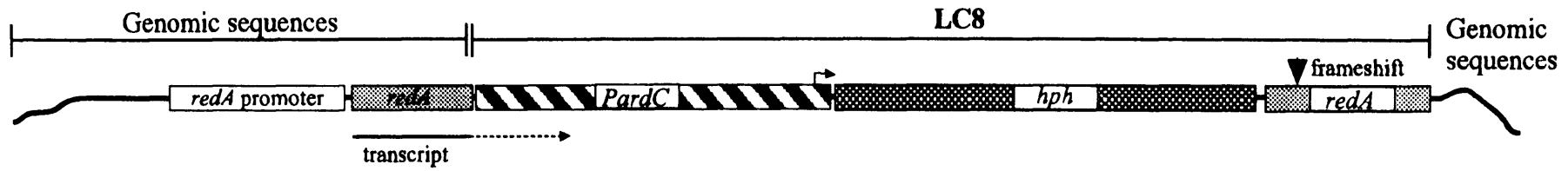


Figure 5.2: Mechanism of disruption of *redA* by LC8 and LC9 as a result of insertion of *PardC-hph*

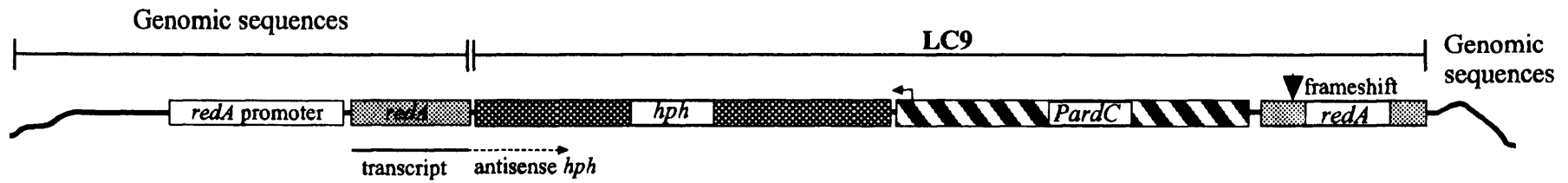
Schematic representation of one possible mechanism for homologous gene replacement of *redA* with the LC8 or LC9 constructs (Figure 5.1). The transcription start site within the *PardC* promoter and the direction of *hph* transcription is indicated by a bent arrow (\lrcorner). The position of the *XcmI* frameshift is included for reference (\blacktriangledown frameshift) but is unlikely to affect the transcript produced (see below).

If the LC8 or LC9 constructs were integrated to the genome in their entirety at the region of *redA* where homology to the cDNA clone begins, transcription from the *redA* promoter would proceed first through the 70bp of coding sequence not covered by the cDNA clone and then into the selectable marker, *PardC-hph*. Thus, *redA* transcription would be disrupted by the presence of the selectable marker (Section 5.2.1.2).

Figure 5.2



Transcription at start of *redA* as normal, then into *PardC*.



Transcription at start of *redA* as normal, then into *hph* to generate an antisense *hph* RNA.

transcript (Figure 5.2); LC10 and LC11 are effectively the only two 'genuine' 1bp frameshift designs (Figure 5.1). Constructs with similar action to LC8 and LC9 could have been constructed from the unaltered cDNA clone instead of the *XcmI* frameshifted sequence. Since one aim of this research was to optimise vector design, the *XcmI* frameshift cDNA was selected to standardise the construction procedures, thus providing a better basis for comparison with LC10 and LC11.

5.2.2 Construction of vectors where *PardC-hph* is positioned within the *redA* coding region

An alternative design for gene replacement vectors, which was used by Burland & Pallotta (1995), positions the selectable marker inside the target gene such that regions of homology existed at both ends of the construct (Design B, Section 5.1.1); similar constructs were designed for *redA* as alternatives to constructs LC8–LC11.

The coding region of *redA* was disrupted by insertion of *PardC-hph* at the same *XcmI* site that was selected for the second frameshift (Section 5.2.1.2). Klenow-treated *PardC-hph* was ligated to the *XcmI* digested *redA* cDNA, which had been treated with Klenow and Shrimp alkaline phosphatase (Section 2.3.3), to generate two transformation vectors; LC4 and LC5, with *PardC-hph* inserted in opposite orientations (Figure 5.1). As with the second frameshift design, the RedA protein will only contain the first 63 amino acids before the sequence is disrupted by the insertion of *PardC-hph*. However, since the junctions from *redA* to the selectable marker for LC4 and LC5 were not confirmed by sequencing, the sequences for the chimeric proteins were not determined; the chimeric regions would be produced from the foreign sequences of *PardC* or the reversed *hph* gene (Figure 5.1), both of which contain stop codons in all three reading frames within 160bp of the ligation site.

The design of constructs LC4 & LC5 is such that *PardC-hph* is flanked by regions with homology to *redA* (Figure 5.1). Since no genomic clone was available for construction of these vectors, the regions of homology were limited in size. The smallest region of homology is at the 5' end of *redA* and consists of the 130bp located ahead of the *XcmI* site (Figure 4.2 & Figure 5.1). It is unclear whether this is sufficient to target integration at *redA*, however, gene replacement vectors with just 100bp of flanking homology have been used successfully for homologous gene replacement in *Dictyostelium* (reviewed by Kuspa

& Loomis, 1994). The largest region of homology to the *Physarum* genome for the LC4 & LC5 constructs comprises the 1.1kb *PardC* sequence although, since *ardC* encodes the major actin transcript, it is unlikely that transformants generated through integration at *PardC* would survive.

5.3 CONSTRUCTION OF A *REDA* ANTISENSE RNA MUTAGENESIS VECTOR

Antisense RNA mutagenesis does not depend on homologous integration at the target locus and, therefore, only a single transformant is theoretically required. Since the majority of *Physarum* transformants generated to date are the product of random integration of the transformation construct within the genome (Burland & Pallotta, 1995; Burland *et al.*, 1992b & 1993a), it was anticipated that antisense RNA mutagenesis would help to elucidate the role of *redA* more rapidly than homologous gene replacement.

The mechanism by which RNA transcripts are generated was considered when deciding which portion of the *redA* cDNA to use for the antisense vector. Transcription by RNA polymerase II is initiated by promoter sequences and proceeds until a transcriptional terminator is reached to produce the primary RNA transcript. This transcriptional terminator is not the same as the translational terminators, the stop codons. Introns are subsequently removed from the primary transcript and a poly(A)⁺ tail is added to the 3' end to produce mRNA. Simple transcriptional terminators consist of a G/C-rich hairpin structure followed by a series of T residues (Stryer, 1988). Therefore, there is a possibility that the A/T-rich region of the *redA* cDNA located at the 3' end, which contains the polyadenylation signal and poly(A)⁺ residues, may be recognised as a transcriptional terminator. This would generate a very short antisense transcript, since in reverse orientation it would be located close to the promoter. Such a transcript would only be complimentary to the 3' end of mRNA and, therefore, would be less likely to alter the function of the protein. To avoid this, the 3' sequence of the *redA* cDNA was removed to exclude the A/T-rich region, including the putative polyadenylation sequence. The *redA* cDNA was digested with *Sau3AI* to release a 1.8kb fragment containing some pBluescript II sequence and the first 630bp of *redA* cDNA (Figure 4.1). This fragment was purified by DEAE membrane isolation and then digested with *EcoRV* to separate the Bluescript II and cDNA sequences. The 635bp *EcoRV* - *Sau3AI* cDNA fragment was isolated using DEAE membrane and klenow-treated to fill in the 5' overhang generated by *Sau3AI*. It was necessary to perform this digest in two stages, since *Sau3AI* digestion

of Bluescript II releases a 730bp fragment that would be difficult to separate from the 635bp *EcoRV* – *Sau3AI* *redA* cDNA fragment.

The selectable marker, *PardC-hph-TardC*, was included in the antisense vector. The *ardC* termination sequence, *TardC*, was included to improve stability of the *hph* transcripts by controlling the termination of *hph* independent of the site of integration, for reasons discussed previously (Section 1.6.7). The 3kb *PardC-hph-TardC* fragment was isolated from pTB40 following digestion with *HindIII* and *KpnI* (Burland *et al.*, 1993a), ligated to *HindIII* – *KpnI* digested *pPardB* (Burland *et al.*, 1992a) that had been purified and pre-treated with alkaline phosphatase to prevent self-ligation (Section 2.3.3) and then transformed into XL1-Blue (Section 2.3.5). The resulting 7.9kb vector was digested with *HindIII*, to linearise the vector between *PardB* and *PardC-hph-TardC*, and then treated with DNA polymerase I large (klenow) fragment and alkaline phosphatase (Section 2.3.3).

The antisense-*redA* vector was constructed by ligating the blunt-ended 635bp partial cDNA for *redA* in reverse orientation under the control of the *PardB* promoter in the prepared 7.9kb vector molecule; this was transformed to XL1-Blue (Section 2.3.5). Since the blunt cDNA fragment could insert in either orientation or in multiple numbers, plasmids were screened using *EcoRI* and *BamHI* digestion to select a construct with the antisense orientation of a single *redA* fragment. The final antisense *redA* construct was designated LC17 (Figure 5.1).

If the antisense *redA* mRNA generated by LC17 is transcribed, it will produce a very short peptide since stop codons are located within 100bp of the *Sau3AI* site in all three reading frames (data not shown); the junction between *PardB* and the *Sau3AI* site of the *redA* cDNA was not sequenced, therefore, it is unclear which reading frame is correct.

5.4 TRANSFORMATION OF AMOEBAE WITH THE GENE DISRUPTION VECTORS AND ANALYSIS OF TRANSFORMANTS

The gene disruption vectors, described above, were used in *redA* gene knockout experiments. The frameshift and internal disruption gene replacement plasmids (pLC4-5, pLC8-11; Figure 5.1) were digested with *HindIII-SstI* and the antisense plasmid (pLC17; Figure 5.1) was digested with *KpnI-SstI* to release transformation construct inserts. Axenically grown amoebae of strain LU352 were used for all transformation experiments

(Section 1.6.2). Optimisation of the electrical parameters for transformation and the subsequent transformation experiments were performed as described in Section 2.1.7. Selection was performed using DSPB plates containing $100\mu\text{g ml}^{-1}$ Hygromycin B (Sigma) over a period of 3–4 weeks (Section 2.1.7). Transformation in *P. polycephalum* is performed using haploid amoebae, thus since only a single copy of *redA* is present, it is easy to identify changes to the gene and phenotype resulting from homologous integration of the transformation vector.

Details of the stable hygromycin resistant amoebae (transformants) generated from several independent transformation experiments performed using the different *redA* constructs (Figure 5.1) are shown in Table 5.1. All transformants were assigned a unique code based on the construct used for the transformation, of the format [construct code]T[number] (e.g. LC4T1 for the first transformant obtained using the LC4 construct).

The number of unique transformants for each construct, determined by Southern blotting (see below), was used to calculate the overall efficiency of transformation for each vector. The total number of amoebae surviving the transformation was calculated from the haemocytometer counts performed 2–3 hours after electroporation (Table 5.1). This total was then divided by the number of unique transformants generated to determine the overall efficiency for each construct (Table 5.1). In addition to this figure, the highest efficiency from each individual experiment was also determined. Where transformants for a single construct were generated from more than one experiment, the most efficient is shown (Table 5.1).

The transformants were screened for their ability to undergo apogamic plasmodium development, since it was anticipated that disruption of *redA* would affect plasmodium development (Section 5.4.1). Following electroporation, amoebae typically undergo two or three cell divisions during the outgrowth period before selective plating (Section 2.1.7). Therefore, assuming integration occurs prior to the first mitosis after electroporation, for every unique transformant one would expect a maximum of four to eight amoebal colonies to grow on the selective plates. However, it is possible that integration of the construct occurs at or after the first mitosis, in which case only half of the progeny would be drug resistant and only two to four amoebal colonies would grow on selective plates. In addition, viable count data demonstrate that not all amoebae survive the replating process;

Table 5.1: Details of transformation experiments conducted using the *redA* constructs

Each transformation was performed using 5×10^7 axenically grown amoebae of *Physarum polycephalum* strain LU352 (Section 1.6.1) and 1-10 μ g of linearised LC construct DNA (Figure 5.1) as described in Section 2.1.7.

Pooled data from transformation experiments with *redA*-hygromycin constructs (Figure 5.1) are shown. The overall frequency of transformants does not include an allowance for differences in the size of construct used (Section 1.6.5); however, this would only affect pLC17 since the other vectors are the same size (Section 5.4.4).

[§] The number of independent stable transformants was determined from the Southern blot data (Section 5.4.2).

Table 5.1

Vector	Number of experiments	Total DNA (μg)	Total survivors of electroporation	Number of transformants	Number of independent integration events ^s	Overall frequency of transformants (per cell)	Best frequency from a single experiment (per cell)
pLC4	18	32	4.2×10^8	5	3	1.4×10^{-8}	2.2×10^{-7}
pLC5	18	32	4.2×10^8	8	3	1.4×10^{-8}	1.7×10^{-7}
pLC8	16	31	4.0×10^8	1	1	4.0×10^{-8}	2.2×10^{-7}
pLC9	17	36	3.8×10^8	10	4	9.6×10^{-7}	8.3×10^{-6}
pLC10	16	34	3.8×10^8	0	0	-	-
pLC11	12	18	2.7×10^8	1	1	2.7×10^{-8}	1.3×10^{-7}
pLC17	8	25	1.6×10^8	0	0	-	-

losses can be as high as 50% (data not shown). Therefore, although a maximum of eight sibling amoebal colonies could theoretically be recovered from one transformed cell, generally only one or two are recovered. Since individual experiments sometimes yield several resistant colonies, transformants from the same experiment may be unique or sibling clones. Southern blotting analysis was performed in order to determine the relationship between individual transformants from the same transformation experiment and to check whether homologous integration at *redA* was successful (Section 5.4.2).

5.4.1 Apogamic plasmodium development in transformants

The *redA* gene is first transcribed during the APT (Chapter 3) suggesting that mutation of *redA* would affect this stage of development, either by blocking plasmodium development, as seen with many of the *npf* mutations (Section 1.4.2), or generating phenotypically abnormal plasmodia. Alternatively, *redA* gene knockout may have no discernible effect on plasmodium development, suggesting that it is not essential to plasmodium development perhaps because other genes are able to compensate for its loss. All stable transformants were, therefore, tested for the ability to undergo apogamic plasmodium development and the phenotypes of the resulting plasmodia were examined.

Amoebae from each transformant and a LU352 control were tested for the ability to undergo apogamic development (Section 2.1.8). LU352 amoebae from sub-culture 61 were included as a control to confirm the phenotype expected for cells that had grown in axenic culture for a prolonged period. All of the transformants were capable of apogamic development (Table 5.2), except LC4T4 and LC4T5 which were later identified as sibling clones (Section 5.4.2). All the plasmodia were morphologically abnormal and often resembled the apogamic plasmodia of transformants derived from unrelated experiments (Figure 5.3). The LC9T1–LC9T7, LC8T1 and LC11T1 transformants initially resembled plasmodia with a vein-rich morphology similar to that shown in Figure 5.3c or grew as small fragmented plasmodia that were just a few millimetres in diameter. The majority of these eventually grew larger and developed growth fronts, resembling that shown in Figure 5.3b; the only exception being LC8T1, which developed one or two small plasmodia (approximately 2mm in diameter) that were migratory but grew no larger and eventually died. Plasmodia from transformants derived from subsequent transformation experiments (LC9T8–LC9T10, LC4T1–LC4T3 and LC5T1–LC5T8) also often failed to grow larger than a few millimetres in diameter before dying (picture not shown); the only

Table 5.2

Transformant code	Sub-culture number of amoebae	relationship from Southern blot data	Apogamic plasmodium development?
LC4T1	63	sib LC4T2	Yes
LC4T3	63	unique?	Yes
LC4T4	73	sib LC4T5	No
LC5T1	59	sib LC5T2	Yes
LC5T3	61	sib LC5T4	Yes
LC5T5	75	sib LC5T6-8?	Yes
LC8T1	29	Unique	Yes
LC9T1	20	sib LC9T2	Yes
LC9T3	33	sib LC9T5&6	Yes
LC9T4	33	sib LC9T7	Yes
LC9T8	45	sib LC9T9&10	Yes
LC11T1	27	Unique	Yes

Summary of data from the LC construct-derived stable transformants

Transformants were assigned a unique code based on the construct used for the transformation, of the format [construct code]T[number] (e.g. LC4T1 for the first transformant obtained using the LC4 construct).

Each unique transformant is listed. Southern blotting analysis enabled sibling clones (sib) to be identified and these are included for reference (Section 5.4.2). The sub-culture number for the LU352 amoebae used in the transformation experiments is shown (discussed in Section 5.4.1).

Each transformant and LU352 amoebae from sub-culture 61, as a control (data not shown) were tested for the ability to undergo apogamic development. The phenotype observed is not shown, since all were morphologically abnormal, including the control (discussed in Sections 5.4.1 & 5.5.3).

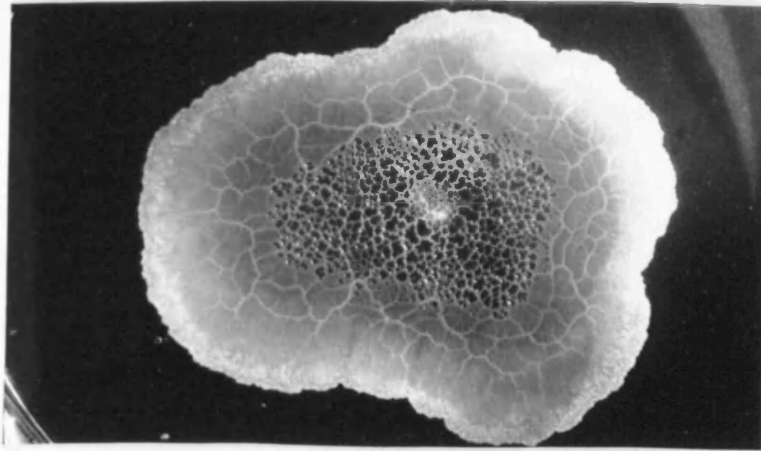
Figure 5.3 Plasmodial morphologies

a. Normal plasmodial morphology. Reproduced from Dee (1975) with permission.

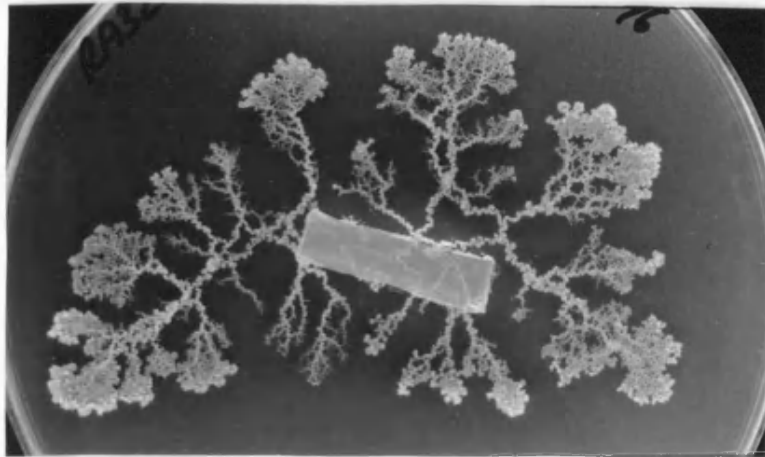
b. & c. Examples of abnormal apogamic plasmodial morphologies generated after prolonged axenic culture of amoebae used for transformation experiments (unpublished data).

Plasmodia were cultured on SDM agar plates at 26°C for 2-3 days; each plasmodium has grown outward from the central inoculum.

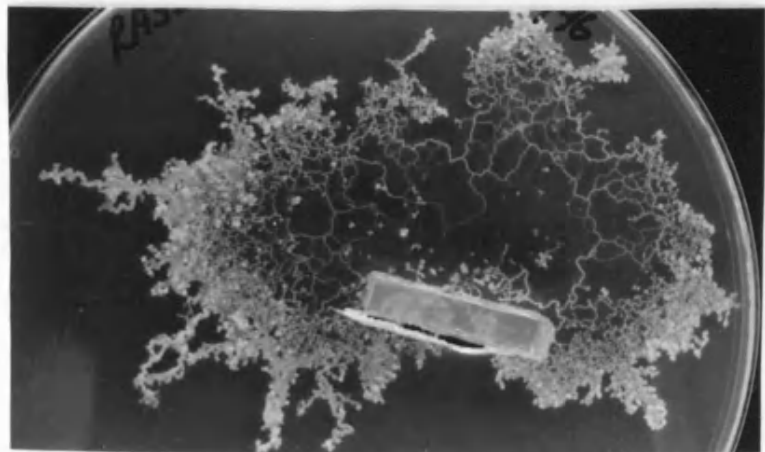
a.



b.



c.



exception was LC4T1, which developed into a small plasmodium (approximately 2cm in diameter) that had no distinct veins but did exhibit cytoplasmic streaming. It is possible that some of these small plasmodia would have grown larger under different culturing conditions. However, further analysis was not performed since the Southern blot data (Section 5.4.2) indicated that all of the transformants resulted from random integration of the transformation construct and, therefore, none of these morphological abnormalities were a consequence of *redA* gene knockout.

All of the transformants and the control were derived from the same LU352 sub-culture line. A variety of abnormalities similar to those seen in the transformants was observed when sub-culture 61 LU352 amoebae were left to develop apogamically. Therefore, it is considered unlikely that any of these morphological abnormalities were caused by the integration of the transformation constructs at random loci affecting for plasmodial morphology. The implications of these and similar findings are discussed further in Sections 5.5.3 & 5.5.6.

5.4.2 Southern blotting analysis of transformants

Southern blotting analysis was performed to determine whether homologous replacement of *redA* had occurred in any of the transformants (Section 2.4.1). Homologous integration of the constructs at *redA* should cause a shift in the size of *redA* genomic fragment(s) observed on Southern blots, due to the insertion of the selectable marker. Since the mechanism of integration is unknown, it is unclear how integration at *redA* will occur. Using LC4 (Figure 5.1) as an example, it is possible to predict the shift in fragment sizes. If the introduced LC4 construct replaces the genomic copy of *redA* (and is integrated in its entirety), the *redA* region will contain a sequence lacking introns and will also gain *PardC-hph* (Figure 5.4b). If the LC4 construct is added to the genome ahead of the *redA* gene, but does not lead to excision of the wild-type gene, the *redA* region will contain an additional 3kb (Figure 5.4c). Both of these described alterations to the *redA* genomic region will change the restriction pattern detected on Southern blots (Figure 5.4). However, if the construct is not integrated to the *redA* genomic region, two *redA* bands should be detected on Southern blots; the only exception to this would be if the part of the construct carrying *redA* was lost on integration, as has been observed in previous transformation experiments (Section 1.6.5; Pierron *et al.*, 1999).

Figure 5.4: Schematic representation of possible mechanisms of disruption of *redA* by integration of LC4

Schematic model of possible mechanisms for targeted disruption or homologous gene replacement of *redA* using the LC4 constructs (Section 5.4.2).

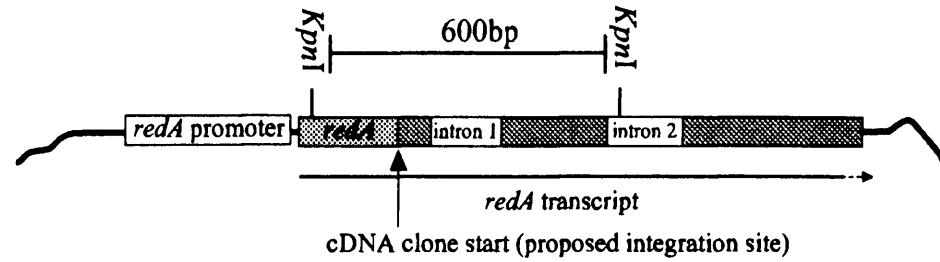
a. Genomic region of *redA* including the proposed integration site, which in these hypothetical examples corresponds with the start of the cDNA clone. The coding region of *redA* is shown as shaded boxes () and the darker shaded boxes () represent regions of identity with the cDNA clone. The location of the *KpnI* sites is indicated; these are situated ahead of the region of identity with the cDNA clone and within the second intron of *redA*. Therefore, the presence of a wild-type genomic copy of *redA* will produce a distinct 600bp *KpnI* band on Southern blots.

b. Hypothetical homologous replacement of the entire region of *redA* with homology to the cDNA clone by the complete LC4 construct. If such a transformation event occurred, the *KpnI* site in the second intron would be lost and the *redA* coding region would be disrupted by the *PardC-hph* sequence at the *XcmI* site (Section 5.2.2). Therefore, the 600bp *KpnI* band would not be present on Southern blots (Section 5.4.2).

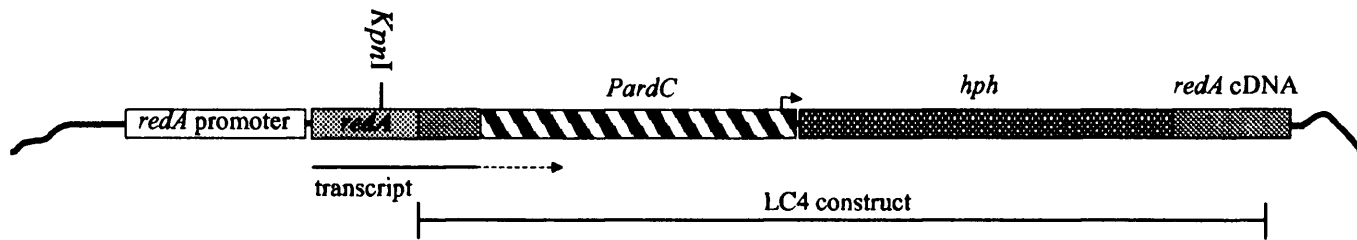
c. Hypothetical integration of the complete LC4 construct at the site corresponding to the start of the region of identity to the cDNA clone. If such an event occurred, the *KpnI* site in the second intron would be separated from the first site by an additional 3kb of sequence, thus a 3.6kb *KpnI* band would be observed on Southern blots instead of the 600bp fragment (Section 5.4.2).

For both b. and c. the *redA* transcript would be chimeric, containing part *redA* and part *PardC* sequences (discussed in Section 5.2.2).

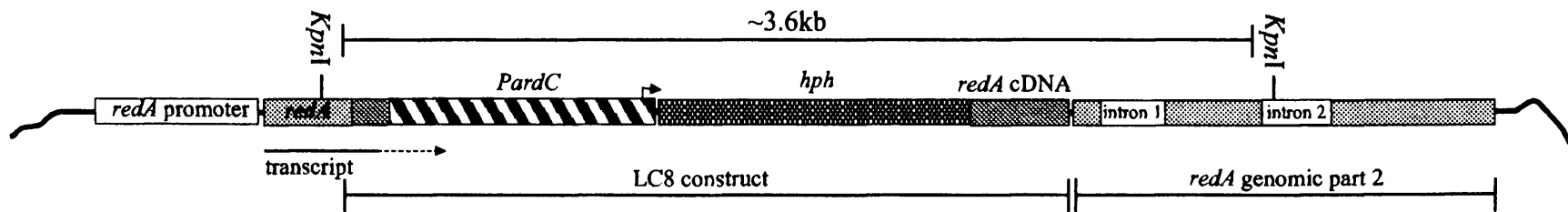
Figure 5.4



a. Genomic region containing *redA*



b. Hypothetical homologous replacement of *redA* with LC4



c. Hypothetical integration of LC4 near the start of *redA*

A single copy of the *ardC* promoter, *PardC*, exists in the haploid *Physarum* genome. Since *ardC* accounts for the majority of actin transcripts (Section 1.3.2), targeted integration of the transformation constructs at *PardC* would be highly detrimental to the amoeba and such transformants are unlikely to survive. Therefore, a wild-type copy of *PardC* was expected on the Southern blots from all transformants. The level of hygromycin selected for screening is sufficient to suppress spontaneous resistance of 10¹⁰ amoebae (Section 1.6.5; Burland *et al.*, 1993a). To reduce the possibility of selecting amoebae with spontaneous mutations conferring resistance to hygromycin as a result of reduced activity of hygromycin in the selective plates, two rounds of selective screening were performed (Section 2.1.7). In order to survive such screening, all transformants must contain at least one functional copy of *PardC-hph*. Therefore, Southern blotting analysis of transformants should identify both the wild-type and integrated *PardC* sequences.

Southern blotting of digested DNA from transformants was expected to generate one of three distinct restriction patterns, provided restriction enzymes with no internal sites for either the construct or *redA* are used:

- i. Two *PardC* bands (one wild-type and one integrated) plus two *redA* bands (one wild-type and one integrated); such a pattern would suggest non-homologous integration.
- ii. Two *PardC* bands (one wild-type and one integrated) plus one *redA* band of the same size as the integrated *PardC*; such a pattern would suggest targeted disruption of *redA*.
- iii. Two *PardC* fragments (one wild-type and one integrated) plus one wild-type *redA* fragment; such a pattern would suggest non-homologous integration of *PardC-hph* alone (Section 1.6.5; Pierron *et al.*, 1999).

5.4.2.1 Southern blotting analysis of transformants derived from LC4 and LC5

Five transformant colonies were obtained from two experiments using the LC4 construct (Table 5.1); LC4T1, LC4T2 and LC4T3 were derived from one transformation experiment whilst clones LC4T4 and LC4T5 were derived from a second experiment. The LC5 construct (Figure 5.1) generated eight transformants from three separate transformation experiments (Table 5.1); LC5T1 and LC5T2 were derived from one experiment, LC5T3 and LC5T4 from a second and LC5T5–LC5T8 from a third.

Genomic DNA for Southern blotting (Section 2.2.1) from LC4T1–LC4T3 and LC5T1–LC5T4 was digested with *Hind*III and *Bam*HI, since these enzymes generate a single *redA* genomic band that is less than 10kb in size (7.6–7.3kb for *Bam*HI and 6.6–6.3kb for *redA*; LU352, Table 5.3). Differences in the sizes of detected bands are considered likely to be an artefact of the blotting procedure. By limiting the size of the genomic fragment to less than 10kb, changes to fragment sizes, due to integration of the selectable marker would be easy to detect on the Southern blots; the larger a fragment becomes, the harder it is to see small size changes using agarose gels. Digestion with *Bam*HI separates the *PardC* and *hph* components of *PardC-hph* and therefore three bands were expected for this digest when probed with *PardC-hph* (one for wild-type *PardC*, one for the introduced *PardC* and one for *hph*). Southern blots were probed first for *redA* and then for *PardC-hph*.

When the first Southern blot was probed for *PardC-hph*, it became apparent that the LU352 wild-type *PardC* and *redA* bands generated using these enzymes were coincidentally of similar sizes (both 7.6–7.3kb for *Bam*HI and 6.6–6.3kb for *Hind*III; Table 5.3). This created difficulties in confirming that the *PardC-hph* component was present since the signal may have been attributable to background remaining after the initial *redA* probing; however, since the colonies were hygromycin resistant, it was assumed that the *PardC-hph* component must be present.

The LC4T1–LC4T3 transformants appeared to contain just a single copy of *PardC* (Table 5.3), perhaps because the fragments for the integrated and wild-type sequences were of similar sizes (*Hind*III; Table 5.3) or as a result of uneven hybridisation of the probe. The only *Bam*HI band detected using *PardC-hph* as a probe was smaller than expected for the wild-type copy of *PardC* suggesting that this could be the integrated copy of *PardC* or *hph*. However, no wild-type band could be detected for *PardC* (Table 5.3). Furthermore, the only *Bam*HI and *Hind*III *redA* fragments detected were of the sizes expected for the wild-type copy of *redA* (Table 5.3). Therefore, there was insufficient evidence to determine whether homologous integration at *redA* had occurred. Since the Southern blot data was inconclusive, further Southern blotting was performed using *Kpn*I. *Kpn*I was selected as a replacement for *Bam*HI because the two *Kpn*I sites situated in the *redA* gene, which generate an internal 600bp band, are located ahead of the region covered by the cDNA clone and in the second intron (Figure 4.4 & 5.4a); since there are no introns

Table 5.3: Data from Southern blotting analyses of transformants derived from the *redA* constructs

These data were compiled from several Southern blots and some digests were repeated (data not shown). When a particular digest was repeated, there were sometimes small discrepancies with the calculated size of the fragment(s) produced as an artefact of the blotting procedure. In these cases the range of estimated sizes is given. The sizes of these bands were determined relative to λ *Hind*III and ϕ X174 *Hae*III DNA size markers. All Southern blots were probed first for *redA* and then for *PardC-hph*.

The banding patterns expected for wild-type sequences were determined from the parental strain, LU352 (†). Fragments shown in **bold** were deduced to correspond to wild-type sequences. Fragments shown in (brackets) produced a low intensity signal on the Southern blot and those larger than 22kb were considered likely to represent undigested genomic DNA. Where a hyphen is shown (-), no signal could be detected on the blot. Where n/a is shown, the enzyme listed was not included on the Southern blot. Transformants derived from the same transformation experiment are grouped together, separated by solid lines in the table.

Table 5.3

Transformant	<i>redA</i>			<i>PardC-hph</i>		
	<i>Bam</i> HI	<i>Hind</i> III	<i>Kpn</i> I	<i>Bam</i> HI	<i>Hind</i> III	<i>Kpn</i> I
LU352 †	7.6-7.4kb	6.6-6.3kb	6kb, 600bp	7.6-7.3kb	6.6 kb-6.3kb	20kb
LC4T1	7.6kb	6.6kb, 6.4kb	6.2kb, 6kb, 600bp	4.8kb	6.6kb	20kb, (25kb)
LC4T2	(25kb), 7.6kb	6.6kb	6.2kb, 6kb, 600bp	4.8kb	6.6kb	20kb, (25kb)
LC4T3	7.6kb	6.6kb	6kb, 600bp, 580bp	4.8kb	6.6kb	20kb, (25kb)
LC4T4	n/a	6.6kb,6.4kb	6.2kb, 6kb, 600bp	n/a	-	20kb, 6.2kb
LC4T5	n/a	6.6kb,6.4kb	6.2kb, 600bp(faint)	n/a	-	-
LC5T1	16kb, 7.6kb	6.6kb, 5.3kb	6.2kb, 6kb, 600bp	16kb	6.6kb, 5.3kb	-
LC5T2	16kb, 7.6kb	6.6kb,6.4kb, 5.3kb	20kb, 6.2kb, 6kb, 600bp	16kb	6.6kb, 5.3kb	20kb
LC5T3	(25kb), 7.6kb	6.6kb,6.4kb, (25kb)	20kb, 18kb,6.2kb, 6kb, 600bp	(25kb), (10kb)	6.6kb	20kb
LC5T4	7.6kb	6.6kb,6.4kb, (25kb)	22kb, 20kb,6.2kb, 6kb, 580bp	-	6.6kb	20kb
LC5T5	n/a	6.6kb,6.4kb	6.2kb, 6kb, 600bp	n/a	6.6kb	20kb
LC5T6	n/a	6.6kb,6.4kb	6.2kb, 6kb, 600bp	n/a	-	20kb
LC5T7	n/a	6.6kb,6.4kb	6.2kb, 6kb, 600bp	n/a	-	20kb
LC5T8	n/a	-	6.2kb, 6kb, 600bp	n/a	-	20kb
LC8T1	7.4kb	6.3kb	6kb, 600bp	7.4kb	6.3kb	-
LC9T1	7.4kb	(25kb), 6.3kb	n/a	7.3kb, 5.3kb	6.3kb	n/a
LC9T2	7.4kb	(25kb), 6.3kb	n/a	7.3kb, 5.3kb	6.3kb	n/a
LC9T3	7.4kb, 5.8kb	18kb, 6.3kb	n/a	5.6kb	18kb, 6.3kb	n/a
LC9T4	7.4kb, 6.2kb, 5.8kb	18kb, 6.3kb	10kb, 6.2kb, 6kb, 600bp	6.4kb, 6.2kb, 4.5kb, 1.2kb	6.4kb, 6.3kb	20kb, 10kb
LC9T5	7.4kb, 5.8kb	18kb, 6.3kb	n/a	5.6kb	18kb, 6.3kb	n/a
LC9T6	7.4kb, 5.8kb	18kb, 6.3kb	n/a	5.6kb	18kb, 6.3kb	n/a
LC9T7	7.4kb, 5.8kb	18kb, 6.3kb	n/a	6.2kb, 4.5kb, 1.2kb	6.3kb	n/a
LC9T8	7.6kb	6.6kb,6.4kb	6.2kb, 6kb, 600bp	-	6.6kb	-
LC9T9	7.6kb	6.6kb,6.4kb	6kb(faint), 600bp	-	6.6kb	-
LC9T10	7.6kb	6.6kb	(25kb), 20kb,6.2kb, 6kb, 580bp	-	6.6kb	-
LC11T1	7.4kb	6.3kb	n/a	(25kb),4.2kb	5.2kb	n/a

in the cDNA and hence no internal *KpnI* site, the 600bp internal fragment would be lost if the wild-type *redA* gene is replaced by the cDNA-based constructs (e.g. construct LC4; Figure 5.4b). However, if the construct was integrated close to the start of the wild-type gene such that it was added to the region rather than replacing the gene, the second *KpnI* site would be shifted approximately 3.6kb away from the first (Figure 5.4c). In addition to the *KpnI* digestion, the *HindIII* digestions were repeated, in order to confirm the preliminary observations. Thereafter, Southern blots for newly isolated transformants (LC4T4 & LC4T5, LC5T4–LC5T8; Table 5.3) were performed using *KpnI* and *HindIII* digestions only.

The *KpnI* data for *redA* was the most informative for determining whether homologous replacement of *redA* had occurred in any of the transformants. When the only bands observed using the *redA* probe were of the size(s) expected for the wild-type *redA*, it was assumed that the integrated and wild-type *redA* sequences were either on similar-sized restriction fragments or that one of the sequences had failed to produce a strong hybridisation signal (e.g. LC4T3; Table 5.3). In many instances, *redA* bands of the sizes expected for the wild-type *redA* gene were observed along with an additional band(s) (e.g. LC5T1; Table 5.3); in such cases, it was deduced that the additional *redA* fragment(s) was derived from random integration of the construct. If the probe for *PardC-hph* hybridised to the same additional band (for *HindIII* and *KpnI* only), this confirmed that the band was due to random integration of the construct (e.g. 5.3kb LC5T1 fragment; Table 5.3).

Both LC4T1 & LC4T2 produced the same extra bands on Southern blots; a 4.8kb *BamHI* *PardC-hph* band and a 6.2kb *KpnI* *redA* band (Table 5.3). Since these two clones were derived from the same transformation experiment and share similar banding patterns on the Southern blots, it is clear that they are sibling clones (Table 5.3). It is possible that LC4T3 is also a sibling to LC4T1 & LC4T2, but the *KpnI* data for this clone differs from the other two in that a faint band was observed at approximately 580bp, in addition to the wild-type 600bp fragment (Table 5.3). Further Southern blot analysis is required to determine whether this clone is unique or a sibling to LC4T1 & LC4T2. Clones LC4T4 & LC4T5 were both derived from the same transformation experiment and the Southern blot data indicate that these are probably sibling clones (diagnostic bands: 6.4kb *HindIII* *redA* band and 6.2kb *KpnI* *redA* bands; Table 5.3) although, once more, further Southern

blotting analysis is required to confirm this. Therefore, the five clones isolated from the transformation experiments using LC4 probably represent three unique independent integration events (Table 5.1).

Since the LC5 transformants were derived from three separate experiments, at least three unique integration events had occurred. The Southern blot data showed that LC5T1 & LC5T2 are siblings (diagnostic bands: 6.4kb *Hind*III and 6.2kb *Kpn*I *redA* fragments; Table 5.3), LC5T3 & LC5T4 are probably siblings (diagnostic bands: 16kb *Bam*HI & 5.3kb *Hind*III fragments; Table 5.3) and LC5T5–LC5T8 are also probably siblings (diagnostic bands: 6.4kb *Hind*III & 6.2kb *Kpn*I *redA* fragments; Table 5.3), although the Southern data for LC5T5–LC5T8 are incomplete due to limited success with the genomic DNA isolation (Table 5.3).

In summary, since both wild-type and introduced *redA* sequences were detected on the Southern blots for all the LC4 and LC5-derived transformants, it is clear that homologous gene replacement of *redA* has not occurred in any of these transformants.

5.4.2.2 Southern blotting analysis of transformants derived from LC8, LC9, LC10 and LC11

The same strategy described above for the analysis of LC4 and LC5 transformants was applied to the transformants derived from LC8, LC9 and LC11; the construct LC10 (Figure 5.1) failed to generate any transformants in these experiments (Table 5.1).

LC8 generated a single transformant (LC8T1; Table 5.1). Only single bands of the sizes expected for wild-type *redA* and *PardC* sequences were observed on the Southern blots (Table 5.3). Since the clone was resistant to hygromycin, it is odd that it did not generate additional bands for the three digests selected. Further analysis of this clone would clarify why no second *PardC* fragment was detected. It is unlikely that this clone became spontaneously resistant to hygromycin, since previous experiments found no spontaneous resistance in 10^{10} amoebae and two rounds of selection were used (Section 1.6.5; Burland *et al.*, 1993a). The presence of the 600bp *Kpn*I *redA* fragment clearly demonstrates that homologous replacement of *redA* had not occurred; therefore, no further investigation was performed.

LC9 was the only construct, other than LC4 and LC5, that generated more than one transformant clone; 10 transformants were obtained from three separate experiments (Table 5.1). LC9T1 & LC9T2 were derived from the first experiment, LC9T3–LC9T7 from the second and LC9T8–LC9T10 from the third. The Southern blot data indicate that LC9T1 & LC9T2 are siblings (diagnostic bands: 5.3kb *PardC Bam*HI fragment; Table 5.3), LC9T3, LC9T5 & LC9T6 are siblings (diagnostic bands: 5.6kb *PardC Bam*HI and 18kb *PardC Hind*III fragments; Table 5.3), LC9T4 & LC9T7 are siblings (diagnostic bands: 6.2kb, 4.5kb & 1.2kb *PardC Bam*HI fragments; Table 5.3) and LC9T8–LC9T10 are probably siblings (diagnostic bands: all *redA* data; Table 5.3). However, further Southern blotting analyses of LC9T8–LC9T10 are required to clarify this result. Therefore, four unique transformants were generated and two of these came from the same experiment (LC9T3/5/6 and LC9T4/7). It is clear from the Southern blot data that none of these transformants is the result of homologous gene replacement at *redA*, since all contain both the introduced and wild-type *redA* sequences (e.g. LC5T1; Table 5.3).

A single transformant was obtained using the LC11 construct (LC11T1; Table 5.3). Clone LC11T1 produced a band that hybridised to *PardC-hph* (4.2kb; Table 5.3), which was smaller than the wild-type *PardC* band (7.5kb; Table 5.3) and was therefore deduced to be a product of the transformation. However, the *redA* probe failed to hybridise to the same band and only generated wild-type bands (Table 5.3). Since this 4.2kb band did not label with *redA*, it is possible that the *redA* portion of this construct was lost on integration to the genome; such losses have been observed before (Section 1.6.5; Pierron *et al.*, 1999). Sequencing of the integrated DNA would confirm this, but since homologous replacement of *redA* had not occurred, this was not necessary.

5.5 DISCUSSION

5.5.1 Summary of results

Vectors designed for gene knockout were constructed successfully and used for transformation in *P. polycephalum*. The vectors designed to target homologous gene replacement of *redA* (LC4–5, LC8–11; Figure 5.1) generated 12 unique transformants (Tables 5.1 & 5.2) from nine different experiments. Unfortunately, Southern blotting analysis revealed that all of the transformants were the result of random integration into the *Physarum* genome, and not homologous integration at *redA* as desired (Table 5.3). Since a maximum of just four unique transformants were obtained for a single construct

(LC9; Table 5.1), the lack of homologous integration was not surprising. Burland & Pallotta (1995) found that only 1 in 20 of their transformants was the product of homologous integration of the vector at the target locus. Their data suggest that as many as 60 transformants may be required for each construct to be certain of obtaining a homologous transformant (95% confidence limit; Burland & Pallotta, 1995). It is anticipated that further transformation experiments using these vectors could eventually generate a homologous *redA* transformant.

The *redA* antisense vector LC17 was used in eight transformation experiments (Table 5.1). However, no transformants were recovered. Further discussion of antisense RNA mutagenesis and possible future experiments based on this procedure is included in Section 5.5.4.

5.5.2 Optimisation of gene disruption vector design

The transformants generated in this study provide no clarification of the optimum design strategy for DNA transformation in *Physarum*. The constructs designed in this Chapter either contained homology to *redA* at just one end of the fragment, with the selectable marker at the other end (LC8–LC11; Figure 5.1), or homology at both ends of the fragment, with the selectable marker in the middle (LC4 & LC5; Figure 5.1). Burland & Pallotta (1995) failed to generate any transformants using vectors with similar designs to LC4 & LC5. Therefore, the studies reported in this Chapter have demonstrated that this type of vector design is suitable for transformation studies in *P. polycephalum*. In total, the same number of unique transformants was generated using both vector design strategies. It is noteworthy that the first construct design (LC8–LC11; Table 5.2) was most successful when cells from a lower sub-culture were used, while the opposite was observed for the second construct design (LC4 & LC5; Table 5.2). The significance of this observation cannot be ascertained from such a small pool of transformants. Since no homologous recombination occurred between the LC vectors and *redA*, it is still unclear whether a particular vector design is more suitable for homologous gene replacement.

Studies by Hernon (1996) and E. Swanston (personal communication) indicate that a transcriptional terminator, such as *TardC*, may be necessary to reduce the risk of generating transcripts with reduced stability or function (discussed in Section 1.6.7). The orientation of *PardC-hph* in constructs LC4 and LC8 is such that transcription proceeds

from *PardC* through *hph* and then into the *redA* cDNA. As discussed in Section 5.3, the 3' end of the *redA* cDNA containing the polyadenylation signal for *redA* is A/T-rich and may act as a transcriptional terminator. Therefore, although the 3' untranslated region of the *hph* transcripts generated by these two constructs will be slightly larger than usual, the transcript may be relatively stable. In LC11, the *hph* gene is positioned such that transcription proceeds from *PardC* through *hph* and into the 3' end of the reversed *redA* cDNA. As discussed above, this region may be sufficient to act as a transcriptional terminator for *hph* and thus prevent long, potentially unstable transcripts. The direction of transcription for *hph* in the LC5 and LC9 constructs is such that the 3' untranslated region of the *hph* transcript will correspond with either reversed 5' *redA* and *redA* promoter sequences (for homologous integration at *redA*), or sequences situated upstream of the site of integration (for random integration) until reaching a transcriptional terminator. Similarly for LC10, transcription of *hph* will proceed into sequences situated downstream of the site of integration. For LC5, LC9 and LC10, the recovery of hygromycin resistant transformants will, therefore, depend largely on the stability of the *hph* transcript, influenced largely by the 3' untranslated region. Theoretically, of all these designs, LC11 may produce the most stable *hph* mRNA transcript.

5.5.3 Factors affecting the transformation efficiency

The highest frequency of transformation reported in the literature is 1×10^{-7} per cell, in which a single copy of linearised selectable marker, *PardC-hph*, had integrated to random sites in the *Physarum* genome (Section 1.6.6; Burland *et al.*, 1992b). The highest transformation frequency obtained using an individual construct in the experiments described in this Chapter was 8.3×10^{-6} per cell for an single experiment and a mean frequency of 9.6×10^{-7} per cell for the experimental period (LC9; Table 5.1); thus, consistent with previous observations (Burland & Pallotta, 1995; Burland *et al.*, 1993a).

Several independent factors may affect the transformation efficiency. One factor was the amount of DNA used for each transformation experiment. The yield of plasmid DNA from the bacterial stocks used in this study was often low and provided limited quantities of DNA for experimentation. Therefore, in most of the experiments reported in this Chapter, approximately 2 μ g of DNA was used for each electroporation sample (Table 5.1). It is possible that increasing the amount of DNA used for these experiments would have generated more transformants. Generally, transformation efficiencies increase

linearly with increasing DNA concentration until a 'plateau' is reached (Miller, 1994; Lurquin, 1997). To my knowledge, no studies have been performed in *Physarum* to determine the concentration of DNA at which a 'plateau effect' is observed. With such low transformation efficiencies, it would be time-consuming to conduct such a study since numerous experiments would be required. Previously, 1µg to 20µg of DNA have been used for each transformation (Burland *et al.*, 1993a; Burland & Bailey, 1995; Burland & Pallotta, 1995). Whilst it is tempting to use increasing amounts of input DNA on the assumption that the 'plateau' has not been reached, reducing the amount of DNA may increase the efficiency of some experiments (D. Pallotta, personal communication). In my studies, the highest transformation efficiency for a single experiment was obtained using 1µg of LC9 vector DNA (data not shown).

Other factors that affect the efficiency of transformation, such as the buffer composition and amoebal cell density, have been optimised for transformation (reviewed by Burland & Bailey, 1995) and it is unlikely that major improvements to the transformation efficiency can be made in these areas.

An additional factor that can affect the transformation efficiency is the condition of the axenic amoebal cell culture. For example, if the sub-culture line becomes contaminated with bacteria or other micro-organisms, antibiotics are added to the culture and the rate of cell doublings drops substantially for the following 2-3 sub-cultures (personal observation). This reduction in cell growth may reflect a decrease in the cell growth rate or may be associated with substantial cell death within the cell population. Either of these could lead to a reduced transformation efficiency. However, since the cells used in this study were from uncontaminated, actively growing axenic culture, this is considered unlikely to have affected the transformation efficiency.

The growth rate of axenically grown LU352 amoebae is slow during the first 10 sub-cultures and then settles to a doubling time of approximately 24 hours (Dee *et al.*, 1989); the reasons for this change are unclear. Transformation is inefficient during these first sub-cultures. Once a stable doubling time of 24 hours is obtained, the amoebae transform well. However, prolonged axenic growth leads to an accumulation of abnormalities in the axenic strain (Section 1.6.1; Dee *et al.*, 1989). Dee *et al.*, (1989) maintained LU352 amoebae in axenic conditions for up to 28 sub-cultures to assess

changes to the strain “during prolonged culture in liquid axenic medium” and found that the frequency of flagellate formation decreased; it was suggested that continuous axenic culture could lead to a complete loss of this transition.

The extent to which abnormalities occur varies; such abnormalities are inherited by progeny and are thus genetic in origin (Dee *et al.*, 1989). The majority of mutations that cause the abnormalities do not appear to affect axenically grown amoebae. However, if by chance a mutation happens to confer improved axenic growth on the amoebae, it is easy to see how it could rapidly accumulate in the cell population. Assuming the mutations that cause these abnormalities arise on a random basis, it would follow that different sub-cultures may exhibit different properties. This is supported by the fact that abnormal plasmodial morphologies arose as early as sub-culture 20 in these studies (LC9T1; Table 5.2). However, it is possible that some of the abnormalities observed were caused by integration of the transformation construct at a locus that affects plasmodial morphology. Genetic analysis of progeny from a cross between transformant and normal amoebae would help clarify this.

Such genetic analysis was performed on several stable hygromycin-resistant transformants from previous transformation experiments, which developed into morphologically abnormal plasmodia (Figure 5.3). These transformants were generated from several independent experiments using amoebae that had been maintained in axenic culture for 47–80 sub-cultures prior to transformation. The linkage studies confirmed that all the mutations leading to abnormal plasmodial morphologies were independent of the integration of the transformation construct. This analysis also suggested that the morphological abnormalities were associated with mutations involving more than one locus in each transformant examined (data not shown).

The LC transformants, described in this Chapter, were all maintained in axenic conditions prior to transformation for as many as 75 sub-cultures (Table 5.2) and all exhibited abnormal plasmodial morphologies. Functional gene analysis of *redA* would be extremely difficult using populations of cells with inherent abnormalities. It is therefore important that axenic cultures are re-initiated from frozen stock at regular intervals if the problems described above and by Dee *et al.* (1989) are to be avoided in future transformation studies. Further evidence for this was obtained by Pallotta and colleagues whilst

attempting gene knockout of the profilinP gene (*proP*) in *Physarum*. For some time, they believed a *proP* gene knockout had produced abnormal plasmodial morphology, only to subsequently discover that the mutation they were studying was in fact unlinked to the recombination event (personal communication). Pallotta and colleagues have since taken heed of the warnings from Dee *et al.* (1989) regarding prolonged axenic culture of amoebae and are routinely re-initiating axenic amoebae approximately once every 3 months (personal communication), which is equivalent to 20–30 sub-cultures. It may be prudent to limit the number of sub-cultures to a maximum of 40 for future transformation studies. Further investigation of the affects of prolonged axenic culture on strain LU352 for sub-cultures between 20 and 60, based on Dee *et al.* (1989), would allow a more accurate estimate of the safe limit for prolonged axenic culture.

5.5.4 Antisense RNA-mediated gene inactivation

Antisense RNA-mediated gene inactivation was selected as a method to eliminate *redA* gene function, since it does not require homologous integration of the introduced DNA. However, no hygromycin-resistant antisense *redA* transformants were generated in this study. Had a hygromycin resistant transformant been isolated, there was no guarantee that the antisense-*redA* would have knocked out *redA* gene function. A defined ‘set of rules’ for antisense RNA mediated gene inactivation has never been compiled, due to the complex nature of antisense transcription (Section 5.1.2; Kuspa *et al.*, 1995). The sequence of antisense RNA and its associated secondary structure differs for each antisense experiment and may cause interference to the sense-antisense RNA interaction. In many cases, the antisense transcripts are unstable, possibly due to the lack of polyadenylation signal (Kuspa *et al.*, 1995). Inclusion of termination sequences, such as *TardC*, may improve the stability of the antisense transcript. Although *TardC* was included in the *redA* antisense vector used for these studies, it was positioned such that it would improve the stability of the *hph* transcript to aid the selection process and would not, therefore, have helped stabilise the antisense *redA* transcript.

Since it is difficult to predict the most effective design for an antisense construct, it is generally recommended that different sized fragments from different locations within the cDNA are tested (Kuspa *et al.*, 1995). During the study reported in this Chapter only one fragment was tested (*EcoRV-Sau3AI*) mainly due to time constraints but also because

there were a limited number of cDNA fragments that were suitable for antisense studies, since the *redA* cDNA is only 660bp in size.

The length of the linearised LC17 antisense fragment was approximately 5.5kb, almost twice that of the gene replacement vectors (Figure 5.1). Similar-sized constructs have been used successfully in transformation of *Physarum*, although the frequency of transformation was reported as less than that obtained for the same construct located on a smaller fragment (Burland & Pallotta, 1995). As discussed previously (Section 1.6.5), this difference may have been largely due to differences in the number of molecules used for each transformation (Ohse *et al.*, 1995). For this study, slightly more DNA was used for each antisense RNA experiment (approximately 3 μ g compared with 2 μ g) to compensate for such size differences.

The region where *PardB* was ligated to the klenow-treated *Sau3AI* site of *redA* was not sequenced; therefore, the exact coding region of this transcript was not determined. However, investigation of the potential transcripts of the antisense *redA* identified stop codons in all three reading frames within 100bp of the *Sau3AI* site. Therefore, any translation of the antisense mRNA would generate very small proteins (data not shown).

Pallotta and colleagues recently used antisense RNA mutagenesis in an attempt to inactivate *proP* (Section 1.3.2). Although stable transformants were obtained, the antisense *proP* transcripts had no discernible effect on the phenotype (D. Pallotta; personal communication). This was possibly because they used the *proP*-promoter to drive the antisense expression instead of using a stronger promoter. Since the *proP*-promoter would induce equal expression of both the native *proP* and the antisense construct, there would not be an excess of antisense transcripts in relation to *proP* mRNA. In addition, the potential instability of the antisense transcript could lead to an overall reduction in the ratio of antisense:native *proP* transcripts; thus, leaving insufficient antisense transcripts to affect *proP* function.

The antisense-*redA* was placed under the control of *PardB*, the constitutive *ardB* promoter from *Physarum*. This promoter is known to be a strong constitutive promoter, although not as strong as *PardC* (Section 1.3.2; Burland *et al.*, 1992a). Therefore, antisense *redA* transcripts would be present at all stages of the life cycle. Northern

analysis demonstrates that *ardB* is transcribed at much higher levels than *redA*. Thus, using *PardB* to drive the expression of the antisense *redA* should generate an excess of antisense *redA* transcripts, hopefully sufficient to knockout RedA function. Clearly, with such an experiment, it is possible that the expression of antisense transcripts are deleterious to the amoebae and may lead to cell death. Construction of an antisense system using a promoter with no amoebal activity, such as a *red* gene promoter or a plasmodium-specific promoter (e.g. the *proP*-promoter) would eliminate any potential deleterious effect that antisense-*redA* transcripts have on amoebae.

5.5.5 Future studies on *redA*

The *redA* constructs designed for these studies utilised the *redA* cDNA clone, since a genomic clone for *redA* was not available. One problem with using the cDNA clone was that it provided limited continuous homology with which to target gene replacement (Section 5.2.2), since the region of homology was broken into smaller fragments by the intron sequences. If the altered *redA* cDNA replaced the native *redA* gene, there is a possibility that the lack of intron sequences will be detrimental, e.g. to the stability of the *redA* region or transcription of the sequence. A genomic *redA* clone would enable constructs to be designed that contained much more homology to the *redA* gene and would eliminate potential problems associated with the intron sequences.

Once homologous gene replacement of *redA* is achieved, a combination of studies could be performed to investigate the effect of the gene replacement, using techniques already developed for *Physarum*. Such studies could include time-lapse cinematography and immunofluorescence microscopy of cells undergoing the APT. Time-lapse studies (Bailey *et al.*, 1987 & 1990) may identify changes in the acquisition of plasmodial characteristics, such as the ability to ingest amoebae, or in the size and behaviour of the cell and/or nucleus during plasmodium development. Immunofluorescence microscopy, similar to that used by Solnica-Krezel *et al.* (1988 & 1991), would enable changes to the organisation of the cytoskeleton and mitotic spindle to be examined. Any changes to the nucleus could be investigated further by flow cytometry to check the DNA content of the cells (Bailey *et al.*, 1992a). Using a classical genetic approach, linkage studies would enable the relationship of *redA* and other previously characterised genes to be ascertained, e.g. the mating-type genes and the *npf* genes (Anderson *et al.*, 1989; Bailey *et al.*, 1992a; Solnica-Krezel *et al.*, 1995). If the above studies reveal that *redA* knockout prevents or

disrupts plasmodium development, strains carrying the *redA* knockout and an *npf* mutation, generated as a result of the linkage studies, could be examined further to determine whether the genes lie in the same developmental pathway (Section 1.4.2.2; Solnica-Krezel *et al.*, 1995). In addition, such linkage studies could facilitate the cloning of linked loci, by direct cloning or using the *hph* gene as a primer target for techniques such as inverse PCR or sequence 'walking'.

5.5.6 Other future transformation studies

Restriction enzyme mediated integration (REMI) is a transformation method that has been successfully applied to *D. discoideum* and *Aspergillus nidulans* (Kuspa & Loomis, 1992; Kuspa *et al.*, 1995; Sánchez *et al.*, 1998). REMI-based transformation is performed in the presence of restriction enzymes that cleave the genome of the host; the linear constructs are then ligated to the host DNA on a random basis *via* the hosts DNA repair mechanisms. REMI was found to increase the transformation efficiency in *D. discoideum* and *A. nidulans* by 20 to 60-fold (Kuspa *et al.*, 1995; Sánchez *et al.*, 1998) and could potentially also increase the rate of non-homologous integration in *Physarum*. Since antisense RNA mutagenesis does not require homologous integration, REMI has potential for future antisense studies in *Physarum*. Such studies would first need to assess how the restriction mixture affects the transformation efficiency for *P. polycephalum*.

Another gene knockout technique that has increased in popularity in recent years is RNAi (RNA interference; reviewed by Hunter, 1999). RNAi has been used successfully to manipulate gene expression in *Caenorhabditis elegans* (Fire *et al.*, 1998), *Trypanosoma brucei* (Ngô *et al.*, 1998) and *Drosophila melanogaster* (Misquitta & Paterson, 1999). The introduction of sense, antisense or double-stranded RNA (ds-RNA) corresponding to either part or the entire coding region of a gene of interest leads to the down-regulation of expression of that gene. Interestingly, ds-RNA was more effective than either sense or antisense RNA transcripts alone (Fire *et al.*, 1998). The major benefit of such a system is that no integration is required. Instead, RNA for the gene of interest is produced *in vitro* from the cDNA, using the RNA polymerase sites located in the vector, and then transfected into the cells (Fire *et al.*, 1998; Ngô *et al.*, 1998). Some residual mRNA was observed during the RNAi studies using *T. brucei* and was thought to result from transcription in the 5–10% of cells that had escaped transformation (Ngô *et al.*, 1998). One problem with RNAi in *Physarum* would be the lack of selectable or screenable

marker to identify non-transformed cells. If suitable RNA could be electroporated into a high proportion of *Physarum* amoebae, this would be unlikely to cause problems. However, without some kind of marker, it would be difficult to determine the proportion of amoebae that contained the transformed ds-RNA. Fluorescent markers such as green fluorescent protein (GFP) could prove useful in determining the proportion of amoebae that receive the sample used for transformation.

Another significant factor when considering the potential of RNAi is the stability of the ds-RNA in the host cell. The transient studies using luciferase vectors have shown that although DNA is easily transformed into *P. polycephalum* amoebae, the expression of luciferase from the non-integrated molecule peaks 2–5 hours after electroporation and drops rapidly thereafter (Bailey *et al.*, 1994). Luciferase used similarly in other systems appears to be more stable, with expression peaking around 24 hours after transformation and remaining present for several days, consistent with losses due to dilution at cell division (Brasier & Ron, 1992; discussed by Bailey *et al.*, 1994). The rapid decline in *Physarum* was not associated with plasmid loss at cell division since the levels dropped faster than that expected for a non-replicating plasmid (Bailey *et al.*, 1994). Therefore, it is likely that some active mechanism is responsible for the rapid decline of luciferase expression, although it was unclear whether RNA, DNA or protein was degraded (Bailey *et al.*, 1994). Therefore, ds-RNA may not be stable for sufficient time for RNAi studies of the APT in *Physarum*, but may be adequate for functional analysis of amoeba-specific genes. In *C. elegans*, the interference was seen to persist into the next generation despite the fact that many endogenous RNA transcripts degrade rapidly in the early embryo, suggesting that these ds-RNA molecules are more stable than native transcripts (Fire *et al.*, 1998). If such stability existed in *Physarum*, it would allow time-lapse cinematography of the APT, in order to investigate a potential role for the *red* genes, provided such a 'gene knockout' has a discernible phenotype.

Another possible way to investigate the role of *redA* is by over-expression studies. In this case, the *redA* cDNA would be placed under the control of promoters with high levels of expression in plasmodia, such as *proP*, to determine the effects of over-expression of *redA* during the APT and in plasmodia. Although it would also be possible to design vectors such that *redA* is under the control of amoeba-specific or constitutive promoters

such as the *proA* promoter or *PardB*, the transcripts produced may have deleterious effects on the amoebae, such that it could be impossible to select for them after transformation.

Functional analysis by gene knockout, over-expression studies, antisense RNA mutagenesis or RNAi would not be possible without the recently developed transformation methodologies (reviewed by Burland & Bailey, 1995). However, *hph* is the only selectable marker that is currently available for transformation in *P. polycephalum* (Section 1.6). Development of additional selectable markers would expand the usefulness of the transformation system and simplify the analysis of multiple gene functions, for example the relationship of *redA* and *redB* during the APT. Attempts to develop a second selectable marker are discussed further in Chapter 7.

CHAPTER SIX

**EXPRESSION OF THE FRAGMIN
GENE FAMILY DURING
PLASMODIUM DEVELOPMENT**

CHAPTER 6: EXPRESSION OF THE FRAGMIN GENE FAMILY DURING PLASMODIUM DEVELOPMENT

6.1 INTRODUCTION

The work discussed in this Chapter results from collaboration between the Leicester (UK) and Gent (Belgium) University *Physarum* groups that began in 1996. Dr. J. Bailey provided Dr. J. Gettemans at Gent, with an aliquot of the ML8A cDNA library (Chapter 3), from which a fragmin cDNA clone was isolated following screening with antibodies raised against plasmodial fragmin (T'Jampens *et al.*, 1997). The *Physarum* group at Gent had no expertise in culturing amoebae or inducing development, nor with the type of northern blotting analysis that is routinely performed at Leicester. Therefore, Dr. Bailey and I helped to characterise the plasmodial fragmin gene and other members of the fragmin gene family. This collaboration has already resulted in two joint publications (T'Jampens *et al.*, 1997 & 1999) and a third manuscript is in preparation.

6.1.1 The role of fragmin and cell-type specific isoforms

Fragmin is a calcium-dependant, actin-binding protein (Section 1.3.2) that regulates the polymeric state of actin and is present in *Physarum polycephalum* plasmodia at concentrations approximately 5% of those of actin (Hinssen 1981a). Fragmin is closely related to gelsolin from vertebrates (Section 1.3.2). Interestingly, gelsolin can be cleaved roughly in half by proteases to produce two 44 kDa fragments that are similar to fragmin (Matsudaira & Janmey, 1988); therefore, gelsolin is believed to have evolved by duplication of a fragmin-like gene (reviews: Matsudaira & Janmey, 1988; Friederich *et al.*, 1990; Hatano 1994). Like gelsolin, fragmin can nucleate, cap and sever F-actin at high Ca^{2+} concentrations (Section 1.3.2; Gettemans *et al.*, 1995). Fragmin can bind two actin molecules in the presence of Ca^{2+} to form a trimer, which is stable and cannot be phosphorylated by actin fragmin kinase (Waelkens *et al.*, 1995; Eichinger *et al.*, 1996). In the presence of EGTA, the actin₂-fragmin trimer releases one actin molecule and the resulting heterodimer (actin-fragmin) possesses actin-nucleating and capping activity (Section 1.3.2; Gettemans *et al.*, 1995). Phosphatidylinositol-4,5-bisphosphate (PIP₂) partially inhibits the actin-capping and nucleating activity of this actin-fragmin heterodimer by binding to it (Waelkens *et al.*, 1995). After association with fragmin, as an actin-fragmin dimer, the actin can be phosphorylated by AFK (Gettemans *et al.*, 1995; Waelkens *et al.*, 1995). This phosphorylation leads to inhibition of the actin-nucleating

activity of the actin-fragmin complex and renders the F-actin-capping activity Ca^{2+} -dependent (Waelkens *et al.*, 1995; Constantin *et al.*, 1998).

As with profilin, there are cell-type-specific fragmin isoforms in *Physarum*. Fragmin was first isolated as plasmodial actinin (a complex of fragmin and actin) by Hasegawa *et al.* (1980) and Hinssen (1981a & b). The fragmin was separated from the actin by ion exchange chromatography (Hasegawa *et al.*, 1980; Hinssen, 1981a). Hasegawa *et al.* (1980) and Hinssen (1981a & b) demonstrated that fragmin is able to regulate actin polymerisation in a calcium-dependent manner. Immunolocalisation of fragmin in microplasmodia revealed that fragmin co-localises with actin and myosin in the fibrillar system under the plasmodium membrane (Section 1.3.2; Osborn *et al.*, 1983). Flagellates contain a backbone of microfilaments that is thought to be essential in maintaining the elongated shape of the cell (Uyeda *et al.*, 1988). If flagellates are cooled, the cellular Ca^{2+} concentration increases and the backbone disintegrates rapidly leading to cell deformation (Uyeda *et al.*, 1988). Since fragmin activity is regulated by the cellular Ca^{2+} concentrations, Uyeda *et al.* (1988) investigated the involvement of fragmin in the deformation of the flagellate microfilament backbone and isolated a protein from amoebae that was functionally similar to plasmodial fragmin: myxamoebal fragmin. Immunoblot analysis and antibody specificity suggested that the myxamoebal and plasmodial fragmins are encoded by different genes (Uyeda *et al.*, 1988).

6.1.2 Comparison of gene expression during apogamic and heterothallic development

The Leicester and Gent *Physarum* groups were interested in examining fragmin gene expression during the APT since this is when the complex cytoskeletal changes associated with plasmodium development are initiated (discussed in Section 1.4). Techniques for the analysis of gene expression during the apogamic APT are well established (Chapter 3; Bailey *et al.*, 1999; Solnica-Krezel *et al.*, 1988; Sweeney *et al.*, 1987). Much of the *P. polycephalum* research is conducted using apogamic strains since they remain haploid throughout the life cycle and, therefore, the effects of recessive genes or mutations are visible in the plasmodia (Section 1.2.4). In addition, it is comparatively easy to generate populations of cells undergoing apogamic plasmodium development that contain a high proportion of developing uninucleate cells.

Apogamic strains arose through mutation in the laboratory and similar strains may not exist in nature. Therefore, it has become of increasing importance to establish the degree of similarity between apogamic and heterothallic plasmodium development. Amongst the most obvious differences between the two types of development are the requirements for cell and nuclear fusion at the onset of heterothallic development and the ploidy of the plasmodia generated (discussed in Chapter 1). In addition, there are subtle differences in the two types of development at the cellular and behavioural level (Section 1.2). Generally, the similarities between the two types of development far outreach the differences, thus making apogamic strains a good experimental model. Extending the comparison of apogamic and heterothallic plasmodium development could add further to the credibility of apogamic strains as a model for development or may highlight further differences between the two types of development.

Preliminary studies of gene expression during heterothallic plasmodium development were performed by Barber (1998). Initially, he used two heterothallic strains, LU648 and CH508, since development in these two strains had been studied previously by time-lapse cinematography (Bailey *et al.*, 1990) and because they differ at all three *mat* loci, they mate well (Section 1.2.3). However, Barber (1998) had difficulty in obtaining cultures where more than 25% of the cell population were in the extended cell cycle at any one time (fusion cells and developing zygotes); thus, Barber (1998) sought to enrich the population for these cell types. Heterothallic development requires that two compatible amoebae fuse. Therefore, improving the probability that any two amoebae coming into contact are compatible at all three *mat* loci should increase the proportion of zygotes present at any one time. In a population of amoebae containing two strains, which differ at all three *mat* loci, the probability that any two amoebae are compatible for development is 50%. However, if the number of strains is increased to 10, this probability increases to 90%. Using a 10-strain mixture, Barber (1998) was able to obtain populations of cells containing up to 41% developing cells (fusion cells, zygotes and multinucleate plasmodia), which contained a high proportion of zygotes (29.1%; Table 2.2).

6.1.3 Aims

The expression patterns of the fragmin family of genes and *AFK* during development were investigated using RNA samples isolated from both heterothallic (Barber, 1998) and apogamic cultures (Chapter 3; Bailey *et al.*, 1999). Southern-blotting analysis was performed to determine the number of members in the fragmin gene family.

6.2 RESULTS

Northern blots were prepared using RNA isolated from cells undergoing both apogamic and heterothallic development (Section 2.5.2; Chapter 3) and were probed at high (65°C) and low (50–55°C) stringency as indicated; probes for the control genes, *redA* and actin (pPpA35; Hamelin *et al.*, 1988), were only used at high stringency. Southern blots were prepared using CL genomic DNA digested with a selection of restriction enzymes that had 4–6bp recognition sequences and these too were probed at high and low stringency as indicated.

6.2.1 Expression of the two control genes; *redA* and actin

To provide a firm basis for the comparison of the gene expression patterns detected during apogamic and heterothallic development, actin and *redA* were included as control genes. As described in Chapter 3, actin was used to confirm the integrity of the RNA samples and to provide an indication of the relative concentrations of RNA in all lanes. For the heterothallic samples (Figure 6.1), one actin result is shown and this is representative of the signal obtained for all the blots performed using these samples. Since there is smearing within the lanes containing RNA from the samples derived from 10–strain mating (38% and 41% developing cells; Figure 6.1), these samples have undergone a degree of degradation with the highest level of degradation observed in the 41% sample. The actin signal in the remaining heterothallic samples varies in intensity (Figure 6.1); such differences were considered when comparing the signal intensities for the genes of interest. On the upper apogamic northern blot (Figure 6.2a), the low intensity of the actin signal for the lanes containing 10% developing cells and macroplasmodia (Ma) suggests that these lanes were substantially underloaded compared to the other lanes. The variation in the actin signal intensity for the remaining apogamic samples was less striking (Figure 6.2a & 6.2b) and, as with the heterothallic northern blots (Figure 6.1), such differences were considered when comparing the signal intensities for the genes of interest.

The developmentally–regulated gene, *redA* (Chapters 3, 4 & 5), was used as a second control for the comparison of gene expression during apogamic and heterothallic plasmodium development. The expression pattern for *redA* in apogamic development was as expected from previous studies (Chapter 3). In heterothallic samples, expression of *redA* is first detected when 17% committed cells are present in the culture (Figure 6.1) and

Figure 6.1: Northern analysis of gene expression during heterothallic development

Total RNA was isolated from amoebae of the heterothallic strains CH508 and LU648 [A(CH508) and A(LU648)], plasmodia derived from LU648 × CH508 (Mi: microplasmodia, Ma: macroplasmodia) and populations of heterothallic developing cells (2% – 24%[‡], 38%[†] & 41%[†]) as described in Section 2.4.2; for more information on these samples see Table 2.2. 10µg denatured total RNA and 3µg denatured RNA size markers (Promega) were size-fractionated in 1.1% agarose gels as described in Section 2.4.2. The sample RNA was blotted to Hybond-N membrane using the 20 × SSC alkaline transfer method (Sambrook *et al.*, 1989) and the RNA was fixed to the membrane by exposure to UV (Section 2.4.1). The RNA size markers were stained and photographed as described in Section 2.4.2 and were used to estimate the transcript sizes detected on autoradiographs following probing (see below).

The cDNA clones for actin (pPpA35; Hamelin *et al.*, 1988), *frgA* (Section 6.2.3; T'Jampens *et al.*, 1999), *frgP* (Section 6.2.2; T'Jampens *et al.*, 1997), D13/3D (*redA*; Chapter 3) and the 850bp C-terminal region of the *frg60* cDNA clone (Section 6.2.4) were radio-labelled using the method of Feinberg and Vogelstein (1983), as described in Section 2.4.4. These radio-labelled probes were hybridised at high stringency (65°C) to northern blots; the results shown are representative of the signals obtained from three independent blots containing the same samples.

The probes hybridised to transcripts of the following sizes, as estimated from the RNA size markers: Actin, 1400 nucleotides; *frgA*, 1200 nucleotides; *frgP*, 1200 nucleotides; *frg60*, 1800 nucleotides; *redA* (D13/3D), 800 nucleotides.

[‡] total percentage of developing cells in cultures derived from 2-strain cultures of LU648 × CH508 (Table 2.2)

[†] total percentage of developing cells in cultures derived from 10-strain cultures (strains listed in Table 2.2).

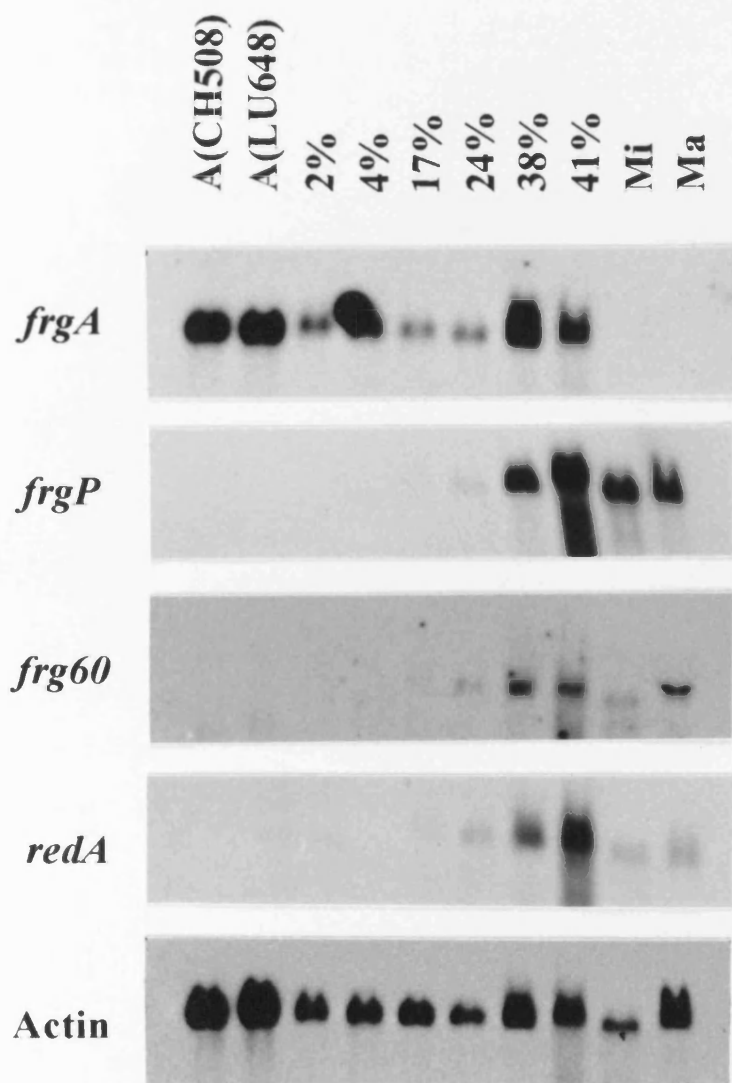
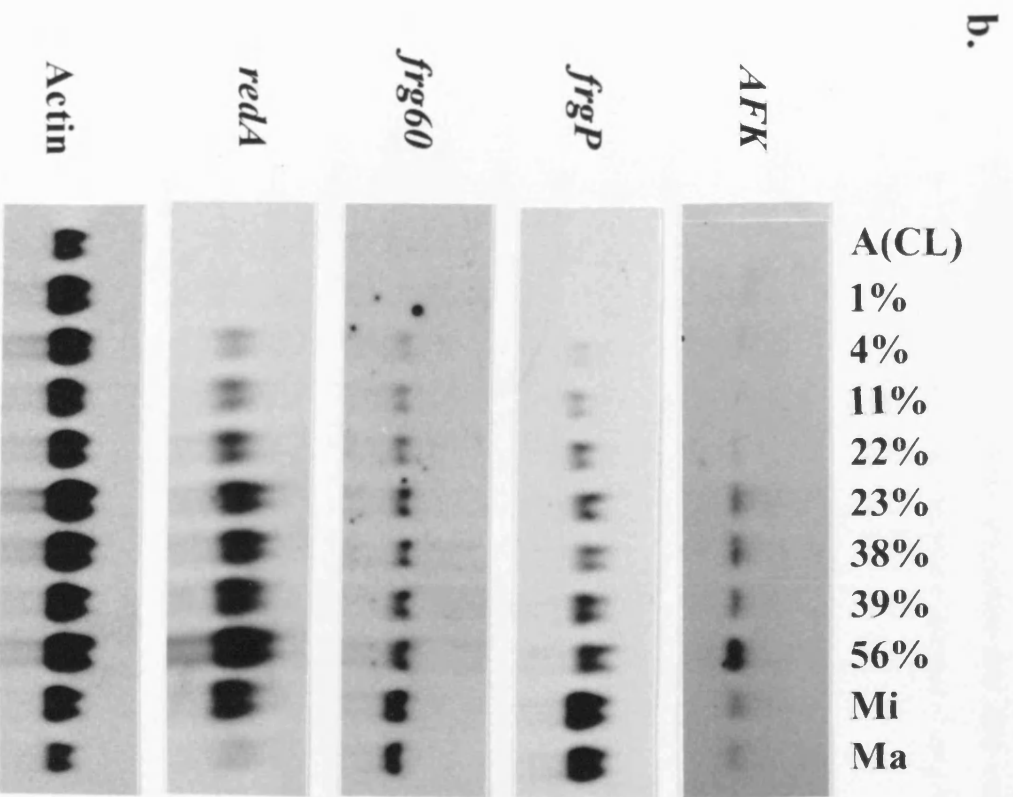
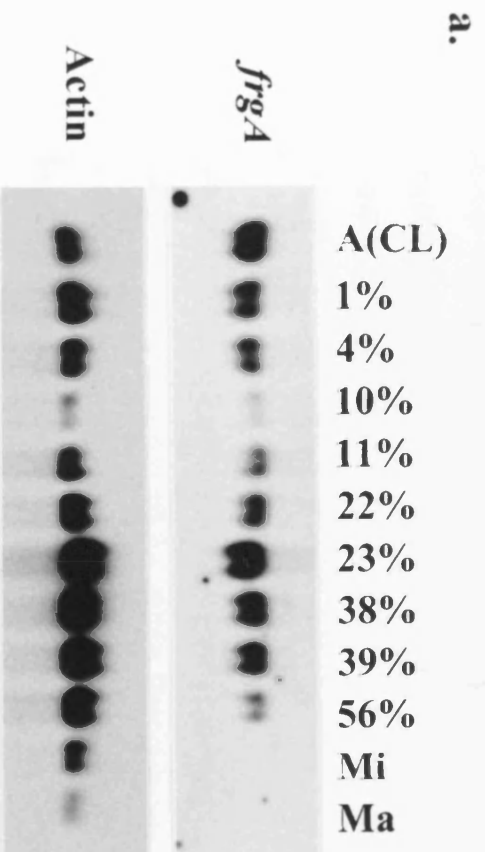


Figure 6.2: Northern analysis of gene expression during apogamic development

Total RNA was isolated from amoebae (A), plasmodia (Mi: microplasmodia, Ma: macroplasmodia) and populations of developing cells (1-56%) of the apogamic strain CL as described in Section 2.4.2; for more information on these samples see Table 2.1. 10µg denatured total RNA and 3µg denatured RNA size markers (Promega) were size-fractionated in 1.1% agarose gels as described in Section 2.4.2. The sample RNA was blotted to Hybond-N membrane using the 20 × SSC alkaline transfer method (Sambrook *et al.*, 1989) and the RNA was fixed to the membrane by exposure to UV (Section 2.4.1). The RNA size markers were stained and photographed as described in Section 2.4.2 and were used to estimate the transcript sizes detected on autoradiographs following probing (see below).

The cDNA clones for *actin* (pPpA35; Hamelin *et al.*, 1988), *frgA* (Section 6.2.3; T'Jampens *et al.*, 1999), *frgP* (Section 6.2.2; T'Jampens *et al.*, 1997), *AFK* (Section 6.2.5; Eichinger *et al.*, 1996), D13/3D (*redA*; Chapter 3) and the 850bp C-terminal region of the *frg60* cDNA clone (Section 6.2.4) were radio-labelled using the method of Feinberg and Vogelstein (1983), as described in Section 2.4.4. These radio-labelled probes were hybridised at high stringency (65°C) to northern blots; the results shown are representative of the signals obtained from three independent blots containing the same samples.

The probes hybridised to transcripts of the following sizes, as estimated from the RNA size markers: *Actin*, 1400 nucleotides; *frgA*, 1200 nucleotides; *frgP*, 1200 nucleotides; *frg60*, 1800 nucleotides; *AFK*, 2300 nucleotides; *redA* (D13/3D), 800 nucleotides.



reaches a peak when the number increases to 41% (Figure 6.1). Lower levels of expression are detected in plasmodia (Mi & Ma; Figures 6.1) and no expression is detected in amoebae or cultures with a low proportion of developing cells (CH508, LU648 or 2–4%; Figure 6.1). The overall pattern of expression in heterothallic development is similar to that seen in apogamic development; comparison of the expression pattern for *redA* during apogamic and heterothallic development is discussed further in Section 6.3.1.

6.2.2 Analysis of the fragmin clone by northern and Southern blotting

The Gent group isolated a fragmin clone from the ML8A cDNA library by using IPTG to induce expression from the *lac* promoter located in the cDNA vector and then screening against antibodies to plasmodial fragmin to identify clones that expressed fragmin (T’Jampens *et al.*, 1997). As with other clones isolated from this cDNA library (Chapter 3), some 5’ coding sequence was missing. The missing nucleotides were deduced by reverse translation of the amino acid sequence and this revealed that the cDNA clone was missing only 7bp and was therefore almost complete (Accession number: U70047; T’Jampens *et al.*, 1997).

I used this cDNA clone to probe northern and Southern blots. Northern blotting analysis at high stringency revealed that the fragmin cDNA clone hybridises to a 1200 nucleotide transcript, which is first detected in developing populations of cells (24%: Figure 6.1; 4%: Figure 6.2b) and increases throughout development to reach peak levels in plasmodia (Mi and Ma; Figures 6.1 & 6.2b) but is not detected in amoebae (A; Figures 6.1 & 6.2b). Therefore, this fragmin gene exhibits a plasmodium-specific expression pattern in both apogamic and heterothallic development (Figures 6.1 & 6.2b). This fragmin cDNA was the first plasmodium-specific fragmin gene to be cloned and was named *frgP* (**f**ragmin **P**lasmodial; T’Jampens *et al.*, 1997). A second, less intense, plasmodium-specific signal was observed when the apogamic northern blots were probed at low stringency (data not shown), suggesting that *P. polycephalum* has a fragmin gene family. This low-abundance transcript is approximately 2600 nucleotides in size and was named *frgR* (**f**ragmin-**R**elated; T’Jampens *et al.*, 1997).

To confirm that the *P. polycephalum* genome contained several fragmin genes indicative of a gene family and to extend the characterisation of the *frgP* gene, Southern blotting analysis was performed. At high stringency, digestion of CL genomic DNA with *Pst*I

generates two bands (3.5kb and 2kb; Table 6.1); since the cDNA sequence contains a single *Pst*I site, this result is as expected. Digestion with *Hind*III generates intense 7.2kb and 1.5kb bands and a faint 6.6kb band at high stringency (Table 6.1). Since the cDNA clone contains a *Hind*III site located close to the 5' end, two of these bands can be attributed to the *frgP* gene. However, the third band may be the product of either partial digestion, digestion within a *frgP* intron or cross hybridisation to *frgR*; this is discussed further below. The *frgP* cDNA sequence contains no *Kpn*I sites, yet at high stringency, digestion with *Kpn*I generates intense 9kb and 1.7kb bands and a faint 14kb band (Table 6.1) indicating the presence of at least one intron in the *frgP* gene.

In addition to the major bands, faint bands were sometimes observed on the Southern blots at high stringency; e.g. the 14kb band generated by *Kpn*I digestion (Table 6.1). These faint bands may have been the product of uneven or 'asymmetric' digestion of the *frgP* gene as was often observed with *redA* (Chapter 4). For example, the *Pst*I site in *frgP* is located two thirds of the way through the cDNA clone, therefore, twice as much probe would hybridise to the 5' fragment than to the 3' fragment and the faint 3.5kb *Pst*I fragment could thus, correlate to the 3' fragment (Table 6.1). Where no internal site was identified from the cDNA sequence, such faint bands could indicate the existence of an intron in the *frgP* gene or may have arisen through partial digestion. The two smallest *Kpn*I fragments collectively cover 10.7kb (Table 6.1), yet the faint band is 14kb and is thus almost 3.3kb larger than expected (Table 6.1). Since a 3.3kb band was not visible on the gel, this could suggest that a second *Kpn*I site is situated outside the gene, approximately 3.3kb from a *Kpn*I site located within an intron.

Even though no *frgR* transcript could be detected on northern blots at high stringency, closely-related genes are more likely to cross hybridise at high stringency on Southern blots since they do not depend upon transcript levels. Therefore, it is considered highly likely that some of the faint bands observed on Southern blots at high stringency correspond to fragments bearing the *frgR* gene, such as the 14kb *Kpn*I band and the 6.6kb *Hind*III band (Table 6.1). Low stringency probing of Southern blots with *frgP* produced numerous low intensity fragments in addition to the expected major bands, which strongly suggests the presence of more than just *frgP* and *frgR* in the fragmin gene family (data not shown).

Table 6.1: Data from Southern blotting analyses of AFK and the fragmin family of genes

The sizes of bands observed on Southern blots probed high stringency using the cDNA clones for *AFK* and the members of the fragmin gene family. The sizes of these bands were determined relative to λ *HindIII* and ϕ X174 *HaeIII* DNA size markers. The fragments shown in (brackets) produced a low intensity signal on the Southern blot and were considered to be the product of either digestion at an internal site or partial digestion (discussed in text). Where a hyphen is shown (-), no signal could be detected on the blot. Where n/a is shown, the enzyme listed was not included on the Southern blot.

Table 6.1

	<i>frgP</i>	<i>frgA</i>	<i>frg60</i>	<i>AFK</i>
<i>Bam</i> HI	n/a	6.2 kb	-	25 kb
<i>Eco</i> RI	n/a	4 kb 3 kb (5.8 kb) (5.0 kb)	1.5 kb	28 kb
<i>Eco</i> RV	n/a	-	2.8 kb (23 kb)	18 kb
<i>Hind</i> III	7.2 kb 1.5 kb (6.6 kb)	2.5 kb	-	3.4 kb (4.9 kb)
<i>Kpn</i> I	9 kb 1.7 kb (14 kb)	4.1 kb (5.1 kb)	6 kb	10 kb
<i>Pst</i> I	2 kb (3.5 kb)	4.3 kb (2.0 kb)	-	6 kb (4.2 kb)
<i>Alu</i> I	n/a	-	3.8 kb	-
<i>Rsa</i> I	n/a	1 kb	2.4 kb	900 bp 620 bp 250 bp
<i>Taq</i> I	n/a	3.2 kb 2.9 kb	1.9 kb 1.7 kb	2 kb 1.8 kb 1.1 kb (3.6 kb) (1.4 kb) (800 bp) (600 bp) (350 bp)

6.2.3 Characterisation of an amoeba-specific fragmin gene

The northern blot data for *frgP* provided evidence in support of the biochemical data of Uyeda *et al.* (1988; Section 6.1.1), which indicated that the myxamoebal and plasmodial fragmins are encoded by different genes. Since fragmin protein is found in amoebae but the *frgP* mRNA was only detected in plasmodia and developing cells, it was postulated that a separate amoeba-specific fragmin gene existed and this was named *frgA* (fragmin Amoebal; T'Jampens *et al.* 1997).

In order to clone the amoeba-specific fragmin isoform, the Gent group purified fragmin from amoebae, deduced the partial amino acid sequence by peptide sequencing and then used the amino acid sequence to design degenerate PCR primers (McPherson *et al.*, 1995) for use with the cDNA library, ML8A. They successfully identified partial cDNAs by PCR against ML8A and then constructed a new cDNA library from amoebal mRNA to identify the rest of the coding region (T'Jampens *et al.*, 1999); further PCR using a new degenerate primer and a primer designed against the partial cDNA sequence obtained from ML8A, resulted in the isolation of a longer cDNA clone (T'Jampens *et al.*, 1999). RACE-PCR (Rapid amplification of cDNA ends; McPherson *et al.*, 1991 & 1995) was then performed and the missing 5' and 3' regions of the cDNA were identified (Accession number: AF135270; T'Jampens *et al.*, 1999).

This cDNA was used to probe northern and Southern blots at Leicester, as described for *frgP*. At high stringency, the cDNA hybridises to a 1200 nucleotide transcript with an amoeba-specific gene expression pattern, confirming it is the *frgA* isoform (Figures 6.1 & 6.2a); the 4% sample on Figure 6.1 is obscured by strong background hybridisation and therefore should be ignored. Like *proA* (Section 3.3.2), *frgA* can be detected in all samples containing amoebae and is not detected in micro- (Mi) or macroplasmodia (Ma; Figures 6.1 & 6.2a). This transcription pattern was distinct from that observed for *frgP* and *frgR* and did not cross hybridise to the transcripts from either of these genes at high stringency. Low stringency probing was not performed due to time constraints, although, since *frgP* did not cross hybridise to the *frgA* transcript at low stringency, it is considered unlikely that *frgA* would cross hybridise with *frgP* or *frgR* at low stringency. However, low stringency probing may have identified further fragmin gene family members, if any remain to be identified. Since the fragminA antibodies react with only one protein on western blots of amoebal extracts, this suggests that only one amoeba-specific fragmin

isoform exists (T'Jampens *et al.*, 1999). Since *frgR* is the only transcript that *frgP* cross hybridises to at low stringency, it is considered likely that *frgP* and *frgR* will share greater homology than *frgP* and *frgA*. The *frgR* transcript is much larger than *frgP* and may, therefore, encode a much larger protein that could be isolated by fractionation using the established techniques (e.g. Furuhashi & Hatano, 1989).

Southern blotting analysis of *frgA* at high stringency produced no cross hybridisation to the other fragmin genes; low stringency probing was not performed. Digestion of CL genomic DNA with *Bam*HI, *Hind*III or *Rsa*I all generated a single *frgA* fragment (Table 6.1), as expected from the cDNA sequence. Restriction sites for *Pst*I and *Taq*I are present in the cDNA sequence and, in agreement with this, two fragments were detected on the Southern blot for each of these digests (4.3kb & 2kb for *Pst* I, 3.2kb & 2.9kb for *Taq* I; Table 6.1). The cDNA sequence contains no *Kpn*I sites, yet digestion with *Kpn*I generates 5.1kb and 4.1kb fragments (Table 6.1) suggesting the presence of at least one intron. Since the fragment sizes detected for *frgA* at high stringency differ greatly from those obtained by probing with *frgP*, the Southern blot data clearly demonstrate that these fragmins are encoded by different genes. This was confirmed by sequence comparisons, which revealed 65% identity between the proteins encoded by *frgP* and *frgA* (T'Jampens *et al.*, 1999).

6.2.4 Characterisation of a second plasmodium-specific fragmin gene

Antibodies raised against FragminP cross-react, on western blots of plasmodial extracts, with a 60 kDa protein named Fragmin60 (Furuhashi & Hatano, 1989). Since the northern blotting with the *frgP* clone had identified a second plasmodium-specific transcript, *frgR*, it was possible that the *frgR* gene encoded the Fragmin60 protein. The Gent group sequenced part of the Fragmin60 protein and designed degenerate primers from this amino acid sequence for PCR against a cDNA library constructed from plasmodia; this resulted in the isolation of a partial cDNA clone for Fragmin60 (J. Gettemans, personal communication). The missing portions of the cDNA clone were obtained by 5' and 3' RACE PCR (J. Gettemans, personal communication).

Sequence analysis of this clone revealed that the C-terminus encoded a peptide that contained a region with 55% identity to the FrgP protein and 54% identity to the FrgA protein. The N-terminus was found to contain a C₂ domain; this kind of domain is not

usually found in Gelsolin-like proteins, (J. Gettemans; unpublished data). The C₂ domain is one of four sequence motifs that are commonly found in protein kinase C (Knopf *et al.*, 1986) and is the only one of the four motifs that is Ca²⁺ dependent and is commonly found in a variety of proteins (Sutton *et al.*, 1995).

The C-terminal region of the *frg60* clone, which contains the fragmin-like sequence, was used as a probe for northern and Southern blotting analysis. The *frg60* clone hybridises to a 1800 nucleotide transcript that is clearly not the same size as the previously identified *frgR* mRNA (2600 nucleotides; data not shown) and exhibits a plasmodium-specific expression pattern that closely resembles that of *frgP* (Figures 6.1 & 6.2). The similarities in *frgP* and *frg60* gene expression are discussed further in Section 6.3.1. Low stringency probing of northern blots with the entire *frg60* clone, including the unusual N-terminal domain, produces low levels of hybridisation to numerous transcripts ranging in size from 600–2800 nucleotides, in addition to the major 1800 nucleotide transcript (data not shown). However, since the C₂ domain is found in many genes (Sutton *et al.*, 1995), it is likely that some, if not all, of these transcripts are from genes that share homology with this N-terminal domain rather than with the fragmin-like region.

Southern blotting analysis using the fragmin-like C-terminal region of *frg60*, at high stringency, generates a single genomic fragment for all but one of the digestions performed (Table 6.1); low stringency probing was not performed. The cDNA sequence contains numerous *TaqI* sites (J. Gettemans; personal communication), and digestion with *TaqI* generates two detectable fragments, 1.9kb and 1.7kb (Table 6.1). Therefore, none of the digestions selected for Southern blotting provide evidence that the C-terminal region of *frg60* contains introns (Table 6.1). Probing was not done with the whole *frg60* clone due to the likelihood that cross-hybridisation would occur to other genes containing the C₂ domain.

6.2.5 Characterisation of AFK by northern and Southern blotting analysis

The phosphorylation of actin is correlated with reorganisation of the cytoskeleton in *Dictyostelium discoideum* (Noegal & Luna, 1995); in *Physarum polycephalum*, the actin-fragmin complex is a target for phosphorylation and the protein kinase that specifically phosphorylates the actin-fragmin complex is the 80 kDa enzyme, AFK (Waelkens *et al.*, 1995; Section 6.1.1). During the APT, the actin cytoskeleton is

re-organised and the plasmodium-specific fragmin genes are activated. Since the roles of AFK and fragmin seem so intimately linked, my studies were expanded to include AFK. A cDNA clone for *AFK* was obtained by reverse transcription-PCR (RT-PCR) and RACE-PCR using ML8A (Accession number: U64722; Eichinger *et al.*, 1996). This was used to probe northern blots to determine whether *AFK* gene expression changes during development.

Northern blotting analysis shows that the *AFK* cDNA hybridises to a 2300 nucleotide transcript. The signal for *AFK* was very faint on both apogamic and heterothallic northern blots; the result obtained for the apogamic samples after a long exposure period is shown in Figure 6.2b. The expression pattern obtained from the heterothallic northern blot is not shown since the result did not reproduce well from the X-ray film. Although no transcript could be detected in amoebal RNA samples from strain CL (Figure 6.2b), a low level of hybridisation was detected when amoebal RNA samples from strains LU353, CH508 and LU648 were probed (data not shown). Expression of this gene appears to increase during development and in plasmodia relative to amoebal expression (Figure 6.2b). These results suggest that the expression of *AFK* is constitutive. With such low levels of expression, this northern analysis is inconclusive and further analysis of the expression of *AFK* is required, possibly using alternative methods, such as quantitative RT-PCR.

Southern blotting analysis of CL genomic DNA using *AFK* as a probe at high stringency indicates that it is a single copy gene, since the cDNA sequence contains no *KpnI* sites and only a single *KpnI* genomic fragment was detected (10kb; Table 6.1). The cDNA sequence contains no *HindIII* sites, yet digestion with *HindIII* generates a major 3.4kb band and weak hybridisation to a 4.9kb band (Table 6.1). However, the same digestion was performed by Eichinger *et al.* (1996) and only a 4.9kb band was observed. Since Eichinger *et al.* (1996) used a different strain for their analysis to that used here, it is considered likely that this represents an RFLP difference between the two strains. It is possible that the weak hybridisation to the 4.9kb fragment detected in CL (Table 6.1) resulted from partial digestion involving a site situated 1.5kb from one end of the 4.9kb fragment and that this site was outside the *AFK* gene, thereby releasing a 1.5kb fragment with no homology to *AFK* and reducing the *AFK* fragment to 3.4kb. The cDNA sequence reveals the presence of several *RsaI* and *TaqI* restriction sites making it difficult to interpret the banding patterns obtained using these enzymes. Sequencing of partial

genomic clones by Eichinger *et al.* (1996) revealed that the gene contains several short introns and exons and confirms that *AFK* is a single copy gene.

6.3 DISCUSSION

6.3.1 Comparison of gene expression during heterothallic and apogamic development

The expression patterns obtained for the genes investigated were essentially the same in both apogamic and heterothallic development. The expression pattern obtained for *frgA* was typical of amoeba-specific genes, such as *proA* (Section 3.2.4; Bailey *et al.*, 1999); mRNA was detected in all populations of cells that contained amoebae, but not in micro or macropasmodia (Figure 6.1 & 6.2). The expression patterns obtained for *frgP* and *frg60* were typical of plasmodium-specific genes, such as *proP* and β 2-tubulin (Section 3.2.4; Bailey *et al.*, 1999). Although *frgR* also exhibited a plasmodium-specific gene expression pattern, the low intensity of the signal means no meaningful comparison can be made between the two types of development or with the expression patterns observed for *frgP* and *frg60*; further analysis of the *frgR* transcript is therefore required. The *frgP* and *frg60* transcripts were first detected in populations of cells that contained either apogamic (4%; Figure 6.2b) or heterothallic developing cells (24%; Figure 6.1) and then increased during the APT to reach their highest levels in vegetative plasmodia (Ma; Figures 6.1 & 6.2). These results demonstrate that the switch in expression of these actin-binding genes occurs during the APT.

There were minor differences in the timing of expression between apogamic and heterothallic plasmodium development. The *redA* and plasmodium-specific transcripts were apparently detected when fewer developing cells were present in apogamic development (1–4%; Figure 6.2b) than in heterothallic development (17%; Figure 6.1). Similar results were obtained for *proP* and *mynD* (Barber, 1998; Bailey *et al.*, 1999). This difference could represent a minor difference between apogamic and heterothallic development, or it could be a consequence of the methodology used to determine the proportion of developing (committed) cells in a population (Section 1.2.5).

As discussed previously (Section 1.2.5), a committed cell is defined as one that survives replating and continues to develop into a plasmodium. Since ‘commitment’ is an ‘operational’ definition, it does not necessarily follow that commitment in apogamic and

heterothallic development relates to the same developmental stage in terms of gene activation or cell structural rearrangements in zygotes and developing uninucleate apogamic cells (Section 1.2.5). Given these uncertainties in the state of the cells at the time of commitment, the comparison of gene expression between apogamic and heterothallic development is therefore restricted to determining general trends. Within these constraints, there is little difference in the expression of *AFK*, *frg60*, *frgA*, *frgP*, *myxD*, *proA*, *proP*, *redA* or *redB* during apogamic and heterothallic development (Figures 6.1 & 6.2; Barber, 1998; Bailey *et al.*, 1999). Therefore, as previously shown for cellular events (Bailey *et al.*, 1987 & 1990), the general pattern of molecular events during the APT appear to be unaffected by the *gadA* mutation. Thus, this data provides further justification for the use of apogamic strains as a model for development in *P. polycephalum*.

6.3.2 The fragmin gene family

T'Jampens *et al.* (1997 & 1999) isolated cDNAs encoding the plasmodial and amoebal fragmins, *frgP* and *frgA*, confirming the conjecture of Uyeda *et al.* (1988) that these proteins are encoded by different genes. These two *P. polycephalum* fragmins share only 65% sequence homology at the protein level (T'Jampens *et al.*, 1999), which is insufficient for cross hybridisation on northern and Southern blots (Sections 6.2.1 & 6.2.2); a similar level of homology exists between the two profilin genes and likewise, no cross hybridisation occurs between the *proA* and *proP* transcripts at high stringency (Binette *et al.*, 1990).

Antibody staining of FragminP in plasmodia revealed that it is localised to the cortical actin layer under the cell membrane and it could, therefore, be involved in cell motility (T'Jampens *et al.*, 1997). Using similar antibody staining in amoebae, FragminA was found distributed predominantly to regions beneath the cell membrane suggesting this protein may also be involved in cytoskeletal rearrangements (T'Jampens *et al.*, 1999). Antibody staining for myxamoebal fragmin had previously revealed that myxamoebal fragmin remains present in cells undergoing the APT, including some "young" plasmodia (Uyeda *et al.*, 1988). In agreement with these observations, the northern blotting analysis revealed that the concentration of *frgA* mRNA gradually declined as the percentage of developing cells increased (Figures 6.1 & 6.2). Since the mRNA and protein do not

degrade instantly and can therefore remain present for some time after gene expression ceases, this is no surprise.

Antibody staining for FragminP against western blots of plasmodial protein extracts identified a 60 kDa protein that cross reacted with fragmin; Fragmin60 (Furuhashi & Hatano, 1989; T'Jampens *et al.*, 1999). The gene for this was cloned and the C-terminal region was found to share homology with fragmin (J. Gettemans, unpublished data). However, a C₂ domain was identified at the N-terminus, which is Ca²⁺ dependent and specifically binds phosphatidylserine and is not found in other gelsolin-like, actin-binding proteins (J. Gettemans, unpublished data); this suggests that Fragmin60 belongs to the fragmin subfamily (T'Jampens *et al.*, 1999). Further analysis by northern and Southern blotting, together with immunolocalisation data has confirmed that *frg60* is a plasmodium-specific gene and is not the same as *frgR* as originally suspected (Section 6.2.4; manuscript in preparation).

In summary, the fragmin gene family appears to comprise of one amoeba-specific (*frgA*) and three plasmodium-specific (*frgP*, *frg60* and *frgR*) genes. The relationship of *frgR* with the other members of the gene family remains to be determined. However, since the *frgR* transcript was the only one that cross-hybridised with *frgP*, it is likely that at least part of the *frgR* gene will exhibit a high level of homology to *frgP*. The evidence from northern and Southern blotting, together with the antibody studies, suggests there are no further members in this gene family. However, the possibility that more divergent members exist cannot be excluded.

6.3.3 The role of the fragmin isotypes in amoebae and plasmodia

Actin in *P. polycephalum* amoebae is concentrated beneath the cell membrane in an irregular layer, located predominantly where pseudopodia form (Section 1.3.2). In *Dictyostelium discoideum* amoebae, severin is concentrated in cortical actin-rich regions that coincide with pseudopod extension or phagocytosis (Brock & Pardee, 1988). Similarly in *P. polycephalum*, the FragminA protein localises to regions beneath the cell membrane that suggest a role in the regulation of cytoskeletal rearrangements associated with cell motility and the formation of pseudopodia (T'Jampens *et al.*, 1999).

In contrast to that in amoebae, the actin layer in plasmodia has an extremely complex arrangement (Section 1.3.2; reviewed by Stockem & Brix, 1994). Since the organisation of the cortical actin layer is more complex in plasmodia than in amoebae, it is possible that some of the different plasmodium-specific fragmin isoforms have specific roles in its regulation. FragminP is localised to the cortical actin layer at the surface of microplasmodia, which is similar to that found in amoebae (T'Jampens *et al.*, 1997 & 1999). In addition to the complex cortical layer, macroplasmodia and large microplasmodia also possess cytoplasmic fibrils, which are found throughout the veins, and cell matrix both maintaining the cell shape and mediating surface adhesion sites (Section 1.3.2; Stockem & Brix, 1994). Immunofluorescence microscopy with antibodies specific to FragminP revealed that FragminP does not interact with the cytoplasmic fibrillar actin filaments of large microplasmodia (T'Jampens *et al.*, 1997); unfortunately, the distribution of FragminP in macroplasmodia has not been examined. However, the regulation of actin in cytoplasmic fibrils may provide yet another specialised role for one of the other plasmodium-specific fragmin isoforms.

Immunolocalisation of Fragmin60 in microplasmodia revealed a similar distribution to that seen for FragminP, although there appears to be more Fragmin60 present in the cytoplasm, particularly in association with vesicles, than was observed for FragminP; the reason for this difference is unclear (J. Gettemans, personal communication). In plasmodia, it is estimated that 2–5% of actin is phosphorylated, whereas in sclerotia this level increases dramatically to 50% (T'Jampens *et al.*, 1999). Actin in the fragmin60-actin complex is not phosphorylated in plasmodia but is phosphorylated in sclerotia, which strongly suggests that fragmin60 may be involved with regulating actin phosphorylation in sclerotia (J. Gettemans, personal communication).

The FragminA and FragminP proteins share 65% identity and 79% similarity (T'Jampens *et al.*, 1999). The biochemical data and sequence homologies suggest that these two fragmins have similar roles in amoeba and plasmodia, with some degree of specialisation specific to cell-type. Therefore, it would follow that the remaining plasmodium-specific fragmin isoforms perform more divergent roles required to regulate the complex actin cytoskeleton in plasmodia.

Now that isotype-specific antibodies are available for fragmin, the localisation of the FragminP, Fragmin60 and FragminA proteins in individual cells undergoing the APT can be investigated. Such studies may help to determine the role fragmin plays in regulating the dynamic changes to the actin cytoskeleton that occur during plasmodium development. Alternatively, gene knockout studies may provide evidence of specific roles for the fragmin isotypes during vegetative growth in amoebae and plasmodia. However, such studies could be hampered if some of the plasmodium-specific genes are able to substitute for one another functionally, as with the profilin genes in *Dictyostelium discoideum* (Section 1.3.2; Haugwitz *et al.*, 1994). The recently reported over-expression of the two *P. polycephalum* profilin isoforms in profilin-deficient *Saccharomyces cerevisiae* cells suggest that they are not functionally equivalent (Marcoux *et al.*, 1999). Similar studies could be used to determine whether the different plasmodium-specific fragmin isoforms are functionally equivalent and whether any have similar roles to *frgA*.

6.3.4 Regulation of the plasmodial actin microfilament system by AFK

T'Jampens *et al.* (1999) demonstrated that AFK is a very low abundance protein in plasmodia and represents just 0.004% of the total protein. This observation is supported by the low level of expression detected by northern blotting (Figure 6.2b). Phosphorylation of actin in the actin-fragmin complex, by AFK, inhibits the nucleating activity of the complex and renders its capping activity Ca^{2+} -dependent (Gettemans *et al.*, 1995). It is thought that the actin microfilament system in *P. polycephalum* plasmodia may be regulated by changes to actin-fragmin capping activity due to phosphorylation of actin by AFK (Waelkens *et al.*, 1995; Constantin *et al.*, 1998).

Northern analysis of *AFK* gene expression suggests a low level of AFK transcription occurs in amoebae (discussed in Section 6.2.5). However, by analysing amoebal extracts, T'Jampens *et al.* (1999) demonstrated that AFK was enzymatically inactive in amoebae, indicating that the activity of fragmin in amoebae is not regulated by AFK. However, *in vitro*, the actin-fragmin complex from amoebae can be phosphorylated by both AFK and casein kinase II, suggesting it may be phosphorylated by casein kinase II, *in vivo* (T'Jampens *et al.*, 1999). Plasmodial fragmin in association with actin, as an actin fragmin dimer, appears to represent the true substrate for AFK *in vivo*. Functional analysis of AFK, such as those described previously (Sections 1.3.2) may confirm the

involvement of AFK in regulation of the actin microfilament system in *P. polycephalum* plasmodia.

6.4 SUMMARY

The fragmin gene family has recently emerged as a group of genes involved in actin regulation in *Physarum* and appears to contain at least four members. Three of these members, *frgP*, *frg60* and *frgR*, exhibit plasmodium-specific expression patterns, while *frgA* exhibits an amoeba-specific expression pattern. Whether *frgR* closely resembles *frgA* and *frgP* or contains additional domains, like *frg60*, remains to be determined. However, since the *frgR* transcript was the only one that cross-hybridised with *frgP*, it is considered likely that at least part of the *frgR* gene will exhibit a high level of homology to *frgP*. Immunolocalisation of fragmin suggests it is involved in the regulation of cytoskeletal rearrangements associated with cell motility and the formation of pseudopodia (T'Jampens *et al.*, 1997 and 1999). The exact roles that these and other actin-binding proteins have in the different cell types of *P. polycephalum* may be determined by combining studies such as immunofluorescence microscopy and functional analysis by gene knockout.

Comparison of the gene expression patterns for the fragmin gene family during apogamic and heterothallic development provides further justification for the use of apogamic strains as a model for plasmodium development. Each gene examined so far exhibits the same basic expression pattern during both heterothallic development and apogamic development. This suggests that the *gadA* mutation at *matA*, which permits apogamic development, has no major effect on the general pattern of events occurring once development is initiated.

CHAPTER SEVEN

**DEVELOPMENT OF NEW
SELECTABLE MARKERS FOR USE
IN TRANSFORMATION STUDIES**

CHAPTER 7: DEVELOPMENT OF NEW SELECTABLE MARKERS FOR USE IN TRANSFORMATION STUDIES

7.1 INTRODUCTION

Current DNA transformation studies in *Physarum* are limited to the use of only one selectable marker, resistance to hygromycin ($100\mu\text{g ml}^{-1}$) encoded by the hygromycin phosphotransferase (*hph*) gene (Section 1.6.5). Functional gene analysis by gene knockout studies can provide valuable information regarding the role of a particular gene. However, in many cases genes have a functional overlap and more than one gene knockout is necessary to determine the genes' functions. For example, it was only through double knockout of *profilin I* and *profilin II* in *Dictyostelium discoideum* that Haugwitz *et al.* (1994) were able to determine the role of profilin. Since these two profilins were able to substitute for one another, single knockout of either gene had no discernible effect on the phenotype. Simultaneous knockout of both genes altered cell growth, increased the level of F-actin and removed the cells ability to form fruiting bodies (Haugwitz *et al.*, 1994).

Simultaneous gene knockout of two or more genes can also provide insight into the interaction of those genes. Such double knockout studies may help to determine the role of genes such as *redA* and *matA* during the APT (Chapters 3 to 5). It would theoretically be possible to isolate double gene-knockout mutants in *Physarum* using just *PardC-hph*. This would involve generating transformants with single gene knockouts for each of the genes under investigation using strains compatible for heterothallic development, crossing the two strains and then analysing their progeny by Southern blotting to identify clones that carried both gene knockouts. However, such a procedure would be time consuming and would require a second strain, compatible with LU352, that was capable of axenic growth and suitable for use in transformation studies. Although such strains are currently being developed (J. Dee, personal communication), a second selectable marker would simplify the screening for such mutants; a strain with a single knockout could be transformed using a knockout vector incorporating the new selectable marker to generate the second gene knockout.

In other systems such as the yeast, *Saccharomyces cerevisiae*, nutritional markers are often used to aid selection; e.g. *leu2* or *trp1* (leucine and tryptophan auxotrophy,

respectively; Zhang *et al.*, 1996). However, no such markers are available for *P. polycephalum*. Therefore, resistance to xenobiotics provide the only opportunity for development of a new selection system for use in transformation studies. Past research has shown that *P. polycephalum* is naturally resistant to many xenobiotics and, in some cases, spontaneous resistance occurs (e.g. cyclohexamide, acriflavin & chloroquine: Dee, 1966; benzimidazole compounds: Schedl *et al.*, 1984b). Such spontaneous resistance may provide a way to develop a genetic marker or isolate a new resistance gene (e.g. Nelson *et al.*, 1994). However, in many cases, the genetic basis of the spontaneous resistance in *Physarum* could not be determined and may have been multifactoral (e.g. emetine: Dee, 1962; benzimidazole compounds: Schedl *et al.*, 1984b).

7.1.1 Aims

A comprehensive search of literature databases was performed in order to identify markers for which a resistance gene was available, which could potentially be developed as selectable markers for transformation in *P. polycephalum*. The concentration of xenobiotic required to suppress amoebal growth was determined for several candidate markers. For one of these, vectors containing the resistance gene under the control of *PardC* were used in transformation experiments.

7.2 IDENTIFICATION OF CANDIDATE RESISTANCE GENES

The Bath Information and Data Service (BIDS) Institute for Scientific Information (ISI) database was searched for citations to resistance genes used in transformation or transfection experiments in eukaryotes. Several keyword combinations were used, including 'resistance gene', 'antibiotic', 'selectable marker', 'transformation' and 'drug'. Citations to xenobiotics with cloned resistance genes were examined further to determine the suitability of the xenobiotic resistance system for potential use in *P. polycephalum*. Six candidate resistance genes were identified from the literature surveys that may be suitable for use as a selectable marker in *Physarum*. The characteristics of each system are discussed in detail below.

A factor that influenced the selection of candidate markers was the availability and size of a gene conferring resistance to the appropriate xenobiotic combination. Data from previous transformation experiments are insufficient to ascertain whether there is an upper size limit for integrating fragments following DNA transformation. The *PardC* and

PardB promoter sequences are 1.1kb and 1.9kb respectively (Burland *et al.*, 1991; Burland *et al.*, 1992a). Resistance genes larger than 2kb were rejected because the addition of promoter sequences would result in vector inserts in excess of 4kb that may cause problems with cloning and plasmid stability in the bacterial host (Sections 1.5.2 & 4.3.2). In addition, if a gene were attached to target homologous integration, such as *redA*, the construct would become larger still. By limiting the size of the resistance gene, the size of the linear construct used for transformation would be similar to that used in previous experiments. Resistance to the xenobiotic must also be attributable to a single gene product and not as a result of modification in the cell, since *P. polycephalum* may not recognise the modification signal.

To determine the concentration of xenobiotic required to suppress amoebal growth, axenically grown LU352 amoebae were plated on DSDM plates containing a range of concentrations of the xenobiotic. The amoebae were grown in axenic culture and 1.5×10^8 were pelleted and resuspended with 3ml FKB; this provided 15 aliquots each containing 1×10^7 amoebae and 200 μ l FKB. The concentration of xenobiotic required to suppress amoebal growth was determined by plating 1×10^7 amoebae per plate in triplicate on DSDM containing the xenobiotic at 0 μ g ml⁻¹, 10 μ g ml⁻¹, 50 μ g ml⁻¹, 100 μ g ml⁻¹ and 200 μ g ml⁻¹. These plates were incubated at 26°C and the number of colonies on each plate was noted every 2–3 days over a period of 4–6 weeks. The results of such screening are discussed in the relevant sections below.

7.2.1 BASTA

BASTA™ is a non selective herbicide containing 18.5% of the active ingredient, phosphinothricin (PPT), also known as bialaphos or glufosinate ammonia (ammonium-D,L-homoalanin-4-yl[methyl]phosphinate), and 30% surfactant (sodium polyoxyethylene alkylether sulfate; Koyama *et al.*, 1997). PPT is a natural amino acid produced by *Streptomyces hygroscopicus* (Thompson *et al.*, 1987), which acts as a general herbicide by inhibiting glutamine synthetase; this leads to an accumulation of ammonia and affects the metabolism of amino acids in plants (Koyama *et al.*, 1997). The 600bp *bar* gene from *Streptomyces hygroscopicus* encodes PPT acetyltransferase, which inactivates the herbicide by acetylating PPT (Thompson *et al.*, 1987). The *bar* gene is located on a 16kb gene cluster containing the bialaphos production genes (*bap* cluster; Anzai *et al.*, 1987).

The biochemical reaction catalysed by PPT acetyltransferase is similar to that of the well-known reporter gene CAT (Section 1.6.3); Thompson *et al.*, (1987) have adapted the CAT assay for detection of PPT acetylation. Therefore, like CAT, the *bar* gene can serve as both a selectable marker and a reporter gene. Thompson *et al.* (1987) used the *bar* gene as a selectable marker in bacteria and suggested it would be suitable as a selectable marker for both prokaryotic and eukaryotic systems. However, this system seems most suited to plants (Thompson *et al.*, 1987); since the initial trials of Thompson *et al.* (1987) in bacteria, *bar* has only been used successfully for transformation of Japonica and Indica rice (Li *et al.*, 1997). Since the system appears to be most suited to plant studies, it was not tested for use in *Physarum*.

7.2.2 Blasticidin-S

Blasticidin-S was isolated from *Streptomyces griseochromogenes* in 1958 for use against rice blast disease (Izumi *et al.* 1991). It is a potent inhibitor of protein synthesis in both prokaryotic and eukaryotic cells. Two resistance genes have been isolated: *bsr* (blasticidin-S resistance; Izumi *et al.*, 1991) and *bsd* (blasticidin-S deaminase; Kimura *et al.*, 1994a). These genes differ in codon usage and share no nucleotide sequence homology and very little amino acid sequence homology (27%), but both encode deaminases which de-toxify blasticidin (Kimura *et al.*, 1994a). The suitability of the resistance genes seems to depend on the recipient system; e.g. Kimura *et al.* (1994a) found that *bsd* was useful as a selectable marker in *Pyricularia oryzae* where *bsr* had previously failed. Further studies by Kimura *et al.* (1994b) suggested that a bias in codon use by *bsr* may be the reason for its failure and that *bsd* was therefore potentially more suitable for transfection of eukaryotic cells. Both genes are small (<600bp) and have been used successfully for transformation in a variety of systems; e.g. *Schizosaccharomyces pombe*, *Pyricularia oryzae* (Kimura *et al.*, 1994a), *Rhizopus niveus* (Yanai *et al.*, 1991), *Dictyostelium discoideum* (Sutoh, 1993; Barth *et al.*, 1998; Pang *et al.*, 1999) and mammalian cells (Izumi *et al.*, 1991; Kimura *et al.*, 1994b); therefore suggesting that blasticidin was a suitable candidate for *Physarum*.

The concentration of blasticidin used for selection in other systems varies from 10µg ml⁻¹ in *D. discoideum* (Sutoh, 1993) to 400µg ml⁻¹ in mammalian cells (Izumi *et al.*, 1991); the majority of the systems investigated use a concentration at the lower end of this range

(10–30 $\mu\text{g ml}^{-1}$). The concentration of blasticidin required to suppress amoebal growth in *P. polycephalum* was determined. Amoebae were screened for growth in the presence of blasticidin-S (ICN Pharmaceuticals Ltd.), as described above. After 1 week, the amoebae had grown to confluence at all but the highest concentration of blasticidin (200 $\mu\text{g ml}^{-1}$). At 200 $\mu\text{g ml}^{-1}$, a mean of 17 colonies was seen on each plate, which equates to a spontaneous resistance frequency of approximately 6×10^{-5} per cell. Sufficient fungicide was available to conduct a single test of resistance at 500 $\mu\text{g ml}^{-1}$ using the same density of amoebae and bacterial suspension as with the previous tests; there were no signs of amoebal growth after several weeks. However, the cost of Blasticidin-S and the concentration of fungicide required in culture made further work financially non-viable (£89 per 50mg, at 200 $\mu\text{g ml}^{-1}$ \equiv approximately £8.90 per plate). In the future, it may be feasible to conduct trials with the *bsd* (or *bsr*) gene under the control of *PardC* or *PardB*, provided the cost of this fungicide is reduced.

7.2.3 Emetine

Emetine interacts with the S14 ribosomal protein, blocking protein synthesis. It has been used in past *Physarum* research to select emetine resistant strains for development as genetic markers for recombination analysis; Dee (1962) found 10–50 $\mu\text{g ml}^{-1}$ was effective in preventing amoebal growth (spontaneous resistance of one in 3×10^8 amoebae at 15 $\mu\text{g ml}^{-1}$). However, emetine resistance did not segregate amongst the *Physarum* progeny in a manner consistent with mendelian ratios and this was assumed to be due to misclassification for emetine resistance but may have been multifactoral (Dee, 1962). The *CRY-1* gene confers resistance to emetine and cryptopleurine in *Chlamydomonas reinhardtii* and encodes the ribosomal S14 protein with a single base substitution in the conserved C-terminal region (Nelson *et al.*, 1994). This gene has been used successfully for targeted gene disruption in *C. reinhardtii* only (Nelson *et al.*, 1995). Similar S14 resistance mutations have been reported in other systems including Chinese hamster ovary cells and *Saccharomyces cerevisiae* (reviewed by Nelson *et al.*, 1994). Although the *CRY-1* sequence is highly conserved when compared to other S14 encoding homologues (e.g. *S. cerevisiae*; Nelson *et al.*, 1994), it is unclear whether this gene will confer resistance to emetine in *Physarum*. In any case, even if the *CRY-1* gene were able to function in *Physarum*, the fact it is 3.6kb in size may cause problems with vector stability and integration to the *Physarum* genome, for reasons discussed earlier. Therefore, the

emetine/*CRY-1* system was not considered suitable for development as a selectable marker in *Physarum*.

7.2.4 Geneticin or Neomycin

Geneticin (G418; Amersham International) is a synthetic aminoglycosidic antibiotic related to neomycin (Egelhoff *et al.*, 1991) that blocks protein synthesis by interaction with the 80S ribosomal subunit. Resistance to this antibiotic is conferred by the bacterial transposons Tn903 or Tn5 encoding aminoglycoside 3'-phosphotransferases type I and II respectively (APH; Oka *et al.*, 1981; Lang-Hinrichs *et al.*, 1990). The 850bp resistance gene from Tn903 is referred to as aminoglycoside 3'-phosphotransferases type I (*APHI*), *kan* (kanamycin; e.g. Oka *et al.* 1981; Chen & Fukuhara, 1988) or *neo* (neomycin; e.g. Lang-Hinrichs *et al.*, 1990). To avoid confusion, the designation *APH* is used in this Chapter for all further references to this gene. The *APH* resistance gene has been used in a wide variety of systems for transformation experiments, in combination with G418 or neomycin (e.g. *S. cerevisiae*: Chen & Fukuhara, 1988; *D. discoideum*: Egelhoff *et al.*, 1991; Pang *et al.*, 1999; *Trichomonas vaginalis*: Delgadillo *et al.*, 1997). G418 was also used as a selective agent at 20µg ml⁻¹ in the preliminary trials of DNA transformation using *P. polycephalum* performed by Haugli & Johansen (1986). However, no enzymatic activity of APH could be detected in *Physarum* cell lysates, even though the APH gene could be detected in genomic DNA and the cells were apparently G418 resistant (Haugli & Johansen, 1986); the reason for this is unclear. Since the *APH* resistance gene is small (850bp) and has been used successfully for transformation in other systems, this was considered a potentially useful selectable marker and the concentration of G418 required to suppress amoebal growth was re-assessed.

Since the *APHI* gene confers resistance to both neomycin and G418, the concentrations of neomycin sulphate (Sigma Aldrich) and G418 (Amersham International) required to suppress amoebal growth were assessed. After 2 weeks, colonies were observed on neomycin plates containing up to 200µg ml⁻¹, whilst no colonies were seen at any concentration of G418. Further screening was performed using G418 at concentrations ranging from 10µg ml⁻¹ to 80µg ml⁻¹, using increments of 10µg ml⁻¹ per plate. Again, there were no obvious signs of sustained growth, although there were some signs that there had been a delay before the growth of the amoebae was inhibited by the antibiotic at the lowest concentration.

For *Physarum polycephalum* transformation experiments, the working strength of hygromycin chosen for screening was twice the concentration that is required to suppress the development of amoebae with spontaneous resistance (Burland *et al.*, 1993a). Previous testing of G418 by D. Pallotta indicated that 20µg ml⁻¹ should be suitable for *APHI* transformant selection (personal communication). Therefore, since 10µg ml⁻¹ was sufficient to prevent spontaneous resistance of 10⁷ amoebae, this was doubled and 20µg ml⁻¹ G418 was selected for these studies. To confirm no resistant amoebae would develop at higher cell densities, 10 plates containing 20µg ml⁻¹ of G418 were each inoculated with 5 × 10⁷ amoebae. After 4 weeks at 26°C, no amoebal growth was observed; confirming the suitability of this concentration of G418 for selection of *APHI* transformants. Since G418 is commercially available at low prices, each 20 µg ml⁻¹ plate would cost less than 2p. Similar concentrations of G418 are used for *D. discoideum* transformation experiments (e.g. 10µg ml⁻¹: Pang *et al.*, 1999; 20µg ml⁻¹ Barth *et al.*, 1998). Preliminary trials of G418/*APHI* for transformation are described below (Section 7.3).

7.2.5 Puromycin

Puromycin is an aminonucleoside antibiotic that was isolated from *Streptomyces alboniger* and mimics the 3'-end of aminoacyl-tRNAs, causing interruption to protein synthesis on the ribosome (Tercero *et al.*, 1993). The genes involved in puromycin synthesis in *S. alboniger* are clustered on a 13kb fragment; the 600bp puromycin N-acetyltransferase (*pac*; Lacalle *et al.*, 1989) gene is located on a 906bp fragment contained within the 13kb cluster and inactivates puromycin by N-acetylation of the amino group (Lacalle *et al.*, 1993; Tercero *et al.*, 1996). Similarly to PPT (Section 7.2.1), this acetylation resembles the acetylation of CAT and assays for gene activity, based on the CAT assay, have been devised (De La Luna & Ortín, 1992; Mielke *et al.*, 1995). This means puromycin can also be used as both a reporter and a selectable marker. Puromycin has been used as a selectable marker in several systems including *Streptomyces lividens* (Lacalle *et al.*, 1993), *Methanococcus voltae* (Patel *et al.*, 1994) and mammalian cells (De La Luna & Ortín, 1992; Watanabe *et al.*, 1995). The resistance gene is small (600bp) and has a proven track record for transformation in a variety of systems suggesting that puromycin is a suitable candidate for development in *Physarum*.

The concentration of puromycin dihydrochloride (Calbiochem) required to suppress amoebal growth was assessed. After 1 week, amoebae had grown to confluence at all concentrations up to $200\mu\text{g ml}^{-1}$. Therefore, a second screen was conducted using one plate at each of the following concentrations of puromycin: $500\mu\text{g ml}^{-1}$, $750\mu\text{g ml}^{-1}$ and 1mg ml^{-1} . After one month, 11 colonies had appeared on the plate containing $750\mu\text{g ml}^{-1}$ puromycin, and none were observed at 1mg ml^{-1} . The high concentration of puromycin required to suppress amoebal-growth in *Physarum* was unexpected, since the other systems investigated all used $0.1\text{--}10\mu\text{g ml}^{-1}$ for selection (Lacalle *et al.*, 1993; Patel *et al.*, 1994; Watanabe *et al.*, 1995). Like blasticidin, the cost of puromycin and the concentration of antibiotic required to suppress amoebal growth made further work financially non-viable (£89 per 100mg, at $750\mu\text{g ml}^{-1}$ \equiv approximately £16.70 per plate).

7.2.6 Zeocin

The bleomycin family of glycopeptide antibiotics bind to DNA and cause DNA degradation; zeocin[®] is a member of this protein family. DNA replication is disrupted and this affects cell division; cells already committed to division will not be affected until the next round of replication, and thus divide once before the affects of the antibiotic are observed (Pfeifer *et al.*, 1997). The product of the resistance gene interacts with the antibiotic and prevents it from binding to the DNA (Gautier *et al.*, 1996). Several bleomycin resistance genes have been cloned and these confer resistance to all members of the bleomycin protein family (*Sh ble* from *Streptoalloteichus hindustanus*: Drocourt *et al.*, 1990; *ble* from Tn5: Blot *et al.*, 1994; *Sa ble* from *Staphylococcus aureus*: Semon *et al.*, 1987; *blmA* from *Streptomyces verticillus*: Calcutt & Schmidt, 1994; Sugiyama *et al.*, 1994). Interestingly, the *ble* gene from Tn5 has also been shown to benefit bacterial hosts even when bleomycin is not present and is thus thought to function in DNA repair (Blot *et al.*, 1994).

The 375bp *Sh ble* gene from *Streptoalloteichus hindustanus* has been developed for use in transformation (Invitrogen; Drocourt *et al.*, 1990). Zeocin was selected for development as the first selectable marker for transformation in both wild-type and mutants strains of the multicellular green alga, *Volvox* (Hallmann & Rappel, 1999). Hallmann & Rappel (1999) tested the level of sensitivity of *Volvox* to both zeocin and phleomycin; although zeocin was a weaker toxin than phleomycin, they found that the minimum concentration of zeocin required to suppress growth of the algae was reproducible, whereas phleomycin

was not. In addition to *Volvox*, the bleomycin family of antibiotics have been used successfully as a selectable marker for several systems including avian cells (Gautier *et al.*, 1996), insect cell lines (Pfeifer *et al.*, 1997) and *Toxoplasma gondii* (Messina *et al.*, 1995). This proven track record combined with the commercial availability and small size of the resistance gene suggested that it was a potentially useful selectable marker and the concentration of zeocin required to suppress amoebal growth was therefore assessed.

The level of sensitivity of *Physarum* amoebae to Zeocin® (Invitrogen) was tested. DSPB was used instead of DSDM for the plates as zeocin is sensitive to acidic conditions (manufacturers data sheet). After a 4-week period, a concentration of 200 µg ml⁻¹ had suppressed amoebal growth, but some amoebae appeared to have grown or encysted. After a further 2–3 weeks, small plasmodia were forming on the 200 µg ml⁻¹ plates. Therefore, further tests were conducted using antibiotic concentrations of 200 µg ml⁻¹ to 500 µg ml⁻¹, using increments of 50 µg ml⁻¹ per plate over this range. After a 7-week period, a mean of two colonies formed on each of the plates containing 250 µg ml⁻¹ and no colonies were observed at concentrations exceeding this. This indicated that 300 µg ml⁻¹ was a suitable concentration for selective plating in *P. polycephalum*. At this concentration further experiments are considered to be financially viable (<£1.00 per plate); similar concentrations are used for selection of transfected insect cells (150–500 µg ml⁻¹, Pfeifer *et al.*, 1997). To confirm the suitability of this concentration, 12 plates containing 300 µg ml⁻¹ zeocin were inoculated with 5×10^7 *Physarum* amoebae per plate and incubated at 26°C for 6 weeks; no amoebal growth was detected. However, due to a lack of time and resources, no transformation experiments were performed using this system.

7.3 PRELIMINARY TRIALS OF THE G418-*APHI* TRANSFORMATION SYSTEM

The literature review suggested that G418 and *APHI* were suitable candidates for development as a new selectable marker for use in *Physarum* transformation experiments (Section 7.2.4). Vectors containing the aminoglycoside 3'-phosphotransferase (*APHI*) gene from the bacterial transposon Tn903 (Oka *et al.*, 1981) under the control of *PardC*, both with and without *TardC*, were kindly provided by D. Pallotta (pLAV-T10 and

pLAV-T20 respectively); Pallotta and colleagues had not performed any transformation experiments with these vectors (personal communication).

Prof. Pallotta had cloned the *APHI* gene into a vector containing *PardC* plus the first 25bp of the *ardC* coding region, including the transcriptional start (ATG), followed by 19bp of the pBluescript KS- (Stratagene) polylinker (see below). The *APHI* gene was cloned such that it is missing the first 29bp of coding sequence; sequence analysis confirmed that the *APHI* gene was in frame with the ATG from *PardC* (Pallotta, personal communication; see below). Provided the correct reading frame is maintained, the first 19 codons (57bp) of the *APHI*-resistance gene from Tn903 can be removed without loss of activity of the gene product (Chen & Fukuhara, 1988). This is due to a second ATG at codon 19 (ATG; illustrated below). Chen & Fukuhara (1988) also created vectors where the *APHI* gene was fused to the 3' end of different sequences and found that APH activity was maintained provided the *APHI* sequence was in the correct reading frame. Therefore, the 15 amino acids from *ardC* and pBluescript encoded ahead of the *APHI* gene are unlikely to affect the activity of the *APHI* protein.

APHI gene from Tn903 (Oka *et al.*, 1981)

Region fused to *PardC* (see below)

.....
ATGAGCCATATTCAACGGGAAACGTCTTGCTCGAGGCCGCGATTAAATTCCAACATG...
 M S H I Q R E T S C S R P R L N S N M .

Fusion of *PardC* and the *APHI* gene used to generate pLAV-T10 and pLAV-T20 (Pallotta, personal communication)

PardC region Bluescript polylinker *APHI* gene

.....
 .. **ATGGAAGGAGAAGACGTTCAAGCTTatcgataaccgtcgatcgacCTCGAGGCCGCGA...**
 M E G E D V Q A Y R Y R R S T S R P R .

The *APHI* plasmids were digested with *Sst*I to release the 2.2kb pLAV-T10 (*PardC-APHI*) and 2.9kb pLAV-T20 (*PardC-APHI-TardC*) inserts from the vectors. Transformation was performed using 1-10µg of digested vector (Section 2.1.7). The hygromycin plasmids, pTB37 (*PardC-hph*; Burland *et al.*, 1993a) and pTB40 (*PardC-hph-TardC*; Burland *et al.*, 1993a), were included as controls in all experiments to confirm that the transformation procedure was working and that the cells were

transformable. The results of these transformation experiments are summarised in Table 7.1 and discussed below and in Section 7.4.2.

Selective plating was initially performed on plates containing $20\mu\text{g ml}^{-1}$ G418; this concentration was later reduced to $15\mu\text{g ml}^{-1}$ or $10\mu\text{g ml}^{-1}$ (Table 7.1). The lower concentrations were selected to increase the likelihood of recovering a transformant, for reasons discussed in Section 7.4.2. At these lower concentrations, the amoebae had shown no signs of sustained growth during the initial screening (Section 7.2.4). No transformants were recovered at any of these concentrations (Table 7.1)

During one experiment, several colonies appeared on the G418 ($15\mu\text{g ml}^{-1}$) selective plates containing cells that had been transformed with either of the *APHI* vectors (data not shown). However, the negative control cells were plated on a different batch of G418 plates and therefore did not give an indication of whether the colonies were genuine transformants or had resulted from spontaneous amoebal growth. When these putative transformants were sub-cultured to fresh selective plates, the amoebal growth ceased. Therefore, it is considered likely that a problem occurred within the batch of selective plates prepared for that particular experiment, which resulted in a lower activity of G418 within the plates, facilitating spontaneous growth of a small proportion of the amoebae.

A few colonies also appeared on a single G418 selective plate ($15\mu\text{g ml}^{-1}$) from a separate experiment after transformation with pLAV-T10. In this case, no amoebal growth was observed on the negative control plates or with the second vector (pLAV-T20). These putative *APHI*-transformants were sub-cultured to fresh selective plates and again, no further growth occurred suggesting that they too were the result of spontaneous amoebal growth.

Both of the experiments that resulted in spontaneous amoebal growth on selective plates were performed during the same fortnight; such problems were avoided in subsequent experiments by using a fresh batch of G418 stock solution to prepare the selective plates. These data suggest that the G418 stock solution is stable at 4°C for approximately four months. Past experiments suggest that problems associated with instability of hygromycin do not occur as frequently as those seen with G418 (personal observation). This suggests that G418 may be less stable than hygromycin in plates or as stock solutions stored at 4°C .

Table 7.1

Vector	Concentration of selective agent	Number of experiments	Total DNA	Total survivors of electroporation	Number of transformants	Transformation efficiency (per cell)
pLAV-T10	20µg ml ⁻¹ G418	6	8.5µg	1.5 × 10 ⁸	0	-
	15µg ml ⁻¹ G418	4	30µg	5.8 × 10 ⁷	0	-
	10µg ml ⁻¹ G418	2	6µg	8.1 × 10 ⁷	0	-
pLAV-T20	20µg ml ⁻¹ G418	7	10µg	1.9 × 10 ⁸	0	-
	15µg ml ⁻¹ G418	4	30µg	6.6 × 10 ⁷	0	-
	10µg ml ⁻¹ G418	2	6µg	7.9 × 10 ⁷	0	-
pTB37	100µg ml ⁻¹ Hyg	10	38µg	2.6 × 10 ⁸	1	2.6 × 10 ⁻⁸
pTB40	100µg ml ⁻¹ Hyg	10	38µg	2.4 × 10 ⁸	4 †	6 × 10 ⁻⁷ to 1.2 × 10 ⁻⁸

Details of preliminary transformation experiments to test the G418/APHI selection system (Section 7.3)

† Three of these clones were derived from the same transformation experiment and no attempt was made to determine if any were siblings. Thus, a range of transformation efficiencies was calculated for pTB40, allowing for all clones being unique (i.e. four transformants) or for the three transformants derived from the same experiment being siblings (two transformants).

7.4 DISCUSSION

7.4.1 Prospects for development of the zeocin selection system for use in *Physarum*

The concentration of zeocin required to suppress amoebal growth was determined as $300 \mu\text{g ml}^{-1}$ (Section 7.2.6). However, time constraints and a lack of resources meant that I was unable to begin vector construction and testing. Vectors carrying the 375bp *sh ble* gene from *Streptoalloteichus hindustanus* under the control of various promoters are available from Invitrogen; the most basic of these vectors contains the zeocin resistance gene under the control of the bacterial promoter EM7 (Invitrogen). These vectors were all designed with several cloning sites on either side of the resistance gene and promoter making it relatively simple to either replace the promoter with *PardC* or to transfer the *sh ble* resistance gene to a vector carrying *PardC*; *PardC* vectors are available for all three reading frames (Burland *et al.*, 1993a). The efficiency of transformation with these vectors can then be assessed using similar procedures to those described above for G418.

7.4.2 The G418-*APHI* transformation system

Preliminary trials of the G418-*APHI* transformation system were performed using pLAV-T10 and pLAV-T20 vectors and G418 selective plates; selective plating was initially performed on plates containing $20 \mu\text{g ml}^{-1}$ G418. However, the concentration was later reduced to $15 \mu\text{g ml}^{-1}$ or $10 \mu\text{g ml}^{-1}$ to improve the chance of recovering a transformant (discussed below; Section 7.3; Table 7.1).

Early transformation studies in *P. polycephalum* used geneticin (G418) in conjunction with *APH* genes (Haugli & Johansen, 1986). There were some concerns at that time regarding the suitability of G418 for selection due to potential problems with spontaneous resistance of amoebae to G418 in the presence of Ca^{2+} and Mg^{2+} together with an apparent reduction in the survival of cysts on G418 selective plates when stored for prolonged periods in the cold (Haugli & Johansen, 1986). Spontaneous resistance of amoebae did not appear to be a problem during the tests reported in this Chapter, since no resistant amoebae were detected in 5×10^8 cells plated during the initial tests to determine a suitable working concentration for the antibiotic (Section 7.2.4). If cysts are unable to survive when stored for prolonged periods on G418 selective plates, a simple solution would be to store the cysts as frozen glycerol stocks or on agar plates without G418 selection. Previous experience with hygromycin-resistant transformants suggest that the

integrated DNA will be stable in the cells in the absence of the selective agent (Section 1.6.6; Burland *et al.*, 1993a).

The results of the preliminary trials reported in this Chapter are disappointing; no stable transformants were obtained after electroporation of approximately 3×10^8 LU352 amoebae per vector (Table 7.1). The positive controls produced transformation efficiencies of 2.4×10^{-8} for pTB37 or between 1.2×10^{-8} and 6×10^{-7} for pTB40; these are lower than the reported figure of 2×10^{-7} (Burland & Pallotta, 1995) but were similar to those observed during the *redA* transformation experiments reported in this thesis (Chapter 5). Therefore, the positive controls and *redA* transformation experiments suggest that there was nothing wrong with the amoebae, *per se*. Since the mean transformation efficiency generated in the studies reported throughout this thesis is 2×10^{-8} , the results of the G418/APHI trials are insufficient to categorically state that this system will not work in *Physarum*; further testing is required.

As discussed previously, several contributory factors could have influenced the transformation efficiency, including the amoebae, the DNA template(s), the buffers and the electroporation apparatus (Section 1.6).

The two vectors provided by Prof. Pallotta had not been used in any transformation experiments before (personal communication). Therefore, there were no guarantees that either vector would produce functional APH. Evidence from other systems suggest that the fusion of the APhi gene to *PardC* would produce functional APH (Section 7.3; Chen & Fukuhara, 1988). However, to confirm that these vectors are functional, studies similar to those performed using the *PardC-hph* vectors in fission yeast are required (Burland *et al.*, 1991).

Barth *et al.*, (1998) used G418 for transformation studies in *Dictyostelium* and showed that the plasmid copy number appeared to be directly related to the concentration of G418 used for selection; the higher the concentration, the higher the typical plasmid copy number per cell. A minimum of 8 neomycin plasmid molecules was required to confer resistance to G418 and the average number of neomycin plasmid copies per genome was 14 times greater than the number of blasticidin plasmid copies (Barth *et al.*, 1998). Similar results were obtained by Pang *et al.* (1999) using blasticidin, hygromycin and neomycin vectors

fused to GFP (green fluorescent protein) in *Dictyostelium*. They found that the level of GFP directly related to the copy number of the vector. They compared the hygromycin and neomycin vectors and showed that both vectors were present at high copy number, although the hygromycin copy number was the lower of the two (a mean of 300 compared to 500 for neomycin).

Physarum transformants result from integration of a single linear molecule into the genome. Given the data from *Dictyostelium* (Barth *et al.*, 1998; Pang *et al.*, 1999), the concentration of G418 was decreased during the experiments reported in this Chapter, in case the presence of just one copy of the *APHI* gene was insufficient to confer resistance to G418 at the higher concentration. Since *PardC* is a strong promoter, it may produce enough transcripts to confer resistance to G418 when just one copy of the resistance gene is present. A single copy of *PardC-hph* is sufficient to confer resistance to hygromycin in *Physarum*. Since a high copy number (300) for hygromycin vectors was also observed for the *Dictyostelium* transformation studies reported by Pang *et al.* (1999), it is possible that APH may also function in *Physarum* when just a single copy of the APHI gene is present. However, if multiple copies of the *APHI* gene are required for resistance to G418 in *Physarum*, this system will not work unless the vector is altered to increase the gene copy number.

A 'cassette multiplication technique' was devised during vector construction for transformation of *Volvox* (Hallmann & Rappel, 1999). Hallmann & Rappel (1999) increased the number of selectable marker cassettes carried by a single plasmid molecule to 16. The vectors containing multiple *ble*-cassettes were tolerant to higher levels of zeocin than those containing a single cassette. The multiplication of cassettes was limited only by the capacity of the vector and host organism (Hallmann & Rappel, 1999). Whether this kind of strategy could succeed in *Physarum* remains to be determined. However, given the problems associated with stability of repetitive elements in vectors (Sections 1.5.2 & 4.3.2) and the potential truncation of cassettes on integration to the *Physarum* genome (Pierron *et al.*, 1999), this strategy may prove problematic. An alternative strategy that could increase the copy number for integration would be the use of Tp elements to target integration (Section 1.5.1); vectors incorporating Tp sequences have been designed by J. Bailey and such vectors do target multiple integration events (personal communication). However, such integrated fragments may have reduced or

little activity due to *de novo* methylation, since the Tp sequences have only been found in association with methylated DNA (Section 1.5.1; Rothnie *et al.*, 1991).

The main objective of developing a new selectable marker was for use in future double gene knockout experiments; this system would not be suited to such studies if multiple copies of *APHI* are required. The cassette multiplication technique of Hallmann & Rappel (1999) may enable a single fragment for transformation to be produced containing several copies of the *APHI* gene under the control of a single *PardC* promoter; previous studies suggest that such tandem copies would retain APH activity (Chen & Fukuhara, 1988). However, such repetition of sequence may be unstable in both the bacterial hosts and the *Physarum* genome. In addition, the multiplication would lead to a large selectable marker that would be difficult to incorporate effectively into vectors for homologous gene replacement. If multiple copies of *APHI* are required, the G418/*APHI* system may only be suited to other types of transformation experiment such as over-expression studies (Section 5.5.6) or protein localisation studies using GFP-fusion vectors.

7.4.3 Summary

Both the G418-*APHI* and Zeocin-*sh ble* systems require further testing to determine whether they are suitable for use in transformation studies in *Physarum polycephalum*. Although no transformants were generated during the preliminary trials of the G418-*APHI* transformation system, only approximately 3×10^8 LU352 amoebae were used per vector (Table 7.1). Therefore, it is possible that continued testing of the G418-*APHI* transformation system, including methods to increase the copy number, will lead to G418-resistant transformants. This will expand the potential for the study of gene function in *Physarum polycephalum* by electroporation.

CHAPTER EIGHT

GENERAL DISCUSSION

CHAPTER 8: GENERAL DISCUSSION

8.1 *PHYSARUM POLYCEPHALUM* AS A USEFUL EXPERIMENTAL SYSTEM

Physarum polycephalum possesses some interesting features, which make it a useful experimental system for studies of development. The large acellular plasmodium can contain several million nuclei and provides an abundant supply of nuclear material synchronised to a particular stage of the cell cycle, without the need for artificially induced synchronisation. The cytoplasmic streaming that occurs in the plasmodium provides a good model for studies of cellular contractility and motility and the abundance of plasmodial structural proteins facilitated the discovery and investigation of the properties of the actin-binding proteins, profilin and fragmin (Section 1.3.2; Chapter 6). The organisation of the genome is similar to that of other eukaryotes with alternating sequences of unique and repetitive DNA (e.g. *Xenopus*; Hardman *et al.*, 1980). Yet, for such a 'simple' eukaryote, the genome is comparatively large at 2.7×10^8 bp (Burland *et al.*, 1993b); with repetitive sequence comprising one third of this. The mechanism of differentiation of individual cells within complex, multicellular organisms has been a focus of much research within the scientific community and studies of *P. polycephalum* may help address such problems on a simplified level. The apogamic *P. polycephalum* strains provide an ideal system for such studies, since they remain haploid throughout the life cycle and therefore the effects of even recessive mutations are visible in the plasmodium (Section 1.2.4).

Since apogamic strains arose through mutation in the laboratory, recent studies have investigated the differences in gene expression during both apogamic and heterothallic development in *P. polycephalum* (Barber, 1998; Bailey *et al.*, 1999). I expanded these studies to include the fragmin gene family (*frgA*, *frgP* & *frg60*) and actin-fragmin kinase (*AFK*; Chapter 6). Although gene expression appeared to be activated when fewer apogamically developing cells were present than compared with heterothallically developing cells, these differences may be due to differences in timing of commitment, as described in Section 6.3.1. Since there is no apogamic event equivalent to the cell and nuclear fusion observed in heterothallic development, which could be used as a marker for the initiation of apogamic development, 'commitment', the point of no return, was assigned based on the ability of a cell to survive replating and continue to develop into a

plasmodium. Thus, commitment may not represent the same state of gene expression or cellular organisation in both apogamic and heterothallic development (Section 6.3.1; Barber, 1998; Bailey *et al.*, 1999). Within such constraints, each gene examined so far appears to exhibit the same individual expression pattern during both heterothallic and apogamic development (Section 6.3.1; Barber, 1998; Bailey *et al.*, 1999).

These expression data together with the general similarities that were observed during time-lapse cinematography studies (Bailey *et al.*, 1987 & 1990) and immunofluorescence studies of apogamic and heterothallic development (Bailey *et al.*, 1990; Solnica-Krezel *et al.*, 1988 & 1991) strongly suggest that the *gadA* mutation, which permits apogamic development, has no major consequences on the general pattern of events occurring during development.

8.2 DIFFERENTIALLY EXPRESSED GENES

Several distinct cell types occur during the life cycle of *P. polycephalum*; these are linked by reversible and irreversible transitions; some of which are well characterised (Section 1.2). The two vegetative cell types, amoebae and plasmodia are linked by an irreversible developmental transition that has been of key interest to the studies reported in this thesis.

Amoebae and plasmodia are considerably different in appearance and behaviour; consistent with this observation, a comparison of abundant proteins from amoebae and plasmodia revealed that approximately 20% of the abundant proteins were cell-type specific (Section 1.4.1; Turnock *et al.* 1981).

Time lapse-cinematography of both apogamic and heterothallic development showed that a critical stage in the amoebal-plasmodial transition (APT) is an extended cell cycle (Section 1.2.5; Bailey *et al.*, 1987 & 1990). During the extended cell cycle, cells become committed to development, lose the ability to undergo the amoeba-flagellate transformation and acquire the ability to undergo plasmodial fusion and phagocytose vegetative amoebae (Bailey *et al.*, 1987 & 1990). Analyses of the APT, which begins with the extended cell cycle, indicated that plasmodium development is completed over several cell cycles and is associated with a gradual acquisition of plasmodium-specific proteins and characteristics, concomitant with a loss of amoebal-specific proteins and

characteristics (Section 1.4; Pallotta *et al.*, 1986; Sweeney *et al.*, 1987; Solnica-Krezel *et al.*, 1989 & 1991).

Mutagenesis of amoebae generated a class of mutants that are unable to develop normal apogamic plasmodia; the *npf* mutants (Section 1.4.2; Wheals, 1973; Anderson & Dee, 1977; Bailey *et al.*, 1992a; Solnica-Krezel *et al.*, 1995). Characterisation of these mutants revealed that the genes affected by the mutations are normally active at different times during development, suggesting a cascade of gene activation occurs; analysis of double mutants provides evidence that such cascades may involve several developmental pathways (Section 1.4.2).

Bailey *et al.* (1992) sought to clone and characterise genes expressed primarily during the APT and constructed a cDNA library from a developing population of apogamic amoebae containing a high proportion of cells in the extended cell cycle. Screening of a small proportion of this library has led to the isolation of four *red* genes (*redA*, *redB* and *mynD*: Chapters 3–5; Bailey *et al.*, 1999; *redE*: E. Swanston, personal communication); more *red* genes undoubtedly exist within the cDNA library (Chapter 3). It was anticipated that the *red* genes could be classified into two categories: genes required for the structural rearrangements occurring during the APT (e.g. *mynD*: myosin type II heavy chain; Bailey *et al.*, 1999) or genes involved in the regulation of gene activity (Chapter 3). It is the latter category of genes that are of particular interest to understanding the regulation of this transition.

Using northern blotting analysis, I investigated the changes in gene expression for *redA* and *redB*, *proA* and *proP* (Chapter 3) and the recently identified fragmin gene family (*frgA*, *frgP*, *frg60*, and *frgR*; Chapter 6; T'Jampens *et al.* 1997 & 1999) during the APT; this confirmed that the extended cell cycle is a critical stage in the APT and is when many of the changes in gene expression are initiated. In addition, these northern analyses confirmed the existence of the *red* genes and examined their expression pattern in more detail.

Functional analysis of the *red* genes by gene disruption could identify genes that are essential for completion of the APT; I attempted such an analysis with *redA* (Chapter 5). It is predicted that continued transformation studies using the vectors I designed and

similar vectors, incorporating a *redA* genomic clone, will generate a strain(s) carrying a gene knockout for *redA* that can be analysed using techniques such as time-lapse cinematography and immunofluorescence microscopy to clarify whether RedA is essential for plasmodium development (Section 5.5). A combination of functional analysis of the *red* genes by gene knockout and immunolocalisation studies may determine the roles of the *red* genes and ultimately identify the gene hierarchy within the developmental cascade.

Future experiments that may provide insight as to how gene expression is regulated during the APT could examine the promoters of the *red* genes and plasmodium-specific genes, such as *proP*. In addition, other developmental promoters could be identified using “promoter-trap” techniques (e.g. Chang *et al.*, 1995; Kuspa *et al.*, 1995), modified for *Physarum* by replacing the reporter gene, *lacZ*, with GFP. By attaching such promoters to GFP or *luc* for transformation studies, promoter activity during plasmodium development could be examined; this technique is far more sensitive than expression analysis by northern blotting and would allow gene expression to be correlated to a particular stage of development.

Sequence analysis of the promoters may identify conserved regions that represent putative regulatory elements. Alternatively, the regulatory regions of the promoters could be identified by creating deletions within the promoter and then using these altered promoters to drive expression of luciferase in transformation experiments; such an approach has been used successfully in *Dictyostelium discoideum* to identify and characterise elements that control expression from actin promoters (Hori & Firtel, 1994). This may identify regulatory regions that suppress or enhance transcription from *red* gene promoters in *P. polycephalum*. The binding of transcription factors to such regions could be confirmed by gel retardation assays using nuclear extracts from amoebae and plasmodia (Carey, 1991). In addition to identifying the regions of the promoter that suppress or enhance transcription, a yeast hybrid system could be used to identify the genes that encode the transcription factors that bind to these regions. The effect any enhancer proteins identified have on plasmodium development in *Physarum* could then also be investigated using gene knockout techniques such as those described in Chapter 5.

A combination of functional analysis of the *red* genes, characterisation of *red* gene promoters and the identification of transcription factors involved in the regulation of gene

expression driven by these promoters may ultimately identify the cascade of regulatory events, initiated by *matA*, that are essential to plasmodium development.

8.3 THE ROLE OF *MATA* IN PLASMODIUM DEVELOPMENT

The APT in *P. polycephalum* involves various loci, the most important being *matA*, which is responsible for the initiation of development (Sections 1.2.3 & 1.4; Bailey, 1995 & 1997). For heterothallic development to occur, two fusing amoebae must possess different alleles of *matA* (Section 1.2.3). In amoebae carrying a *gadA* mutation at *matA*, apogamic development can occur (Section 1.2.4), although the frequency at which this occurs is influenced by *npfB* and *npfC* mutations, which are also tightly-linked to *matA* (Section 1.2.4). Finally, *matA* also influences uniparental inheritance of mitochondrial DNA (Section 1.5). These observations indicate that the *matA* genetic region is a complex multi-functional locus with at least four roles in plasmodium development. Although *matA* has been well characterised by classical genetic approaches, nothing is known at a molecular level (reviewed by Bailey 1995 & 1997).

Sexual development in the Basidiomycetes is regulated by two independent mating-type loci (reviews: Casselton & Olesnicky, 1998; Kothe, 1996; Kahmann & Bölker, 1996). One mating-type locus contains pairs of genes that encode homeodomain (HD) transcription factors, which heterodimerise to form an active regulatory protein while the second contains genes that encode pheromones and transmembrane receptors (reviews: Casselton & Olesnicky, 1998; Kothe, 1996; Kahmann & Bölker, 1996). Development only proceeds if the two mating strains possess different alleles of the mating-type loci. Interestingly, development in *Ustilago hordei* is regulated by a single mating-type locus that contains a complex of genes for both a regulatory protein/transcription factor and a pheromone receptor system (reviewed by Casselton & Olesnicky, 1998). The multifunctional *matA* locus in *P. polycephalum* could share similarities with either of the two mating-type systems found in the Basidiomycetes or may even be similar to *U. hordei* and contain a complex of both systems.

Both mating-type systems in Basidiomycetes possess self/non-self recognition mechanisms (reviewed by Casselton & Olesnicky, 1998). For example, the amino-terminal domains of the two HD proteins encoded by each pair of genes found in the *b* mating-type are responsible for self/non-self recognition in *Ustilago maydis* and a single amino acid

substitution in the N-terminal domain of one of the HD proteins can alter the protein sufficiently to enable compatibility between HD factors that are normally incompatible (reviewed by Casselton & Olesnicky, 1998). A mutation that generated a chimeric gene as a result of fusion of a HD1 and HD2 gene in the *A* mating-type locus of *Coprinus cinereus* produced a protein that was effectively a heterodimer and was sufficiently active to promote self-compatibility for development (reviewed by Casselton & Olesnicky, 1998). Similarly, “self-compatible” mutations have been identified in the Basidiomycete pheromone receptor systems that lead to constitutive activation of the receptors (reviewed by Casselton & Olesnicky, 1998). Similar mutations may have occurred at *matA* in *P. polycephalum* to permit apogamic development.

A “positive selection” technique that was first developed in order to clone probes for the Y chromosome in the mouse (Lamar & Palmer, 1984) has been used successfully to clone genes in other systems, including the mating-type *A* genes from *C. cinereus* encoding the HD proteins (Kües *et al.*, 1992). With such a technique, genomic DNA known to contain the desired gene (the tracer) is digested with a restriction enzyme with a 4bp recognition sequence to generate small fragments with cohesive ends. Genomic DNA known not to be carrying the desired gene (the driver) is sonicated to generate larger fragments with ragged ends. An excess of driver is then hybridised with tracer and the tracer-tracer hybrids are selected using one of several methods including ligation to vectors with cohesive ends (the same cohesive sequence as the tracer) or ligation to PCR adapters with cohesive ends followed by PCR (reviewed by Sagerström *et al.*, 1997; Lisitsyn *et al.*, 1993). A similar approach was proposed by Dr. Anderson and Dr. Bailey to isolate *matA* from *P. polycephalum*, using genomic DNA prepared from two closely related strains that differ at *matA* (personal communication). However, it is considered unlikely that a complete clone of *matA* would be obtained using such an approach. Therefore, genomic techniques such as the construction and screening of size-fractionated genomic libraries or inverse PCR (Chapter 5) may be required to clone the complete locus. To identify DNA containing a functional *matAx*, heterothallic amoebae of a different *matA*-type could be transformed with the DNA, under the control of a constitutive *Physarum* promoter, such as *PardB* or *PardC* (Section 1.6); if the transformant amoebae readily develop into plasmodia or have changed *matA* allele, this would indicate the cloned gene is indeed *matAx*.

The application of the 'positive selection' techniques to *P. polycephalum* depends primarily on the assumption that the *matA* loci are idiomorphs (i.e. non-homologous alleles); this is considered likely since no recombination has been observed in the *matA* region. The isolation of a *matA* clone may clarify:

- i. How *matA* regulates the APT (Sections 1.2 & 1.4),
- ii. The genetic basis of the *gada*, *npfB* and *npfC* mutations at *matA* and how they affect the function of *matA* (Section 1.2)
- iii. How *matA* influences the inheritance of mitochondria (Section 1.5.3).

8.4 CONCLUSION

The *red* genes have recently emerged as a new class of genes expressed at their highest levels during the amoebal-plasmodial transition in *P. polycephalum* (Bailey *et al.*, 1999). Of the four putative *red* gene cDNA clones previously identified from a subtracted cDNA library (Bailey *et al.*, 1992b), the research reported in this thesis confirms that two are clones of *red* genes (*redA* and *redB*; Chapter 3). Sequence analysis provided no clues as to the roles of *redA* and *redB* during plasmodium development. However, the subsequent identification of a third *red* gene encoding the structural protein myosin type II heavy chain by E. Swanston (*mynD*; Bailey *et al.*, 1999) together with past evidence from *npf* mutation studies (Section 1.4.2; Bailey *et al.*, 1992a; Solnica-Krezel *et al.*, 1995) suggests that the *red* genes are likely to comprise of two distinct categories; those required for structural rearrangement of the cell during the APT and those involved in the regulation of gene activity.

The analysis of promoters from plasmodium-specific genes and some *red* genes may provide information on the regulation of the APT. Further studies to identify and characterise *matA* and additional *red* genes may ultimately unveil the molecular mechanism by which amoebae develop into plasmodia. Some of these regulatory mechanisms might have been well conserved throughout evolution and thus, such studies could contribute to the understanding of developmental processes in other organisms.

LITERATURE CITED

LITERATURE CITED

- Adam L., Laroche A., Barden A., Lemieux G. and Pallotta D. (1991). An unusual actin-encoding gene in *Physarum polycephalum*. *Gene* **106**: 79–86.
- Adams M. D., Kelley J. M., Gocayne J. D., Dubnick M., Polymeropoulos M. H., Xiao C. R., Merril C. R., Wu A., Olde B., Moreno R. F., Kerlavage A. R., McCombie W. R., Venter J. C. (1991). Complementary DNA sequencing: expressed sequence tags and the human genome project. *Science* **252**: 1651–1656.
- Adler P.N. and Holt C. E. (1977). Mutations increasing asexual plasmodium formation in *Physarum polycephalum*. *Genetics* **87**: 401–420.
- Anderson R. W. (1977). Short paper: A plasmodial colour mutant in the myxomycete *Physarum polycephalum*. *Genetical Research, Cambridge* **30**: 301–306.
- Anderson R. W. and Dee J. (1977). Isolation and analysis of amoebal-plasmodial transition mutants in the myxomycete *Physarum polycephalum*. *Genetical Research, Cambridge*. **29**: 21–34.
- Anderson R. W. and Hutchins G. (1986). Uncertainty in the mapping of *GAD* mutations. *Physarum Newsletter* Dec 1986. 6–8.
- Anderson R. W., Cooke D. J. and Dee J. (1976). Apogamic development of plasmodia in the myxomycete *Physarum polycephalum*: A cinematographic analysis. *Protoplasma* **89**: 29–40.
- Anderson R. W., Hutchins G., Gray A., Price J. and Anderson S. E. (1989). Regulation of development by the *matA* complex locus in *Physarum polycephalum*. *Journal of General Microbiology* **135**: 1347–1359.
- Anzai H., Murakami T., Imai S., Satoh A., Nagaoka K. and Thompson C. J. (1987). Transcriptional regulation of bialaphos biosynthesis in *Streptomyces hygroscopicus* *Journal of Bacteriology* **169**: 3482–3488.
- Arellano O. L., Pallotta D. and Sauer H. W. (1992). Differential expression of three actin genes in the cell cycle of *Physarum polycephalum*. *Cell Biology International Reports* **16**: 1077–1081.
- Bailey J. (1995). Plasmodium development in the Myxomycete *Physarum polycephalum*: genetic control and cellular events. *Microbiology* **141**: 2355–2365.
- Bailey J. (1997). Building a plasmodium: development in the acellular slime mould *Physarum polycephalum*. *Bioessays* **19**: 985–992.
- Bailey J., Anderson R. W. and Dee J. (1987). Growth and development in relation to the cell cycle in *Physarum polycephalum*. *Protoplasma* **141**: 101–111.
- Bailey J., Anderson R. W. and Dee J. (1990). Cellular events during sexual development from amoeba to plasmodium in the slime mould *Physarum polycephalum*. *Journal of General Microbiology* **136**: 739–751.

- Bailey J., Solnica-Krezel L., Anderson R. W. and Dee J., (1992a). A developmental mutation (*npfL1*) resulting in cell death in *Physarum polycephalum*. *Journal of General Microbiology* **138**: 2575–2588.
- Bailey J., Solnica-Krezel L., Lohman K., Dee J., Anderson R. W. and Dove W. F. (1992b). Cellular and molecular analysis of plasmodium development in *Physarum*. *Cell Biology International Reports* **16**: 1083–1090.
- Bailey J., Bénard M. and Burland T. G. (1994). A luciferase expression system for *Physarum* that facilitates analysis of regulatory elements. *Current Genetics*. **26**: 126–131.
- Bailey J., Cook L. J., Kilmer-Barber R., Swanston E., Solnica-Krezel L., Lohman K. N., Dove W. F., Dee J. and Anderson R. W. (1999). Identification of three genes expressed primarily during development in *Physarum polycephalum*. *Archives of Microbiology* **172**: 364–376.
- Baldauf S. L. and Doolittle W. F. (1997). Origin and evolution of the slime moulds (Mycetozoa). *Proceedings of the National Academy of Science (USA)* **94**: 12007–12012.
- Barber R. (1998). Changes in cell fusion behaviour and gene expression during sexual development of *Physarum polycephalum*. PhD Thesis, University of Leicester, Leicester, UK.
- Barth C., Fraser D. J. and Fisher P. R. (1998). Co-insertional replication is responsible for tandem multimer formation during plasmid integration into the *Dictyostelium* genome. *Plasmid* **39**: 141–153.
- Bénard M. and Pierron G. (1992). Mapping of a *Physarum* chromosomal origin of replication tightly linked to a developmentally-regulated profilin gene. *Nucleic Acids Research* **20**: 3309–3315.
- Bertioli D. J., Schlichter U. H. A., Adams M. J., Burrows P. A., Steinbib H-H and Antoniw J. F. (1995). An analysis of differential display shows a strong bias towards high copy number mRNAs. *Nucleic Acids Research* **23**: 4520–4523.
- Binette F., Bénard M., Laroche A., Pierron G., Lemieux G. and Pallotta D. (1990). Cell specific expression of a profilin gene family. *DNA and Cell Biology* **9**: 323–334.
- Blindt A. B. (1987). Changes in cellular organisation during apogamic development in *Physarum polycephalum*. PhD thesis, University of Leicester, Leicester, UK.
- Blindt A. B., Chainey A. M., Dee J. and Gull K. (1986). Events in the amoebal-plasmodial transition of *Physarum polycephalum* studied by enrichment for committed cells. *Protoplasma* **132**: 149–159.
- Blot M., Hauer B. and Monnet G. (1994). The Tn5 bleomycin resistance gene confers improved survival and growth advantage on *Escherichia coli*. *Molecular and General Genetics* **242**: 595–601.
- Brasier A. R. and Ron D. (1992). Luciferase reporter gene assay in mammalian cells. *Methods in Enzymology*. Ed. Ray Wu. Academic Press **216**: 386–397.

- Brock A. M. and Pardee J. D. (1988). Cytoimmunofluorescent localisation of severin in *Dictyostelium* amoebae. *Developmental Biology* **128**: 30–39.
- Brown A. J. P. and Hardman H. (1981). The effect of age on the properties of Poly(A)-containing messenger RNA in *Physarum polycephalum*. *Journal of General Microbiology* **122**: 143–150.
- Burland T. G. and Bailey J. (1995). Electroporation of *Physarum*. *Methods in Molecular Biology, Vol. 47: Electroporation Protocols for Microorganisms*. Ed. Nickoloff J. A. 303–320.
- Burland T. G. and Pallotta D. (1995). Homologous gene replacement in *Physarum*. *Genetics* **139**: 147–158.
- Burland T. G., Chainey A. M., Dee J. and Foxon J. L. (1981). Analysis of development and growth in a mutant of *Physarum polycephalum* with defective cytokinesis. *Developmental Biology* **85**: 26–38.
- Burland T. G., Pallotta D., Tardif M. C., Lemieux G. and Dove W. F. (1991). Fission yeast promoter–probe vectors based on hygromycin resistance. *Gene* **100**: 241–245.
- Burland T. G., Bailey J., Adam L., Mukhopadhyay M., Dove W. F. and Pallotta D. (1992a). Transient expression in *Physarum* of a chloramphenicol acetyltransferase gene under the control of actin gene promoters. *Current Genetics* **21**: 393–398.
- Burland T. G., Bailey J., Dove W. F., Mukhopadhyay M. and Pallotta D. (1992b). Methods for transient and stable expression of heterologous genes in *Physarum*. *Cell Biology International Reports* **16**: 1111–1117.
- Burland T. G., Bailey J., Pallotta D. and Dove W.F. (1993a). Stable, selectable, integrative DNA transformation in *Physarum*. *Gene* **132**: 207–212.
- Burland T. G., Solnica–Krezel L., Bailey J., Cunningham D. B. and Dove W. F. (1993b). Patterns of inheritance, development and the mitotic cycle in the protist *Physarum polycephalum*. *Advances in Microbial Physiology* **35**: 1–69.
- Carey J. (1991). Gel retardation. *Methods in Enzymology* **208**: 103–117.
- Carulli J. P., Artinger M., Swain P. M., Root C. D., Chee L., Tulig C., Guerin J., Osborne M., Stein G. and Lomedico P. T. (1998). High throughput analysis of differential gene expression. *Journal of Cellular Biochemistry Supplements* **30/31**: 286–296.
- Casselton L. A. and Olesnicky N. A. (1998). Molecular genetics of mating recognition in *Basidiomycete* fungi. *Microbiology and Molecular Biology Reviews*. **62**: 55–70.
- Chen X. J. and Fukuhara H. (1988). A gene fusion system using the aminoglycoside 3'-phosphotransferase gene of the kanamycin-resistance transposon Tn903: use in the yeasts *Kluyveromyces lactis* and *Saccharomyces cerevisiae*. *Gene* **69**: 181–192.

- Chomczynski P. and Sacchi N. (1987). Single step method of RNA isolation by acid guanidium thiocyanate- phenol - chloroform extraction. *Analytical Biochemistry* **162**: 156-159.
- Church G. M. and Gilbert W. (1984). Genomic Sequencing. *Proceedings of the National Academy of Sciences* **81**: 1991-1995.
- Constantin B., Meerschaert K., Vandekerckhove J. and Gettemans J. (1998). Disruption of the actin cytoskeleton of mammalian cells by the capping complex actin-fragmin is inhibited by actin phosphorylation and regulated by Ca²⁺ ions. *Journal of Cell Science* **111**: 1695-1706.
- Cunningham D. B. and Dove W. F. (1993). Two alleles of a developmentally regulated α -tubulin locus in *Physarum polycephalum* replicate on different schedules. *Molecular and Cell Biology* **13**: 449-461.
- Cunningham D. B., Buchschacher G. L., Burland T. G., Dove W. F., Kessler D. and Paul E.C.A. (1993). Cloning and characterisation of the *altA* α -tubulin gene of *Physarum*. *Journal of General Microbiology* **139**: 137-151.
- Daniel J.W. and Rusch H.P. (1961). The pure culture of *Physarum polycephalum* on a partially defined soluble medium. *Journal of General Microbiology* **25**: 47-59.
- De La Luna S. and Ortín J. (1992). *pac* gene as efficient dominant marker and reporter gene in mammalian cells. *Methods in Enzymology*. Ed. Ray Wu. Academic Press **216**: 376-385.
- Dee J. (1962). Recombination in a Myxomycete, *Physarum polycephalum*. *Genetical Research*. **3**: 11-23
- Dee J. (1966). Genetic analysis of actidione-resistant mutants in the Myxomycete *Physarum polycephalum*, Schw. *Genetical Research* **8**: 101-110.
- Dee J. (1975). Slime moulds in biological research. *Scientific Progress, Oxford* **62**: 523-542.
- Dee J. (1982). Genetic control of mating in cell biology of *Physarum* and *Didymium*. In *Cell Biology of Physarum and Didymium Vol. I*. Eds. Aldrich, H. C. and Daniel, J.W. 229-231.
- Dee J. (1986). The culture of *Physarum* amoebae in axenic media. In *The Molecular Biology of Physarum polycephalum* Eds. Dove W. F., Dee J., Hatano F. B., Haugli F. B. & Wohlfarth-Bottermann K-E. 253-269.
- Dee J. and Anderson R. W. (1984). The effect of ploidy on the stability of plasmodial heterokaryons in *Physarum polycephalum*. *Journal of General Microbiology* **131**: 1167-1179.
- Dee J., Foxon J. L and Anderson R. W. (1989). Growth, development and genetic characteristics of *Physarum polycephalum* amoebae able to grow in liquid, axenic medium. *Journal of General Microbiology* **135**: 1567-1588.

- Dee J., Foxon J. L., Hill W., Roberts E. M. and Walker M. H. (1997). Contact with a solid substratum induces cysts in axenic cultures of *Physarum polycephalum* amoebae: Mannitol-induced detergent-resistant cells are not true cysts. *Microbiology* **143**: 1059–1069.
- Delgadillo M. G., Liston D. R., Niazi K. and Johnson P. J. (1997). Transient and selectable transformation of the parasitic protist *Trichomonas vaginalis*. *Proceedings of the National Academy of Sciences* **94**: 4716–4720.
- Drocourt D., Calmels T., Reynes J–P., Baron M. and Tiraby G. (1990). Cassettes of the *Streptoalloteichus hindustanus ble* gene for transformation of lower and higher eukaryotes to phleomycin resistance. *Nucleic Acids Research* **18**: 4009.
- Egelhoff T. T., Titus M. A., Manstein D. J., Ruppel K. M. and Spudich J. A. (1991). Molecular genetic tools for the study of the cytoskeleton in *Dictyostelium*. *Methods in Enzymology* **196**: 319–334.
- Eichinger L., Bombliès L., Vandekerckhove J., Schleicher M. and Gettemans J. (1996). A novel type of protein kinase phosphorylates actin in the actin–fragmin complex. *The EMBO journal*. **15**: 5547–5556.
- Esser K. and Lemke P. A. (1994). *The Mycota: A Comprehensive Treatise on Fungi as Experimental Systems for Basic and Applied Research. I; Growth, Differentiation and Sexuality*. Wessels J. G. H. and Meinhardt F. (Vol Eds.). Springer–Verlag.
- Evans K. (1997). Studies on the developmentally regulated gene, *redC*, in the acellular slime mould *Physarum polycephalum*. Project report submitted for the MSc in Molecular Genetics. Leicester University.
- Feinberg A. P. and Vogelstein B. (1983). A technique for radiolabelling DNA restriction endonuclease fragments to high specific activity. *Analytical Biochemistry* **132**: 6–13.
- Fire A., SiQun X., Montgomery M. K., Kostas S. A., Driver S. E. and Mello C. C. (1998). Potent and specific genetic interference by double-stranded RNA in *Caenorhabditis elegans*. *Nature* **391**: 806–811.
- Friederich E., Pringault E., Arpin M. and Louvard D. (1990). From the structure to the function of Villin, an actin-binding protein of the brush border. *Bioessays*. **12**: 403–408.
- Furuhashi K. and Hatano S. (1989). A fragmin-like protein from plasmodium of *Physarum polycephalum* that severs F-actin and caps the barbed end of F-actin in a Ca²⁺-sensitive way. *Journal of Biochemistry (Tokyo)* **106**: 311–318.
- Gaertig J., Gu L., Hai B. and Gorovsky M. A. (1994). High frequency vector-mediated transformation and gene replacement in *Tetrahymena*. *Nucleic Acids Research* **22**: 5391–5398.
- Gautier R., Drocourt D. and Jaffredo T. (1996). Generation of small fusion genes carrying phleomycin resistance and *Drosophila* alcohol dehydrogenase reporter properties: Their application in retroviral vectors. *Experimental Cell Research* **224**: 291–301.

Gettemans J., De Ville Y., Waelkens E, and Vandekerckhove J. (1995). The actin-binding properties of the *Physarum* actin fragmin complex: regulation by calcium, phospholipids and phosphorylation. *Journal of Biological Chemistry* **270**: 2644–2651.

Gorman J. A. and Wilkins A. S. (1980). Developmental phases in the life cycle of *Physarum* and related myxomycetes. In *Growth and Differentiation in Physarum polycephalum*. Eds. Dove W. F. and Rusch H. P. Princeton University Press.

Gorman J. A., Dove W. F. and Shaibe E. (1977). Anisomycin sensitive mutants of *Physarum polycephalum* isolated by cyst selection. *Molecular and General Genetics* **151**: 253–259.

Green L. L. and Dove W. F. (1988). Correlation between tubulin mRNA stability and poly(A) length over the cell cycle of *Physarum polycephalum*. *Journal of Molecular Biology* **200**: 321–328.

Gritz L. and Davies J. (1983). Plasmid-encoded hygromycin B resistance: the sequence of hygromycin B phosphotransferase gene and its expression in *Escherichia coli* and *Saccharomyces cerevisiae*. *Gene* **25**: 179–188.

Gull K., Birkett C. R., Blindt A. R., Dee J., Foster K. E. and Paul E. C. A. (1985). Expression of a multi-tubulin family and the in vivo assembly of microtubular organelles in *Physarum polycephalum*. *Microtubules and Microtubule Inhibitors*. De Brabander M. and De Mey J. (Eds.) Elsevier Science Publishers.

Hallmann A. and Rappel A. (1999). Genetic engineering of the multicellular green alga *Volvox*: a modified and multiplied bacterial antibiotic resistance gene as a dominant selectable marker. *The Plant Journal* **17**: 99–109.

Hamelin M., Adam L., Lemieux G. and Pallotta D. (1988). Expression of the three unlinked isocoding actin genes of *Physarum polycephalum*. *DNA* **7**: 317–328.

Hardman N. and Jack P. L. (1978). Periodic organisation of foldback sequences in *Physarum polycephalum* nuclear DNA. *Nucleic Acids Research* **5**: 2415–2423.

Hardman N., Jack P. L., Fergie R. C. and Gerrie L. M. (1980). Sequence Organisation in Nuclear DNA from *Physarum polycephalum*: interspersed repetitive and single-copy sequences. *European Journal of Biochemistry* **103**: 247–257.

Hasegawa T., Takahashi S., Hayashi H. and Hatano S. (1980). Fragmin: A calcium sensitive regulatory factor on the formation of actin filaments. *Biochemistry* **19**: 2677–2683.

Hatano S. (1994). Actin-binding proteins in cell motility. *International Review of Cytology* **156**: 199–273.

- Haugli F. and Johansen T. (1986). Toward a DNA transformation system for *Physarum polycephalum*. In *The Molecular Biology of Physarum polycephalum*. Eds. Dove W. F., Dee J., Hatano S., Haugli F. B. and Wohlfarth-Bottermann K-E. Plenum Press.
- Haugli F. B., Cooke D. and Sudbery P. (1980). The genetic approach in the analysis of the biology of *Physarum polycephalum*. In *Growth and Differentiation in Physarum polycephalum*. Eds. Dove W. F. and Rusch H. P. Princeton University Press.
- Haugwitz M., Noegel A. A., Karakesisoglou J. and Schleicher M. (1994). *Dictyostelium* amoebae that lack G-actin sequestering profilins show defects in F-actin content, cytokinesis and development. *Cell* **79**: 303–314.
- Hausmann K. and Hülsmann N. (1996) in *Spezielle Zoologie Teil 1: Einzeller und Wirbellose Tiere* Eds.: Westheide W. & Reiger R. Gustav Fischer Verlag, Stuttgart: 32–33.
- Havercroft J. C. and Gull K. (1983). Demonstration of different patterns of microtubule organisation in *Physarum polycephalum* myxamoebae and plasmodia using immunofluorescence microscopy. *European Journal of Cell Biology* **32**: 67–74.
- Hernon F. (1996). The development of a luciferase reporter gene system in *Physarum polycephalum*. Report submitted for the MSc by individually supervised study, University of Leicester, Leicester, UK.
- Hinssen H. (1981a). An actin-modulating protein from *Physarum polycephalum* I. Isolation and purification. *European Journal of Cell Biology* **23**: 225–233.
- Hinssen H. (1981b). An actin-modulating protein from *Physarum polycephalum*. 2. Ca²⁺-dependence and other properties. *European Journal of Cell Biology* **23**: 234–240.
- Hori R. and Firtel R.A. (1994). Identification and characterisation of A/T-rich cis-acting elements that control expression from *Dictyostelium* actin promoters: the *Dictyostelium* upstream activating sequence confers growth phase expression and has enhancer-like properties. *Nucleic Acids Research* **22**: 5099–5111.
- Hunter C. P. (1999). Genetics: A touch of elegance with RNAi. *Current Biology* **9**: R440–R442.
- Izumi M., Miyazawa H., Kamakura T., Yamaguchi I., Endo T., and Hanaoka F. (1991). Blasticidin S-resistance gene (*bsr*): A novel selectable marker for mammalian cells. *Experimental Cell Research* **197**: 229–233.
- Johansen T., Johansen S. and Haugli F. B. (1988). Nucleotide sequence of the *Physarum polycephalum* small subunit ribosomal RNA as inferred from the gene sequence: secondary structure and evolutionary implications. *Current Genetics* **14**: 265–273.
- Johansen , S., Johansen, T. and Haugli, F. (1992). Extrachromosomal ribosomal DNA of *Didymium iridis*: Sequence analysis of the large subunit ribosomal RNA gene and sub-telomeric region. *Current Genetics* **22**: 305–312.

- Kahmann R. and Bölker M. (1996). Self/nonself recognition in fungi: old mysteries and simple solutions. *Cell* **85**: 145–148.
- Kawano, S. and Kuroiwa, T. (1989). Transmission pattern of mitochondrial DNA during plasmodium formation in *Physarum polycephalum*. *Journal of General Microbiology* **135**: 1559–1566.
- Kawano S., Anderson R. W., Nanba T. and Kuroiwa T. (1987a). Polymorphism and uniparental inheritance of mitochondrial DNA in *Physarum polycephalum*. *Journal of General Microbiology* **133**: 3175–3182.
- Kawano S., Kuroiwa T. and Anderson R. W. (1987b). A third multiallelic mating type locus in *Physarum polycephalum*. *Journal of General Microbiology* **133**: 2539–2546.
- Kawano S., Takano H., Mori K. and Kuroiwa T. (1991). A mitochondrial plasmid that promotes mitochondrial fusion in *Physarum polycephalum*. *Protoplasma* **160**: 167–169.
- Kimura M., Kamakura T., Tao Q. Z., Kaneko I. and Yamaguchi I. (1994a). Cloning of the blasticidin S deaminase gene (BSD) from *Aspergillus terreus* and its use as a selectable marker for *Schizosaccharomyces pombe* and *Pyricularia oryzae*. *Molecular and General Genetics* **242**: 121–129.
- Kimura M., Takatsuki A. and Yamaguchi I. (1994b). Blasticidin S deaminase gene from *Aspergillus terreus* (BSD): a new drug resistance gene for transfection of mammalian cells. *Biochimica et Biophysica Acta* **1219**: 653–659.
- Knopf J. L., Lee M. H., Sultzman L. A., Kriz R. W., Loomis C. R., Hewick R. M. and Bell R. M. (1986). Cloning and expression of multiple protein kinase C cDNAs. *Cell* **46**: 491–502.
- Kothe E. (1996). Tetrapolar fungal mating types: sexes by the thousands. *FEMS Microbiology Reviews* **18**: 65–87.
- Koyama K., Koyama K. and Goto K. (1997). Cardiovascular effects of a herbicide containing glufosinate and a surfactant: *in vitro* and *in vivo* analyses in rats. *Toxicology and Applied Pharmacology* **145**: 409–414.
- Kozłowski P., Tymowska Z. and Toczko K. (1993). Nucleotide and predicted amino acid sequence of a new member of the *ras* gene family from the slime mold *Physarum polycephalum*. *Biochimica et Biophysica Acta* **1174**: 299–302.
- Kruse L., Meyer G. and Hildebrandt A. (1993). A highly conserved repetitive sequence from *Physarum polycephalum* contains nucleotide arrangements similar to replicator sequences. *Biochimica et Biophysica Acta* **1216**: 129–133.
- Kües U., Richardson W. V. J., Tymon A. M., Mutasa E. S., Göttgens B., Gaubatz S., Gregoriades A. and Casselton L. A. (1992). The combination of dissimilar alleles of the *A α* and *A β* gene complexes, whose proteins contain homeodomain motifs, determines sexual development in the mushroom *Coprinus cinereus*. *Genes and Development* **6**: 568–577.

- Kukulies J., Brix K. and Stockem W. (1987). Studies on microplasmidia of *Physarum polycephalum* VI. Functional analysis of a cortical and fibrillar actin system by use of fluorescent - analog cytochemistry. *Cell Tissue Research* **250**: 125–134.
- Kuspa A. and Loomis W. F. (1992). Tagging developmental genes in *Dictyostelium* by restriction enzyme-mediated integration of plasmid DNA. *Proceedings of the National Academy of Sciences (USA)* **89**: 8803–8807.
- Kuspa A. and Loomis W. F. (1994). Transformation of *Dictyostelium*: gene disruptions, insertional mutagenesis and promoter traps. *Methods in Molecular Genetics* **3**: 3–21.
- Kuspa A., Dingermann T. and Nellen W. (1995). Analysis of Gene Function in *Dictyostelium*. *Experientia* **51**: 1116–1123.
- Laane M. M and Haugli F. B. (1976). Nuclear behaviour during meiosis in the myxomycete *Physarum polycephalum*. *Norwegian Journal of Botany* **23**: 7–21.
- Lacalle R. A., Pulido D., Vara J., Zalacain M. and Jiménez A. (1989). Molecular analysis of the *pac* gene encoding a puromycin-N-acetyltransferase from *Streptomyces alboniger*. *Gene* **79**: 375–380.
- Lacalle R. A., Tercero J. A., Vara J. and Jimenez A. (1993). Identification of the gene encoding an N-acetylpuromycin N-acetylhydrolase in the puromycin biosynthetic gene cluster from *Streptomyces alboniger*. *Journal of Bacteriology* **175**: 7474–7478.
- Laffler T. G. and Dove W. F. (1977). Viability of *Physarum polycephalum* spores and ploidy of plasmodial nuclei. *Journal of Bacteriology* **131**: 473–476.
- Lamar E. E. and Palmer E. (1984). Y-encoded, species-specific DNA in mice—evidence that the Y-chromosome exists in 2 polymorphic forms in inbred strains. *Cell* **37**: 171–177.
- Lang-Hinrichs C., Dössereck C., Fath I and Stahl U. (1990). Use of the Tn903 neomycin-resistance gene for promoter analysis in the fission yeast *Schizosaccharomyces pombe*. *Current Genetics* **18**: 511–516.
- Li Z., Upadhyaya N. M., Meena S., Gibbs A. J. and Waterhouse P. M. (1997). Comparison of promoters and selectable markers for use in Indica rice transformation. *Molecular Breeding* **3**: 1–14.
- Liang P. and Pardee A. B. (1992). Differential display of the eukaryotic messenger RNA by means of the polymerase chain reaction. *Science* **257**: 967–971.
- Liang P. and Pardee A. B. (1995). Recent advances in differential display. *Current Opinion in Immunology* **7**: 274–280.
- Lisitsyn N., Lisitsyn N. and Wigler M. (1993). Cloning the differences between two complex genomes. *Science* **259**: 946–951.

- Lister G. (1925). *A Monograph of the Mycetozoa*, 3rd Edition. Oxford University Press.
- Luehrsen K. R., De Wet J. and Walbot V. (1997). Transient expression analysis in plants using Firefly luciferase reporter gene. *Methods in Enzymology*. Ed. Ray Wu. Academic Press **216**: 397–414.
- Lurquin P. F. (1997). Gene transfer by electroporation. *Molecular Biotechnology* **7**: 5–35.
- Marcoux N., LaForest M. and Pallotta D. (1999). The two *Physarum polycephalum* profilins are not functionally equivalent in yeast cells. *Protoplasma* **210**: 45–51.
- Matsudaira P. and Janmey P. (1988). Pieces in the actin–severing protein puzzle. *Cell* **54**: 139–140.
- Matz M. V. and Lukyanov S. A. (1998). Different strategies of differential display: areas of application. *Nucleic Acids Research* **26**: 5537–5543.
- McCullough C. H. R., Cooke D. J., Foxon J. L., Sudbery P. E. and Grant W. D. (1973). Nuclear DNA content and senescence in *Physarum polycephalum*. *Nature New Biology* **245**: 263–265.
- McCullough C. H. R., Dee J. and Foxon J. L. (1978). Genetic factors determining the growth of *Physarum polycephalum* amoebae in axenic medium. *Journal of General Microbiology* **106**: 297–306.
- McCurrach K., Glover L. A. and Hardman N. (1988). Transient expression of a *chloramphenicol acetyltransferase* gene following transfection of *Physarum polycephalum* myxamoebae. *Current Genetics* **13**: 71–74.
- McCurrach K. J., Rothnie H. M., Hardman N. and Glover L. A. (1990). Identification of a second retrotransposon–related element in the genome of *Physarum polycephalum*. *Current Genetics* **17**: 403–408.
- McPherson M. J., Quirke P., and Taylor G. R. eds. (1991). *PCR : A practical approach*. IRL press, Oxford.
- McPherson M. J., Hames B. D. and Taylor G. R. eds. (1995). *PCR 2: A practical approach*. IRL press, Oxford.
- Meerschaert K., De Corte V., De Ville Y., Vandekerckhove J. and Gettemans J. (1998). Gelsolin and functionally similar actin–binding proteins are regulated by lysophosphatidic acid. *The EMBO Journal* **17**: 5923–5932.
- Meland S., Johansen S., Johansen T., Haugli K. and Haugli F. (1991). Rapid disappearance of one parental mitochondrial genotype after isogamous mating in the myxomycete *Physarum polycephalum*. *Current Genetics* **19**: 55–60.
- Messina M., Niesman I., Mercier C. and Sibley L. D. (1995). Stable DNA transformation of *Toxoplasma gondii* using phleomycin selection. *Gene* **165**: 213–217.

- Mielke C., Tummler M. and Bode J. (1995). A simple assay for puromycin *N*-acetyltransferase: selectable marker and reporter. *Trends in Genetics* **11**: 258–259.
- Miller J. F. (1994). Bacterial transformation by electroporation. *Methods in Enzymology* **235**: 375–385.
- Misquitta L. and Paterson B. M. (1999). Targeted disruption of gene function in *Drosophila* by RNA interference (RNA-i): A role for *nautilus* in embryonic somatic muscle formation. *Proceedings of the National Academy of Science (USA)* **96**: 1451–1456.
- Mohberg J. (1977). Nuclear DNA content and chromosome numbers throughout the life cycle of the Colonia strain of the myxomycete *Physarum polycephalum*. *Journal of Cell Science* **24**: 95–108.
- Mohberg J. and Babcock K.L. (1982). Genealogy and characteristics of some cultivated isolates of *Physarum polycephalum*. In *Cell biology of Physarum and Didymium*, Vol. I. Ed Aldrich, H. C. and Daniel, J. W. Academic Press.
- Mohberg J., Babcock K. L., Haugli F. B. and Rusch H. P. (1973). Nuclear DNA content and chromosome numbers in the myxomycete *Physarum polycephalum*. *Developmental Biology* **34**: 228–245.
- Morita M. (1998). Molecular analysis of *Physarum* haemagglutinin I, lack of a signal sequence, sulphur amino acids and post-translational modifications. *Microbiology* **144**: 1077–1084.
- Murray M., Foxon J., Sweeney F. and Orr E. (1994). Identification, partial sequence and genetic analysis of *mlpA*, a novel gene encoding a myosin-related protein in *Physarum polycephalum*. *Current Genet* **25**: 114–121.
- Nader W. F. (1986). Gene cloning and construction of genomic libraries in *Physarum*. In *The Molecular Biology of Physarum polycephalum* Eds. Dove W. F., Dee J., Hatano F. B., Haugli F. B. & Wohlfarth-Bottermann K-E: 291–300.
- Nader W. F., Shipley G. L., Huettermann A. and Holt C. E. (1984). Analysis of an inducer of the amoebal-plasmodial transition in the Myxomycetes *Didymium iridis* and *Physarum polycephalum*. *Developmental Biology* **103**: 504–510.
- Nader W. F., Edlind T. D., Huettermann A. and Sauer H. W. (1985). Cloning of *Physarum* actin sequences in an exonuclease-deficient bacterial host. *Proceedings of the National Academy of Science (USA)* **82**: 2698–2702.
- Nader W. F., Isenberg G. and Sauer H. W. (1986). Structure of *Physarum* actin gene locus *ardA*: a nonpalindromic sequence causes inviability of phage lambda and *recA*-independent deletions. *Gene* **48**: 133–144.
- Nakagawa, C. C. Jones, E. P. and Miller, D. L. (1998). Mitochondrial DNA rearrangements associated with mF plasmid integration and plasmodial longevity in *Physarum polycephalum*. *Current Genetics* **33**: 178–187.

- Nelson J. A. E. and Lefebvre P. A. (1995). Targeted disruption of the *NIT8* gene in *Chlamydomonas reinhardtii*. *Molecular and Cellular Biology* **15**: 5762–5769.
- Nelson J. A. E., Savereide P. B. and Lefebvre P. A. (1994). The *CRY1* gene in *Chlamydomonas reinhardtii*: Structure and use as a dominant selectable marker for nuclear transformation. *Molecular and Cellular Biology* **14**: 4011–4019.
- Ngô H., Tschuldi C., Gull K. and Ullu E. (1998). Double-stranded RNA induces mRNA degradation in *Trypanosoma brucei*. *Proceedings of the National Academy of Science (USA)* **95**: 14687–14692.
- Noegal A. A. and Luna J. E. (1995). The *Dictyostelium* cytoskeleton. *Experientia* **51**: 1135–1142.
- Nowak A. and Steffan B. (1997). Physarorubinic acid, a polynoyltetramic acid type plasmodial pigment from the slime mould *Physarum polycephalum* (Myxomycetes) *Leibigs Annalen* **9**: 1817–1821.
- Ochman H., Gerber A. S. and Hartl D. L. (1988). Genetic applications of an inverse polymerase chain reaction. *Genetics* **120**: 621–625.
- Ohse M., Takahashi K., Kadowaki Y. and Kusaoka H. (1995). Effects of plasmid DNA sizes and several other factors on transformation of *Bacillus subtilis* ISW1214 with plasmid DNA by electroporation. *Bioscience, Biotechnology and Biochemistry* **59**: 1433–1437.
- Oka A., Sugisaki H. and Takanami M. (1981). Nucleotide sequence of the Kanamycin resistance transposon *Tn903*. *Journal of Molecular Biology* **147**: 217–226.
- Osborn M., Weber K., Naib-Majani W., Hinssen H., Stockem W., and Wohlfarth-Botterman K-E. (1983). Immunocytochemistry of the acellular slime mould *P. polycephalum*. III. Distribution of myosin and the actin-modulating protein (fragmin) in sandwiched plasmodia. *European Journal of Cell Biology* **29**: 179–186
- Otsuka T., Nomiyama H., Yoshida T., Kahara S. and Sakaki Y. (1983). Complete nucleotide sequence of the 26S rRNA gene of *Physarum polycephalum*: it's significance in gene evolution. *Proceedings of the National Academy of Science (USA)* **80**: 3163–3167.
- Pallotta D., Laroche A. and Tessier A. (1986). Molecular cloning of stage-specific mRNAs from amoebae and plasmodia of *Physarum polycephalum*. *Biochemistry and Cell Biology* **64**: 1294–1302.
- Pallotta D., Adam L. and Lemieux G. (1989). The cloning and nucleotide sequencing of the actin gene family in *Physarum polycephalum*. Abstracts of the North American *Physarum* meeting, July 1989, Cornell University, Ithaca, New York.
- Pang K. M., Lynes M. A. and Knecht D. A. (1999). Variables controlling the expression level of exogenous genes in *Dictyostelium*. *Plasmid* **41**: 187–197.

Pardinas J. R., Combates N. J., Prouty S. M., Stenn K. S. and Parimo S. (1998). Differential Subtraction Display: A unified approach for isolation of cDNAs from differentially expressed genes. *Analytical Biochemistry* **257**: 161–168.

Patel G. B., Nash J. H. E., Agnew B. J. and Sprott G. D. (1994). Natural and electropration-mediated transformation of *Methanococcus voltae* protoplasts. *Applied and Environmental Microbiology*. **60**: 903–907.

Paul E. C. A., Buchschacher G. L., Cunningham D. B., Dove W. F. and Burland T. G. (1992). Preferential expression of one β -tubulin gene during flagellate development in *Physarum*. *Journal of General Microbiology* **138**: 229–238.

Pearston D. H., Gordon M. and Hardman N. (1985). Transposon-like properties of the major, long repetitive sequence family in the genome of *Physarum polycephalum*. *The EMBO Journal* **4**: 3557–3562.

Peoples O. P. and Hardman N. (1983). An abundant family of methylated repetitive sequences dominates the genome of *Physarum polycephalum*. *Nucleic Acids Research* **11**: 7777–7788.

Pfeifer T. A., Hegedus D. D., Grigliatti T. A. and Theilmann D. A. (1997). Baculovirus immediate-early promoter-mediated expression of the Zeocin resistance gene for use as a dominant selectable marker in Dipteran and Lepidopteran insect cell lines. *Gene* **188**: 183–190.

Pierron G., Pallotta D. and Bénard M. (1999). The one-kilobase DNA fragment upstream of the *ardC* actin gene of *Physarum polycephalum* is both a replicator and promoter. *Molecular and Cellular Biology* **19**: 3506–3514.

Poulter R. T. M. (1969). Senescence in the myxomycete *Physarum polycephalum*. PhD thesis, University of Leicester, Leicester, UK.

Puissant C. and Houdebine L-M. (1990). An improvement of the single-step method of RNA isolation by acid guanidinium thiocyanate-phenol-chloroform extraction. *Biotechniques* **8**: 148–149.

Root-Bernstein R. S. and Holsworth D. D. (1998). Antisense peptides: A critical mini-review. *Journal of Theoretical Biology* **190**: 107–119.

Rothnie H. M., McCurrach K. J., Glover L. A. and Hardman N. (1991). Retrotransposon-like nature of Tpl elements: implications for the organisation of highly repetitive, hypermethylated DNA in the genome of *Physarum polycephalum*. *Nucleic Acids Research* **19**: 279–285.

Sagerström C. G., Sun B. I. And Sive H. L. (1997). Subtractive cloning: past, present and future. *Annual review of biochemistry* **66**: 751–783.

Salles-Passador I., Moisand A., Planques V. and Wright M. (1991). *Physarum* plasmodia do contain microtubules. *Journal of Cell Science* **100**: 509–520.

Salles-Passador I., Lajoie-Mazenc I., Tollon Y., Ahkavan-Niaki H., Oustrin M. L. Moisand A., Raynaud-Messina B. and Wright M. (1992). The intranuclear microtubule organising centre in the plasmodium of the myxomycete *Physarum polycephalum*. *Cell Biology International Reports* **16**: 1193–1204.

Sambrook J., Fritsch E. F. and Maniatis T. (1989). *Molecular Cloning: A laboratory manual*. 2nd Edition. Cold Spring Harbour Laboratory Press.

Sánchez O., Navarro R. E. and Aguirre J. (1998). Increased transformation frequency and tagging of developmental genes in *Aspergillus nidulans* by restriction enzyme-mediated integration (REMI). *Molecular General Genetics* **258**: 89–94.

Sasaki N., Suzuki T., Ohta T., Kawano S. and Kuroiwa T. (1994). Behaviour of mitochondria and their nuclei during amoebae cell proliferation in *Physarum polycephalum*. *Protoplasma* **182**: 115–125.

Schedl T. and Dove W. F. (1982). Mendelian analysis of the organisation of actin sequences in *Physarum polycephalum*. *Journal of Molecular Biology* **160**: 41–57.

Schedl T., Burland T.G. Gull K. and Dove W.F. (1984a). Cell cycle regulation of tubulin RNA level, tubulin protein synthesis, and assembly of microtubules in *Physarum*. *Journal of Cell Biology*. **99**: 155–165.

Schedl T., Owens J., Dove W. F. and Burland T. G. (1984b). Genetics of the tubulin families of genes in *Physarum*. *Genetics* **108**: 143–164.

Schlüter K., Jockusch B. M. and Rothkegel M. (1997). Profilins as regulators of actin dynamics. *Biochimica et Biophysica Acta* **1359**: 97–109.

Schreckenbach T. and Werenskiold A-K. (1986). Gene expression during plasmodial differentiation. In *The Molecular Biology of Physarum polycephalum* Eds. Dove W. F., Dee J., Hatano F. B., Haugli F. B. & Wohlfarth-Bottermann K-E: 131–150.

Semon D., Rao Movva N., Smith T. F., El Alama M. and Davies J. (1987). Plasmid-determined bleomycin resistance in *Staphylococcus aureus*. *Plasmid* **17**: 46–53.

Sharpe P. T. and Goodman E. M. (1986). Evidence that a low- M_r diffusible factor is involved in communication between compatible mating-types of the slime mould *Physarum polycephalum*. *Journal of General Microbiology* **132**: 3491–3495.

Shinnick T. M. and Holt C. E. (1977). A mutation (*gad*) linked to *mt* and affecting plasmodium formation in *Physarum polycephalum*. *Journal of Bacteriology* **131**: 247–250.

Shipley G. L. and Holt C. E. (1982). Cell fusion competence and its induction in *Physarum polycephalum* and *Didymium iridis*. *Developmental Biology* **90**: 110–117.

Sohn R. H. and Goldschmidt–Clermont P. J. (1994). Profilin: At the crossroads of signal transduction and the actin cytoskeleton. *Bioessays* **7**: 465–472.

Solnica–Krezel L., Dove W. F. and Burland T. G. (1988). Activation of a β -Tubulin gene during early development of the plasmodium in *Physarum polycephalum*. *Journal of General Microbiology* **134**: 1323–1331.

Solnica–Krezel L., Burland T. G. and Dove, W. F. (1991). Variable pathways for developmental changes of mitosis and cytokinesis in *Physarum polycephalum*. *Journal of Cell Biology* **113**: 591–604.

Solnica–Krezel L., Bailey J., Gruer D. P., Price J. M., Dove W. F., Dee J. and Anderson R. W. (1995). Characterisation of *npf* mutants identifying developmental genes in *Physarum*. *Microbiology* **141**: 799–816.

Stockem W. and Brix K. (1994). Analysis of microfilament organisation and contractile activities in *Physarum*. *International Review of Cytology* **149**: 145–215.

Stryer L. (1988). *Biochemistry*. Third edition. Freeman & Company, New York.

Sugiyama M., Thompson C. J., Kumagai T., Suzuki K., Deblaere R., Villarroel R. and Davies J. (1994). Characterisation by molecular cloning of two genes from *Streptomyces verticillus* encoding resistance to bleomycin. *Gene* **151**: 11–16.

Summers D. (1998). Timing, self-control and a sense of direction are the secrets of multicopy plasmid stability. *Molecular Microbiology* **29**: 1137–1145.

Sun H. Q., Kwiatkowska K. and Yin H. L. (1995). Actin monomer binding proteins. *Current Opinion in Cell Biology*. **7**: 102–110.

Surin B. P. and Downie J. A. (1988). Characterization of the *Rhizobium leguminosarum* genes *nodLMN* involved in efficient host-specific nodulation. *Molecular Microbiology* **2**: 173–183.

Sutherland J. D. and Witke W. (1999). Molecular genetic approaches to understanding the actin cytoskeleton. *Current Opinion in Cell Biology* **11**: 142–151.

Sutoh K. (1993). A transformation vector for *Dictyostelium discoideum* with a new selectable marker *bsr*. *Plasmid* **30**: 150–154.

Sutton R. B., Davletov B. A., Berghuis A. M., Südhof T. C. and Sprang S. R. (1995). Structure of the first C₂ domain of Synaptotagmin I: A novel Ca²⁺/Phospholipid-binding fold. *Cell* **80**: 929–938.

Sweeney G. E., Watts D. I. and Turnock G. (1987). Differential gene expression during the amoebal–plasmodial transition in *Physarum*. *Nucleic Acids Research* **15**: 933–945.

Tautz D. and Schmid K. J. (1998). From genes to individuals: developmental genes and the generation of the phenotype. *Philosophical transactions of the royal society of London Series B* **353**: 231–240.

Tercero J. A., Lacalle R. A. and Jiménez A. (1993). The *puo8* gene from the *pur* cluster of *Streptomyces alboniger* encodes a highly hydrophobic polypeptide which confers resistance to puromycin. *European Journal of Biochemistry* **218**: 963–971.

Tercero J. A., Espinosa C., Lacalle R. A. and Jiménez A. (1996). The biosynthetic pathway of the aminonucleoside antibiotic Puromycin, as deduced from the molecular analysis of the *pur* cluster of *Streptomyces alboniger*. *The Journal of Biological Chemistry* **271**: 1579–1590.

Theriot J. A. and Mitchison T. J. (1993). The three faces of profilin. *Cell* **75**: 835–838.

Thompson C. J., Movva N. R., Tizard R., Cramer R., Davies J. E., Lauwereys M. and Botterman J. (1987). Characterisation of the herbicide-resistance gene *bar* from *Streptomyces hygroscopicus*. *The EMBO Journal* **6**: 2519–2523.

T'Jampens D., Meerschaert K., Constantin B., Bailey J., Cook L. J., De Mol H., Goethals M., Van Damme J., Vandekerckhove J. and Gettemans J. (1997). Molecular cloning, over-expression, developmental regulation and immunolocalisation of fragminP, a gelsolin-related actin binding protein from *Physarum polycephalum* plasmodia. *Journal of Cell Science* **110**: 1215–1226.

T'Jampens D., Bailey J., Cook L. J., Constantin B., Vandekerckhove J. and Gettemans J. (1999). *Physarum* amoebae express a distinct fragmin-like actin-binding protein that controls *in vitro* phosphorylation of actin by the actin-fragmin kinase. *European Journal of Biochemistry* **265**: 240–250.

Trzcinska-Danielewicz J., Kozolowski P. and Toczko K. (1996). Cloning and genomic sequence of the *Physarum polycephalum Ppras1* gene, a homologue of the *ras* protooncogene. *Gene* **169**: 143–144.

Turnock G., Morris S. R. and Dee J. (1981). A comparison of the proteins of the amoebal and plasmodial phases of the slime mould, *Physarum polycephalum*. *European Journal of Biochemistry* **115**: 533–538.

Uyeda T. Q. P., Hatano S., Kohama K. and Furuya M. (1988). Purification of myxamoebal fragmin, and switching of myxamoebal fragmin to plasmodial fragmin during differentiation of *Physarum polycephalum*. *Journal of Muscle Research and Cell motility* **9**: 233–240.

Vanhée-Brossollet C. and Vaquero C. (1998). Do natural antisense transcripts make sense in eukaryotes? *Gene* **211**: 1–9.

Velculescu V. E., Zhang L., Vogelstein B. and Kinzler K. W. (1995). Serial analysis of gene expression. *Science* **270**: 484–488.

Von Stosch H. A., Van Zel-Pischinger M. and Dersch G. (1964). Nuclear phase alternance in the myxomycete *Physarum polycephalum*. Abstracts of the 10th International Botanical Congress, Edinburgh.

- Waelkens E., Gettemans J., De Corte V., De Ville E., Goris J., Vandekerckhove J. and Merlevede W. (1995). Microfilament dynamics: regulation of actin polymerisation by actin-fragmin kinase and phosphates. *Advances in Enzyme Regulation* **35**: 199–227.
- Wakasugi M. and Ohta J. (1973). Studies on the Amoeboid-flagellate transformation in *Physarum polycephalum*. *Botanical Magazine Tokyo* **86**: 299–308.
- Wan J. S., Sharp S. J., Poirier G. M-C., Wagaman P. C., Chambers J., Pyati J., Hom Y-L., Galindo J. E., Huvar A., Peterson P. A., Jackson M. R. and Erlander M. G. (1996). Cloning differentially expressed mRNAs. *Nature Biotechnology* **14**: 1685–1691.
- Watanabe S., Kai N., Yasuda M., Kohmura N., Sanbo M., Mishina M. and Yagi T. (1995). Stable production of mutant mice from double gene converted ES cells with puromycin and neomycin. *Biochemical and Biophysical Research Communications* **213**: 130–137.
- Welsh J., Chada K., Dalal S. S., Chang R., Ralph D. and McClelland M. M. (1992). Arbitrary primed PCR fingerprinting of RNA. *Nucleic Acids Research* **20**: 4965–4970.
- Wheals A. E. (1970). A homothallic strain of the myxomycete *Physarum polycephalum*. *Genetics* **66**: 623–633.
- Wheals A. E. (1973). Developmental mutants in a homothallic strain of *Physarum polycephalum*. *Genetical Research* **21**: 79–86.
- Woese C.R. (1996). Phylogenetic trees: Whither microbiology? *Current Biology* **6**: 1060–1063.
- Wright M. (1982). The microtubular systems in the amoebal and plasmodial forms of *Physarum polycephalum* (Myxomycetes). *Microtubules in Microorganisms*. Cappuccinelli P. and Morris N. R. (Eds). Marcell Dekker Inc., New York and Bassel.
- Yanai K., Horiuchi H., Takagi M., Yano K. (1991). Transformation of *Rhizopus niveus* using a bacterial blasticidin-s resistance gene as a dominant selectable marker. *Current Genetics* **19**: 221–226.
- Youngman P. J., Adler P. N. Shinnick T. M. and Holt C. E. (1977). An extracellular inducer of asexual plasmodial formation in *Physarum polycephalum*. *Proceedings of the National Academy of Sciences (USA)* **74**: 1120–1124.
- Youngman P. J., Pallotta D. J., Hosler B., Struhl G. and Holt C. E. (1979). A new mating compatibility locus in *Physarum polycephalum*. *Genetics* **91**: 683–693.
- Youngman P. J., Anderson R. W. and Holt C. E. (1981). Two multiallelic mating compatibility loci separately regulate zygote formation and zygote differentiation in the Myxomycete *Physarum polycephalum*. *Genetics* **97**: 513–530.

Zalacain M., González A., Guerrero M. C., Mattaliano R. J., Malpartida F. and Jiménez A. (1986). Nucleotide sequence of the hygromycin B phosphotransferase gene from *Streptomyces hygroscopicus*. *Nucleic Acids Research* **14**: 1565–1581.

Zhang Z., Moo-Young M. and Chisti Y. (1996). Plasmid stability in recombinant *Saccharomyces cerevisiae*. *Biotechnology Advances* **14**: 401–435.